DRYING OF PORTLAND CEMENT RAW MATERIAL SLURRIES

(Predicting the Performance of a

Counter-Current Spray Drier)

by

AKINPELU OLA. ESUBIYI, B.Sc., M.Sc.

A Thesis submitted to the

University of Aston in Birmingham

for the Degree of

Doctor of Philosophy

Department of Chemical Engineering

University of Aston in Birmingham

August 1980

DRYING OF PORTLAND CEMENT RAW MATERIAL SLURRIES

by

Akinpelu Ola. Esubiyi, B.Sc., M.Sc.

A thesis submitted to the
University of Aston in Birmingham
for the degree of
Doctor of Philosophy 1980

Summary

An extensive review of literature has been carried out concerning the drying of single drops, sprays of droplets and the prediction of spray drier performances.

The experimental investigation has been divided into two broad parts mainly: (1) Single Drop Experiments, and (2) Spray Drying and Residence Time Distribution Experiments.

The thermal conductivity of slurry cakes from five different sources have been experimentally determined using a modified Lee's Disc Apparatus and the data collected was correlated by the polynomial:

$$K = A + BT + CT^2 + DT^3 + \ldots.$$

Good agreement was observed between the experimental thermal conductivity values and the predicted ones. The fit gave a variance of between 5.877×10^{-3} and 1.124×10^{-3} for the various samples experimented on.

A mathematical model for estimating crust mass transfer coefficient at high drying temperatures was derived and the following equation is proposed:

$$K_c = \frac{\varepsilon^3 \rho}{5(1-\varepsilon)^2 \mu S^2 \beta}$$

The proposed overall mass transfer coefficient was predicted from the following equation where the gas phase coefficient was estimated by the correlation proposed by Audu.

$$\frac{1}{K_T} = \frac{1}{H_C K_G} + \frac{1}{K_C}$$

The agreement between the experimental and the proposed overall mass transfer coefficient was very good with a correlation coefficient of 0.9960 and a standard deviation of 5.841×10^{-3}.

The residence time distribution of the drying air in the spray drier was experimentally determined by Tracer Analysis and numerically simulated by an appropriate model which was analysed by a computer program. The agreement between experimental and the simulated responses for the model was very good. The sum of squared errors ranged between 0.145 and 0.245 with variances between 1.716×10^{-3} and 2.956×10^{-3}.

Spray drying experiments were carried out on a pilot plant spray drier and the factors predicting its performance were determined by a derived design model. The prediction by the design model was very good.

Keywords

CRUST THICKNESS, MASS TRANSFER COEFFICIENTS, RESIDENCE TIME DISTRIBUTION, TRACER ANALYSIS, SPRAY DRYING

DEDICATED

TO

FATHER

ACKNOWLEDGEMENTS

The author is indebted to and wishes to record his gratitude to the following:

Professor G. V. Jeffereys, Head of Department of Chemical Engineering, University of Aston in Birmingham, for his continued interest, and personal supervision of the research programme.

Blue Circle Cement Manufacturing Limited, for providing the grant for this project.

Blue Circle Technical (Research and Development) for supplying the slurry samples and arranging site trips to their Humber Works.

Dr. B. Gay, for his help in the development of the "Honeywell Basic 16" computer program.

Mr. N. Roberts, Chief Technician, Mr. A. Whyle the Process Laboratory Technician and the rest of the Technical Staff for their technical assistance both at the University and at Humber Works.

My family for their moral support throughout the period of the research programme.

Mrs. H. Turner for typing the thesis with consummate skill.

CONTENTS

INDEX OF FIGURES

INDEX OF TABLES

INDEX OF PLATES

CHAPTER ONE

INTRODUCTION

INTRODUCTION

Spray Driers are direct, dispersion type driers which operate on the principle of atomising a fluid feed to form a spray of droplets which mix with and pass through hot gases to evaporate a liquid and produce a dispered, dry product. Spray drying operation finds very extensive use both in the food and process industries. Its applications range from the production of dried milk, lactose, coffee powders etc., in the food industries to more massive scale of production of detergents, dyestuffs, chemicals, etc., in the process industries.

Despite these wide applications, spray drier design is still very much given to empiricsm. This is so because of the large number of factors that need to be considered in order to predict the performance of a spray drier. A review of literature has shown that among other things the Drying Characteristics of the material to be dried play a very important part in the prediction of the spray drier performance. To this end, the experimental programme had been carried out as follows:-

(1) Single Drops Experiments, during which the Drying Characteristics of the drops were determined.

(2) Spray Drying and Residence Time Distribution Experiments in a pilot plant spray drier; and on an industrial scale drier.

(3) A design model which considered all the factors developed

in (1) and (2) was derived and tested with the experimental data collected.

A mathematical model for predicting the crust mass transfer coefficient at high temperatures was derived in Sections 3.1 to 3.3.

A numerical method utilising the computer was used to analyse Residence Time Distribution data and is presented in Section 3.4.

The results of the experimental programme have been presented and analysed in Chapter 5, while the development of the design model is presented in Chapter 6.

CHAPTER TWO

LITERATURE REVIEW

LITERATURE REVIEW

2.1 MASS TRANSFER ACROSS A PHASE BOUNDARY

Most of the major industrial transfer processes, e.g. drying, distillation, crystallization, etc. are characterised by a transference of material across an interface. The transfer is brought about as a result of the existence of a concentration gradient[1] within a fluid comprising of two or more components. This process takes place in either a gas or liquid phase or in both simultaneously, and it continues until the whole liquid has evaporated or until all the gas is saturated and the concentration gradient is zero[1].

The mass transfer rate between two fluid phases will depend on the following:

(a) the physical properties of the two phases

(b) the concentration gradients existing in the fluids

(c) the interfacial area and the degree of turbulence.

The earliest attempt to explain the mechanism of mass transfer across an interface was by Whitman[1]. He suggested that the resistance to transfer in each phase could be regarded as lying in a thin film close to the interface. Higbie[3] in 1935, further suggested that the transfer process is largely caused by fresh material being brought by eddies to the interface, where a process of unsteady state transfer takes place for a fixed period at the freshly exposed surface. Danckwerts[4] modified this theory by

suggesting that the material brought to the surface will remain there for varying periods of time. Toor and Marchelo[5] have subsequently proposed a more general theory - the film-penetration theory - and also defined the limits of applicability of the two previous theories.

2.1.1 The Two-Film Theory

Whitman's two-film theory[2] was the pioneering theory on mass transfer across a boundary. In his theory, Whitman assumed that turbulence dies out at the interface and that a laminar layer exists in each of the two fluids. He further proposed that outside the laminar layer exists in each of the two fluids. He further proposed that outside the laminar layer, turbulent eddies the action caused by the random movement of the molecules, and the resistance to transfer becomes progressively smaller. This situation is illustrated by Figure 2.1.

The basis of the theory is the assumption that the zones in which resistance to transfer lies can be replaced by two hypothetical layers L_1 and L_2, each on either side of the interface ODCO. Thus, he proposed that the concentration gradient within L_1 and L_2 is linear and zero outside. Equilibrium is assumed to exist at the interface. The mass transfer is thus treated as a steady state process and therefore the theory can be applied only if the time taken for the concentration gradients to become established is small compared to the time of transfer, or if the capacity of the film is negligible. With these assumptions, the

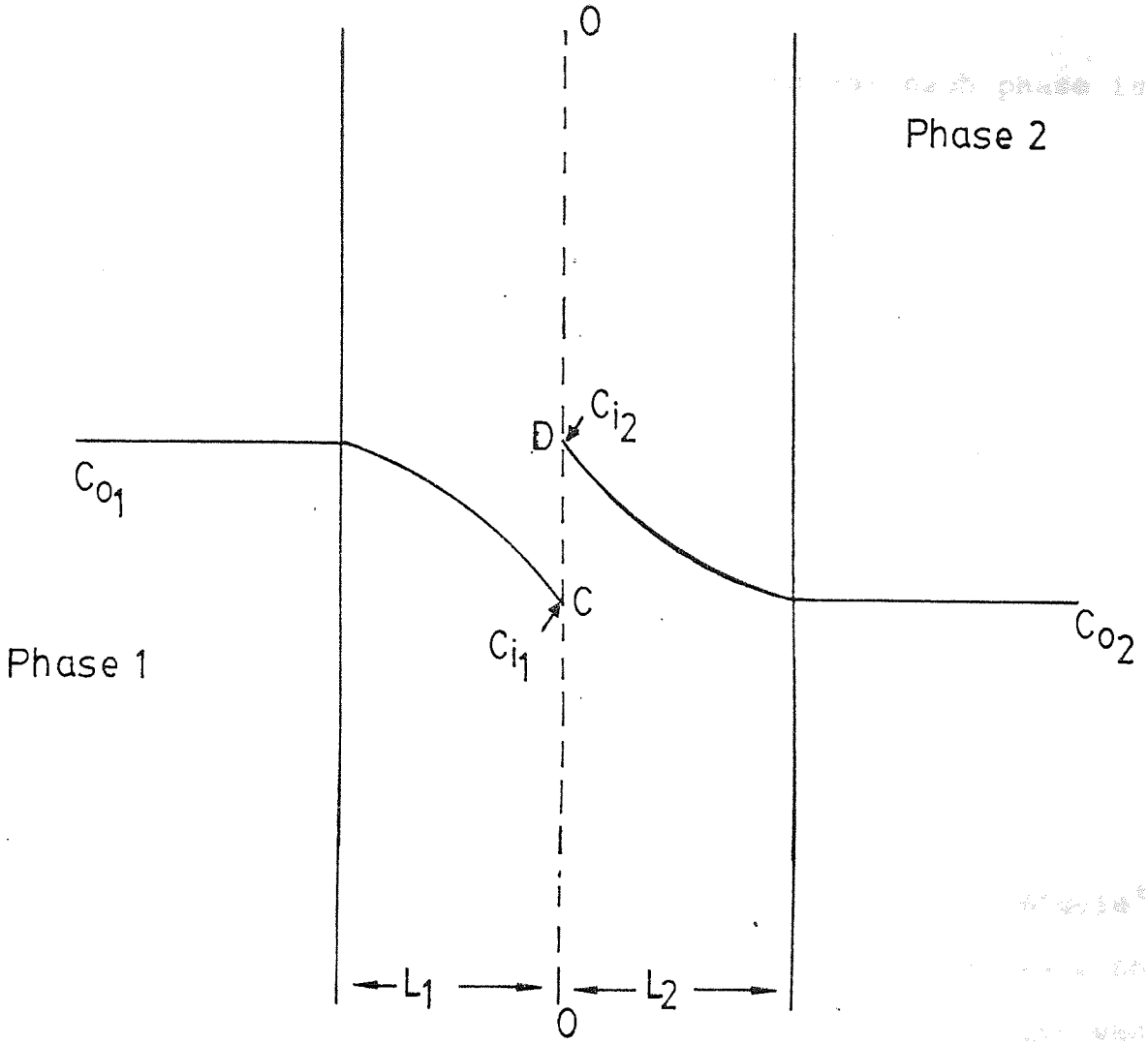

FIGURE 2.1 Concentration Profile across an Interface

relative mass transfer coefficients for each phase is:

$$\frac{K_1}{K_2} = \frac{C_{i_2} - C_{o_2}}{C_{o_1} - C_{i_1}} \qquad (2.1)$$

where

C_{o_1} - Molar concentration outside film L_1

C_{o_2} - Molar concentration outside film L_2

C_{i_1} - Film molar concentration in L_1

C_{i_2} - Film molar concentration in L_2

K_1 - Mass transfer coefficient in phase 1

K_2 - Mass transfer coefficient in phase 2.

2.1.2 The Penetration Theory

The penetration theory was propounded by Higbie[3] who was investigating into whether or not a resistance to transfer existed at the interface when a pure gas was absorbed in a liquid. The work resulted in the theory in which it was assumed that the eddies in the fluid bring an element of fluid to the interface where it is exposed to the second phase for a definite time interval, after which the surface element is mixed with the bulk again.

He proposed a non-linear differential equation to represent the diffusion of a solute A from the interface (Y - direction) such that:

$$\frac{\partial C}{\partial t} = D \frac{\partial C}{\partial y^2} \qquad (2.2)$$

with the boundary conditions:

$t = 0, \quad 0<y<\infty \quad : \quad C = C_o$

$t > 0, \quad y = 0 \quad : \quad C = C_i$

$t > 0, \quad y = \infty \quad : \quad C = C_o$

where

C_o = Concentration of A in the phase

C_i = Equilibrium concentration of A at the interface

D = Diffusivity of the liquid.

Solving equation (2.2), he derived the mass transfer rate, N_A, of a surface element of fluid A as:

$$N_A = 2(C_i - C_o) \left(\frac{D}{\pi t}\right) \qquad (2.3)$$

Danckwerts[4], however modified the Higbie theory. He suggested that each element of surface would not be exposed for the same time, rather a random distribution of ages would exist. He assumed that the probability of any element of surface becoming destroyed and mixed with the bulk of the fluid was independent of the age of that element. On this basis, the transfer rate equation (2.3) was modified thus:-

$$N_A = (C_i - C_o) \int_{t=0}^{t=\infty} \left(\frac{D}{\pi t}\right)^{0.5} s.e^{-st}\, dt \qquad (2.4)$$

where s is the rate of production of fresh surface per unit area of surface and t is the age of a surface element.

2.1.3 The Film-Penetration Theory

The film-penetration theory incorporates some of the principles of both the two-film theory and the penetration theory. It was proposed by Toor and Marchello[5] in 1958. They agreed that the resistance to mass transfer occurs within a laminar layer near the interface as in two-film theory, but claimed that this transfer is an unsteady state process. They also agreed to the theory that material is brought to the surface for exposure for short periods of time as in the penetration theory but that the resistance to mass transfer is confined to the finite film, and the material which goes across the film is immediately and completely mixed with the bulk of the fluid instead of returning to the fluid. They conceded, however, that for a short period of time, mass transfer across a boundary can be modelled by the penetration theory, whereas for prolonged periods of exposure when a steady state concentration gradient has been developed, conditions are pertinent to those considered in the two-film theory.

2.1.4 Mass Transfer Coefficients

The theories so far considered suggest that the rate of mass transfer in the absence of bulk flow is directly proportional to the driving force expressed as the molar concentration difference, thus:-

$$N_A = K_i (C_i - C_o) \qquad (2.5)$$

where K_i is the mass transfer coefficient. The mass transfer coefficient is differently defined in each of the theories discussed. In the two-film theory, K_i is directly proportional to the diffusivity and inversely proportional to the film thickness. By the penetration theory, it is proportional to the square root of the diffusivity and, when all surface elements are exposed for an equal time, it is inversely proportional to the square root of time of exposure; and when random surface renewal is assumed, it is proportional to the square root of the rate of renewal. In the film-penetration theory however, the mass transfer coefficient is a function of diffusivity, film thickness, and either the exposure time or the rate of renewal of the surface.

Since material does not accumulate at the interface the transfer rate on both sides of the interface must equate to one another, thus:

$$N_A = K_1 (C_{o_1} - C_{i_1}) = K_2 (C_{i_2} - C_{o_2}) \qquad (2.6)$$

If there is no resistance to transfer at the interface, C_{i_1} and C_{i_2} will be the corresponding values in the phase-equilibrium relationship. As the values of C_{i_1} and C_{i_2} are generally not known, the mass transfer coefficient is considered for the overall process thus:

$$N_A = K_1 (C_{o_1} - C_{e_1}) = K_2 (C_{e_2} - C_{o_2}) \qquad (2.7)$$

Thus assuming a linearity in the equilibrium relationship

we have

$$H = \frac{C_{i_1}}{C_{i_2}} = \frac{C_{e_1}}{C_{e_2}} = \frac{C_{o_1}}{C_{o_2}} \qquad (2.8)$$

From equations (2.6), (2.7) and (2.8), we derive the relationship between the various transfer coefficients as being:

$$\frac{1}{K} = \frac{1}{HK_1} + \frac{1}{K_2} \qquad (2.9)$$

These equations are valid if the transfer rate is linearly related to the driving force, ΔC[1].

The theories so far discussed find satisfactory applications in problems involving mass transfer between a fluid and the surface of a solid as in the case of drying of drops containing dissolved solids. In this case the basic assumption that turbulence dies out at the interface would be justified. Thus the layer of fluid immediately in contact with the solid is in laminar flow and constitutes the laminar sub-layer. However, in the vicinity of a solid surface, appreciable velocity gradients exist within the fluid and this makes the calculation of the transfer rate very complex if they are taken into consideration.

2.2 PRACTICAL CONSIDERATION OF MASS TRANSFER

In order to design reactors for use in the process industries, it is essential to take into account factors such as heat transfer, mass transfer and fluid dynamics

into consideration. In the light of this fact it is not very conclusive to base the design of mass transfer equipment on the phase boundary theories alone. The pioneering work of Colburn[6] has helped considerably in this respect. He developed a general method for the correlation of forced convection heat transfer data. By this he arrived at the relationship that:

$$St.\ P_r^{2/3} = 0.023\ Re^{-0.2} \qquad (2.10)$$

The basis of this correlation is the Reynold's analogy for flow in pipes, but it also includes a friction term ($C\mu/K$) to correct for differences between temperature and velocity distributions. The equation formed the basis of the analysis which produced the well known j-factors of Chilton and Colburn.

2.2.1 The J-Factor for Heat Transfer

Chilton and Colburn[7] developed the famous j-factors. The latter were developed to represent the results of experimental studies of heat transfer between a turbulent fluid and the wall of a pipe. This was developed from their original equation:

$$Nu = 0.023\ Re^{0.8}\ Pr^{0.33} \qquad (2.11)$$

By dividing both sides of equation (2.11) by Re.Pr, they obtained the relationship:

$$St.\ Pr^{0.67} = j_H = 0.023\ Re^{-0.2} \qquad (2.12)$$

where j_H is the j-factor for heat transfer. The plot of

j_H vs Re, they found, gave approximately the same curve as the friction chart for flow in tubes.

2.2.2 The J-Factor for Mass Transfer

By analogy to the derivation they found in (2.12) for heat transfer, Chilton and Colburn[7, 8] derived the rate of mass transfer to, or from a surface as:

$$\frac{K_G d_p}{D_v} = f(Re, Sc) \qquad (2.13)$$

By the same method as with heat transfer, they developed a j-factor for mass transfer as:-

$$j_d = \frac{K_G P_{bm}}{G_M} \cdot Sc^{0.67} \qquad (2.14)$$

Several workers, including Maisel and Sherwood[9], Sherwood[10], Gilliland and Sherwood[11] have attempted to establish a relationship between j_H and j_D. Introducing the Schmidt group, they were able to formulate the relationship:

$$\frac{K_G P_{bm}}{G_M} \left(\frac{\mu}{\rho D}\right)^{0.56} = 0.023\ Re^{-0.17} \qquad (2.15)$$

The index of the Schmidt group, $(\frac{\mu}{\rho D})$, was much less than 0.67 compared with that of the Prandtl group as obtained during heat transfer. However, the experimental work of Maisel and Sherwood[9] showed a good enough agreement with equation (2.14) of Chilton and Colburn[8]. Sherwood and Pigford[13] showed that if the data of Gilliland and Sherwood[11] and others[9, 10] were plotted with the Schmidt

number having an index number 0.67, a reasonably good correlation also ensued, and they also established that both j_H and j_D were nearly equal to the friction factor $(R_f / \rho U^2)$.

Further confirmation of the Schmidt index of 0.67 was supplied in the work of Linton and Sherwood[13].

2.2.3 Limits of Applicability

The j-factors for heat and mass transfer have been found to be approximately equal. This was confirmed by Maisel and Sherwood[9] in their work when they correlated the mass transfer for various liquids evaporating from different surfaces. Thus the values of mass transfer coefficients could be obtained if the corresponding heat transfer coefficient is known or vice versa.

The j-factors have their limits of applicability though. Now the cases considered in setting up the Chilton-Colburn analogy were those whereby the drag force in the transfer system was due almost entirely to viscous drag at the surface[8]. Sherwood[10], however, when he was investigating the relationship between mass transfer and friction in turbulent flow had to make allowance for cases when another form of drag, namely the form drag, was predominant. The latter was the additional drag caused by addies set up as a result of the fluid impinging on an obstruction. He found that on making this correction, the j-factors for heat and mass transfer were no longer equal. Such cases were thus

the limiting cases for the Chilton-Colburn analogy. The way Sherwood[10], overcame his problem and thus getting a reasonable agreement between the corresponding values of j_H, j_D and $(R/\rho U^2)$ was to subtract the form drag from the total drag force in the system.

Another reason for the limit in the applicability of the Chilton-Colburn analogy is due to the difference in heat and mass transfer paths in a drying droplet. Such cases abound in droplets which form crusts as drying proceeds.

2.3 DRYING AND EVAPORATION OF DROPS CONTAINING DISSOLVED SOLIDS

The drying process can be described as consisting of both the transfer of moisture within a droplet to the surface and the evaporation of the moisture from the surface into the surrounding medium[15]. It is an operation involving simultaneous heat and mass transfer. The heat is being transfered by convection from the hot medium (air or super-heated vapour) to the drop surface, then by conduction into the drop to effect its evaporation. Due to the latter, moisture is transfered through the drop and then by convection into the hot medium.

Various workers[14,16,17,18,19,20,21,22] have carried out investigations into the drying process and they concluded that under constant environmental conditions, the drying process can be divided into a constant rate period and one

or more falling rate periods. The first period of drying i.e. the constant rate period is very amenable to simple analysis[14,16,17,18,19]. This period best describes the drying process in pure drops. The picture is different however in drops containing dissolved solids. Now, as drying proceeds the droplet concentrates to the point where it no longer presents a free liquid interface to the hot air stream. It thus reaches a critical point[20,21,22], whereby drying characteristics is determined by the nature of the solid structure so formed. This is the point it enters the falling rate period and the drying rates begins to decrease with decreasing moisture content.

For a better understanding of the evaporation of drops containing dissolved solids, it is pertinent to consider, first, that of pure single drops.

2.3.1 Pure Single Drops

The theory of evaporation into still air was initiated by Fröessling. He developed an empirical equation for correlating the mass tra-sfer rates from spherical drops. Thus, for mass transfer he obtained:

$$Sh = 2.0 + 0.552\ Re^{0.5}\ Sc^{0.32} \qquad (2.16)$$

The constant value of Sh = 2.0 relates to the condition when Re = 0, that is at zero relative velocity for mass transfer by molecular diffusion.

Another notable contribution to the theory of evaporation

from pure drops is from Ranz and Marshall[29] who investigated the factors influencing the rate of evaporation of pure liquid drops. Their study was in the range $0 \leq Re \leq 200$ as this is representative of the conditions encountered in spray drying operation. The correlated the experimental data for water and benzene drops and they obtained the following equation for mass transfer:

$$Nu' = 2.0 + 0.6\ Sc^{0.33}\ Re^{0.5} \qquad (2.17)$$

For heat transfer they obtained the analogous equation:

$$Nu = 2.0 + 0.6\ Pr^{0.33}\ Re^{0.5} \qquad (2.18)$$

As with Fröessling, also Nu = Nu' when Re = 0. At high values of Re, the constant term becomes significant then equations (2.17) and (2.18) can then be converted through the well known j-factors of Chilton and Colburn[8].

In order to account for bouyancy effects, Ranz and Marshall[18] defined the velocity term in the Reynold's number, Re, as a vector sum $(\bar{V}_o + \bar{V}_{f_c})$, where $\bar{V}_{f_c}$ is the velocity component due to free convection, and

$$|\bar{V}_{f_c}| = (D_p\ g_c\ \sigma\Delta\theta)^{0.5} \qquad (2.19)$$

Then equation (2.17) and (2.18) for V=0 becomes

$$Nu' = 2.0 + 0.6\ (Sc)^{0.33}(Gr)^{0.25} \qquad (2.20)$$

$$Nu = 2.0 + 0.6\ (Pr)^{0.33}.\ (Gr)^{0.25} \qquad (2.21)$$

where

$$Gr = (D_p^3 \rho_g^2 g_c \sigma \Delta\theta)/\mu^2 \qquad (2.22)$$

The equations (2.20) and (2.21), they argue, are consistent with standard empirical correlations for free convections[30,31].

Pei et al.[32], studied the drying of pure single drops in high temperature surrounding and concluded that forced and natural convection were non-additive which contradicts Ranz and Marshall's findings. They suggested however that the transition from one form of convection to the other was a gradual process. Schünder[33] carried out some investigation along the line carried out by Ranz and Marshall except that their experimental procedure was more sophisticated because of the photographic technique[34] they adopted. They reprieved Ranz and Marshall in their reslts except that they modified the Reynold's number, Re, in order to include the effects of both free and forced convections. Their modified Reynold's number was defined thus:

$$Re^* = \frac{\rho U L'}{\mu} + (\tfrac{1}{2}Gr)^{0.25} \qquad (2.23)$$

where $L' = \pi r$, the characteristic length upon which flow impinged; and r = droplet radius.

Their proposed correlation then took the following form:

$$Nu' = \pi + 0.6(Re^*)^{0.5}(Sc)^{0.32} \qquad (2.24)$$

- mass transfer

$$Nu = \pi + 0.6(Re^*)^{0.5}(pr)^{0.33} \qquad (2.25)$$

- heat transfer

More investigations have been carried out on the correlation of experimental data of experiments concerning single drops. Among these was the work of Jeffreys and Audu[23,24]. They carried out experiments on drying of pure water drops. They introduced a novel method whereby the drop to be dried was suspended from a nozzle and rotated in a wind tunnel. By this method the drop is given a uniform exposure to the drying medium. They found that the value of the constant reported by Ranz and Marshall was temperature dependent. In the temperature range $26.5 \leq T \leq 118.5^{\circ}C$ the constant, ψ, for pure water drops varied between 0.38 and 0.47. They proposed a revised correlation of mass transfer coefficient in the form:

$$Sh = 2.0 + 0.44\left(\frac{T_{au} - T_s}{T_{amb}}\right)^{-0.008} Re^{0.5} Sc^{0.33} \qquad (2.26)$$

This correlation was much more practicable in that the experimental procedure simulates more closely the conditions in a spray drier.

2.3.2 Single Drops Containing Dissolved Solids

Ranz and Marshall[29] also carried out experiments on evaporation from droplets of solutions and suspensions,

and concluded that the drop evaporated, initially, as if it were saturated throughout even though its average concentration was less than saturation. The resistance to mass transfer was mainly in the boundary layer of stagnant gas surrounding the drop, and entrained[72] submicroscopic droplets from the evaporating surface. They found that this initial evaporation rate corresponded to that of a pure liquid. When the drop forms a solid however, the falling rate period ensued during which the drop temperature rose continually. They attributed this phenomenon to both the heat of crystallisation and sensible heat transfer in the case of solutions and primarily due to sensible heat transfer in the case of suspensions.

These observations were confirmed by William and Schmidt[35] in their experiments with saturated solutions of ammonium nitrate and magnesium chloride hexahydrate.

The first major work on the drying of single stationary drops containing dissolved solids, however, was by Charlesworth and Marshall[34]. By means of a specially designed sensitive balance, they were able to suspend drops over a hot-air stream and observe their drying characterisatics. They produced a rigorous mathematical model from transient heat and mass balance like Ranz and Marshall[29], but assumed that transfer in the droplet was by diffusion only, and concentration gradients were spherically symmetrical. As drying proceeds the presence of a solid phase was first shown by the formation of crystals at the bottom of the drop. The density of the

crystals grew in time thus forming a surface crust which steadily grew up the sides of the crust. This mode of crust formation contained in stationary drops until the whole drop is encrusted over. On the other hand for rotating drops, the crust tends to dissolve and reform as drying proceeds. They observed also that further drying after the completion of crust formation depended on the nature of the solute and the temperature of the drying air. They produced a comprehensive report on the various resulting crust as a result of different air temperature conditions[34]. In virtually all cases however they reported that the final particle consisted of a hollow, thin, and nearly spherical crust. The latter had a smooth outer surface, whereas the inner surface was rough and uneven, occasionally containing an open network of large crystals.

Other workers[33,41] on drying of drops containing dissolved solids investigated along the lines of Charlesworth and Marshall[34], but with different materials. They too observed the formation of crusts or skins as drying proceeds in the materials.

Of special interest is the recent work of Jeffreys and Audu[23,24] who also included in their work evaporation from aqueous sodium decahydrate drops and slurry drops from various detergent formulations. They also reported the formation of crust as drying proceeds. They were able to measure and study the crust thickness with the aid of a stereoscan, a scanning electron microscope. They found

that when a drop of aqueous sodium sulphate is dried, a hollow crust is formed. This crust they found provides 64.2% of the total resistance to mass transfer. They also found that the crust thickness rate increases with increase in air flowrate past the rotating drop, air temperature and the initial moisture content of the saturated drop. They produced a mathematical model for estimating the variation of crust thickness with drying time, θ, as follows:

$$\beta = R-\left|R^3-(1.5G/\pi C_o)(\Delta H_D-\Delta H_u)\Delta\theta\right|^{1/3} \qquad (2.27)$$

Their crust thickness experimentally evaluated from stereoscan micrographs showed good agreement with those theoretically derived by equation (2.27). In their model they also proposed that the drying characteristics of detergent drops can be evaluated from the porosity:thickness ratio (ε/β), thus:

$$\frac{K_m\beta_m}{D_M\varepsilon^{1.5}} = 0.58\left(\frac{\rho UD_p}{\mu}\right)^{0.5}\left(\frac{\mu}{D_M\varepsilon^{1.5}}\right)^{0.6} \qquad (2.28)$$

Some of their observations on crust structure confirms earlier ones by Charlesworth and Marshall[34] and Trommelen and Crosby[41].

2.3.3 Evaporation and Drying of Drops in Superheated Vapour

Drying in superheated vapours has been claimed to offer numerous advantages over drying with gases, and one of the

main advantages quoted is considerable improvement in thermal efficiency[36,38]. It is also claimed that the problem of dust collection is facilitated[36] since excess vapours ensuing from the system are passed through a total condenser.

Now, a pure liquid evaporating into a gas or dissimilar vapour attains dynamic equilibrium at a temperature somewhat below the dry bulb temperature because of the combined resistances to heat and mass transfer. When the liquid evaporates into a medium of its vapour, though, these resistances become very small indeed and the temperature of the liquid comes close to that of its saturated vapour at the ambient pressure[36,36,39]. This phenomenon predominates during the first period of drying of liquids containing dissolved solids[29,34,40]. It is also the case of single drops in air.

Toei et al.[39] investigated the evaporation of pure water in superheated steam and mixtures of steam and air. For $9 \leq Re \leq 120$ and $0.7 \leq Pr \leq 1.0$, they proposed the following correlations:

$$Nu = 2.0 + 0.65(Re)^{0.5}Sc^{0.33} \qquad (2.29)$$

- for heat transfer

and

$$Sh(P_{av}/P)^{-0.2} = 2.0 + 0.65\ Re^{0.5}Pr^{0.3} \qquad (2.30)$$

- for mass transfer.

where P_{av} is the average partial pressure of air in

transfer path adjacent to drop and P is the total pressure of the system in atmospheres. Their work was supported by Hughmark[38] whose work on spherical drops in superheated steam was in the range $1.0 \leq Re \leq 450$ and $Pr \leq 450$ found the correlation factor in equations (2.29) and (2.30) was 0.6 instead of 0.65. Lee and Ryley[42] also reported a close agreement in their experiments on non-spherical drops of water in superheated steam. Their empirical factor was 0.74. Other workers in this line of investigation include Chu et al.[36,37], and Wenzel and White[43].

In order to understand better the manner in which drops containing dissolved solids dry in superheated vapours as compared with gases, Trommelen and Crosby[41] dried single drops of several aqueous solutions and suspensions in both media. The investigations covered a wide and varied range of materials including commercial clay (6 wt%) potassium nitrate, sodium sulphate, a commercial detergent, tomato juice, coffee concentrate and skimmed milk. They were also interested in the final quality of these materials after drying in both media.

They discovered that water evaporates more slowly in superheated steam than in air. Also, that the medium in which faster drying occurs depended on the material being dried rather than on the medium. For drops containing food products however, they discovered that they did not exhibit a constant temperature period when air was the drying medium. Instead, the temperature rose continuously from its initial value

to that of the air throughout the drying period.

While drying in superheated steam however, a constant temperature period occurred near the saturation temperature of the steam. For drops containing other materials in solution and suspension the picture is quite different. These exhibited a drying pattern similar to the evaporation of water drops in superheated steam. This was characterised by a rather long constant temperature period.

2.4 SPRAY DRIER DESIGN AND PERFORMANCE PREDICTION

Spray drying has of recent found applications in a wide range of products from food to high tonnage chemicals. Master [44] lists several hundreds of products that are being spray dried industrially today. Despite the wide applicability and the appeal of spray driers, their design and performance prediction is still very much a matter of empiricism and experience. One of the main reasons for the lack of unified appraoch to the design of spray driers is the sheer number of operating parameters involved as well as the diversity of products that can be handled.

Spray driers, unlike other flow reactors such as distillation columns or absorption columns, come in a great variety of sizes, shapes, flow and atomizer arrangements. Despite these setbacks, there has been several proposals at design methods. These methods could be classified into three broad categories [45] namely:

1) Empirical and semi-empirical methods.

2) Analytical methods.

3) Numerical methods.

2.4.1 Empirical and Semi-Empirical Methods

These methods have not gained much wide acknowledgements as such. One of the earliest proponents of these methods was Luikov[46]. He derived an equation for the volumetric heat transfer coefficient as a function of droplet mean diameters, droplet velocity and other parameters. The final form of his equation was:

$$\alpha = 1.58 \times 10^{-3} \frac{KW_s}{\rho_s F} \left(\frac{1}{\partial}\right)^{1.6} \left(\frac{1}{U+U_1}\right) \qquad (2.31)$$

where α is the volumetric heat transfer coefficient.

Turba and Nemeth[47], on their work on a spray drying unit tried to apply the above equation in their system. The unit used a slurry of 40% wt chalk as feed material. They evaluated the total volume of drier needed to carry out the drying using equation (2.31). The value predicted by the equation was bigger, by a factor of 10, than the real value. They concluded however that the equation was probably not applicable to cases of slurry feed.

Also together with his works, Fröessling[28], tried to predict spray drier performance. He derived the following equation to evaluate the evaporation of drops in moving air:

$$N_A = 2\pi D.D_V \frac{\Delta\rho}{RT} (1+0.0276\ Re^{0.5} Sc^{0.33}) \qquad (2.32)$$

where N_A is the rate of mass transfer of the species. In his experiments, he used introbenzene, aniline and maphthalene (solid).

Contrary to the methods hitherto discussed, Feder[48] tried a graphical approach in evaluating the rate of evaporation of any fluid in a moving air stream. He based his method entirely on the empirical data of Longwell and Weiss[49] who evaluated the fraction of liquid evaporated in a moving air stream as a function of the liquid "residence time" in the system, the air velocity, and other system parameters. Feder's approach is rather suspect however considering that the data he used were for a limited range of values and he had to extrapolate the data in order to carry out his graphical prediction. Other attempts have been made at spray drier performance prediction, and among them are Borde[50] and Dolinsky [51] who used dimensional analysis.

In conclusion it could be argued that empirical and semi-empirical methods of spray drier performance prediction do not offer a very satisfactory precedent as the experience Turba and Nemeth showed. This is because of the great number of factors involved and this had tempted past workers in this line to make very many over-simplifying assumptions in order to arrive at their equations. At best the advantage these methods offer is in giving a pointer as to the magnitude and general trend and effect of some variables in a spray drying system.

2.4.2 Analytical Methods

Analytical methods so far proposed by investigators can be classified into two broad sections. These represent the two schools of thought now current[45] as to the analytical method suitable to predict the performance of a spray drying system. They are (a) Methods which try to characterise the drying of a spray by that of a single droplet and (b) Methods which assume a size distribution.

2.4.2.1 Methods Which Consider a Single Drop

These methods characterise the behaviour of a polydisperse spray by that of a single droplet. This is usually the largest droplet from the atomiser. Having assumed the latter as being representative of the spray beahviour, the equations of motion and evaporation for the particle are derived using the atomizer parameters as the initial conditions.

One of the earliest exponents of this method is Sjenitzer[52] who developed a graphical method based on the assumptions of constant air conditions, pure liquid droplet and the use of the Ranz and Marshall[29] equation to estimate the heat and mass transfer to spherical particles. He went further by introducing the Height of Transfer Unit concept[53] into spray drier design. Johnstone and Ead[54], however, derived an equation based on Frössling[28] correlation

of mass transfer data from evaporating drops. They claim this equation could be used to predict the time required to completely evaporate a liquid droplet of known size. Miesse[55], assuming a Stokesian regime of Nu = 2 (as for droplets in a quiescent fluid), solved the equation of motion and evaporation for a pure liquid drop in constant descelerating and accelerating gas flows.

Glukert[71] carried out an extensive work on spray drier design, with various atomizer types being considered. He developed the following equations for the rate of heat transfer to a spray for each of the atomizing methods:-

$$q = \frac{6.38k_f V^{0.667}\Delta T}{(D_m)^2} \cdot \frac{W_s}{\rho_s} \sqrt{\left(\frac{\rho_a}{W_a V_a}\right)\left(\frac{\omega_a+\omega_s}{\omega_a}\right)} \qquad (2.33)$$

- Two fluid atomizer

$$q = \frac{10.98k_f V^{0.667}\Delta T}{D_m^2} \cdot D_s \sqrt{\frac{\rho_t}{\rho_s}} \qquad (2.34)$$

- Pressure nozzle atomizer

$$q = \frac{4.19k_f (R_c - r/2)^2}{D_m^2} \cdot \frac{\Delta T}{\rho_s} \sqrt{\frac{\omega_s \rho_T}{rN}} \qquad (2.35)$$

- Centrifugal disk atomizer

He represented the process of heat and mass transfer in the spray as taking place in the maximum drop size D_m where D_m is equal to $3D_{vs}$ the volume-surface diameter of

the spray droplets. It should be pointed out however that almost all the methods so far considered apply only to pure liquid feeds.

2.4.2.2 Methods Which Assume a Size Distribution

In these methods a form of size distribution is assumed and the evaporation in each size range is integrated over the whole size spectrum to yield the total evaporation in the chamber. Of the forms of size distribution favoured by workers, the following are the commonest[56]:-

(i) The Log - Normal Distribution.

$$\frac{dV}{d(\ell_n D_p)} = \frac{1}{\sqrt{p\pi}.\sigma_{LN}}.\exp\left[-\frac{(\ell_n D_p - \mu_{LN})^2}{2\sigma_{LN}^2}\right] \qquad (2.36)$$

(ii) The Root - Normal Distribution.

$$d(\sqrt{D_p}) = \frac{1}{\sqrt{2\pi}.\sigma_{RN}}.\exp\left[-\frac{(\sqrt{D_p} - \mu_{RN})^2}{2\sigma_{RN}^2}\right] \qquad (2.37)$$

(iii) The Rosin-Rammler Distribution[57].

$$\frac{dV}{dD_p} = K\ D_p^{\delta-1}\exp(-aD_p^{\delta}) \qquad (2.38)$$

(iv) The Nukiyama-Tasanawa Distribution[58].

$$\frac{dV}{dD_p} = K\ D_p^{5}\ \exp(-aD_p^{\delta}) \qquad (2.39)$$

In their treatment of the changing size spectrum of particle clouds undergoing evaporation, combustion or acceleration, Shapiro and Erikson[59] developed a vigorous

differential equation governing this size change. They derived this equation as a function of the size, position and the velocity of the spray. They thus postulated that the number/size distribution G could be related to the distance from the nozzle thus:

$$\frac{\partial G}{\partial t} + U\frac{\partial G}{\partial x} + R\frac{\partial G}{\partial D} = -G\left|\frac{\partial U_p}{\partial x} + \frac{U_p\, dA}{A dx} + \frac{\partial R}{\partial D_p}\right| \qquad (2.40)$$

The above equation can be solved for an entire spray by assuming a size distribution as pointed out in the earlier part of this section. The derivative $\frac{dA}{dx}$ is generally assumed to be zero and in most cases $\frac{\partial U_p}{\partial D_p}$ is also assumed to be negligibly small (i.e. uniform cloud motion), such that only $R(D_p)$ and $G(D_p)$ have to be determined after having assumed the size distribution. Various investigators have followed this line of solution. They include Schünder[60], (who assumed a log-normal distribution to arrive at an analytical equation describing evaporation history), Marone[61] and Yaron and Gal-Or[62].

Owing to the complexity of equation (2.40) a variation of this approach has been suggested. This assumes a constant mean evaporative diameter (MED). The MED, D_e is the diameter of a pure liquid droplet that has the same evaporation rate, k, per unit remaining mass as that of the spray drier[45], that is

$$k = \frac{(\pi/2)\ D_e^2\ R(D_e)}{(\pi/6)\ D_e^3} \qquad (2.41)$$

$$= \frac{\int_o^\infty (\pi/2)\ D_p^2\ R(D_p)\ G(D_p)\ dD_p}{\int_o^\infty (\pi/6)\ D_p^3\ G(D_p)\ dD_p}$$

Shapiro and Erickson[59], together with Hopkins and Eisenklam[63], show that k and D_e remain constant as evaporation proceeds provided that

$$G \alpha D_p^{n-1} \exp(-KD_p^n) \qquad (2.42)$$

and

$$R \alpha -D_p^{1-n} \qquad (2.43)$$

Pham and Keey[45] pointed out however that the MED methods have limited application during the early stages of evaporation. This is due to the assumptions made by its proponents. Furthermore, the presence of solids in the slurry were not considered at all in any of these methods. For example, if a crust forms as drying proceeds, it is most likely to affect the transfer processes in the particle. As a result of this the prediciton of the mass transfer process in a spray drier will heavily depend on the characteristic drying curve of the material, and not on the size distribution of the droplets. This is the essential stumbling block in the efforts of an investigator trying to develop a unified method of designing spray driers for industrial purpose.

2.4.3 Numerical Methods

The approach adopted in Numerical Methods of designing of spray drier is to calculate the evaporation of each size range in the spray for a given increment of time or space, then sum over all ranges to get the total evaporation for that increment, proceed to the next increment until the final stage. The size ranges are based on the initial sizes and so each group of droplets is followed throughout its history.

The first worker to apply this method was Marshall[64], and it has then been used with various modifications[65-70] and greater degree of complexity by subsequent workers.

Generally, numerical methods offer a great deal of flexibility of appraoch and a great number of factors which had hitherto been neglected or assumed insignificant can be taken into consideration. A case in view is in the recent work of Keey and Phaam[45], who wrote a program to predict the performance of a tall-form co-current spray drier. The program among other things took into consideration, factors such as the mass flux on heat transfer, radiative heat transfer effects, turbulence effects and the droplets sensible heat.

2.5 CHARACTERISATION OF DROPLET AND AIR FLOW PATTERNS IN SPRAY DRYING SYSTEMS

Air and droplets flow characteristics are of great importance in the performance of spray driers. A good

air flow pattern should provide thorough contacting between the spray and air as soon as possible after the spray emerges from the atomizer in order to maximise thermal efficiency. There are[44,73] four basic methods today used in contacting hot air and droplets in spray drier. They are: Counter-current, Co-current, Parallel and Mixed flow. The contacting in each type of drier is achieved as their names imply. It has been found however, that counter-current flow devices, where the flow of air and droplets are counter to one another, offer the best performance with respect to heat utilization[74,75]. Counter-current flow is generally used with pressure nozzles. This is so because the upward flow of drying air effects a drag on the on-coming droplets and subsequently increases their residence time thus effecting a better evaporation.

Some work has been done on the flow patterns of both air and droplets in spray driers. This includes that of Master[76] who presented a theoretical correlation for predicting the trajectory of droplets from a centrifugal atomizer. On associating with Mohtadi[77], they found that drop size was inversely proportional to the disc speed and a maximum distance of the drops could be attained when drag forces increase to give a critical drop diameter. Their findings compare favourably with that of Friedman and co-workers[78] at lower disc speeds. Gauvin and Katta[68] have derived equations for predicting the three dimensional motion of droplets in a 1.83 m × 1.22 m diameter spray drier.

Their derivations were based on a knowledge of the characteristics of the atomizing device and the air flow patterns of air in the spray chamber.

2.5.1 Air Flow Patterns in Spray Drying Towers

From the works of Masters[76], Kessler[79], Buckham and Moulton[80], it can be inferred that the flow pattern of the drying air, as well as the manner the spray-air contact is achieved, play important roles in the design of spray driers. Kessler's[79], investigation on a co-current laboratory nozzle drier yielded information on the existence of stream-line and vortex motion of air in the spray drier. The same sort of work was carried out by Buckham and Moulton[80] on a 12ft × 4ft diameter tower, and they also studied the air mixing effect.

Chaloud et al.[81] reported on the air flow characteristics in a co-current drier for detergent formulation. They reported the existence of turbulence in the air flow, and this they claim increases the transfer coefficients between the air and droplets. Also this turbulence gives good mixing of the two species along the axis of flow such that the difference in temperature between the top and bottom of the tower was greatly reduced. They also claimed that the flow pattern in the tower was greatly stabilised by the swirling motion of the air.

A new approach which came into use to characterise air flow patterns in spray driers is the use of dispersion

models. Dispersion models have been widely used in connection with flows in tubular reactors, packed beds, and packed columns[82,83]. But Levenspiel and Smith[84], Van der Laan[85] exhibited the equivalence between the longitudinal dispersion model and a series of equally sized, perfectly stirred tanks. This subsequently facilitated the treatment of air flow patterns in spray driers. In this respect the overall flow pattern in a spray drier could then be characterised as a mixture of any of the following[87] 'ideal flows', plug flow and well stirred flow. The presence of an inert pocket[86] of flow is invariably taken into consideration and referred to as by-pass streams.

Paris et al.[87], modelled the flow of air in an 80ft × 20ft diameter counter-current spray drier as consisting of two stirred tanks in parallel with a plug flow by-pass. This they thought represented the existence of a rapidly ascending central stream surrounded by an annular zone of intense turbulence as reported by Chaloud et al[81].

Ade John[86], undertook experiments to confirm his model of the air flow pattern in a pilot plant 9ft × 4ft diameter counter current PVC drying tower. He proposed that the flow model consists of two well stirred tanks at the top and the conical bottom end of the drier. In between these is a plug flow zone and in parallel with the three is an inert by-pass stream. To support his

hypothesis he carried out smoke experiments on the tower, by injecting white smoke at the air inlet port of the drier. Since the tower was transparent, he was able to observe swirling smoke clouds at the conical base as well as at the top section of the tower, and in between these swirls was a regular streamline region. Along the entire length of the tower was a thin clear laminar layer of inactive air which represented the by-pass stream.

Further experiments along the line laid down by Ade-Joh were carried out[90]. These established that the plug flow section between the well stirred tanks diminishes at higher flowrates of air and liquid feed. Furthermore this phenomenon becomes more apparent the more 'squat' the spray drier.

2.5.2 Residence Time Distribution of Air in Spray Driers

There are two fundamental approaches to the mathematical modelling of flow systems. They are the Deterministic Method and the Stochastic Method[92]. The first is the now classical transport phenomena method which consists of writing mass, momentum, and energy balance over certain volume of the reactor. This approach is very desirable when the flow system is relatively simple. But when the nature of the flow is complex, as in a spray drier, this approach fails and the second approach is more applicable[87]. In this case the flowing material is considered as a collection of countable entities which are treated

statistically. Their flow is expressed by various age probability functions, one of which is the Residence Time Distribution (RTD)[91,92]. Treatment of the data from RTD experiments is then referred to as Residence Time Distribution analysis. Fan and Wen[83], Johnson et al.[95] list and compare the various methods available of treating RTD data.

Dankwerts[93] was one of the earliest to introduce the concept of RTD analysis. He suggested that it was possible to have a good knowledge of the flow pattern of a fluid in a continuous flow system by injecting a pulse of tracer at the inlet. He also developed the RTD analysis by introducing the concept of longitudinal dispersion whence the spread in residence time is related to a diffusion process counter to the bulk flow of fluid.

Subsequent to Dackwerts's work there have been some attempts at using RTD method in spray drying systems. Place et al.[94] carried out an investigation into the RTD and flow pattern of the drying air in a 50ft × 20ft diameter spray drier using a pulse of helium as tracer. They injected the tracer at various pre-determined points along the drier and they were able to evaluate the average residence time of the tracer at these points. Their results indicated that a considerable amount of the drying air near the axis of the tower as well as stagnation at the corners.

Other attempts at RTD of air in spray driers are few

and more recent. The basis of these attempts is to determine the RTD of the air in the drier by injecting a pulse of tracer into the inlet streams and measuring the tracer concentration (as a function of time) in the effluenct stream. The difference in their approach is the tracer used and method of analysis of the outlet response curves[95]. Paris et al[87] carried out some RTD experiments on a counter-current flow spray drier. They tried to fit the experimental pulse response data to a model of two stirred tanks in series with plug flow by-pass. They simulated the model on a TR-48 EAI analogue computer. Their findings confirmed earlier propositions by Chaloud et al.[81]. Phaam and Keey[88,89] in their work on RTD in a co-current tall form spray drier used Freon-12 (dichloro-diflouro methane) as tracer. They tried to find the RTD of the drying air by a graphical analysis of the Laplace transform transfer functions of the tracer response data. Their results pointed to the existence of a well-stirred tank zone immediately below the air inlets, followed by a plug flow zone, each occupying about half the chanber. They also concluded that as the Craya-Curtet[96] number increases, the backmixing in the system decreases.

Ade-John[86], used Carbon-dioxide as the tracer in his RTD experiments. The results of his analysis helped to confirm his model of the air flow pattern in the tower. The experimental outlet tracer response curve compared

favourably with the predicted one with a reported standard deviation of between 1.76×10^{-2} and 1.83×10^{-2}.

In conclusion, it can be pointed out that the application of RTD analysis to spray drying system is still very much in the formative stage. The diversity of the spray drying operation is not helping very much in developing a unified approach in this method. It can be inferred however that the more complex the model being proposed, the nearer to the actual state of affairs in the drier.

2.5.3 Hydrodynamic Flow Pattern of Spray Droplets in a Spray Drier

The flow of droplets in a spray drier could be split into two stages[97,98]. The first stage of motion would be in the vicinity of the atomizer, where the flow pattern of the drying air is assumed to have no effect on the droplet flow. The second stage considers the drop trajectory to be that following the air flow profile in the chamber. Pham and Keey[98], observed that depending on the inertia of the droplets, the viscosity and turbulence of the air motion, the droplets may either display plug-flow characteristics or have exactly the same RTD as the air. They observed that in most cases an intermediate situation will occur.

Masters[97] pointed out that the air motion in the spray chamber predetermines the evaporation rate because

it influences the spray passage through the chamber. Baltas and Gauvin[99,100] in their effort at predicting the performance of a co-current spray drier tried to present a model for the motion of droplets in the free-entrainment or free-fall zone of the chamber. They reported a considerable amount of radial mixing of the droplets[99]. They were able to predict mathematically this radial diffusion of the spray droplets on the assumption of equal turbulent diffusivity for spray and gas. This assumption was validated by the work of Soo[100] and Chao[102], who analytically established that the turbulent diffusivity of a majority of the particles is nearly equal to that of the dispersing gas. Baltas and Gauvin also refuted the prevailing theory that the flow of the spray droplets was a plug flow with an absence of any radial gradient.

The rejection of this theory was also further established by a more recent work by Pham and Keey[45,98]. They also identified two distinct zones in the flow profile of spray droplets, namely the jet zone and the free entrainment zone. The flow profile of the former zone is governed mainly by the characteristics of the atomizer in use. They argued that the particles in the jet zone will decelerate more slowly than a single equivalent sized droplet because the cloud of particles travels in a coherent manner to create a parallel flow of gas. As for the flow characteristics of the free-entrainment zone, they completely

agreed with the findings of Baltas and Gauvin[99,100]. In this zone, they claimed that the spray-air mixing is complete within the limits set up by the chamber geometry and the air flow profile.

Guavin et al[103], carried out some extensive investigations to predict droplet trajectory for water sprays in the jet zone, as well as in the free-entrainment zone in a co-current spray drying chamber. Their prediction compared favourably with the experimental results. Katta and Gauvin[68] extended on this work considerably by carrying out the experiments on Calcium Lignosulphate instead of water. They calculated the maximum evaporative capacity of the chamber at steady state on the basis that no incompletely dried particle will hit the wall of the chamber.

They also developed a set of simultaneous equations to predict the trajectory of the droplets. In both centrifugal and gravitational fields, the equation of motion was expressed as[68].

$$\frac{dV_f}{dt} = g_c + r\omega^2 + \frac{V_t V_r}{r^1} - \frac{C_D V_f^2 \rho_g A_p}{2W_d} + \frac{F_1}{W_d} \qquad (2.44)$$

Resolving equation (2.44) in the three dimensions, the droplet velocities were expressed as:-

Tangential motion:-

$$\frac{dV_t}{dt} = -\left(\frac{V_t V_r}{r^1}\right) - \frac{3C_D \rho_g V_f}{4d_i \rho_1}(V_t - V_{at}) \qquad (2.45)$$

Radial motion:

$$\frac{dV_r}{dt} = \frac{V_t^2}{r_1} - \frac{3C_D \rho_g V_f}{4d_i \rho_l}(V_r - V_{ar}) + \frac{F_l}{W_D} \qquad (2.46)$$

and Axial motion:

$$\frac{dV_a}{dt} = g_c - \frac{3C_D \rho_D V_f}{4d_i \rho_l}(V_a - V_{av}) \qquad (2.47)$$

where V_f the velocity of the droplet relative to the fluid is given by:

$$V_f^2 = (V_t - V_{at})^2 + (V_a - V_{at})^2 + (V_r - V_{ar})^2 \qquad (2.48)$$

where V_{at}, V_{ar} and V_{av} were the absolute values of the tangential, radial and axial velocities of air respectively.

A survey of literature yielded the information that so far there is only one published attempt at investigating the hydrodynamic flow profile of spray droplets by the RTD method. This was the recent work of Pham and Keey[98]. They used Carbon-14 in the form of solution of sodium bicarbonate was used as tracer. They reasoned that the factors affecting the relative motion and degree of entrainment of a particle in a turbulent stream are the inertia of the particle and the magnitude of the drag. They then incorporated these factors in a parameter R_D. Thus for the spray drying system they were investigating they defined R_D as follows

$$R_D = \frac{1-m}{1+V_t^2(1 + t_2/t_{pt})/V'^2} \qquad (2.49)$$

where t_{pt} is the terminal velocity of the particle in quiescent air, and defined thus:

$$t_p = \frac{4\rho_D D_p}{3\rho_f C_D V_t} \qquad (2.50)$$

They concluded that working at high air turbulence and entrainment ($R_D >> 10^{-3}$) increases the drag force and hence should also increase the heat and mass transfer rate. They were still very tentative at the conclusion that R_D parameter was a convenient way of measuring the turbulence effect.

CHAPTER THREE

MATHEMATICAL MODELS

MATHEMATICAL MODELS

3.1 INTRODUCTION

It is intended to derive a mathematical model that describes the transport phenomenon taking place in the drop as drying proceeds.

Audu and Jeffreys[23,24] showed that the Chilton-Colburn analogy for drying does not apply after a crust has been formed on a drop surface. The reason for this is that, after formation of a crust on the drop surface, the heat and mass transfer paths differ. As soon as a crust is formed, heat passes into the wet core of the drop by conduction through the solid portion of the crust while evaporation proceeds through the pores. A steady-state model has been developed on this hypothesis and this is the Diffusion Model. The model is strictly mass transfer controlled. The model is so called because on the formation of a crust, the liquid interface recedes into the core of the drop and evaporation occurs by diffusion of vapour through the pores in the crust.

The basis of their model was confirmed by stereoscan analysis of the crust so formed. The model had proved effective under certain conditions. However, examination of spray dried materials often shows that a number of the particles have been ruptured or exploded into small fragments. The occurrence of these ruptured particles has led to the second model for drying of drops.

As drying proceeds in the drop, an intense internal pressure builds up as a result of the expansion of the liquid core and partial vapourisation, and accumulation of vapour within the particle. This is due to the fact that the rate of vapour generation is greater than the rate of mass transfer by diffusion through the pores. Prior to cracking and fragmentation, conditions will exist such that jets of vapour will be discharged through the pores in the crust. When this occurs, there is a transition in the drying phenomenon to that of a Heat-Momentun transfer. The Diffusion model is thus only applicable at low mass and heat transfer rates.

3.2 HEAT-MOMENTUM TRANSFER MODEL

3.2.1 Assumptions

Consider a hemispherical slurry drop suspended from a nozzle as shown in Figure 3.1. Let the following assumptions made by Audu and Jeffreys[23,24] be valid:-

(i) The consistency of the slurry is uniform so that crust formed is composed of pores uniformly dispersed and of similar diameters. Therefore, capillary effects should be similar in all pores within the particle.

(ii) There is a receding interface between the suspension and the crust. As drying proceeds the crust becomes thicker while the external radius of the particle remains constant. Hence the radius of the wet core, r, is a function of time, i.e. $\beta = f(\theta)$.

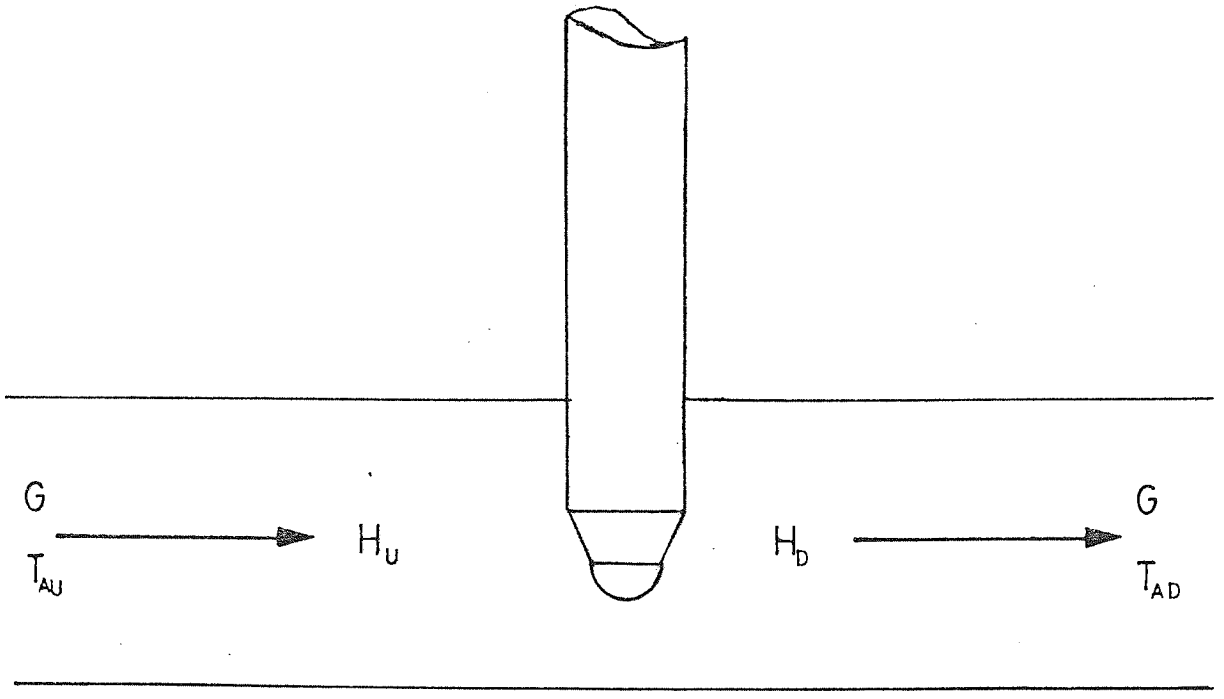

FIGURE 3.1 PARAMETERS IN DROP DRYING MODEL

(iii) The free moisture content of the crust is zero so that the moisture evaporated at any time is a function of the thickness of the crust and the water concentration of the core is constant.

Now consider the core of the drop as shown in Figure 3.2. Thus, the crust once formed is assumed porous. All pores are similar. Then a mass balance over the mass transfer process yields:

$$W' = \frac{\pi D_p^2 \, D_m \, \varepsilon^{2.5}}{\beta} (H_s - H_u) \qquad (3.1)$$

where H_s and H_u are concentrations (kg/m³ solution)

and the heat transfer process:

$$Q = \frac{\pi D_p^2 \, (1-\varepsilon) k}{\lambda \beta} (t_g - t_c) \qquad (3.2)$$

Thus immediately the heat (Q in equation (3.2)) conducted into the wet core exceeds the permissible diffusion rate W' in equation (3.1), vapour will tend to accumulate inside the particle with a corresponding pressure build up.

$$t_g - t_c \geq \frac{D_m \, \varepsilon^{2.5} \, \lambda}{k(1-\varepsilon)} . \Delta H_s \qquad (3.3)$$

When the temperature difference between the surface of the crust and the wet core satisfies that in equation (3.3), the drying rate is determined by the momentum transfer rate through the crust of the particle.

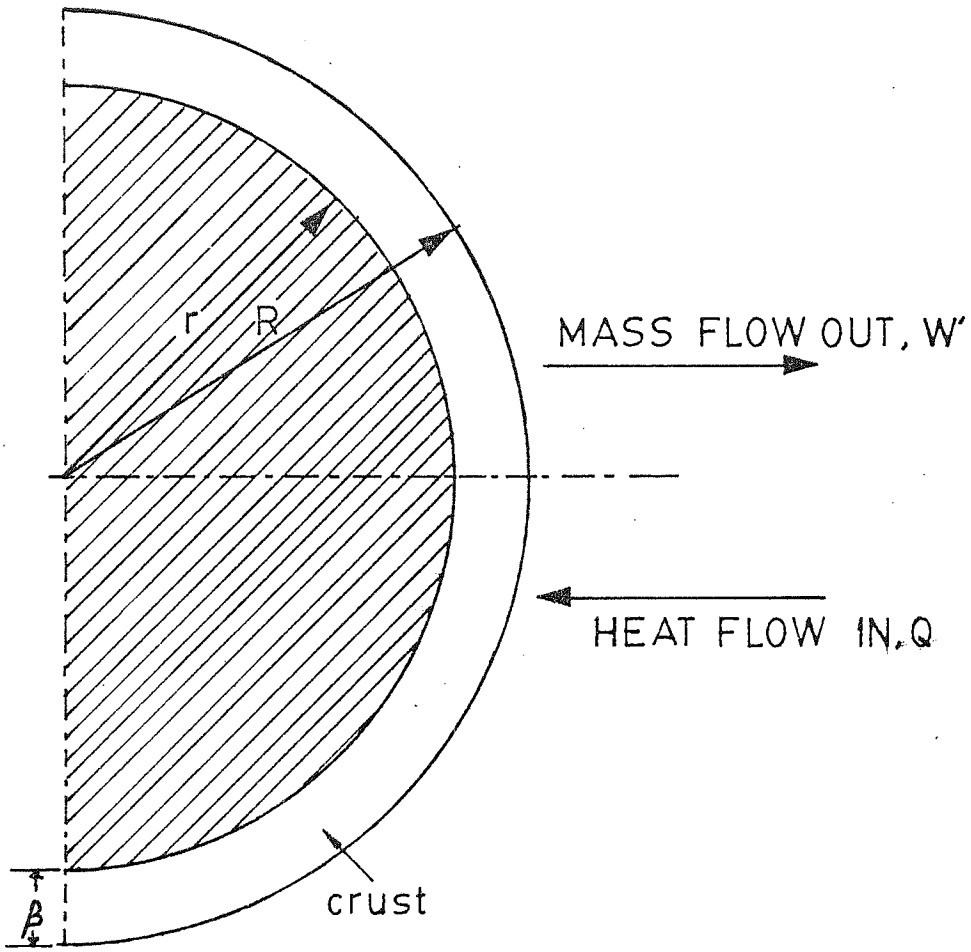

FIGURE 3.2 DROPLET CONFIGURATION

3.2.2 Drop Size

The amount of moisture evaporated in the time interval $\Delta\theta$ is from a mass balance over the drop:

$$\Delta W = G(H_D - H_U)\Delta\theta \qquad (3.4)$$

This is also equal to the quantity of water displaced in forming a crust of thickness (R-r). Thus, for the hemispherical drop at time θ:

$$\Delta W = 2/3\pi(R^3-r^3)C_o \qquad (3.5)$$

Let the drying proceed for a further interval in time $\Delta\theta$. Then the quantity of water further displaced will be:-

$$\Delta W\Big|_{\theta}^{\theta+\Delta\theta} = 2/3\pi C_o\{(R^3-r^3) - |R^3-(r-\Delta r)^3|\}$$

$$= 2\pi\rho R^2 U\Delta\theta \qquad (3.6)$$

Rearranging the above equation and neglecting terms of Δr greater than first order. Then also as $\Delta\theta \to 0$

$$\frac{d\theta}{dr} = -\frac{C_o}{\rho R^2}\left(\frac{r^2}{U}\right) \qquad (3.7)$$

or since $\beta = R-r$

$$\frac{d\theta}{d\beta} = \frac{C_o}{\rho R^2}\left(\frac{r^2}{U}\right) \qquad (3.8)$$

Equation (3.8) is non-linear since U, the vapour

velocity through the pores is a function of the crust thickness, β.

3.2.3 Vapour Velocity

The quantity of water evaporated, ΔW, will be discharged through the pores. The rate of this discharge will depend on the resistance offered by the crust to vapour flow. Since the crust is similar to a packed bed of small particles, the rate of vapour discharge may be estimated from a modified form of Kozeny's equation depending on the Reynold's number of the system. If the latter is less than 10, the following equation[105,106] evaluates the vapour flowrate:-

$$U = \frac{\varepsilon^3}{5(1-\varepsilon)^2 S^2 \mu} \cdot \frac{\Delta P}{\beta} \qquad (3.9)$$

- Kozeny

or

$$U = \frac{\varepsilon^3 g_c D^2}{15(1-\varepsilon)^2 \mu L} \cdot \Delta P \qquad (3.10)$$

- Blake

where D, the effective diameter of the particles defined as:

$$D = 6/S \qquad (3.11)$$

and S is the specific surface area i.e. the surface area per unit volume of solids.

In the transition region when 10<Re<1000 the velocity through the pores could be estimated from a semi-empirical correlation developed by Ergun[107]. Thus:

$$-\frac{\Delta P}{L} = 150\frac{(1-\varepsilon)^2}{\varepsilon^3}.\frac{\mu U}{D_p^2} + 1.75\ \frac{(1-\varepsilon)^2}{\varepsilon^3}.\frac{\rho U^2}{D} \qquad (3.12)$$

At high flowrates when Re>1000, the vapour velocity can be evaluated from the Burke-Plummer[108] equation, thus:-

$$\frac{\Delta P g_c}{L} = 1.75\ \frac{(1-\varepsilon)}{\varepsilon^3}.\ \frac{\rho U^2}{D^2} \qquad (3.13)$$

In order to apply equations(3.9-3.13) it is necessary to evaluate the specific surface area, S. Audu and Jeffreys[24,23] evaluated it in terms of the crust thickness, particle size, and mean pore size. Thus

$$S = \frac{3N\delta L}{R^3-r^3} \qquad (3.14)$$

and L, the mean pore length is:

$$L = 0.72\beta\left|1+(2R-\beta)^{0.5}\right| \qquad (3.15)$$

3.3 MASS TRANSFER COEFFICIENTS

3.3.1 Experimental Mass Transfer Coefficient

The overall mass transfer coefficient for the system would be composed of the transfer coefficient in the crust and the transfer coefficient in the gas film surrounding the drop. Thus,

$$\frac{1}{K_T} = \frac{1}{H_c K_G} + \frac{1}{K_c} \qquad (3.16)$$

where K_T is the total mass transfer coefficient, K_c is the crust mass transfer coefficient and K_G is the gas phase transfer coefficient. Audu and Jeffreys[23,24] have correlated the gas transfer coefficient and arrived at the following empirical equation;

$$\frac{K_G D_p}{D_m} = 2.0 + 0.44\left(\frac{T_a - T_s}{T_{amb}}\right)^{-0.008} . Re^{0.5} Sc^{0.33} \qquad (3.17)$$

They obtained a standard deviation of experimental results from the above equation to be 2.3 and the coefficient of correlation was 0.998.

The experimental mass transfer rate for the system can be evaluated by considering Figure 3.1. Thus for a drying air medium flowing at a rate of $G kgs^{-1}$ with the given humidities. Then by definition:

$$N_A = \frac{G(H_D - H_U)}{A} \qquad (3.18)$$

If one considers the core of the drop being made up of saturated liquid in the form of the slurry material, and if the humidity of this core be H_S. The humidity driving force would thus be $(H_S - H_U)$. If K_E was the mass transfer coefficient between this core of liquid and the hot air, then the rate of mass transfer through the crust would be:

$$N_A = K_E(H_S - H_U) \qquad (3.19)$$

Since N_A in both equations (3.18) and (3.19) are the same for the system then equating both quantities yields:

$$K_E = \frac{G\Delta H}{A\Delta H_S} \qquad (3.20)$$

This transfer coefficient would thus be the overall experimental mass transfer coefficient in the system.

3.3.2 Heat-Momentum Transfer Coefficient

The mass transfer coefficient for the crust when the diffusion model is valid in the system is a function of the crust thickness, porosity and diffusivity of the water vapour. Thus:

$$K_C = \frac{D_m \varepsilon^{1.5}}{\beta} \qquad (3.21)$$

The transfer coefficient of the system during the Momentum-Heat Transfer model phase will be developed as follows.

Consider a jet of vapour being ejected through the pores at a velocity U. The flow regime of this jet would be assumed to be in the region of Re<10, considering the size of the droplet and pores. Thus, then as developed in section 3.2.3.

$$U = \frac{\varepsilon^3}{5(1-\varepsilon)^2 S^2 \mu} \frac{\Delta P}{\beta} \qquad (3.9)$$

Now, the mass transfer rate, N_A, can be defined as

the product of the linear flowrate and the density of the vapour. Thus:

$$N_A = \rho U \tag{3.22}$$

where ρ is the density of the water vapour.

Substituting for U in equation (3.9) we have:

$$N_A = \frac{\varepsilon^3}{5(1-\varepsilon)^2 S^2 \mu} \cdot \frac{\Delta P}{\beta} \cdot \rho \tag{3.23}$$

The mass transfer rate can equally be defined in terms of the pressure gradient across the crust interface, and the crust transfer coefficient, thus:

$$N_A = K_c \Delta P \tag{3.24}$$

Equating equations (3.23) and (3.24) yields

$$K_c \Delta P = \frac{\varepsilon^3}{5(1-\varepsilon)^2 \mu S^2} \frac{\Delta P}{\beta} \cdot \rho \tag{3.25}$$

Thus:

$$K_C = \frac{\varepsilon^3}{5(1-\varepsilon)^2 \mu S^2} \cdot \frac{\rho}{\beta} \tag{3.26}$$

All the terms in R.H.S. of the above equations except β are constants with respect to the fixed set of conditions in the system.

Thus

$$K_C = \frac{\bar{K}}{\beta} \tag{3.27}$$

Thus equations (3.21) and (3.27) gives the mass transfer coefficient of the crust in the system whichever model applies. This value of K_C can then be used in equation (3.16) to evaluate the overall theoretical mass transfer coefficient K_T.

3.4 AIR RESIDENCE TIME DISTRIBUTION MODEL

3.4.1 Introduction

In the R.T.D. model, a known signal of a tracer is introduced into the inlet stream of the spray drying system. The response signals in outlet streams of the system thus constitute the raw data for the RTD model. In the tracer technique to be adopted in this prject, the analysis of the data depends heavily on the responses in the system to the tracer input. There are various methods now available[92-96] for the analysis the raw data from an RTD experiment. In this project, a general and complex flow pattern is proposed for the system. The flow equations describing the response and the various combinations of the zones in the flow patterns will be derived. The simulated graphical response shall then be compared to the experimental response from the system. On obtaining a good enough fit between the two, the parameters would then be used in predicting the performance of the flow system.

3.4.2 Normalisation of Data

The data is in the form of the response in the inlet

and outlet streams in the spray drier. The concentration profile of the tracer inlet pulse is monitored by an adequate method. The inlet response can be represented as X(t) and the outlet as Y(t), while t is time. A typical response curve to a rectangular pulse disturbance is shown in Figure 3.3.

For subsequent analysis of the data, dimensionless variables are used. Thus:

$$X(\theta) = \frac{\bar{t}X(t)}{A_x} \tag{3.28}$$

and

$$Y(\theta) = \frac{\bar{t}Y(t)}{A_y} \tag{3.29}$$

where

$$\bar{t} = V_T/Q_T \tag{3.30}$$

$$\theta = t/\bar{t} \tag{3.31}$$

$$A_x = \int_{tx_o}^{tx_f} X(t)\ dt \tag{3.32}$$

$$A_y = \int_{ty_o}^{ty_f} Y(t)\ dt \tag{3.33}$$

Ideally

$$A_x = A_y$$

= Volume of tracer used in experiment

Having thus evaluated $X(\theta)$ and $Y(\theta)$, they are used to determine the parameters of the model chosen to represent the system.

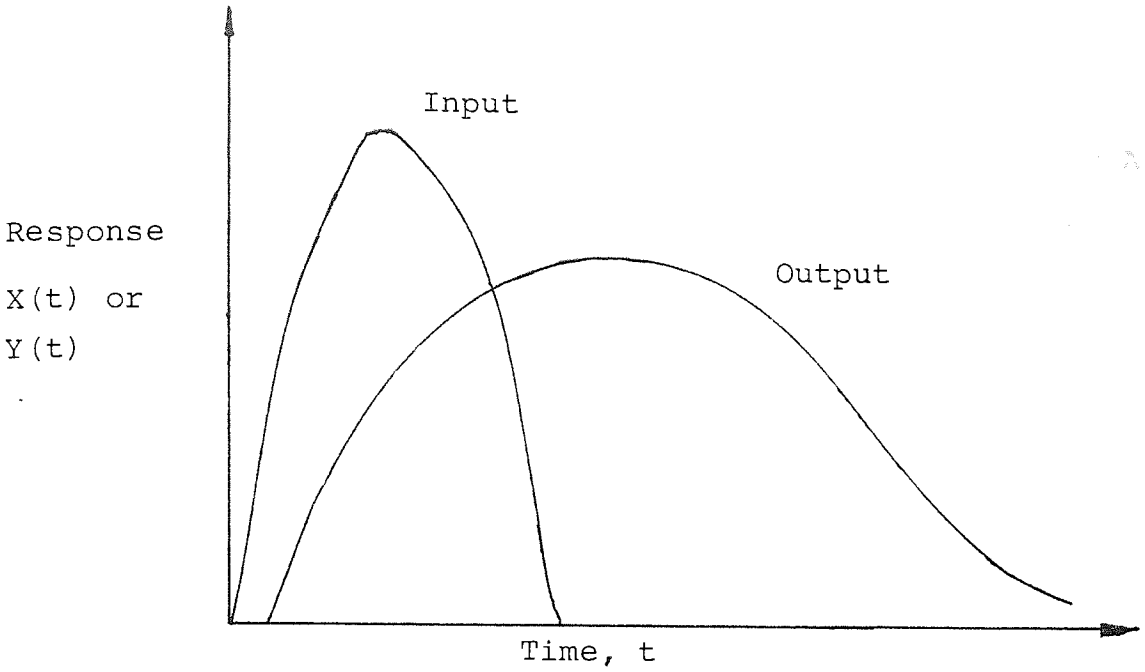

FIGURE 3.3

3.4.3 Residence Time Distribution Model

The following parameters constitute the flow system.

The flow of tracer is distributed in the ratio A:B:C into the three branches of the flow system. If Q_A, Q_B, Q_C are the flow rates respectively, then:

$$A = Q_A/Q_T \tag{3.34}$$

$$B = Q_B/Q_T \tag{3.35}$$

$$C = 1-(A+B) \tag{3.36}$$

The fraction by volume of each zone in the system is thus:

$J = V_J/V_T$ in zone A2

$K = V_K/V_T$ in zone A3

$M = V_M/V_T$ in zone B1

$N = V_N/V_T$ in zone B2

$L = V_L/V_T$ in zone C1

The fraction in the first C.S.T.R. i.e. zone A1 is found by difference. The system of equations describing the flow of tracer through the flow system can be derived by considering mass balances at points 1-6 in the flow diagram in Figure 3.4.

At (1) A well stirred tank zone A1:

$$Q_A(C_o - C_1) = V_1 \frac{dC}{d\theta} \qquad (3.37)$$

Substituting for Q_A from equation (3.34) and

$$V_1/V_T = 1-(J+K+L+M+N)$$

Thus

$$A\ Q_T(C_o - C_1) = V_T(1-(J+K+L+M+N))\frac{dC}{d\theta} \qquad (3.38)$$

Dividing equation (3.38) through by Q_T, we have

$$A\ \Delta C = \frac{V_T}{Q_T}\ (1-(J+K+M+N+L))\ \frac{dC}{d\theta}$$

Therefore:

$$\frac{1}{\Delta C} \cdot \frac{dC}{d\theta} = \frac{A}{\bar{t}(1-(J+K+M+N+L))} \qquad (3.39)$$

The above expression represents the response signal from zone A1.

At (2) A delay zone A2:

The response R_j from this zone can be represented thus:-

$$R_j = \theta - D_j \qquad (3.40)$$

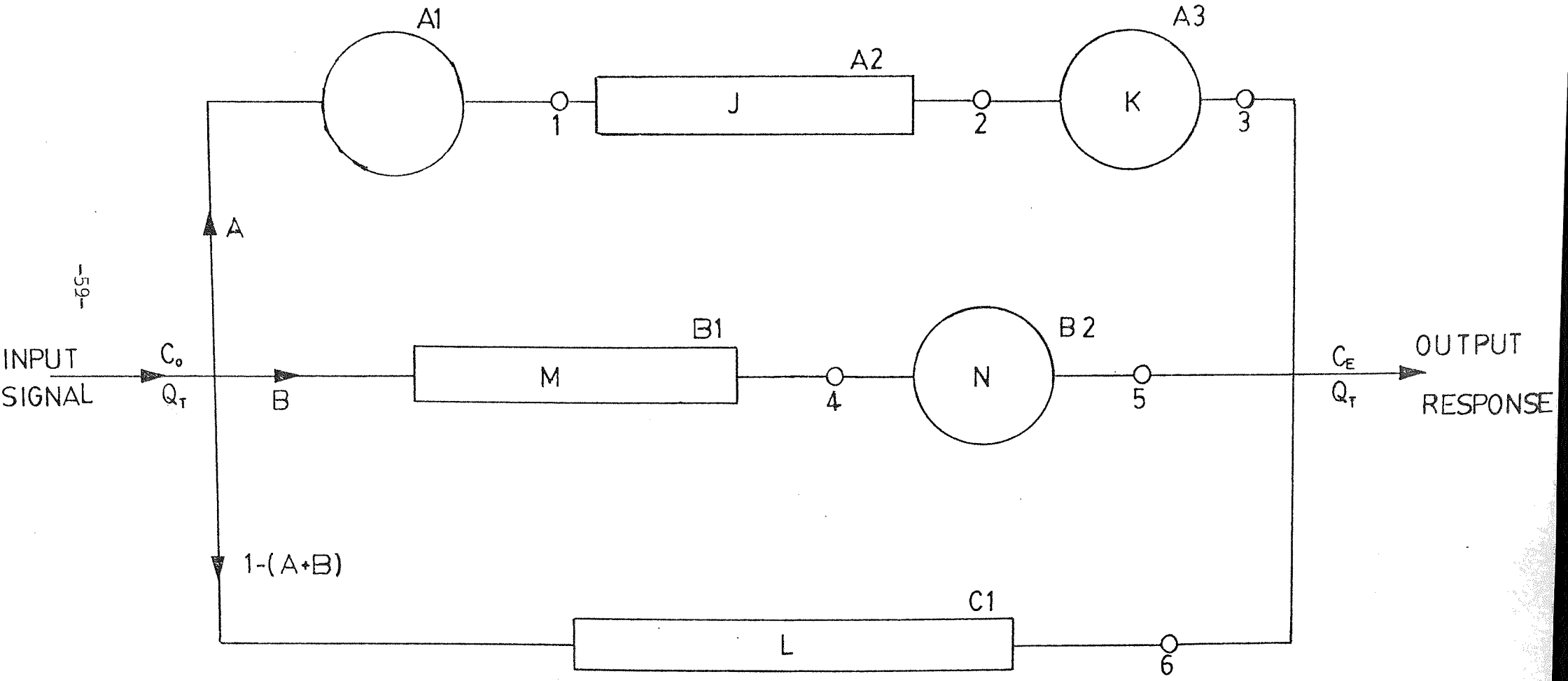

FIGURE 34 - GENERAL AIR FLOW PATTERN FOR SPRAY DRIER

where D_j is the delay time in zone A2. In terms of the system parameters:

$$D_j = V_2/Q_A \tag{3.41}$$

Substituting for Q_A from equation (3.34) and also for the zone fraction J. Then

$$D_j = \frac{J.V_T}{A.Q_T} \tag{3.42}$$

$$= \frac{\bar{t}.J}{A} \tag{3.43}$$

Substituting for D_j in equation (3.40)

$$R_j = \theta - \frac{\bar{t}.J}{A} \tag{3.44}$$

At (3) A well stirred tank zone A3

Following a similar procedure to that of zone A1, yields:

$$\frac{dC}{d\theta} \cdot \frac{1}{\Delta C} = \frac{A}{\bar{t}K} \tag{3.45}$$

At (4) Delay zone B1

The response R_M from this zone is also:

$$R_M = \theta - \frac{\bar{t}M}{B} \tag{3.46}$$

where M is the zone fraction and B is the fraction of tracer diverted through the second breach in the residence time distribution model.

At (5) A well stirred tank zone B2

The zone response can be similarly represented by the following differential equation.

$$\frac{dC}{d\theta} \cdot \frac{1}{\Delta C} = \frac{B}{\bar{t}N} \qquad (3.47)$$

where N is zone fraction by volume.

At (6) A delay zone C1

The response at this zone to a fraction (1-A-B) of tracer input is:

$$R_L = \theta - \frac{\bar{t}.L}{(1-A-B)} \qquad (3.48)$$

The overall exit response C_E to a rectangular tracer input would then be the summation of the final response output from each branch of the distribution model. Solving this set of equations yields the system parameters A, B, J, K, L, M, N and thus predict the overall volume of the reactor.

CHAPTER FOUR

EXPERIMENTAL PROCEDURE, EQUIPMENT

LAYOUT AND MEASUREMENTS

EXPERIMENTAL APPARATUS AND EXPERIMENTAL PROCEDURES

4.1 SINGLE DROP EXPERIMENTAL APPARATUS

4.1.1 Overall Experimental System

The experimental apparatus for single drop experiments is presented by Plate 4.1 and shown diagramatically on Figure 4.1. Essentially it consists of an air receiver, a Birlec air drier, a rotameter metric type 18A, a temperature recorder, a wind tunnel, two sample pumps, a T-piece of brass material, drop suspension device, Shaw Hygrometry unit and the heating elements within the wind tunnel.

Compressed air at about 100 psi was passed into the air receiver from the laboratory mains supply. It was then reduced in pressure and passed into the system via the Birlec air drier; this contained a fixed bed of molecular sieve dessicant. Two pressure regulators were installed; one upstream and the other downstream of the air receiver to dampen any fluctuations in the mains pressure. The air flowrate was monitored, at the inlet to the wind tunnel, by a metric type 18A rotameter, and controlled by a 2.54 cm globe valve connected to the drier outlet.

The wind tunnel was 1.83 m in overall length, and consisted of a Secomark Industrial Heater model 571/3 and a calming section followed by the test section and exit pipe. The heater was cylindrical in shape and the end nearest to the rotameter was 7.62 cm O.D. and flanged. The overall

PLATE 4.1 SINGLE DROP EXPERIMENTAL APPARATUS

FIGURE 4.1 FLOW DIAGRAM – SINGLE DROP EXPERIMENTAL APPARATUS

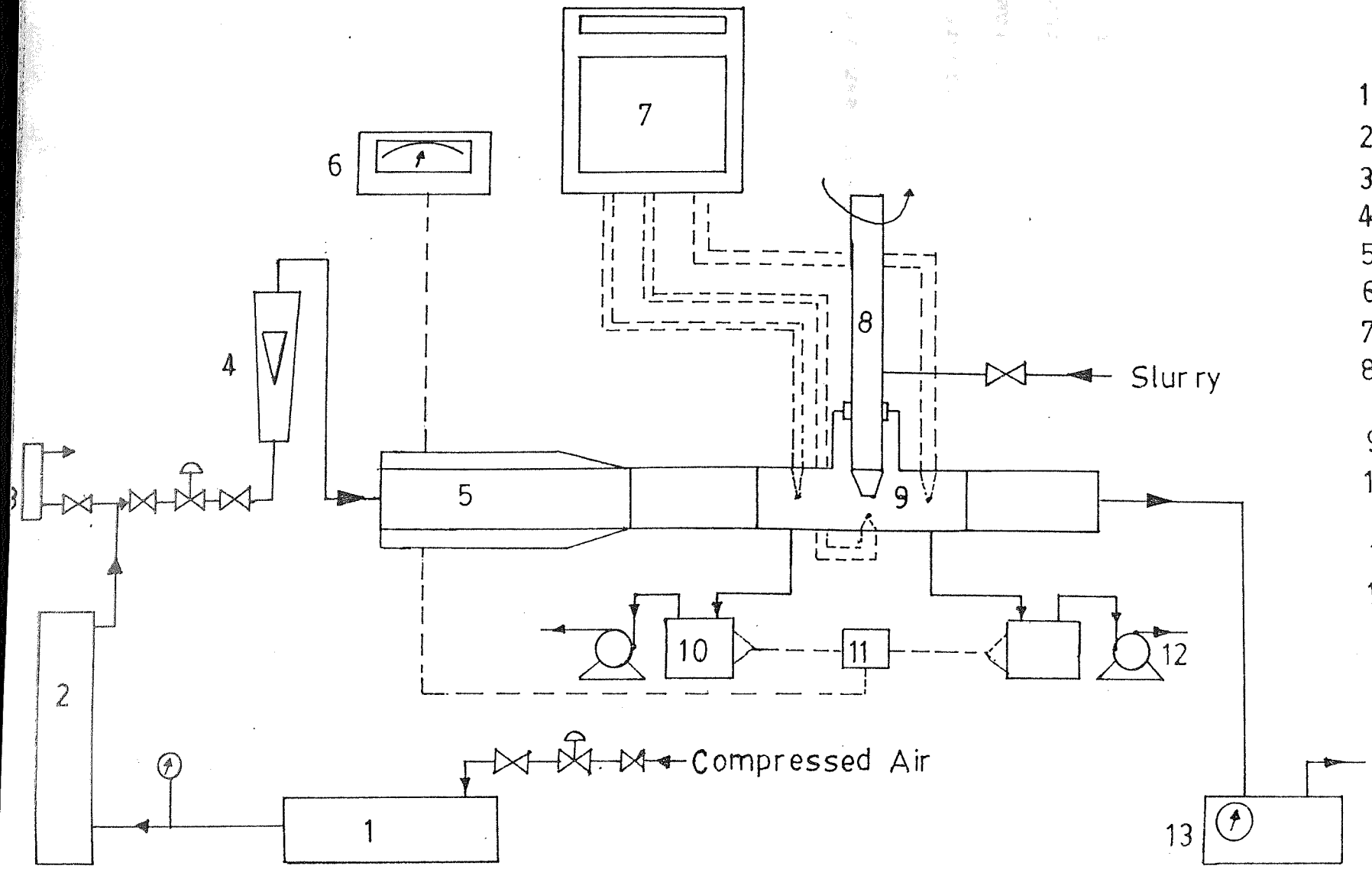

KEY:

1 Air Receiver
2 Birlec Air Drier
3 Purgerator
4 Rotameter Type 18A
5 Air Heater
6 Hygrometer
7 Temperature Recorde
8 Drop–Suspension Device
9 Brass T – piece
10 Constant Temperatur Unit
11 Dipole Valve
12 Sample Pump
13 Pressure Gauge

length of the heater was 0.28m and the cylindrical outlet tapered to a nozzle 3.18 cm O.D. The nozzle end was flanged and connected to a 2.54 cm square mild steel duct which included the test section and the remaining part of the wind tunnel. The industrial heater was capable of delivering up to 3 kW of heat and can be supplied with either A.C. or D.C. 200/220 volts electricity. The heater was controlled by two 6A, 90Ω Cressal Trovolt resistors and it was able to raise the air temperature upto 900°C. The whole wind tunnel was well lagged with a thick swath of fibre glass insulator.

The test section of the system was constructed of a T-piece of brass, and the upstream and downstream air temperatures were measured by thermocouples. The essential details of the working section is presented in Figure 4.2. In order to be able to observe the drying of the drop by the hot air, an observation window was inserted into the brass working section. This consisted of two 5.08 cm × 3.81 cm rectangular holes made on opposite sides of the T-piece test section. These were covered by Vitreosil Transparent glazed plates of thickness 6 mm that could withstand temperatures up to 1000°C. The temperature in the working section was measured by the thermocouples and recorded on a 'Honeywell' automation chart strip temperature recorder capable of reading up to 1200°C. Another thermocouple was installed in such a way that it could measure directly the temperature of the drop

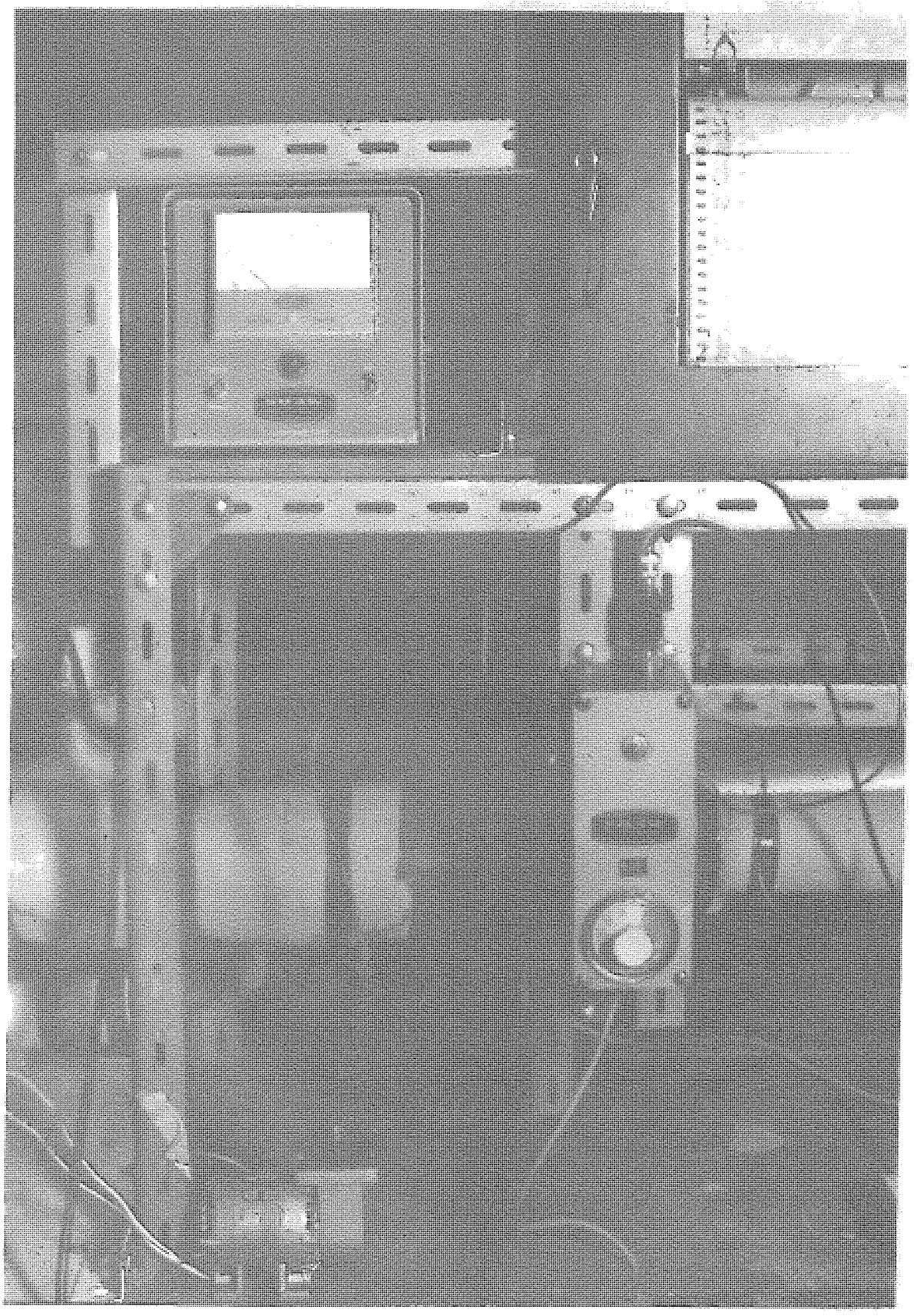

PLATE 4.3 THE HYGROMETRY UNIT

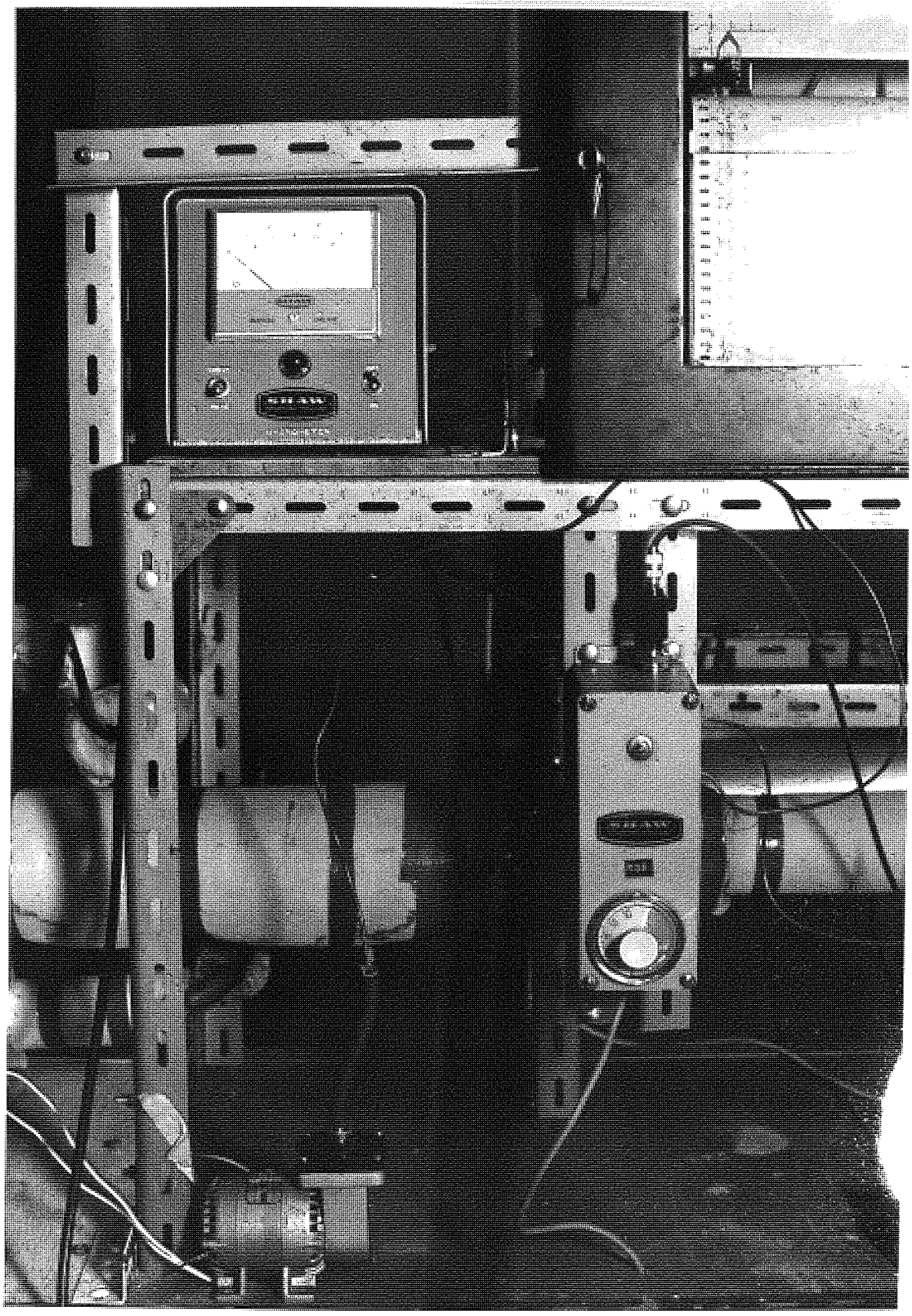

PLATE 4.3 THE HYGROMETRY UNIT

as drying proceeds. Air humidities both upstream and downstream of the drop were monitored by the Shaw Hydrometry Unit.

4.1.2 Drop Suspension Device

The drop suspension device shown in Plate 4.2 consisted of a stainless steel piston inside a 0.95 cm O.D. stainless steel tube. The piston traversed through the vertical shaft and the whole shaft assembly was rotated by a 50 Hz Parvalux electric motor with a maximum speed of 100 rpms. The speed was controlled with a 27 ohm, 10A Cressall Torovolt resistor wired into the armature of the motor. The top part of the stainless steel tube was threaded inside and thus connected to the moving shaft of the Parvalux motor. Halfway down the length of the tube, a brass tap of 0.965 cm diameter was fitted. The tube finally culminated in the brass working section where a stainless steel nozzle was fitted.

4.1.3 Hygrometry Equipment

The hygrometry Unit consisted of a dew point meter, two sensors, two constant temperature units, two sample pumps, three coaxial cables and a diploe valve. The essential components of the unit is shown in Plate 4.3.

The principle of operation of the sensing elements was based on the fact that the capacitance varies in direct proportion to dewpoint of the gas. The probe of

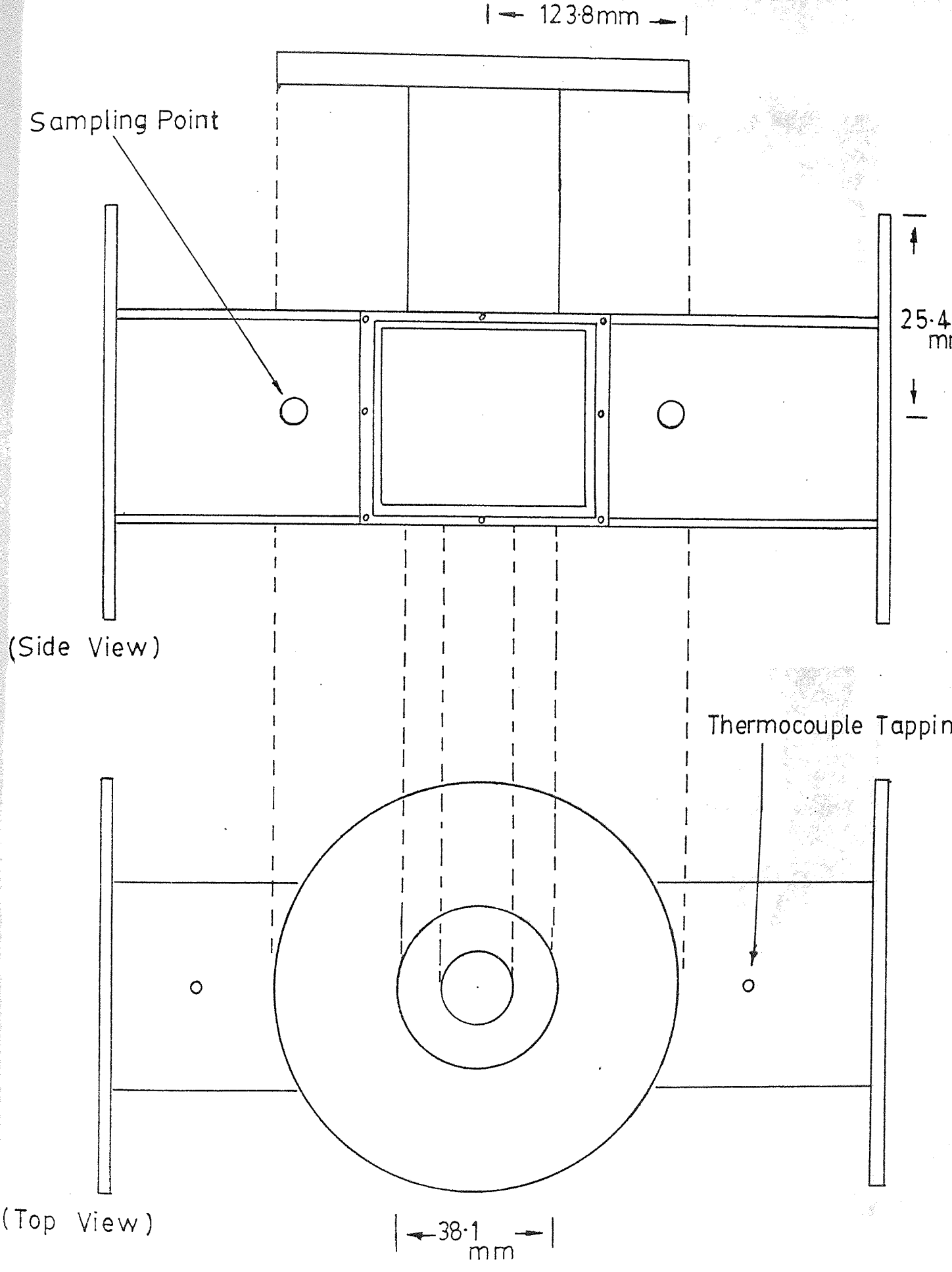

FIGURE 4.2 DRAWING OF WORKING SECTION

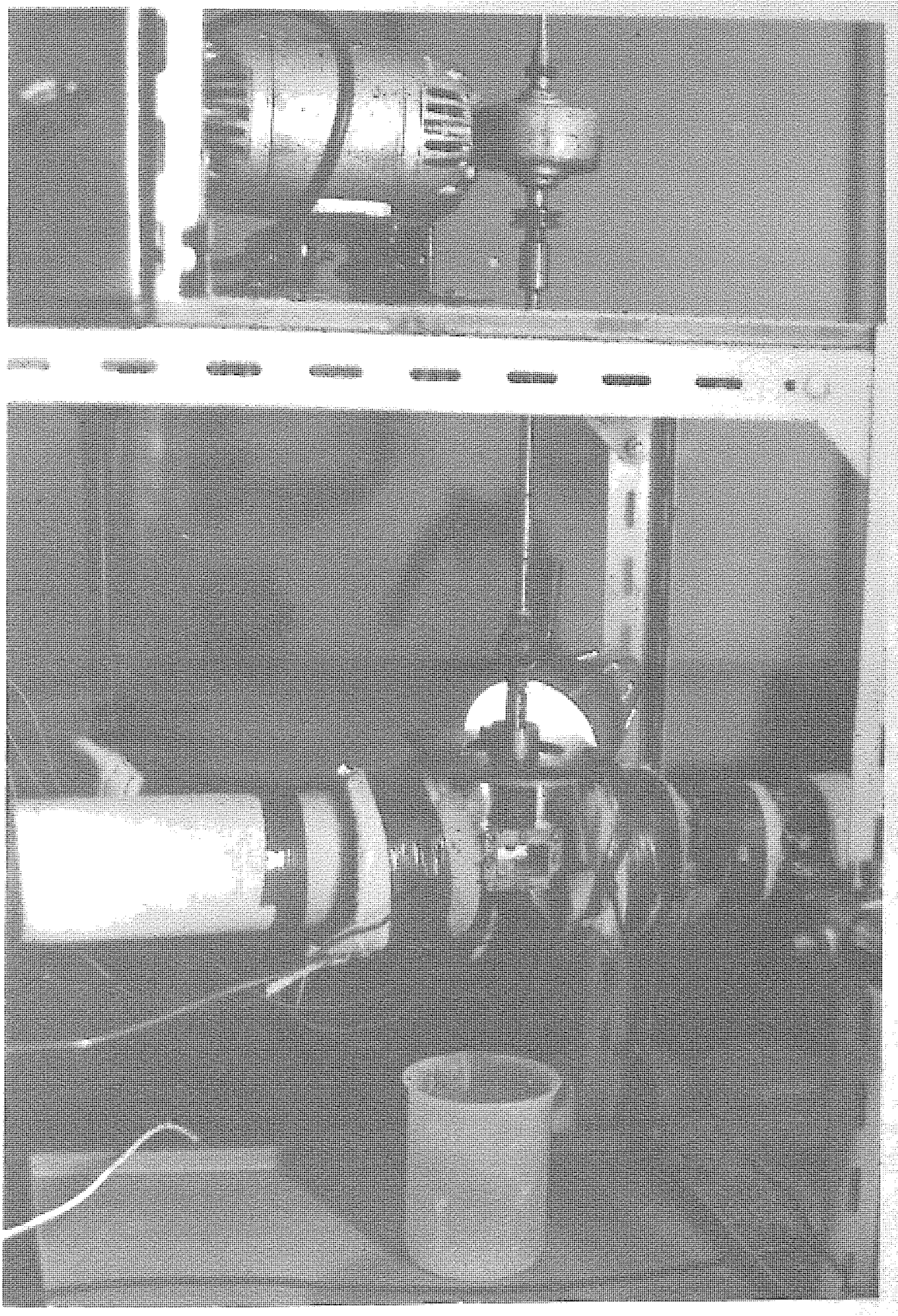

PLATE 4.2 THE DROP SUSPENSION DEVICE

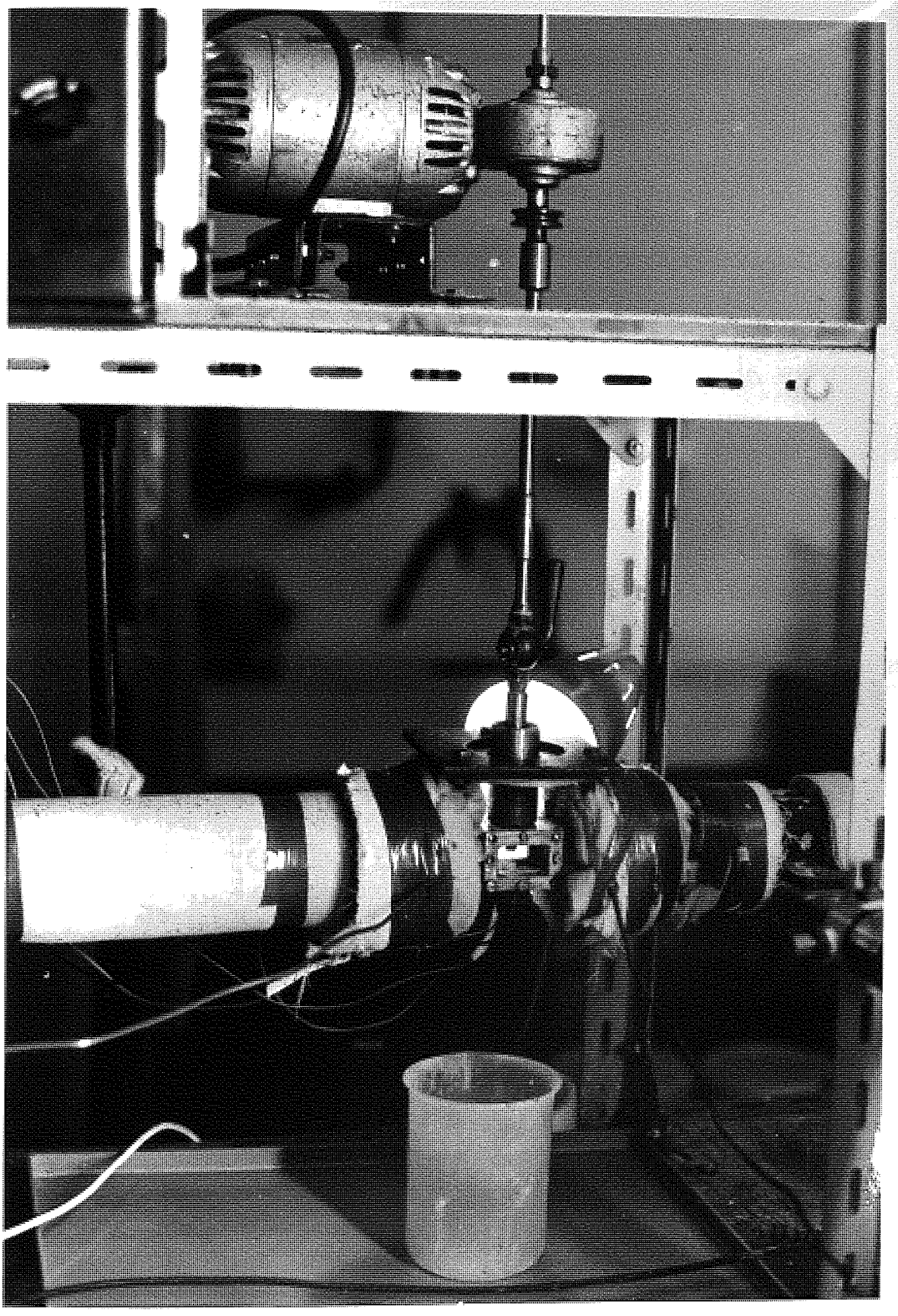

PLATE 4.2 THE DROP SUSPENSION DEVICE

the sensors was protected from dust and moisture by a sintered bronze filter. Once the air flows over this filter, a dynamic equilibrium is set up between water vapour pressure outside the layer and the condensed water absorbed in its fine pores. The sensor estimates the capacitance of the gas and transmits it, via coaxial cables, to the dewpoint meter. The latter is scaled to read dew points from $-80^{o}C$ to $-20^{o}C$. The Constant Temperature Unit, as its name implies maintains a constant temperature of gas flowing to the sensing elements. It also prevents condensation of the flowing gas on to the sensing elements by maintaining the gas at a temperature above its dewpoint. The Unit consisted of a brass container into which the sensor was screwed. A dial switch mounted on the unit operates a sensitive thermostat which maintains a constant temperature indicated by the dial. The latter has a range of $0-110^{o}C$. The unit's heater was 30W rating and heats the sensor chamber which was constructed of heavy brass and chrome plated. The unit had both an inlet and outlet port each of 0.32 cm O.D. copper piping. A constant flow of gas through the unit was supplied by the sampling pump which delivered air at a rate of 0.5 dm^3/min.

4.1.4 The Thermal Conductivity Experimental Apparatus

The thermal conductivity experimental apparatus is a modified form of the Lee's disc apparatus and is shown in Plate 4.4 while a flow diagram is also shown in Figure 4.3. Essentially, it consists of two metallic discs, an asbestos

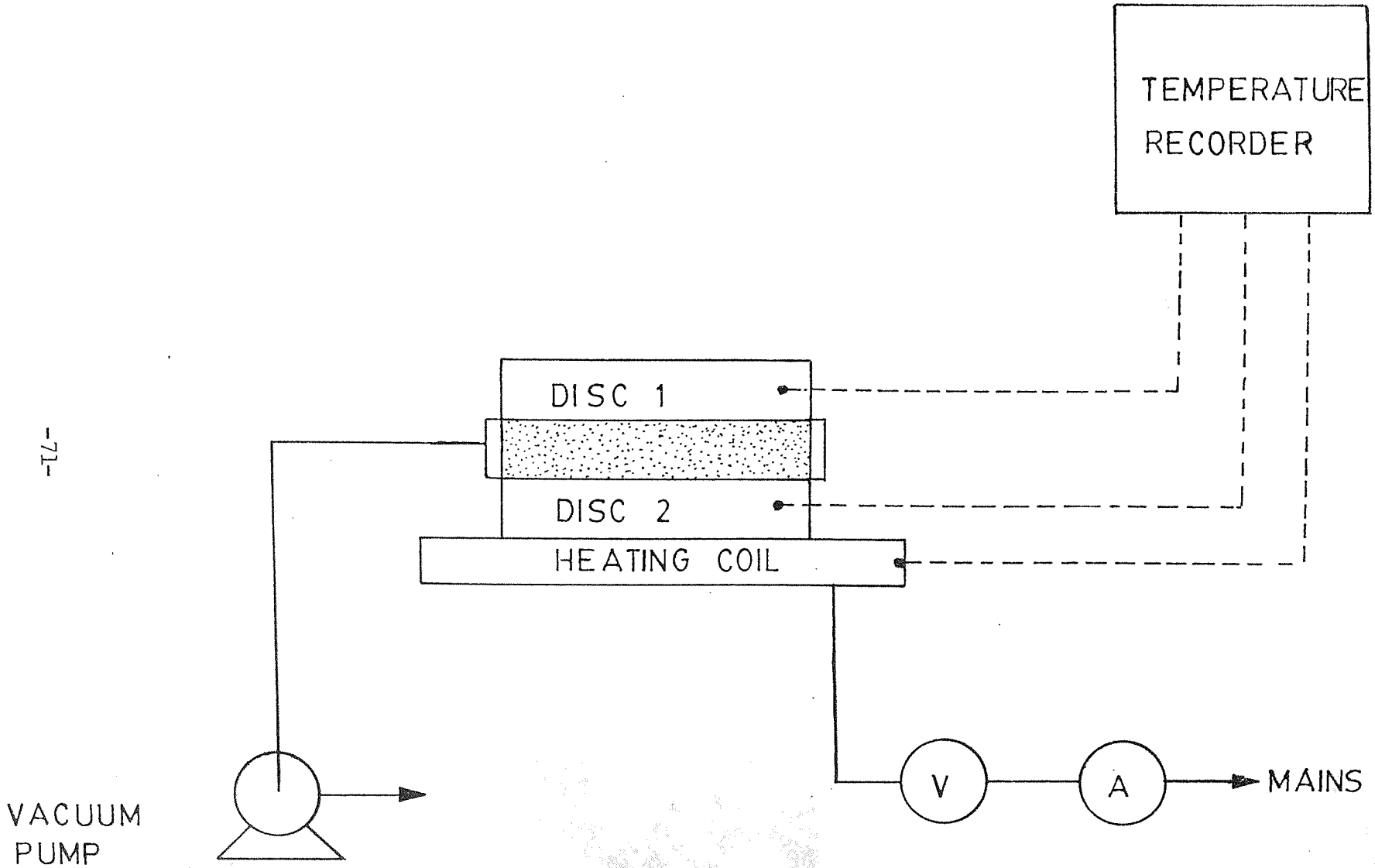

FIGURE 4.3 THE THERMAL CONDUCTIVITY EXPERIMENTAL APPARATUS

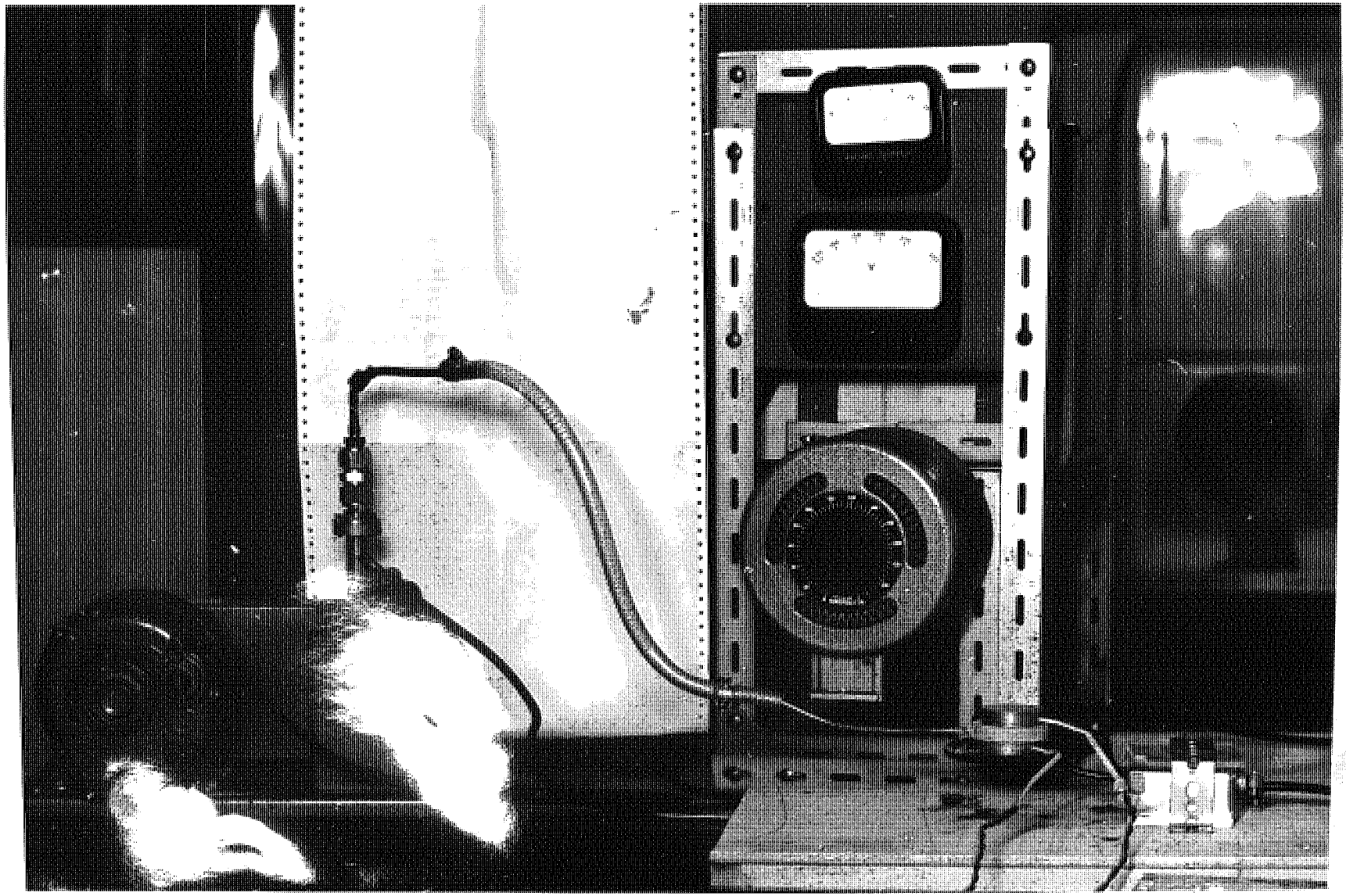

PLATE 4.4 MODIFIED LEE'S DISC APPARATUS

ring, a high vacuum pump, an A.C. voltmeter, an A.C. ampere meter, a multiple point temperature recorder, and a radiant heat ring.

The metal discs were both the same size of diameter 5.06×10^{-2}m, and of thickness 1.26×10^{-2}m. The asbestos ring was 5.06×10^{-2}m I.D. and 6.32×10^{-2}m O.D. Along the side of the ring was bored a hole 1.00×10^{-2}m diameter, into which a copper tube 0.64 cm O.D. was inserted and secured by high temperature cement putty. The copper tube was connected to a 0.64 cm I.D. reinforced P.V.C. tube then connected to the inlet port of a 'Speedivac' high vacuum pump of ¼ H.P. The asbestos ring was secured between the two discs and the whole assembly rested on an electric heating coil controlled by a 10A, 240 volts Cressal Torovolt resistor with a range of 0 to 270 volts. The current flowing through the system was monitored by an A.C. meter with a range of 0.0 to 2.5A and the voltage was measured by an A.C. voltmeter with a full scale of 0 to 300 volts. The temperatures of the hot ring and the discs were monitored by thermocouples specially insulated with fibreglass and were connected to a 'Honeywell' multiple temperature recorder.

4.1.5 Ancillary Equipment

The Stereoscan

The stereoscan microscope is essentially a scanning electron microscope which produces three dimensional photographs of the specimen under observation. The specimen

is scanned by a fine electron beam synchronised with the electron beam of a cathode ray tube. This electron microscope has a wide magnification range from 15 to about 100,000 diameters but over a mangification range of 200,000, the image transmitted becomes rather blurred. This breadth of magnification, together with the ease of zooming in on any point on the specimen for further observation and magnification renders the stereoscan a very powerful instrument for this project. It was used to study the structures of the crusts of the drops of dried slurry.

4.2 SPRAY DRYING EXPERIMENTAL SYSTEM

4.2.1 Overall Spray Drying System

The diagram of the experimental spray drier is shown in Figure 4.4. Atmospheric air was fed into the system via a 10.16 cm diameter mild steel piping by a 20 HP, 3 phase Parkinson fan. The rate of air flow was controlled by the 10.16 cm diameter Audio slim seal valve, and any excess air was vented through a purgerator. The air flowrate was measured on line by a 10.16 cm Dall tube of bore throat 4.64 cm, after which the air flows through two model 15/2 Secomak Industrial Heaters. The heaters were mounted in series and were capable of generating up to 36 kW of heat. Each heater was 0.47 m in length and flanged at each end. The heaters were able to raise the temperature of the air feed to a maximum of 300^{o}C.

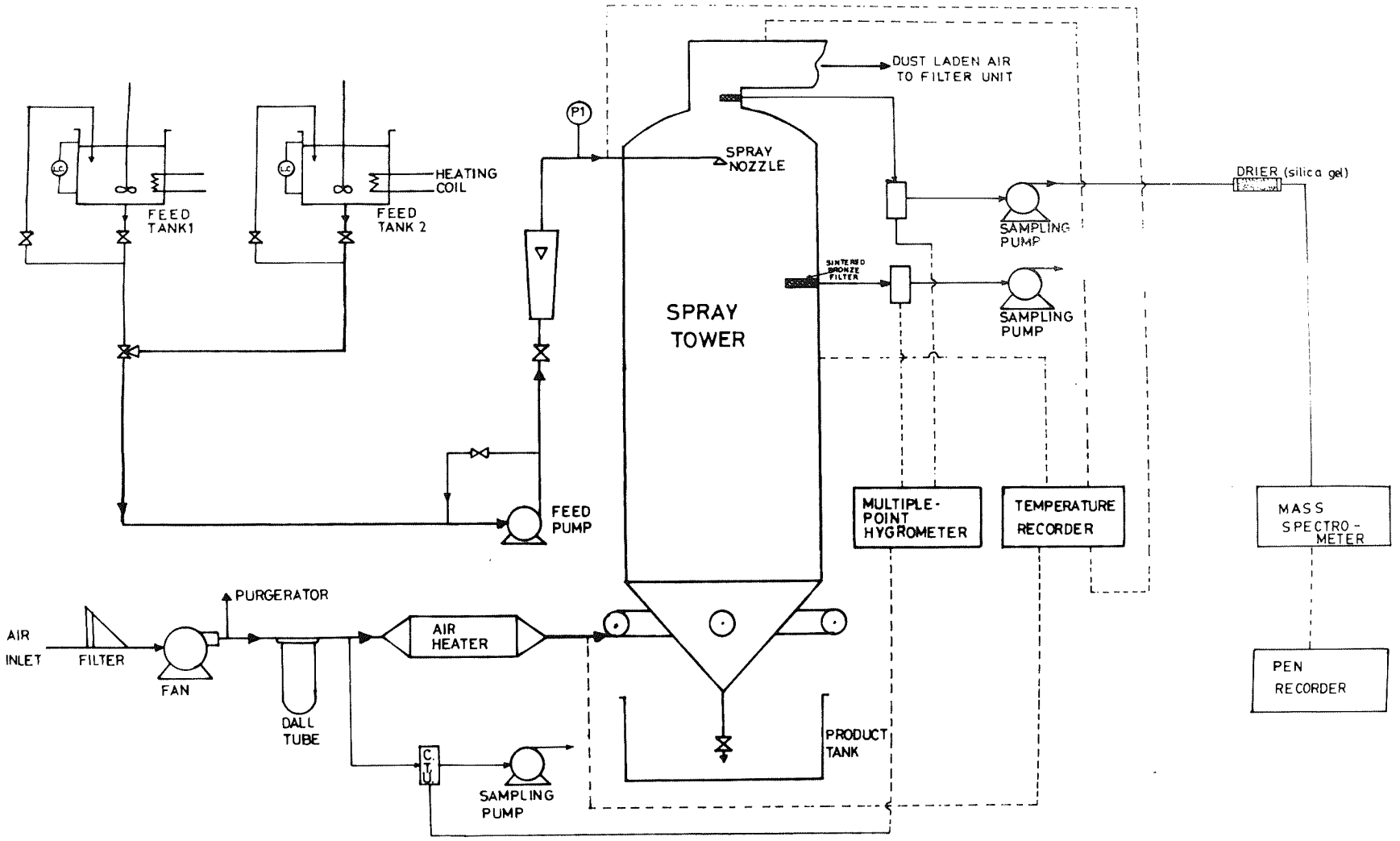

FIGURE 4.4 OVERALL FLOW DIAGRAM OF SPRAY DRYING EXPERIMENTAL APPARATUS

The slurry feed system consisted of two 60.96 cm × 60.96 cm × 91.44 cm stainless steel tanks, each fitted with a stirrer, a heater and an Ether temperature controller. The feed entered the system through 3.81 cm diameter Q.V.F. piping by a 3 phase, Hoover gear pump. The slurry feed flow was controlled by a Q.V.F. needle valve which was connected to a metric type 14F rotameter. The stirrers in the feed tanks kept the slurry in suspension while the Ether temperature controllers maintained the slurry feed at a constant temperature.

The spray in the drying tower was produced by a Delavan Hollow cone nozzle, type SDX-32936/11. It comprised a 303 stainless steel body, stem adaptor, a ceramic swirl chamber and an O-ring seal. The swirl chamber minimised plugging, thus providing a uniform sized distribution of drops. The orifice disc, made of tungsten cabride, was recessed to prevent damage and a stainless steel adaptor was fitted with a 0.64 cm B.S.P. female thread to fit on to a male 0.64 cm B.S.P. steel adaptor for the feed line.

The temperatures of the inlet and outlet air, and the slurry feed were monitored by thermocouples connected to a George Kent temperature recorder. The moisture content of the inlet air, exhaust dust laden air and the air within the spray tower was measured with three Shaw Hygrometry Uits of the type described in Section 4.1.3.

The spray tower itself, 2.43m × 1.21 m diameter, was

made of stainless steel and was completely lagged with a thick layer of fibre glass insulator. A 7.62 cm I.D. ring main was installed in the conical base of the tower at a position 0.61 m from the top of the conical section. The hot drying air passed through this main into four entry ports, each equally spaced around the tower base. This ensured a uniform distribution of the air in the tower.

The Hygrometry Unit was adapted for the tracer experiments in the exit duct of the spray drier, and through this duct was screwed a 30.48cm × 1.27 cm diameter mild steel pipe. At the near end of this pipe in the drier duct was welded a sintered bronze filter with a very fine mesh. The other end of the pipe was connected to a 1.27 cm O.D. copper tube attached to the Constant Temperature Unit and sampling pump. The sintered bronze filter removed the fine powder in the air stream. At the exit port of the sampling pump is connected a 0.965 cm I.D. P.V.C. tube. This led to a drier packing. The packing was a self-indicating silica gel which absorbed moisture from the air sample. When dry the gel is blue in colour, but as soon as it becomes saturated with water vapour, the gel becomes pink. This helped to maintain a constantly dry air sample through the R.T.D. pipeline. The outlet end of the drier packing was fixed to a 0.965 cm I.D. P.V.C. tube of about 4 m in length to the floor level where a hypodermic needle was inserted to the tube wall in order to sample the air stream. This needle was situated at the other end of the

5.08×10^{-2} cm I.D. inlet tube to the MGA 200 Mass Spectrometer. A Pen Recorder attached to the Mass Spectrometer provided a continuous printout of the tracer concentration profile in the air sample.

4.2.2 Ancillary Equipment: The MGA 200 Mass Spectrometer

An MGA 200 Mass Spectrometer was used to analyse the exit air stream after a shot of tracer had been introduced into the spray drying system. Figure 4.5 shows the essential features of the Spectrometer. Essentially it segregates charged gas molecules according to their masses and therefore the air sample containing traces of argon was analysed to give a continuous display of the argon fraction in the stream. A Quadruple analyser was utilised to control and resolve the ions of the charged sample gas according to their m/e ratio, i.e. mass to charge ratio.

It was essential that the ions or charged sample gas molecules have unimpeded progress through the analyser unit thus necessitating a vacuum environment in the latter. Thus, in-built in the Analyser Unit of the 200 MGA, is a mechanical rotary pump which can produce a vacuum of 10^{-3} torr (760 torr = 1 atmosphere). For satisfactory operation a residual vacuum of 10^{-7} torr is needed. The Analyser requires a high vacuum environment for operation, but the sampling gas inlets at atmospheric pressure. In order to overcome this pressure difference and preserve the composition of the sample, an Inlet System was incorporated

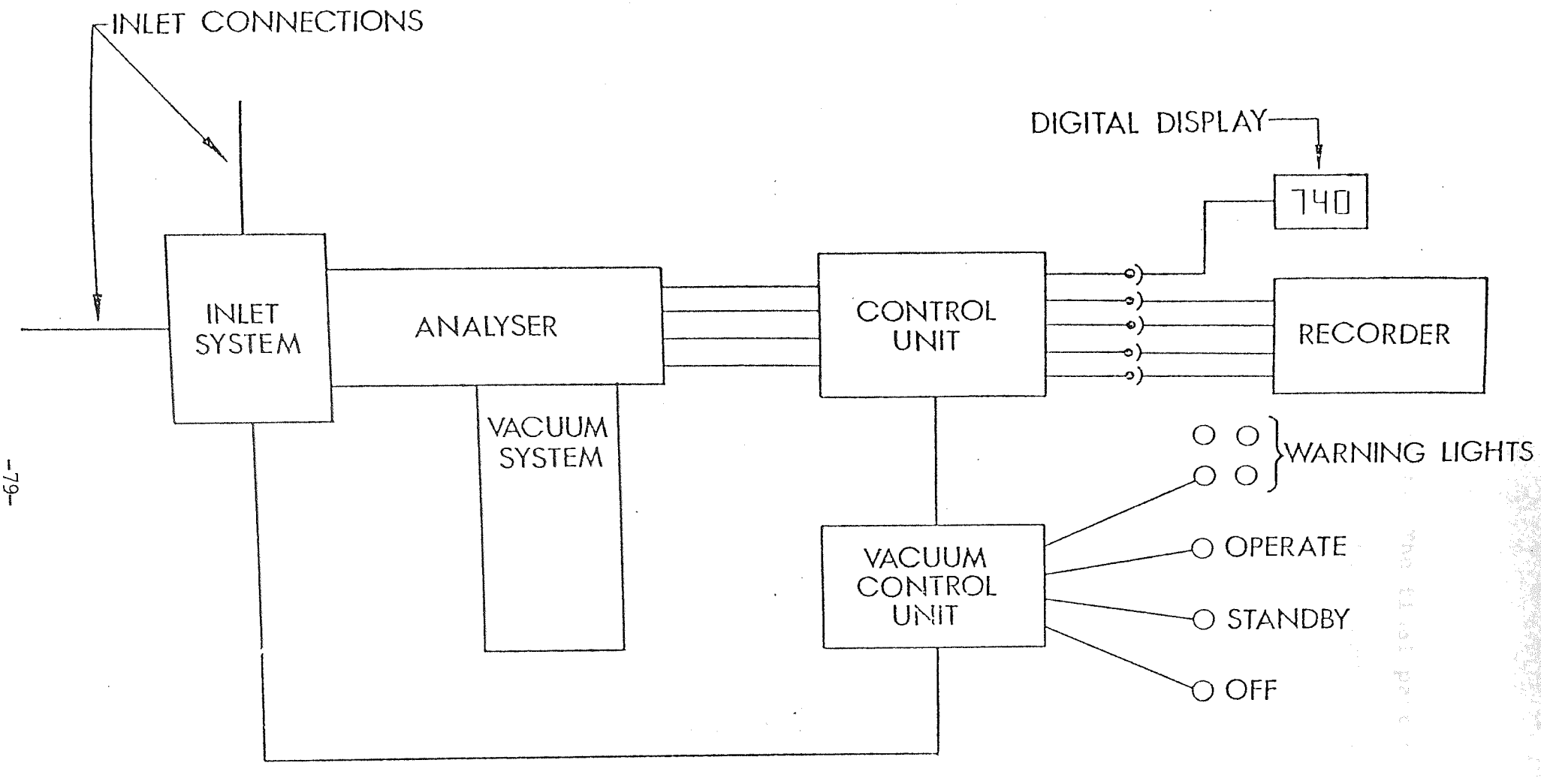

FIGURE 4.5 THE MGA 200 MASS SPECTROMETER SYSTEM

into the mass spectrometer. The final part of the whole mass spectrometer system was the Vacuum Control Unit that controls the overall operational status of the spectrometer, and this includes warning lights, On/Off lights etc.

4.3 CALIBRATION OF MEASURING INSTRUMENTS

4.3.1 Single Drop Experiments

For the Single Drop Experiments, the following instruments were calibrated.

4.3.1.1 The Rotameter

The flowrate of air through the wind tunnel was measured by a Metric type 18A rotameter with a Duralumin float. The quantity of air passing through the system over a specific time interval was measured with the aid of a Parkinson Gas meter placed in the outlet stream of the wind tunnel. This was noted against the float position on the rotameter. Also noted was the temperature of the air. This procedure was repeated over many float positions in the rotameter, and the volume readings were corrected for the effect of temperature. These experimental results of the float position volumetric flowrate was compared with the calculated volume.(90)

4.3.1.2 Hygrometry Equipment

Each sensor supplied by Shaw Limit was delivered with its own calibration graph in which the calibration had been

FIGURE 4.6

A TYPICAL SHAW HYGROMETER CALIBRATION CURVE

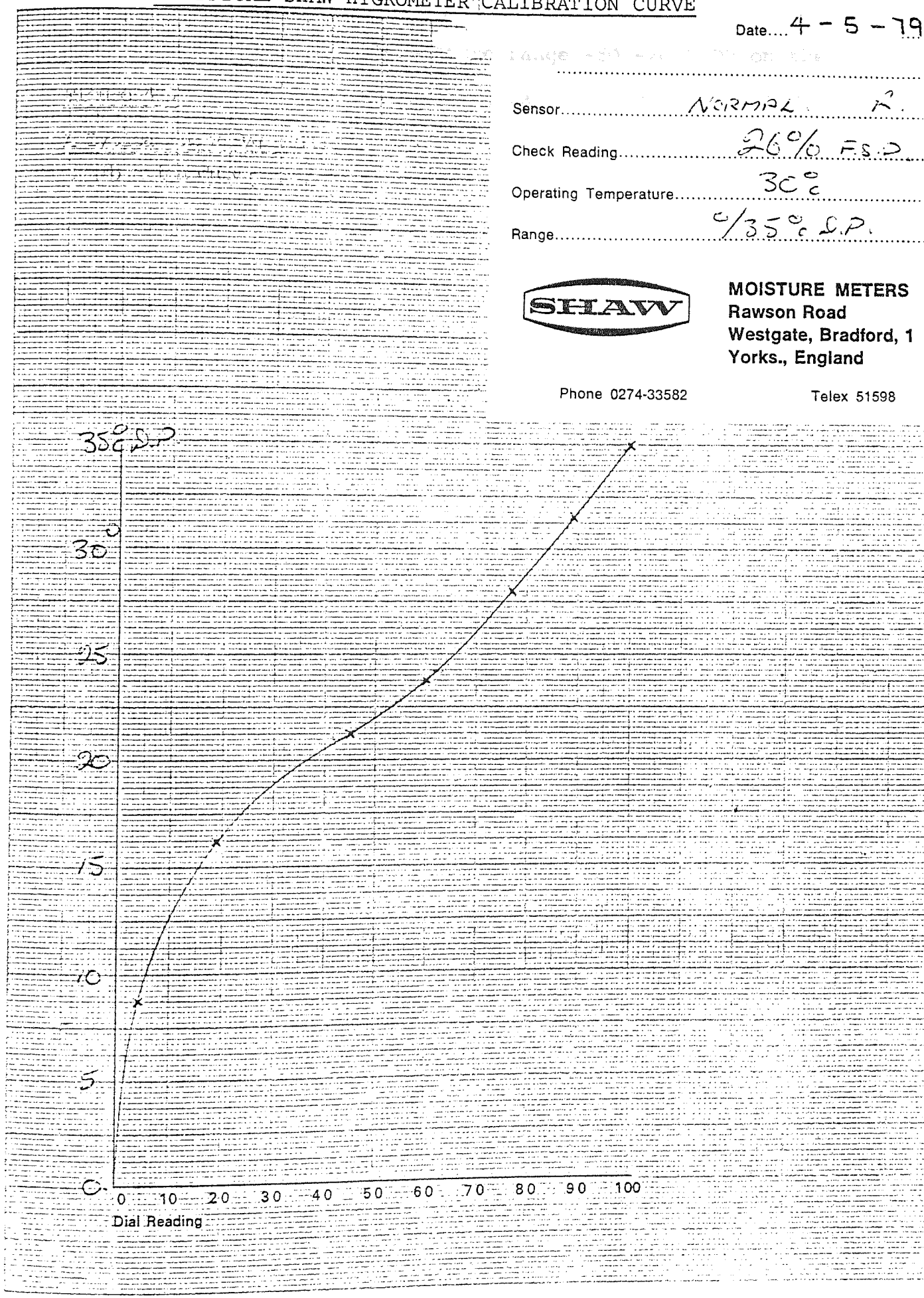

carried out over the temperature range -80/-20°C DP on the moisture meter. The calibration was checked by exposing the sensor to ambient conditions in the laboratory for about five minutes and the value registered on the meter was noted and the Relative Humidity was read from a calibration curve supplied. This was compared to the Relative Humidity of the room evaluated from measurements by a sling hygrometer. They always compared favourably. Similar calibrations were carried out on the air flowing through the wind tunnel. Figure 4.6 gives a typical calibration curve for the Hygrometry Equipments.

4.3.2 Spray Drying Experiments

The following instruments were calibrated for the Spray Drying Experiments.

4.3.2.1 The Dall Tube

The air flowrate was measured by a 10.16 cm Dall tube meter with a throat bore of 4.64 cm. The pressure drop across the meter was measured by a mercury manometer connected to the tapping upstream and downstream. The manometer readings for different positions on the air inlet fan were recorded and the mass flowrate was evaluated and a plot of the flowrate versus pressure drops was then made[90].

4.3.2.2 The Hygrometry Equipment

The Hygrometry Units were calibrated in a similar manner

as that described for the single drop experiments in Section 4.3.1.2 . Only in this case the meter reading range was from 0-100% Relative Humidity. Then the Relative Humidity of the system could be read off directly from the calibration graph.

4.3.2.3 The Mass Spectrometer

The Mass Spectrometer was calibrated for the detection of argon in samples of gas which was arranged to read the minimum and maximum levels possible in a gas sample. The Mass Spectrometer was set to detect the mass number of argon in a gas sample and the inlet pipeline to the instrument was exposed to the laboratory air sucked into the specrometer. Since air contains about 1.1% by weight of argon, a trace of this amount is mapped out on the pen recorder attached to the spectrometer.

The upper extreme was obtained by filling a balloon with 100% pure argon, and inserting this onto the inlet pipeline of the mass spectrometer. The two extremes on the chart were then recorded on the instrument which was then marked off for different discrete percentage level of argon in any sample of gas.

4.4 EXPERIMENTAL PROCEDURES AND MEASUREMENTS

The first part of the project involved the investigation of the drying characterisatics of various portland cement slurries which included slurries from the following Blue

Circle Works:-

i) Northfleet

ii) Humber

iii) Westbury

iv) Shoreham

v) Mason.

The second part of the experimental work was the study of the flow characteristics in the laboratory spray drier and a large scale unit in the Humber Works of the Portland Cement Company Limited.

4.4.1 Single Drop Experiments

The following moisture contents of the slurries were investigated: 30%, 35%, 45%, 50% and 55% and these were prepared from the samples supplied by Blue Circle Limited. Compressed air was passed through the wind tunnel and its flowrate adjusted to 1.0×10^{-3} kg/S. After steady state had been achieved, the Hygrometer Unit, and the Heater in the wind tunnel were switched on and the temperatures of the upstream and downstream portions of the working section were monitored on the temperature recorder. The initial upstream and downstream humidities of the air were recorded and when all readings had remained steady for 15 minutes the prepared slurry was charged into the drop suspension device, by removing the piston and introducing the slurry through the steel tube. The brass tap shown on Plate 4.2 opened and a drop was carefully suspended on the

nozzle in the T-piece working section. The diameter of the drop was measured by a cathetometer and then the drop was rotated at a rate of about 15 rpm. The whole drying process was observed through the observation window and the upstream and downstream humidities were recorded at 1 minute intervals. Experiments were performed at the following temperature range: 200°C, 300°C, 400°C, 500°C, 750°C and 900°C.

In the course of the experiments, it was noted that, as soon as a drop was introduced into the hot air stream at temperatures of above 500°C simply it exploded. Many attempts, to achieve a stable drop throughout the drying process under these conditions was abortive. As a result, the experimental programme was limited to a temperature range of 200°C, 300°C and 400°C. At the end of each run, the ensuing crust was removed, by a guillotine device[23,24], on to a filter paper to remove any excess moisture in the drop. The drops were then glued onto metallic studs with araldite and coated with a thin layer of carbon and gold palladium. This was necessary since the slurry drops could not conduct electricity and the coating maintains a constant electric potential over the surface of the crust. The coatings were of the order of 5×10^{-9} m thick.

In order to study the internal and external structure of the drop as a function of time, the above procedure was repeated at 2, 5, 10, 15, 20 and 30 minute drying periods. Each specimen collected was introduced into the chamber of

the stereoscan microscope for structural analysis and production of photo-micrographs.

The porosity of the drop was estimated from the photo-micrographs[23,24] and recorded.

4.4.2 Thermal Conductivity Experiment

A sample of slurry was filtered and dried to a cake in an oven at about 100°C and the ensuing cake was ground to a fine powder for the Thermal Conductivity Experiment. Enough powder was introduced in the ring sandwiched between the two metal discs. The whole set-up was placed on the heater ring as shown in Figure 4.3 and in Plate 4.4. The vacuum pump was switched on and the duration of the experiment. This evacuated all the air and water vapour released during the course of the experiment and ensured a uniform cake being heated by the high temperature disc. The thermocouple wires were introduced into the holes in the disc and also one was placed on the heater to monitor its temperature. After the pump had been running for about half an hour, the Torovolt resistor was switched on and the voltage and amp noted. The heating continued until the temperature readings of the discs and the heater became steady for about one hour. After this the ambient temperature was recorded and the experiment repeated for various voltmeter and ampmeter readings.

4.4.3 Spray Drier Experiments

The experimental work on the spray drier involved the

Residence Time Distribution experiments. Essentially it entailed the introduction of a shot of argon tracer into the feed system and thereafter monitoring this tracer in the outlet stream of the drier.

After steady state conditions had been attained during which the desired slurry feed and air flowrate, feed and air temperatures remained steady. The argon tracer was introduced at the air inlet.

Meanwhile, the MGA 200 mass spectrometer had been switched on, maintained at a 'standby' switch position and allowed to warm up for about thirty minutes. As soon as the tracer was introduced into the spray system, the mass spectrometer inlet pipeline was opened, and the sampling pump was switched on. Also the pen recorder was switched on, thus providing a continuous display of the tracer concentration profile in the form of narrow width histograms and the speed of the chart determined the time interval between each concentration peak. The air flowrate inlet and outlet temperatures, inlet and outlet humidities were continuously monitored during the course of the experiment, and this was by the method described in Section 4.1. The time interval during which the tracer was introduced into the spray system was recorded by stop clock. The experiment was continued until the concentration profile displayed by the pen recorder had decayed to a very low level. This did not take very long since the mass spectrometer has a very high sensitivity and it

registers trace levels of tracer in a gas sample. The amount of tracer introduced into the system was estimated by monitoring the tracer level in the inlet stream. Having obtained this profile, the volume of tracer input was then estimated by integrating the input residence time distribution curve (refer to Figure 3.3).

The experimental studies were initially carried out on water as slurry feed, and then eventually with cement raw material slurries provided from the Blue Circle Works.

4.5 HUMBER WORKS EXPERIMENTAL PROGRAMME

A series of tracer experiments identical to those described in Section 4.4.3 were undertaken at the Blue Circle Works at Humber in June 1979. The experiments involved the injection of a shot of Argon into the Spray Drying System and thereafter monitoring the outlet concentration profile with the mass spectrometer. Figure 4.7 presents a diagram of the Humber Works Spray Drying equipments. This drier was a counter-current 'squat' type and the hot air feed was the exhaust flue gas from one of the rotary kilns operated on the site. The hot gas exit from the spray drier emerged via two outlet ports into two cyclones mounted on two opposite sides of the spray drier. Excess dust was finally removed by passing the exhaust gas from the cyclones through an electrostatic precipitator.

All the experimental parameters were kept as constant

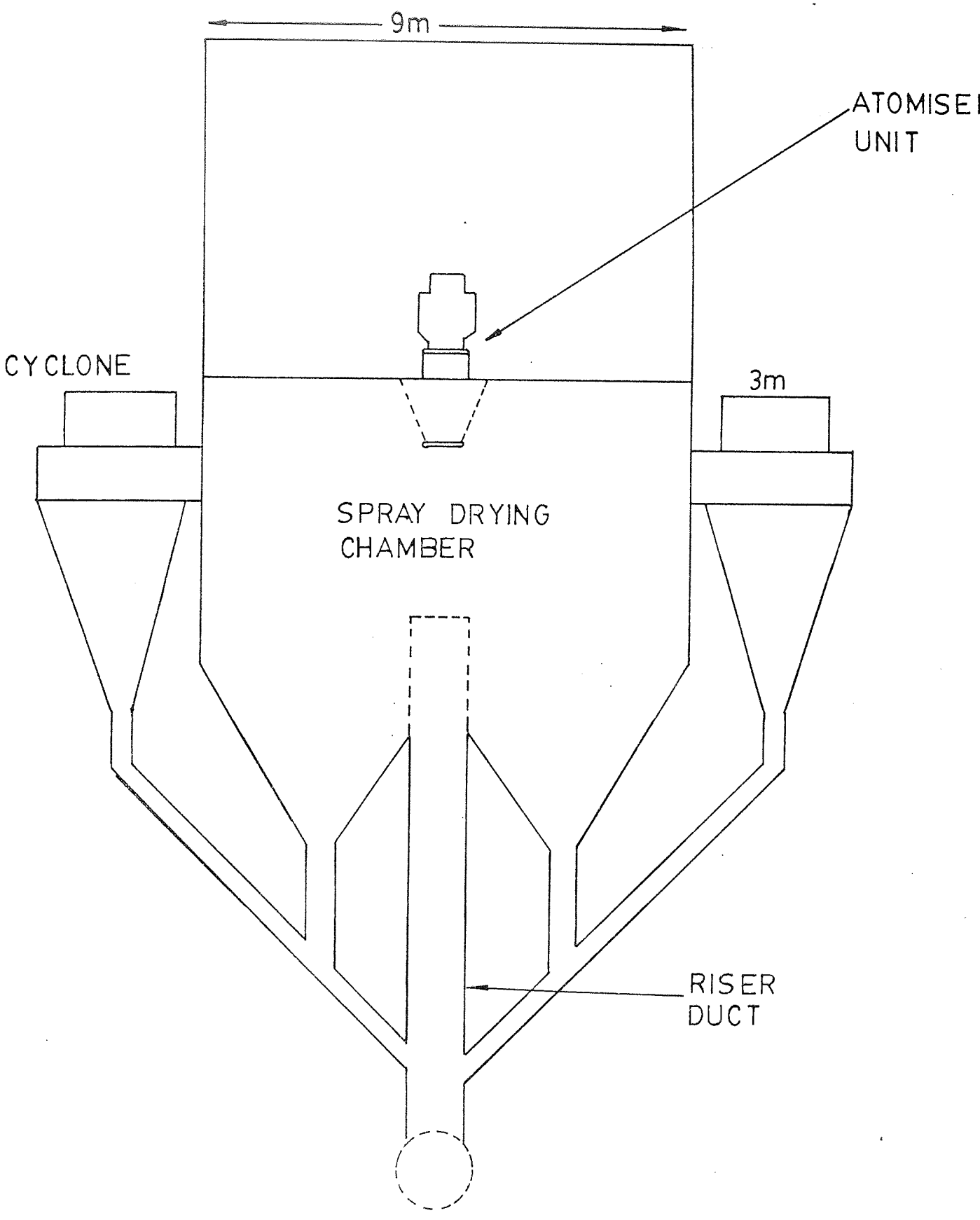

FIGURE 4.7 HUMBER SPRAY DRYING SYSTEM

as possible throughout the experimental programme and Plates 4.5 to 4.7 depict the salient features of this study. Typical tracer outlet concentration profile, as monitored by the mass-spectrometer, are shown on Plates 4.8 and 4.9 .

The experimental data for the programme are:

Spray Drier

Diameter of Spray Drier	8.6 m
Height of Cylindrical Section	4.6 m
Height of Conical Base	4.0 m
Diameter of Gas Riser	1.98 m
Diameter of Top of Conical Base	4.0 m
Drier Volume (V_T)	392.76 m^3
Evaporative Capacity of Drier	10.9 tonnes/hr.

Operating Parameters

Average Inlet Gas Temperature	650°C
Average Outlet Gas Temperature	158°C
Average Slurry Moisture Content	33.9%
Average Final Clinker Moisture Content	≃5.0%
Total Gas Flowrate (Q_T)	26.06×10^3 m^3/hr
Average Residence Time of Air in Spray Drier	54.26 sec
Clinker Flowrate	13.5 tonnes/hr
Waste Gas Flowrate	48.1 tonnes/hr

The waste gas is made up of:

CO_2 - 13.96 tonnes

SO_2 - 0.03 tonnes

N_2 - 20.06 tonnes

O_2 - 2.05 tonnes

H_2O - 12.01 tonnes

Also a typical analysis of a portland cement slurry yields [104]

SiO_2 - 13.19%

Al_2O_3 - 5.41%

Fe_2O_3 - 1.90% (about 5% at Humber)

CaO - 42.87%

MgO - 0.70%

SO_3 - 0.11%

CO_2 - 32.75%

Loss - 2.19%

K_2O - 0.57%

N_2O - 0.26%

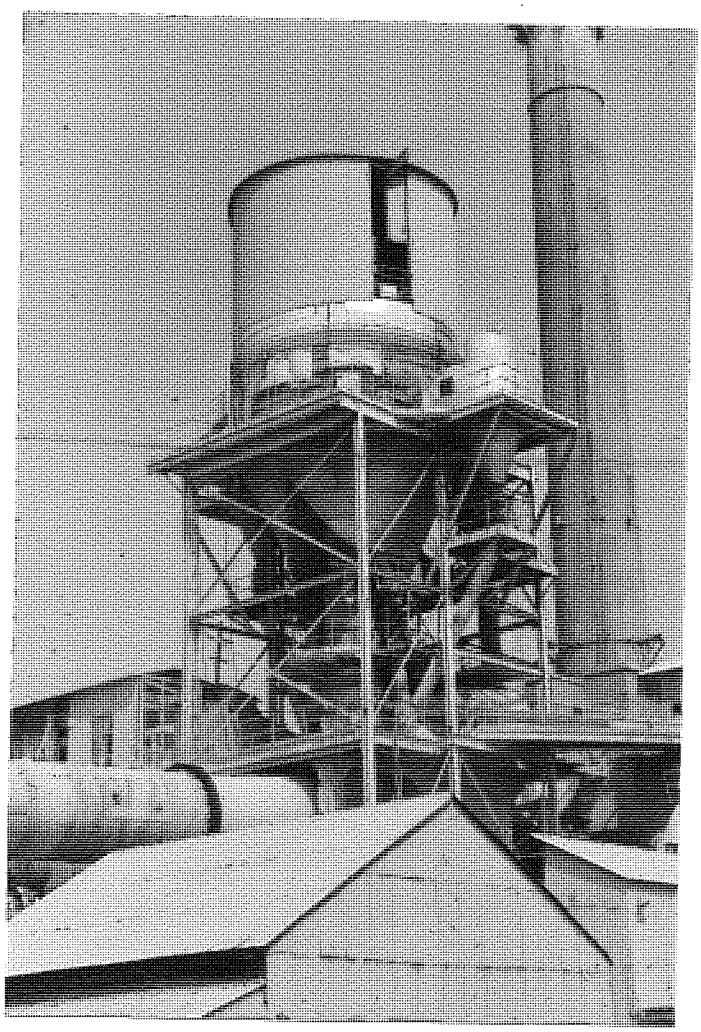

Plate 4.5 The Humber Works Spray Drier

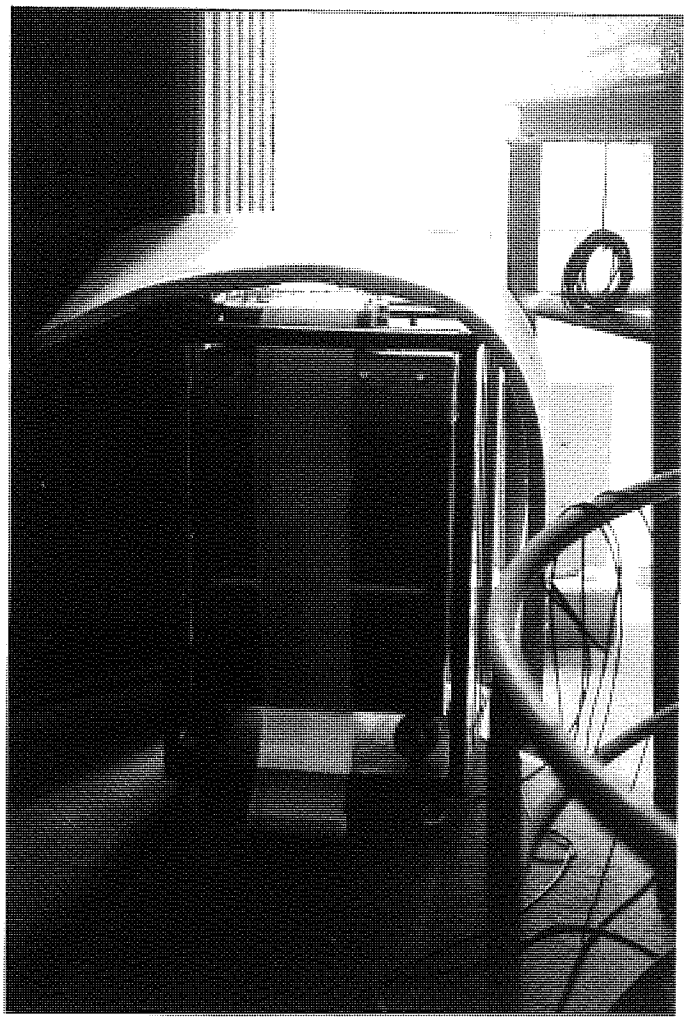

Plate 4.6 The MGA 200 Mass Spectrometer

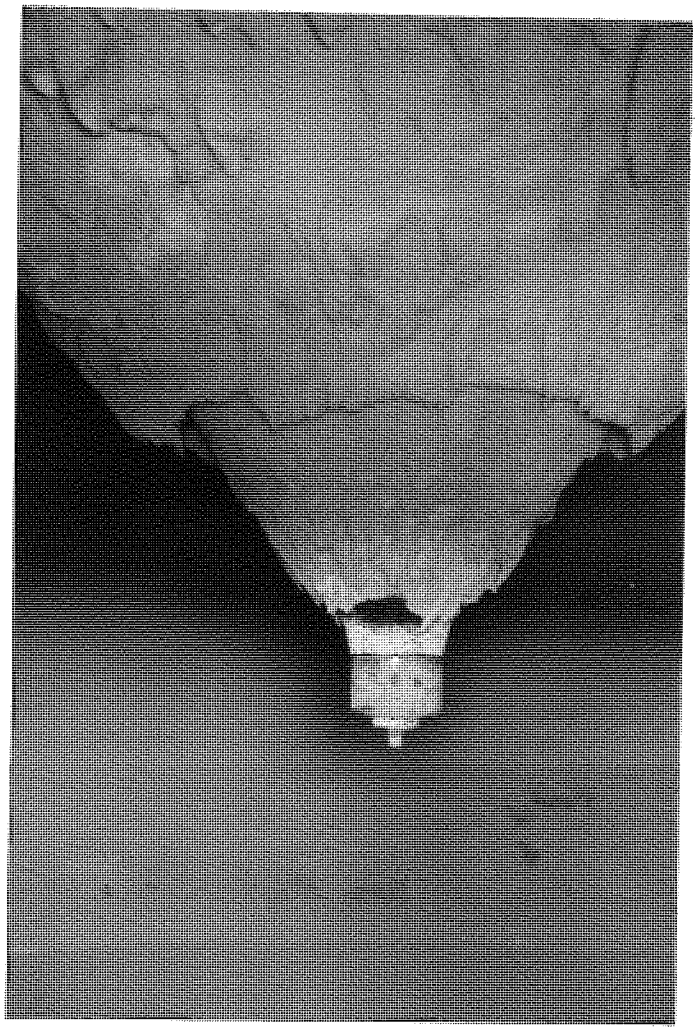

Plate 4.7 The Humber Spray Drier Atomiser.

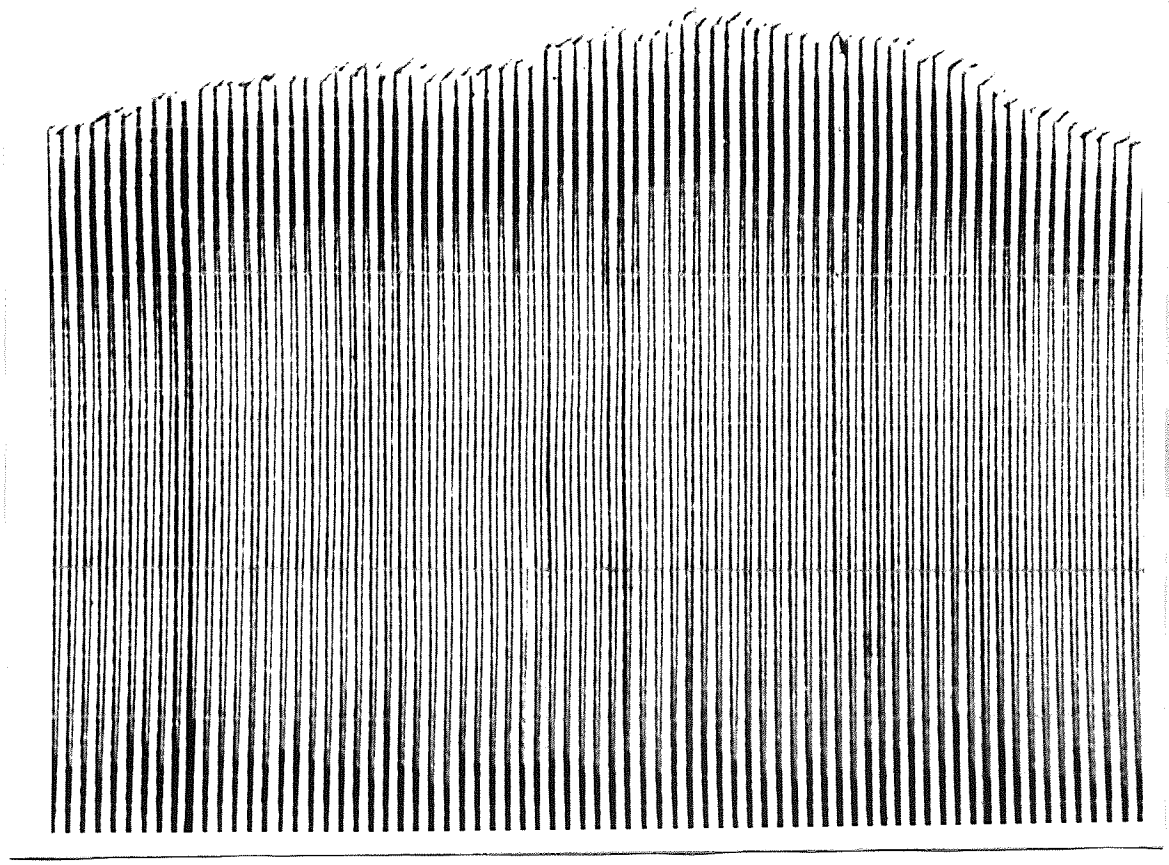

Plate 4.8 A typical Tracer Output Concentration Profile: Experiment No. H1.

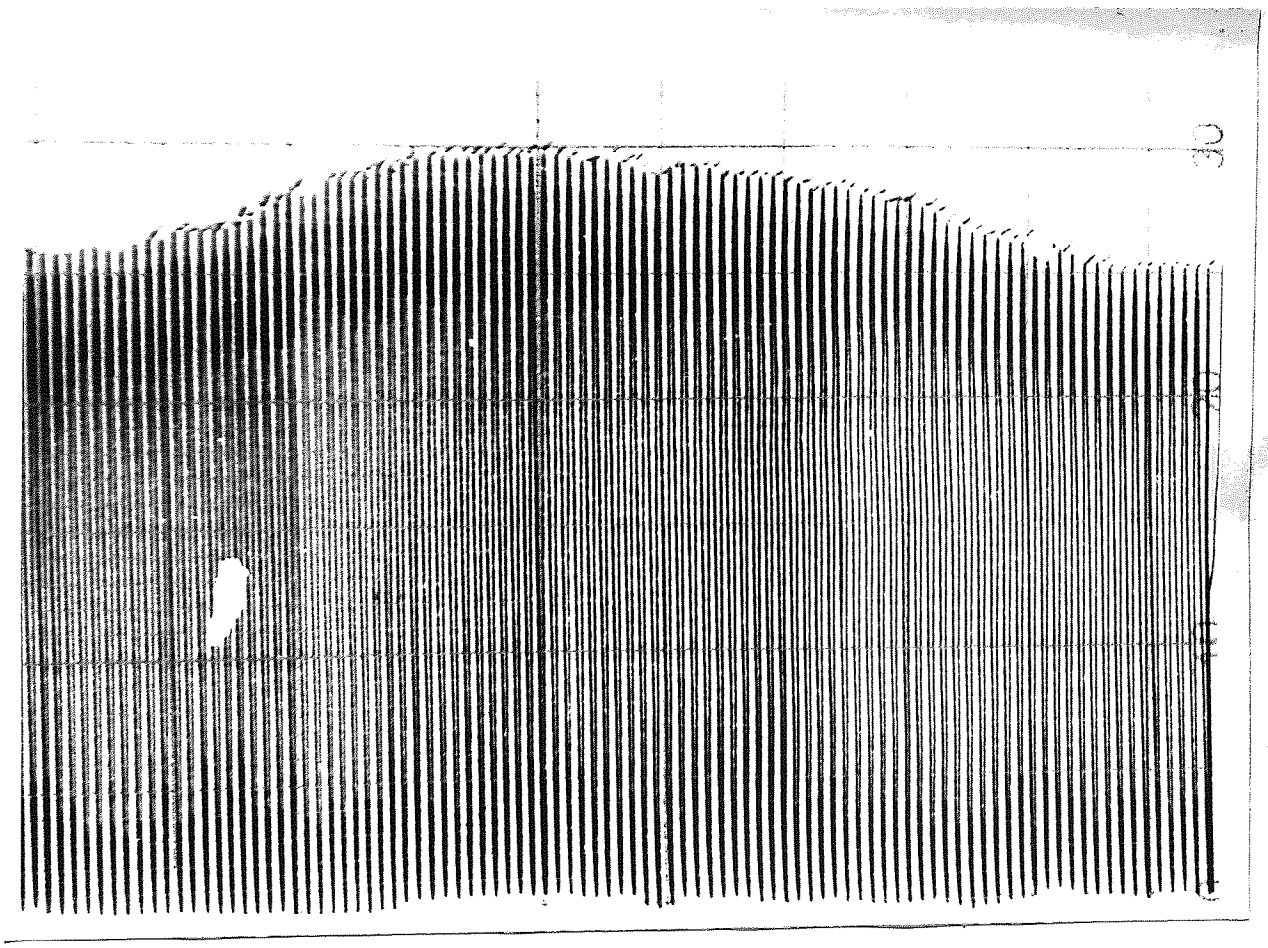

Plate 4.9 A typical Tracer Output Concentration Profile: Experiment No. H5.

CHAPTER FIVE

PRESENTATION AND ANALYSIS OF RESULTS

PRESENTATION AND ANALYSIS OF RESULTS

Results from the Thermal Conductivity Experiments, Single Drop Experiment, Residence Time Distribution Experiments and also Spray Drying Experiments have been presented graphically and where necessary a correlation has been proposed.

Further, observation from stereoscan analysis are presented in form of photo-micrographs. The experimental and proposed mass transfer coefficients are presented and analysed.

5.1 THERMAL CONDUCTIVITY EXPERIMENT

The results of the Thermal Conductivity experiments are shown in Appendix A. Tables A1 to A5 present the measurements made during the experiments. The thermal conductivity was calculated using the Lee's disc equation[86] but allowance was made for the slurry porosity. A Fortran IV computer program was written to evaluate the thermal conductivity. Since the university computer, an ICL 1904S has a device for plotting graphs (CALCOMP), this was also used.

In order to be able to interpolate for the thermal conductivity of the slurry at any temperature within the experimental range, a correlation was carried out on a proposed polynomial of the form:

$$K = A + BT + CT^2 + DT^3 + \ldots\ldots \qquad (5.1)$$

where K = Thermal Conductivity ($W/M/^{o}C$)

T = Temperature (^{o}C)

A,B,C ..... = Coefficients independent of Temperature

The least square method was applied for the correlation and this subroutine was written into the program. A listing of the program is presented in the Appendix A and so also are the outputs for all the slurry samples. Table 5.1 presents the results of the statistical correlation showing a variance of 1.124×10^{-3} for Westbury slurry to a maximum variance of 8.592×10^{-3} for Northfleet. The very good degree of fit between the experimental and correlated thermal conductivity values are shown by the graph plotter printouts in Figures 5.1 to 5.5.

FIGURE 5.1

CORRELATED THERMAL CONDUCTIVITY

FOR SLURRY SAMPLE FROM WESTBURY

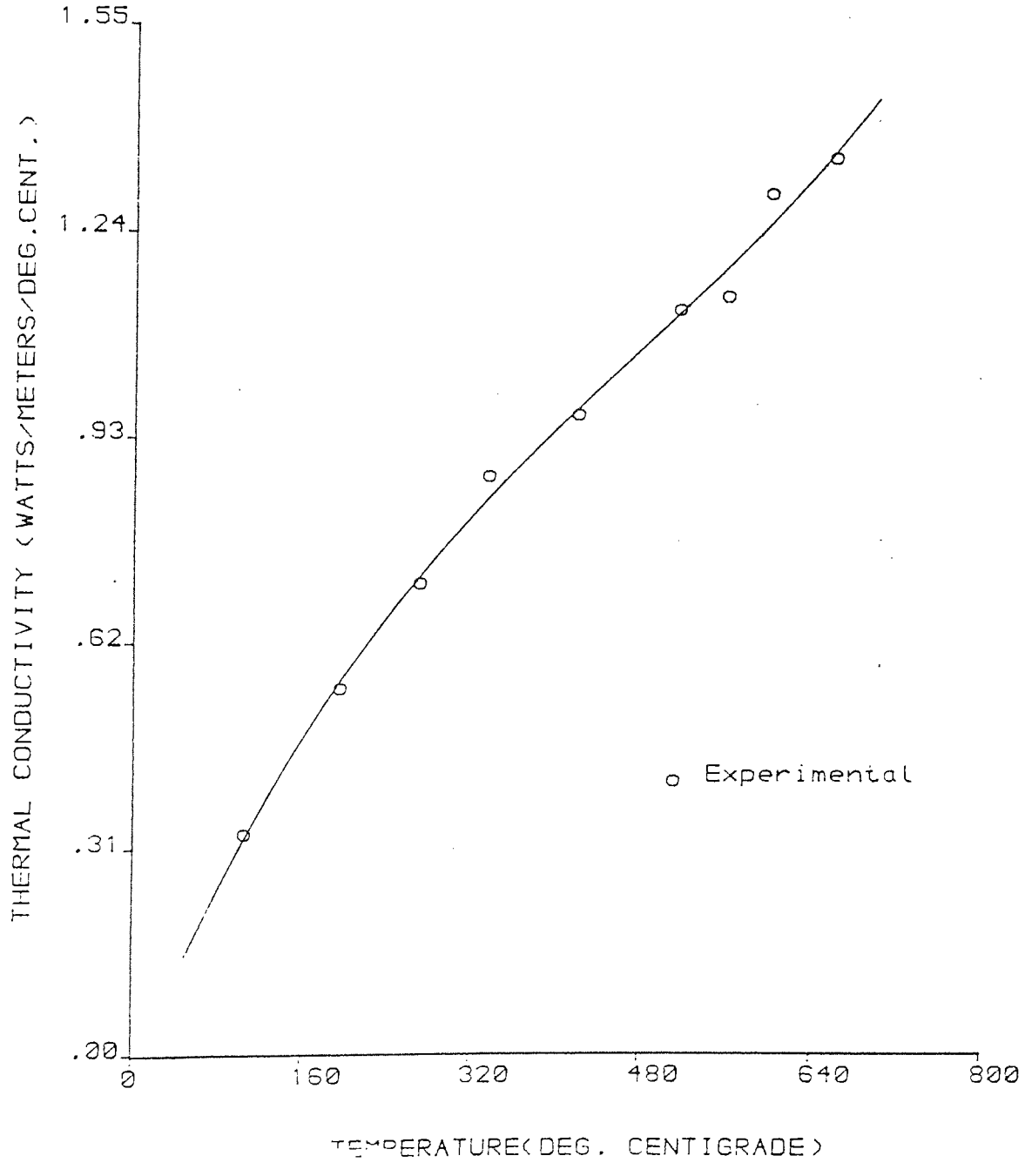

FIGURE 5.2

CORRELATED THERMAL CONDUCTIVITY

FOR SLURRY SAMPLE FROM NORTHFLEET

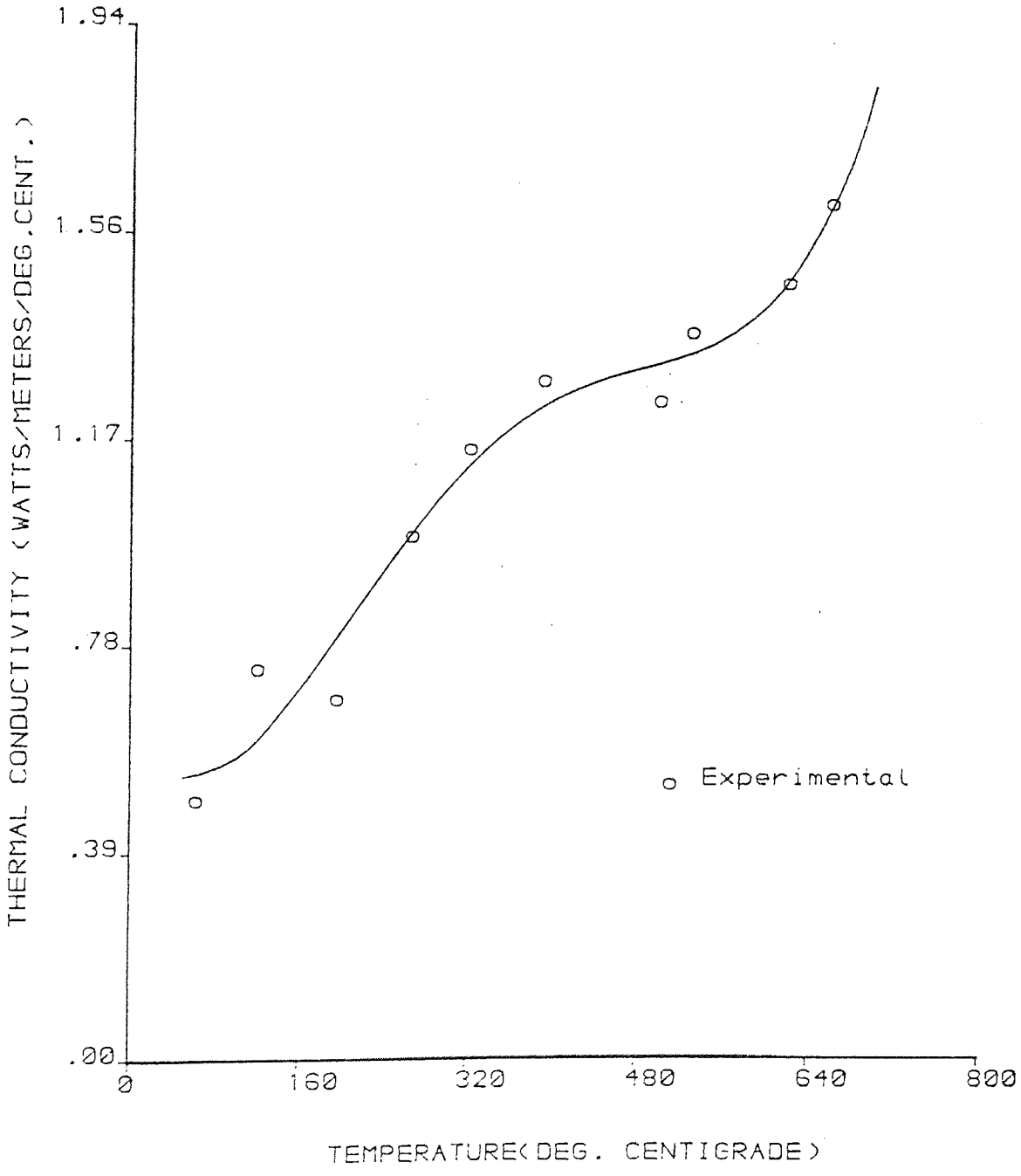

FIGURE 5.3

CORRELATED THERMAL CONDUCTIVITY

FOR SLURRY SAMPLE FROM MASON

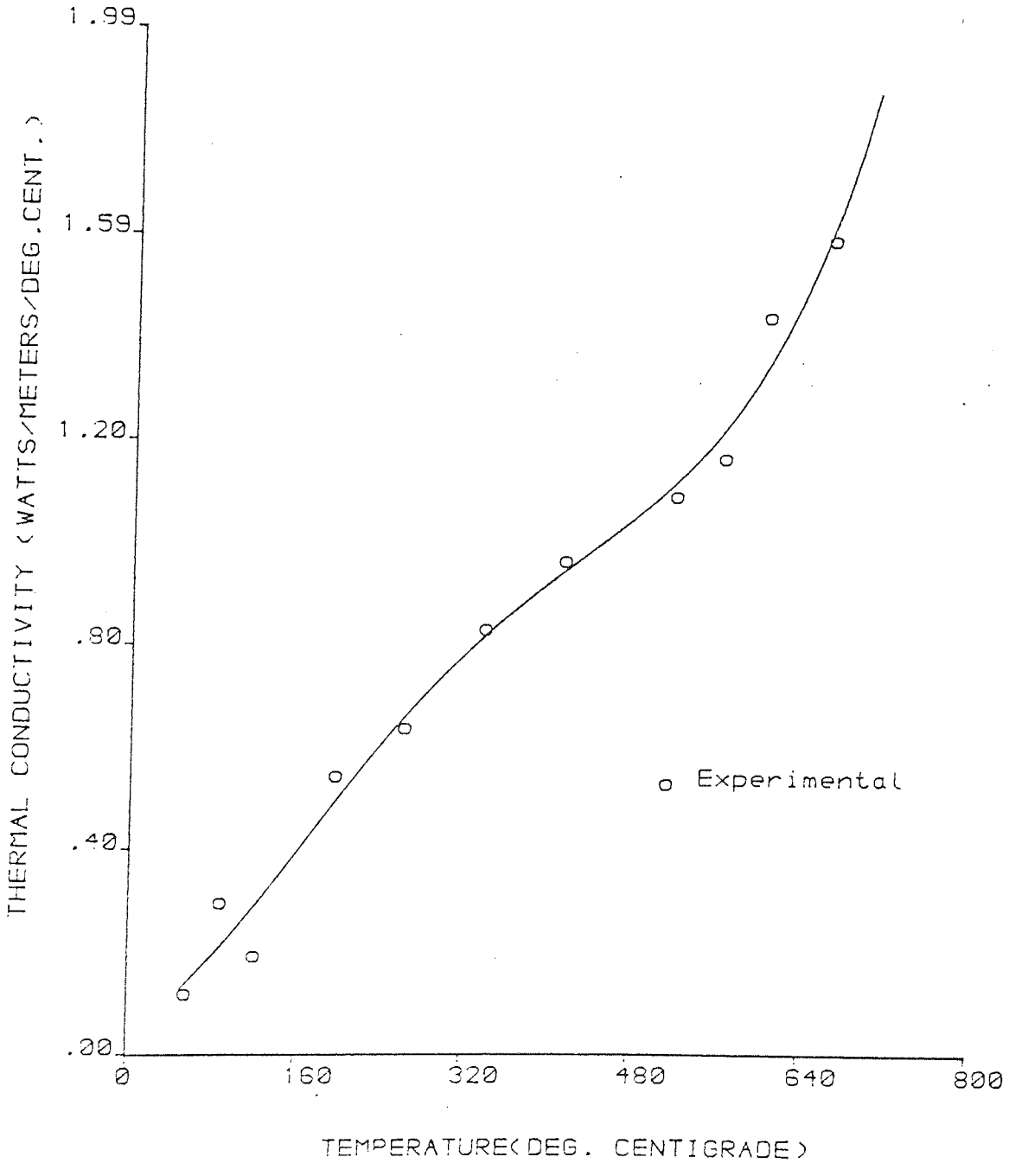

FIGURE 5.4

CORRELATED THERMAL CONDUCTIVITY

FOR SLURRY SAMPLE FROM HUMBER

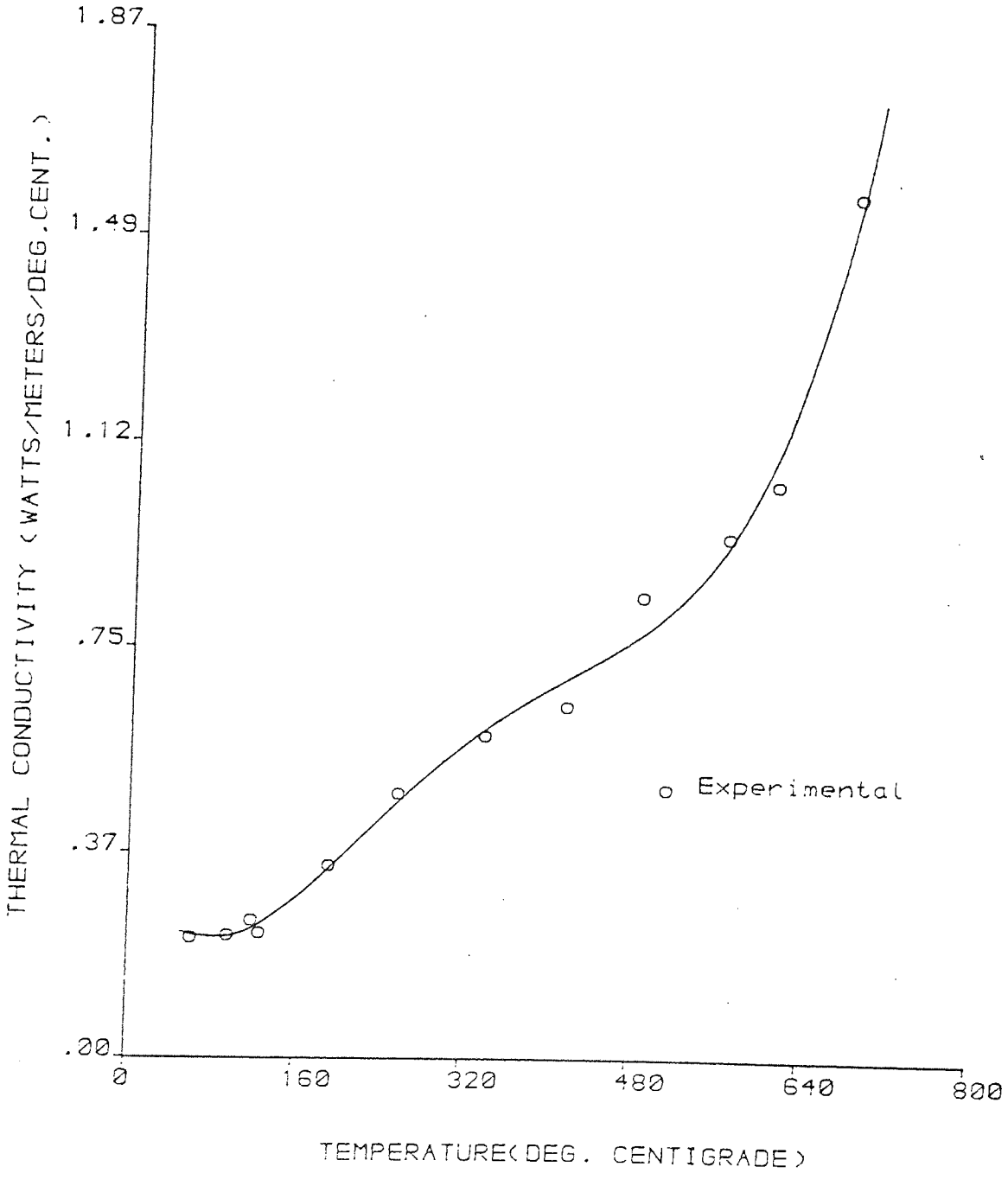

FIGURE 5.5

CORRELATED THERMAL CONDUCTIVITY

FOR SLURRY SAMPLE FROM SHOREHAM

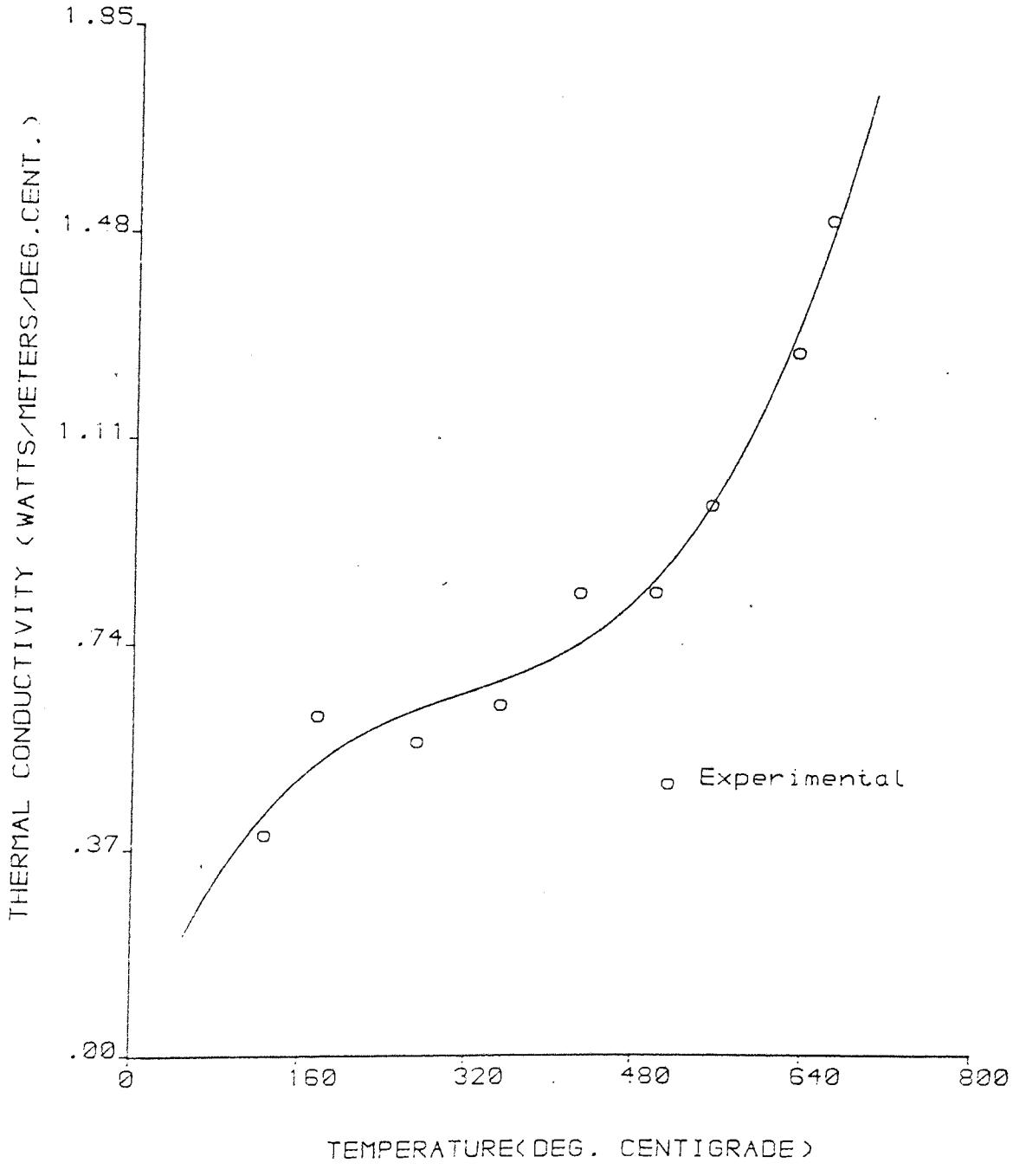

TABLE 5.1

CORRELATED POLYNOMIAL OF THE FORM: $K = A + BT + CT^2 + DT^3 + ET^4 + ...$

SAMPLE	A	B	C	D	E	SUM OF SQUARED ERRORS $\sum_{i=1}^{n} (e_i)^2$	VARIANCE σ^2
MASON	5.292×10^{-2}	9.046×10^{-4}	1.295×10^{-5}	-3.663×10^{-8}	3.093×10^{-11}	0.0353	5.877×10^{-3}
NORTHFLEET	6.117×10^{-1}	-3.036×10^{-3}	3.325×10^{-5}	-7.6217×10^{-8}	5.501×10^{-11}	0.04296	8.592×10^{-3}
WESTBURY	-3.505×10^{-2}	3.949×10^{-3}	5.224×10^{-6}	3.734×10^{-9}	-	0.0056	1.124×10^{-3}
SHOREHAM	5.381×10^{-4}	4.989×10^{-3}	-1.385×10^{-5}	1.479×10^{-8}	-	0.0264	5.288×10^{-3}
HUMBER	3.3389×10^{-1}	-3.3939×10^{-3}	2.8976×10^{-5}	-6.6427×10^{-8}	5.1618×10^{-11}	0.0120	4.528×10^{-3}

5.2 SINGLE DROPS EXPERIMENT

The drying characteristics of the slurry samples were determined by applying equations (3.16) to (3.26). This was done with the aid of the program listed in Appendix B. The program contains various subroutines for evaluating vapour pressures, humidity, graph plotting, and linear regression of the proposed mass transfer coefficients and experimental mass transfer coefficient. Also presented in Appendix B, in the form of Figures B1 to B75 is the data obtained from the single drop experiments. Comments on the effect of the following parameters on the drying characteristics of the slurry drops are made below:-

1) Temperature of drying air.

2) The initial moisture content of the slurry samples.

Also comments on the degree of fit between the experimental and the theoretical mass transfer coefficients and observations from the stereoscan micrographs will be discussed.

5.2.1 Effect of Air Temperature

The effect of the drying air temperature on the drying characteristics are presented in Figure C.1 to C.10 in Appendix C and Figure 5.6 is typical. Each quadrant in the graphs shows the effect of air temperature on each of the following factors:

a) Crust growth,

b) Crust mass transfer coefficient,

c) Overall experimental mass transfer

d) The drying rate.

FIGURE 5.6

o $t_a = 200^{\circ}C$

▽ $t_a = 300^{\circ}C$

* $t_a = 400^{\circ}C$

DRYING CHARACTERISTICS OF WESTBURY SLURRY SAMPLE WITH AN INITIAL M. C. OF 50.00 PER CENT

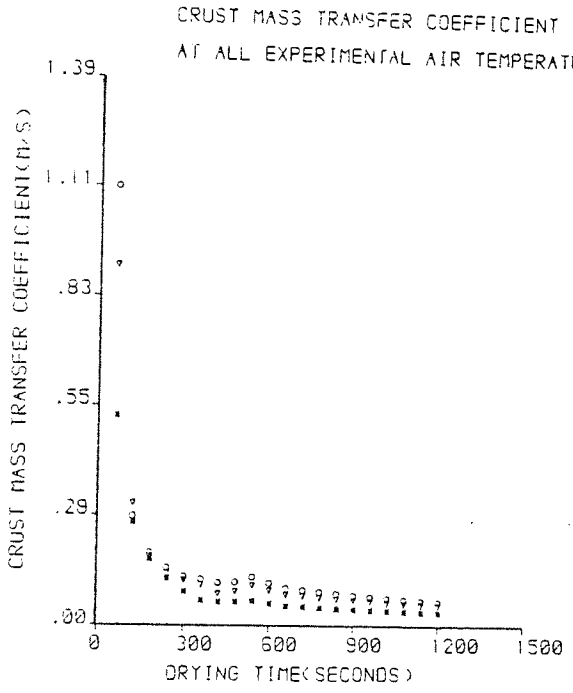

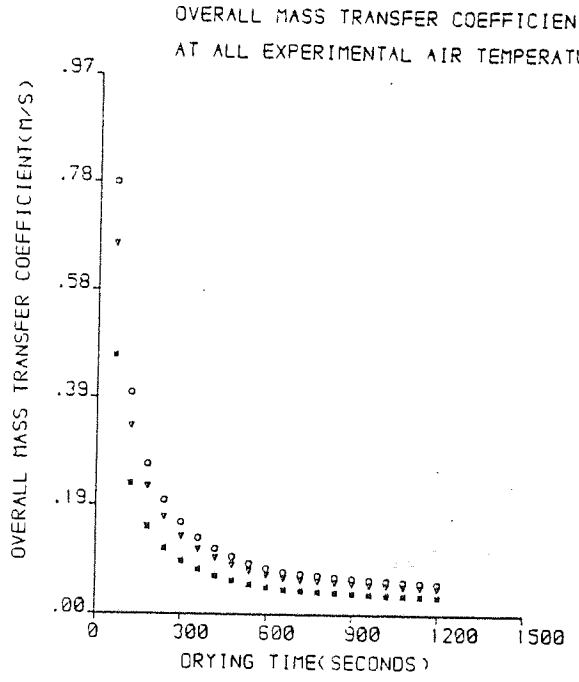

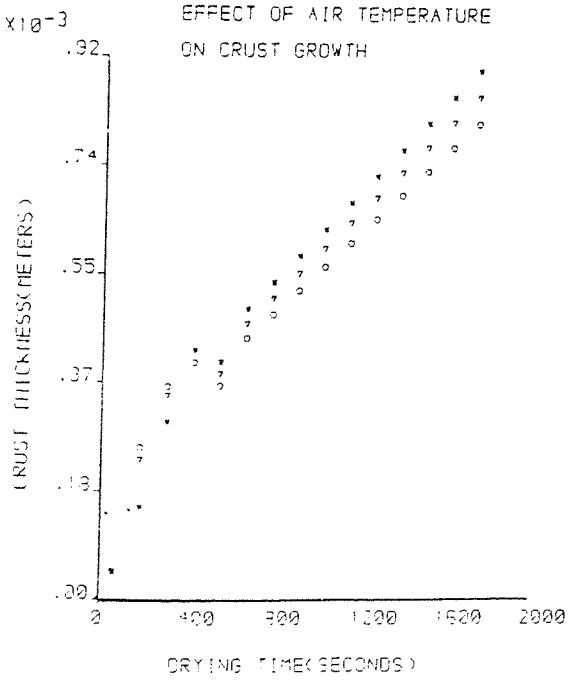

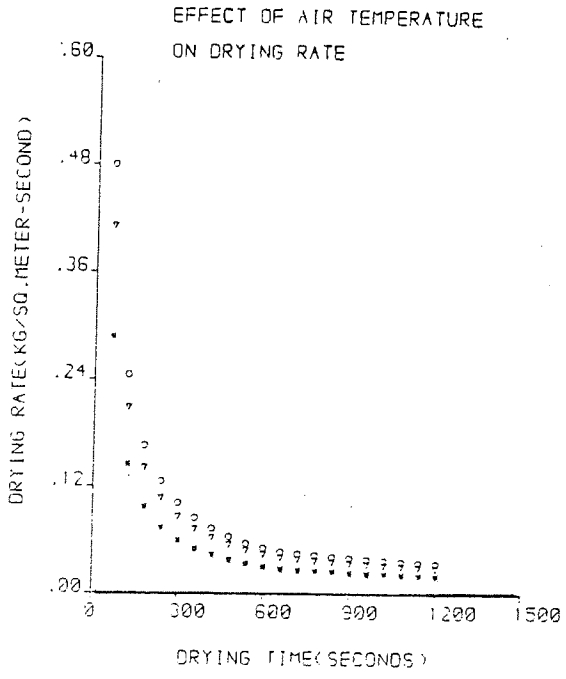

The quadrant showing crust growth rate indicated that the crust grows thicker in most of the samples as the temperature increases. This implies that as drying proceeds, the mass transfer rate decreases accordingly since the growing crust offers increased resistance to mass transfer.

The crust mass transfer rates on the other hand decreases with drying time and increasing temperature but this decrease tends to a constant rate after about 600 seconds of drying. This phenomenon was also observed at all drying air temperatures experimented. This is to be expected by considering the effect of the rate of heat conducted through the crust, which will be limited by the predominance of the crust thickness.

The variation of the overall mass transfer coefficient follows the same pattern noted for the crust mass transfer coefficient. That is the overall mass transfer coefficient decreases with increasing air temperature.

As expected, the drying rate of the slurry drops decrease with drying time; after decreasing for about 600 seconds, the drying rate becomes constant and this confirms the results of other workers[20,21,22,34].

5.2.2 Effect of Initial Moisture Content

The effect of initial slurry moisture content are presented in Figures 5.7 to 5.10. The other graphs showing the effects of the moisture content are shown in Appendix C.

Figures 5.7 to 5.10 indicate that the effect of the initial moisture content on drying characteristics of the

FIGURE 5.7

EFFECT OF INITIAL MOISTURE CONTENT ON CRUST GROWTH RATE FOR WESTBURY SLURRY

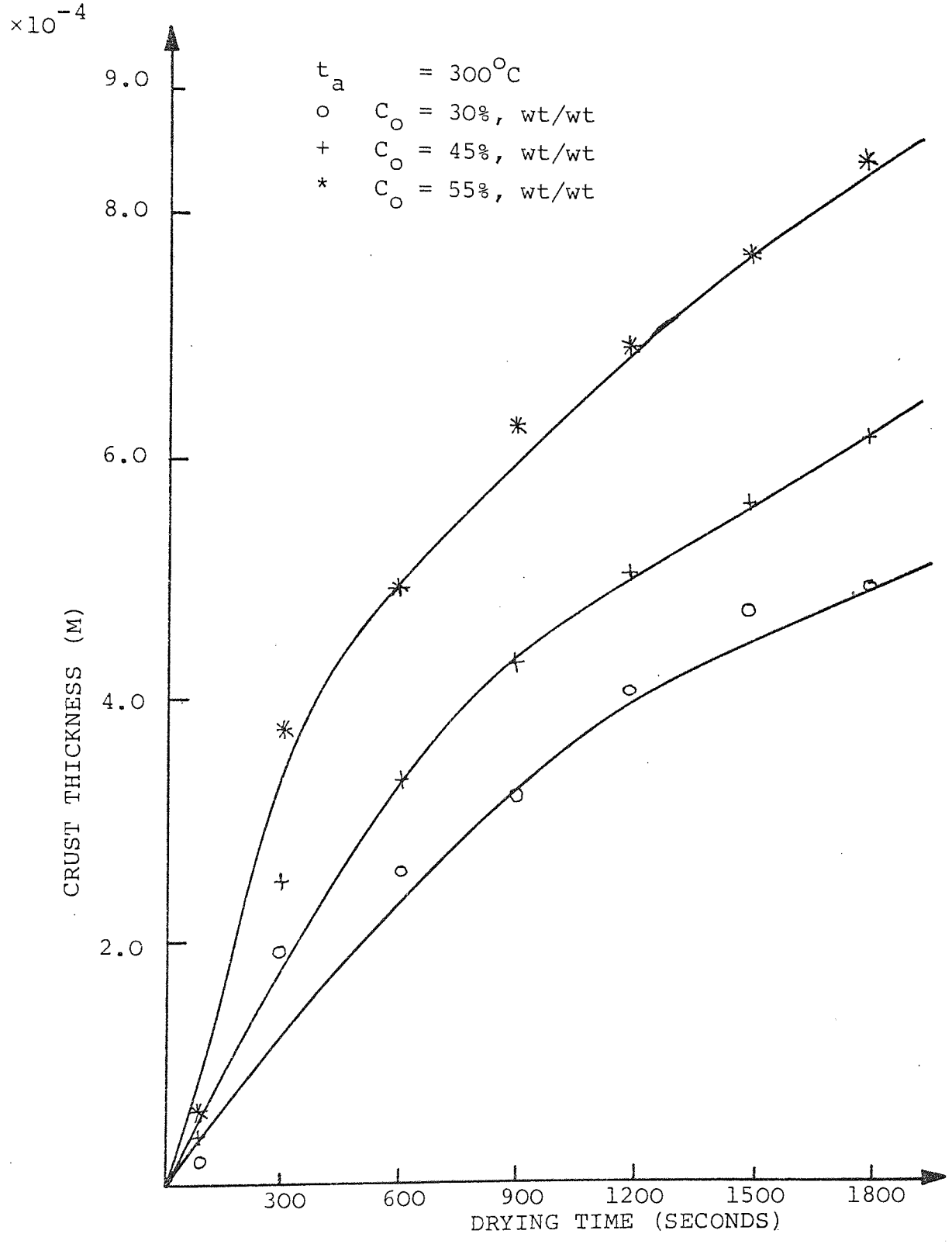

FIGURE 5.8

EFFECT OF INITIAL MOISTURE CONTENT ON CRUST MASS TRANSFER COEFFICIENT FOR WESTBURY SLURRY

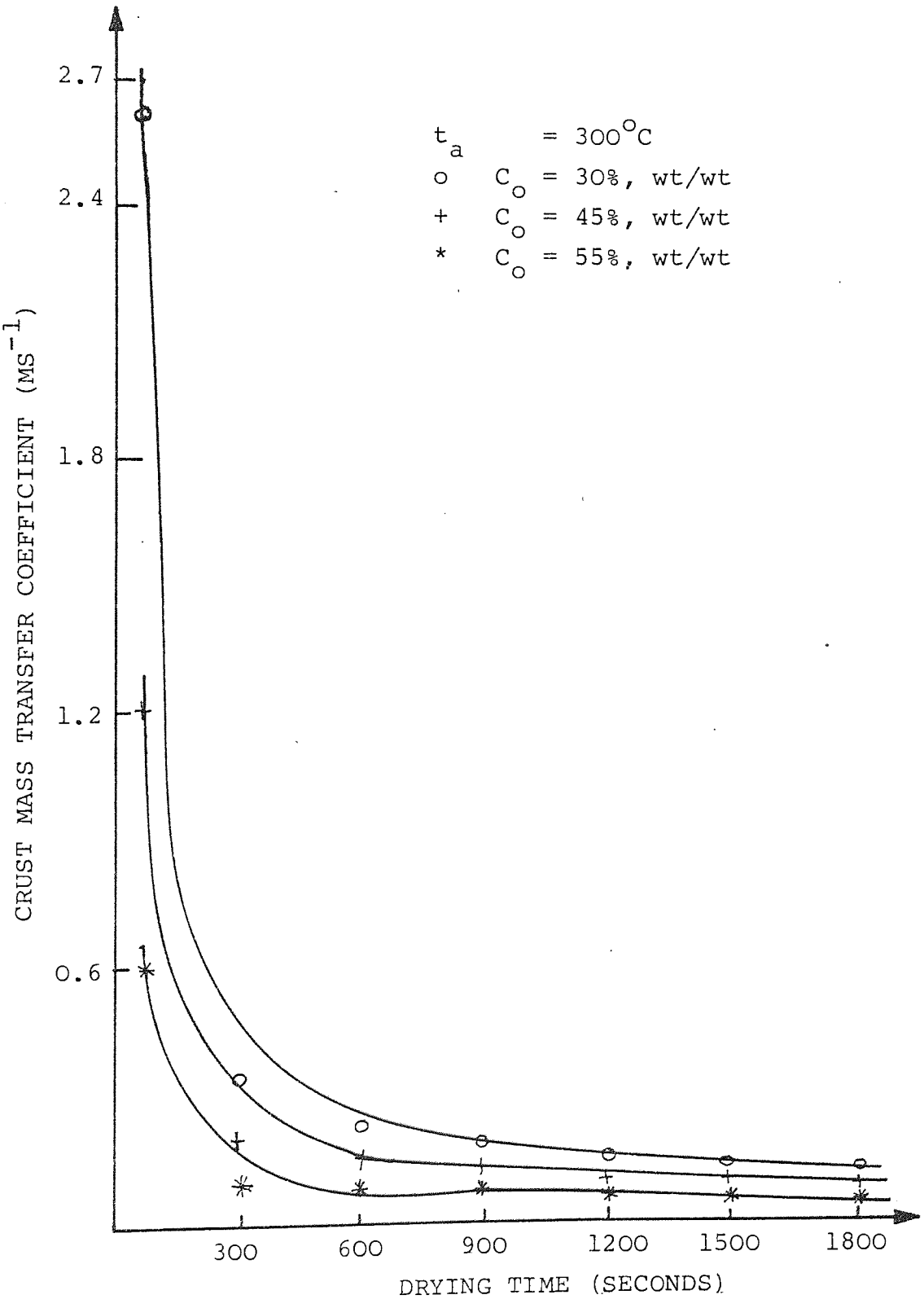

FIGURE 5.9

EFFECT OF INITIAL MOISTURE CONTENT ON EXPERIMENTAL MASS TRANSFER COEFFICIENT FOR WESTBURY SLURRY

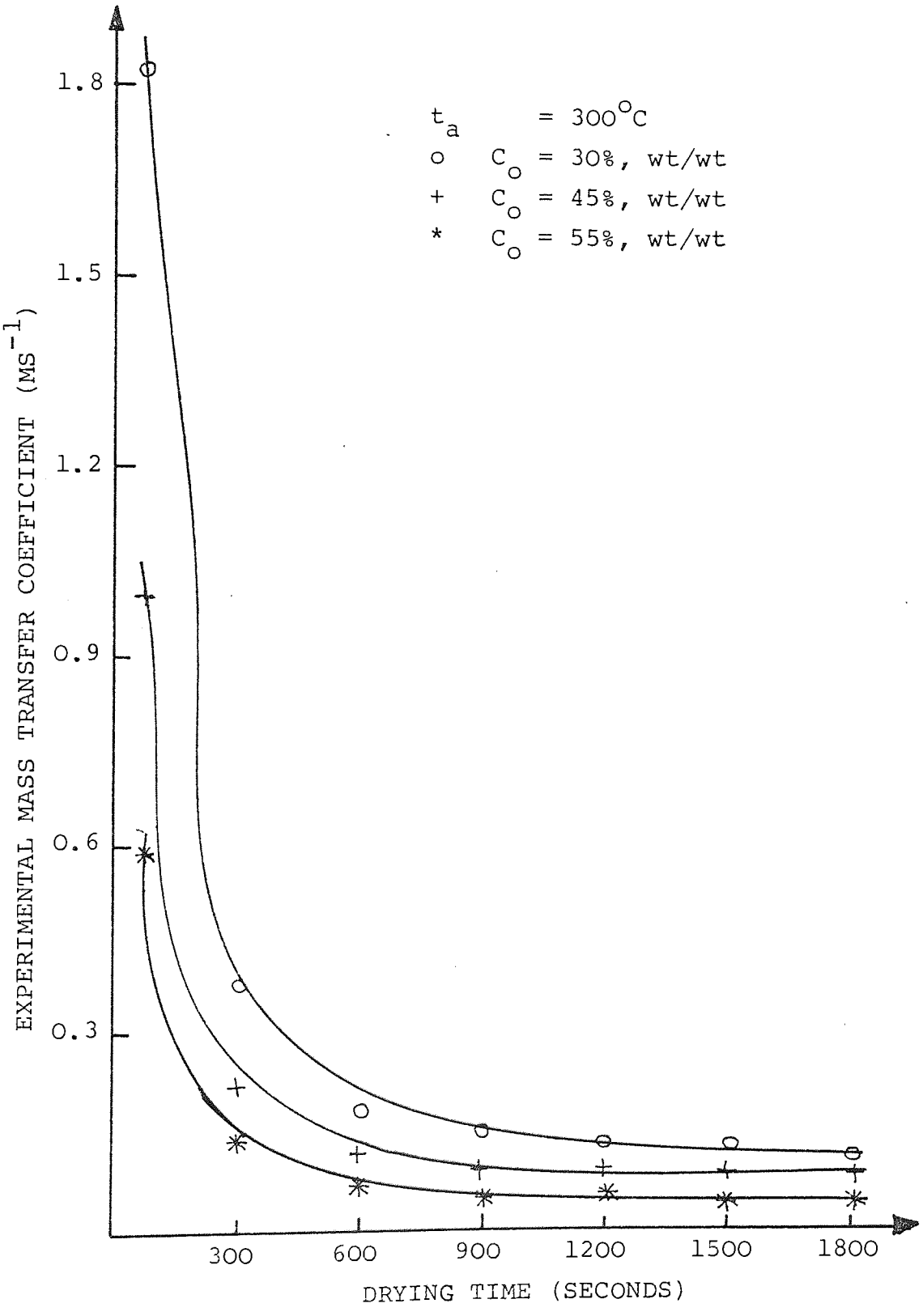

FIGURE 5.10

EFFECT OF MOISTURE CONTENT ON THE DRYING RATE OF WESTBURY SLURRY

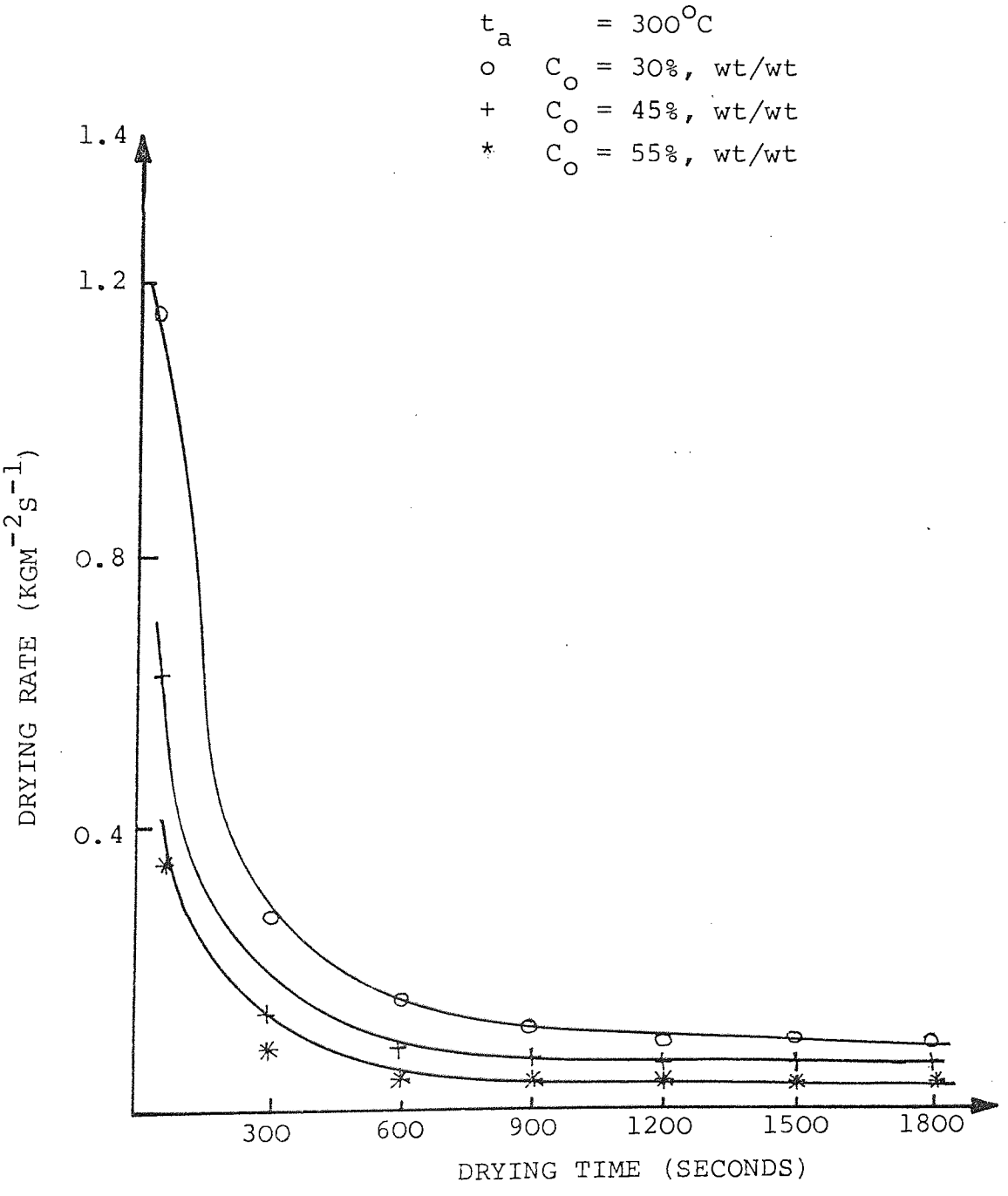

slurry drops are similar to those of temperatures. They show a more pronounced effect on the crust growth rate than is the case with temperature. This could be accounted for by the fact that, as the moisture content increases, the pressure of the resulting vapour formed also increases as drying proceeds. Thus the greater the vapour pressure in the core of the particle the greater the tendency to eject it through the pores thus accelerating the formation of the crust.

Figure 5.8 shows that the crust mass transfer coefficient decreases with increasing moisture content, because of the increasing crust thickness.

Figure 5.9 indicates a similar trend for the overall mass transfer coefficient of the particles.

Figure 5.10 shows that the drying rate of the drop decreases with increasing initial moisture content.

5.2.3 Comparison of Theoretical with the Experimental Mass Transfer Coefficient

The calculated mass transfer coefficients are tabulated in Appendix D and a typical set of results are shown in Table 5.2. The table gives the various parameters of the experiment and also the crust mass transfer coefficient (K_C) the overall theoretical mass transfer coefficient (K_T) and the overall experimental coefficient (K_E).

A linear regression was undertaken between the experimental and theoretical mass transfer coefficient and a typical plot

FIGURE 5.11

EXPERIMENTAL VERSUS THEORETICAL MASS TRANSFER COEFFICIENT FOR WESTBURY SLURRY SAMPLE

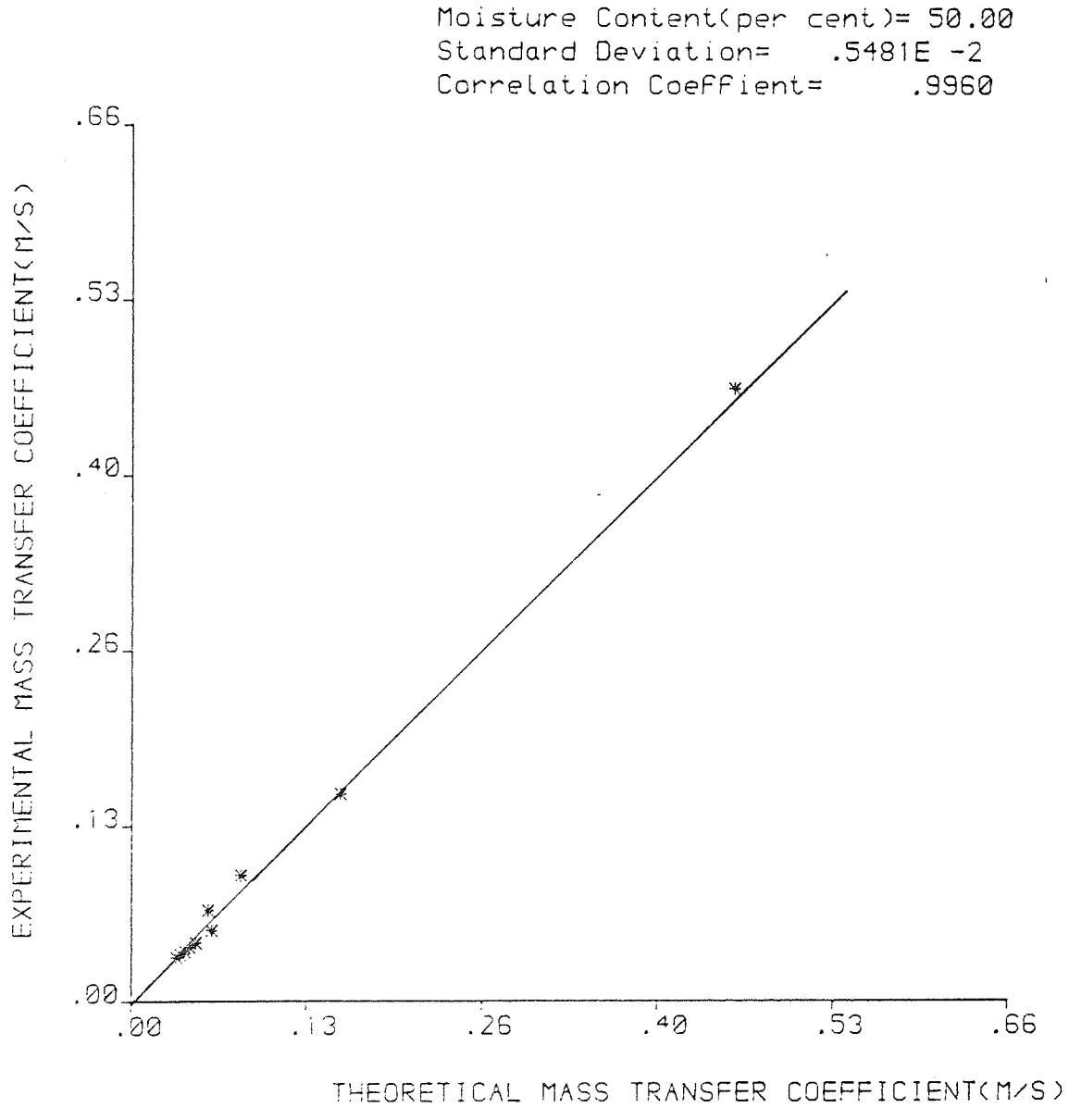

TABLE 5.2

SAMPLE - WESTBURY SLURRY

MEAN SAT. DROP TEMPERATURE= 267.50 DEG.C

CRUST THERMAL CONDUCTIVITY= .7190 W/M/DEG. C

AIR TEMPERATURE = 300.00 DEG. C.

INITIAL MOISTURE CONTENT = 0.550 KG/KG

GAS FILM TRANSFER COEFFIENT = 5.9840 M/S

DRYING TIME(SEC)	KC	KT	KE
6.0000E 01	5.8061E-01	5.2926E-01	5.7035E-01
1.2000E 02	2.8923E-01	2.7589E-01	2.8798E-01
1.8000E 02	1.9487E-01	1.8872E-01	1.9384E-01
2.4000E 02	1.4450E-01	1.4110E-01	1.4686E-01
3.0000E 02	9.5149E-02	9.3660E-02	1.1984E-01
3.6000E 02	9.3297E-02	9.1865E-02	9.9944E-02
4.2000E 02	8.5498E-02	8.4294E-02	8.6091E-02
4.8000E 02	8.7145E-02	8.5894E-02	7.5229E-02
5.4000E 02	8.1145E-02	8.0060E-02	6.7155E-02
6.0000E 02	7.2174E-02	7.1314E-02	6.0901E-02
6.6000E 02	6.4725E-02	6.4032E-02	5.5791E-02
7.2000E 02	6.1454E-02	6.0829E-02	5.3572E-02
7.8000E 02	5.8438E-02	5.7872E-02	5.1539E-02
8.4000E 02	5.5648E-02	5.5135E-02	4.9670E-02
9.0000E 02	5.3060E-02	5.2594E-02	4.7946E-02
9.6000E 02	5.0654E-02	5.0229E-02	4.6352E-02
1.0200E 03	4.8410E-02	4.8021E-02	4.4872E-02
1.0800E 03	4.6313E-02	4.5957E-02	4.3496E-02
1.1400E 03	4.4349E-02	4.4023E-02	4.2214E-02
1.2000E 03	4.2506E-02	4.2207E-02	4.1015E-02

of the regression is shown in Figure 5.11 . The standard deviation and correlation coefficient for the regression are also given. It is noticeable that there is close agreement between the experimental and theoretical transfer coefficients after about 240 seconds of drying. This confirms that hitherto, the drying process was controlled by a combination of the gas film and crust resistances. Once the crust has grown appreciable its resistance to mass transfer predominates. Hence the fact that towards the later period of the drying the K_E and K_T values were close to the K_C values.

The very favourable agreement between the experimental and the proposed theoretical mass transfer coefficient for the system supports the Heat-Momentum transfer model proposed in Section 3.

5.2.4 Photomicrograph Observations

The micrographs made from the stereoscan analysis are presented on Plates 5.1 to 5.4. They show the external and internal structures of typical slurry droplets at various stages of drying during the single drop experiments. The micrographs reveal the internal change occurring in the drop as drying proceeds.

The external structures as shown by Plates 5.1 and 5.2 depict surface of the drop in the early stages of the drying. As drying proceeds, cracks begin to appear on the smooth surface of the drop while craters and holes proliferate . These craters and holes are the exit points of the jets of

Plate 5.1 : Surface Structure

Sample: Humber

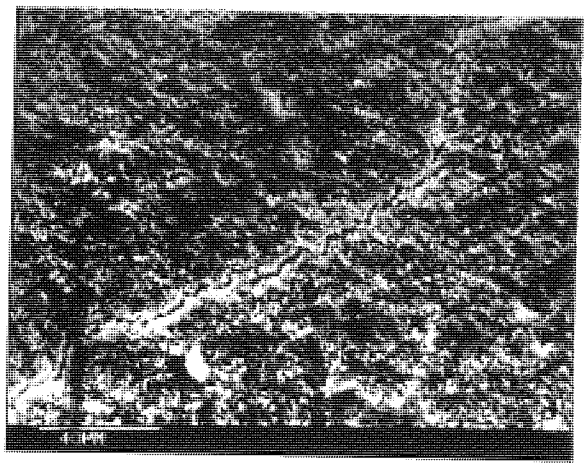

Sample: Humber

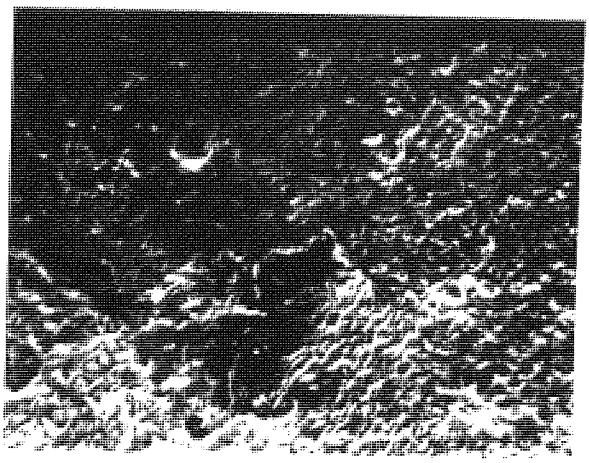

Sample: Northfleet

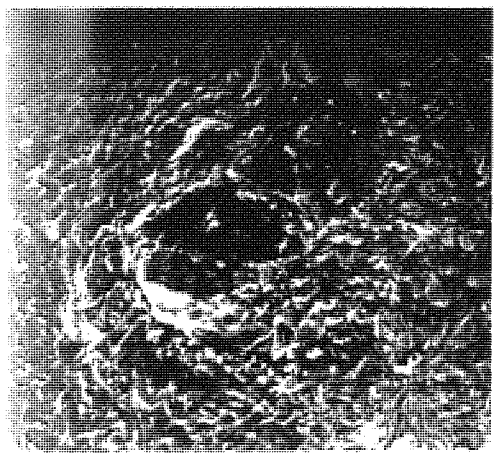

Plate 5.2 : Internal Structure

Sample: Humber

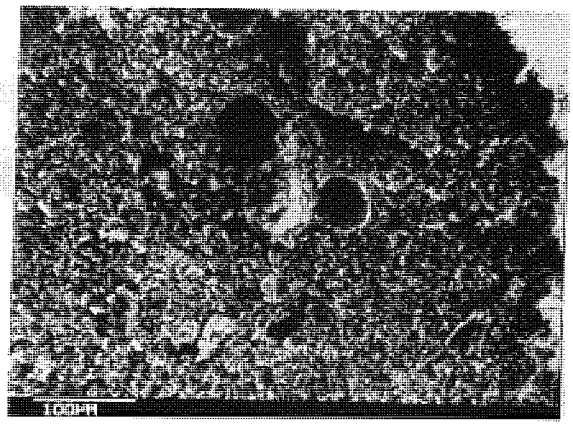

Sample: Humber

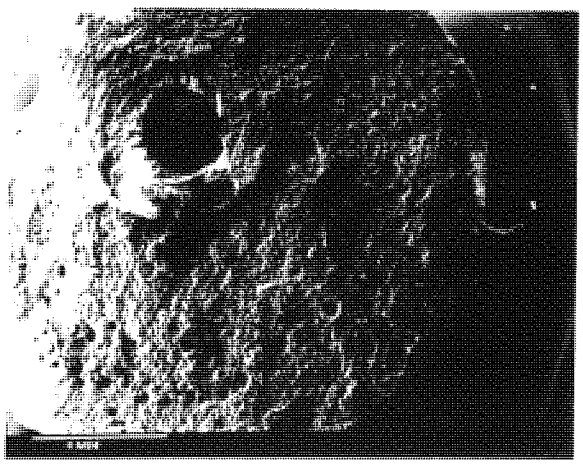

Sample: Northfleet

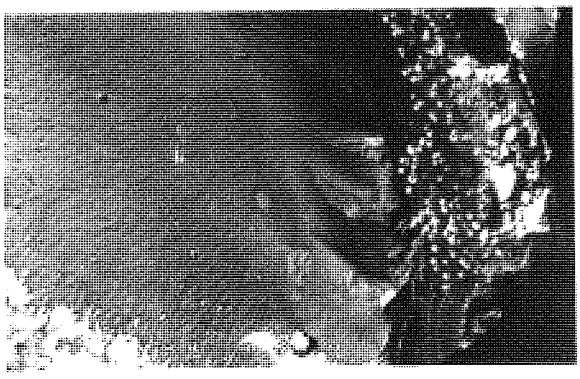

Plate 5.3 : Internal Structure

Sample: Mason

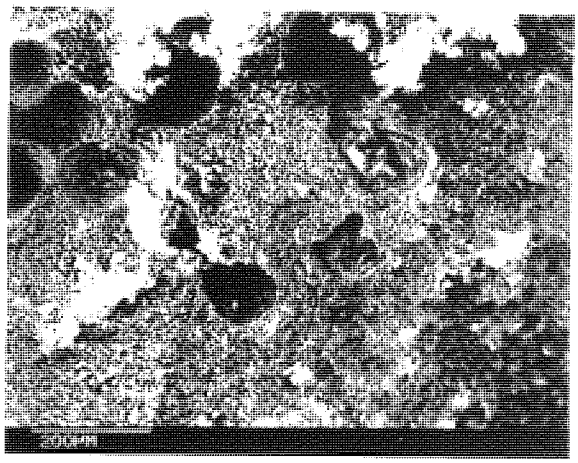

Sample: Mason

Plate 5.4 : Internal Structure

Sample: Westbury

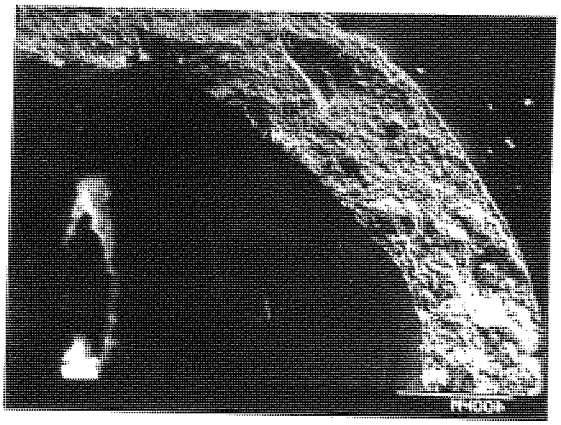

Sample: Westbury

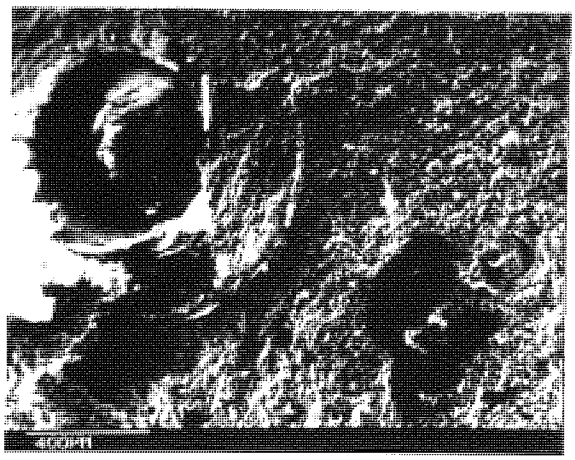

steam ejected from the core of the drop. They give credibility to the proposition that steam spurts out of the drop as drying proceeds at a high rate of drying.

Plates 5.3 and 5.4 show the internal structure of the droplets as drying proceeds. Of particular interest are the circular crater-like structures in the drops. This suggests that water droplets are held in the form of globules inside the slurry drops. Thus the globules are the points from which water vapour is ejected from the core. The micrographs show the proliferation of craters and pores in the core of the drop as drying proceeds, and sometimes as in the case of Plate 5.4c large hollow portions result. The white patches observed on the surface are also present in the internal structure.. These could be attributed to the chalk content of the slurry.

5.3 SPRAY DRYING AND RESIDENCE TIME DISTRIBUTION EXPERIMENTS

The Spray Drying experiments were carried out in two stages. The first stage was a preliminary one, during which the evaporative capacity of the pilot plant spray drier was established by undertaking spray drying experiments using water as the liquid feed. The second stage was the actual spray drying of Portland Cement slurry sample and the data obtained from these experiments are presented in Appendix E in form of Tables E1 to E20.

The Residence Time Distribution experimental programme included Tracer experiments on the pilot plant spray drier and

an industrial spray drier at Humber works of Blue Circle Coy. Limited. The experimental data collected are presented in Appendix F in Tables F1 to F7.

5.3.1 Analysis of Spray Drying Experimental Results

The experimental results from both parts of the Spray Drying experiments have been treated separately; thus for 1) Water drops, and 2) Slurry drops.

5.3.1.1 Water Drops

The results from the water experiments are presented in Appendix E. These data were used to carry out both mass and heat balance calculation on the spray drier and as such determine the evaporative capacity and heat utilisation characteristics of the drier. A typical calculation is presented in Appendix E. The results of the mass balance calculations are presented in Table 5.3, while those for enthalpy balance are presented in Table 5.4.

The experiments were carried out at five air flowrates varying from 0.13 kgs^{-1} to a maximum of 0.23 kgs^{-1}. Two experiments were carried out for each flowrate to assess the reproduceability and the flowrates increased from 0.13 kgs^{-1} to 0.23 kgs^{-1}. The results of the mass balances on moisture content presented in Table 5.3, are as expected in relation to the flow in the spray drier. As the air flowrate increases the total evaporation load in the drier increases and so does the heat load in a corresponding manner. Thus more moisture is transferred from the liquid feed into the air stream. This

phenomenon is presented in Table 5.3 where it can be seen that the evaporative capacity of the drier increases from 3.2448×10^{-3} kgs^{-1} in experiment SD1 to 5.7408×10^{-3} kgs^{-1} in experiment SD9. The accummulation term refers to the unevaporated water collected from the conical base of the drier at the end of each experiment. It will be noticed also that this quantity decreases with increasing air flowrate. Thus in terms of optimum moisture removal from the pilot plant spray drier, the indication is that higher air flowrate is favourable provided that there is no entrainment.

The Enthalpy balance presented in Table 5.4 shows a similar trend as that observed in the case of moisture transfer. The increase in air flowrate necessitates an increased heat load in the spray chamber but the thermal efficiency of the drier remained nearly constant between 0.626 and 0.804, during the whole experimental programme.

5.3.1.2 Slurry Drops

The data collected from the drying of cement slurry drops are presented in Tables E11 to E20. As in the drying of water drops, two experiments were performed for each air flowrate.

Since the evaporative capacity of the spray drier had been determined from the preliminary experiments on a water feed, the slurry feed flowrate was predetermined, and two slurry feed rates were chosen for each air flowrate. This was done in order to observe the effects on the drying of the slurry.

TABLE 5.3

MASS BALANCE ON MOISTURE ON

PILOT PLANT SPRAY DRIER

Feed: WATER

EXPERIMENT NUMBER	TOTAL MOISTURE INPUT $(KGS^{-1}) \times 10^{-3}$	EVAPORATIVE CAPACITY $(KGS^{-1}) \times 10^{-3}$	ACCUMULATION $(KGS^{-1}) \times 10^{-3}$
SD 1	4.9242	3.2448	1.6794
SD 2	5.3299	3.4641	1.8658
SD 3	5.0832	3.8653	1.2179
SD 4	5.5215	3.9936	1.5279
SD 5	5.2816	4.5900	0.6915
SD6	5.8270	4.2999	1.5271
SD 7	5.7130	4.9001	0.8129
SD 8	5.9365	5.4159	0.5207
SD 9	6.0200	5.7408	0.2792
SD 10	5.9683	5.5563	0.4120

TABLE 5.4

ENTHALPY BALANCE ON PILOT

PLANT SPRAY DRIER

Feed: WATER

EXPERIMENT NUMBER	TOTAL HEAT INPUT ($KJKG^{-1}S^{-1}$)	TOTAL HEAT EXHAUST ($KJKG^{-1}S^{-1}$)	THERMAL EFFICIENCY (η)
SD 1	24.736	17.433	0.705
SD 2	40.398	26.661	0.660
SD 3	45.883	31.464	0.686
SD 4	39.744	37.637	0.695
SD 5	46.082	30.060	0.652
SD 6	43.093	26.985	0.626
SD 7	51.038	34.289	0.691
SD 8	50.062	38.213	0.763
SD 9	53.531	43.054	0.804
SD 10	51.047	39.424	0.772

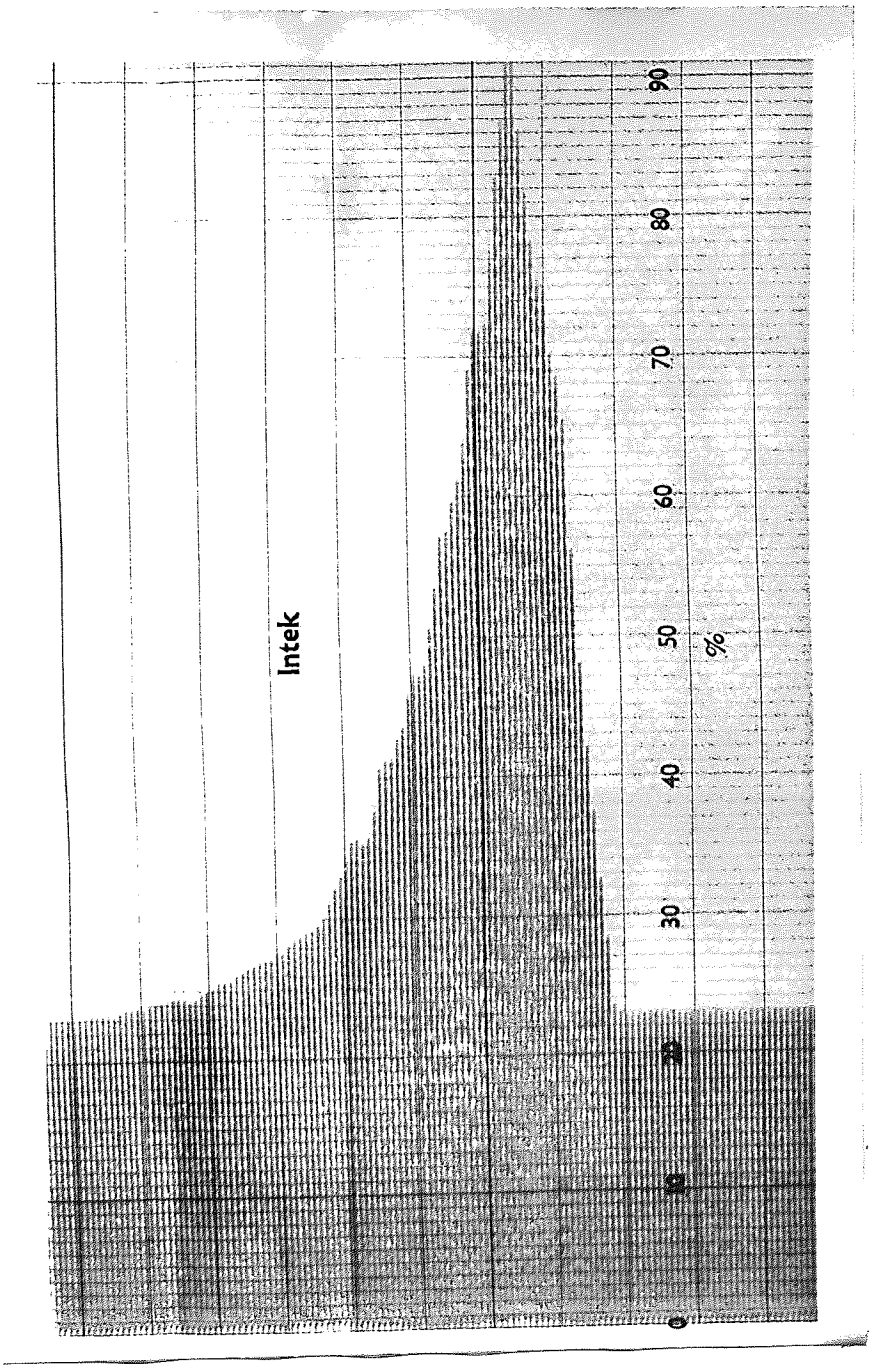

Plate 5.5 A typical Pilot Plant Spray Drier Tracer Output Concentration Profile: Experiment No. SD 21.

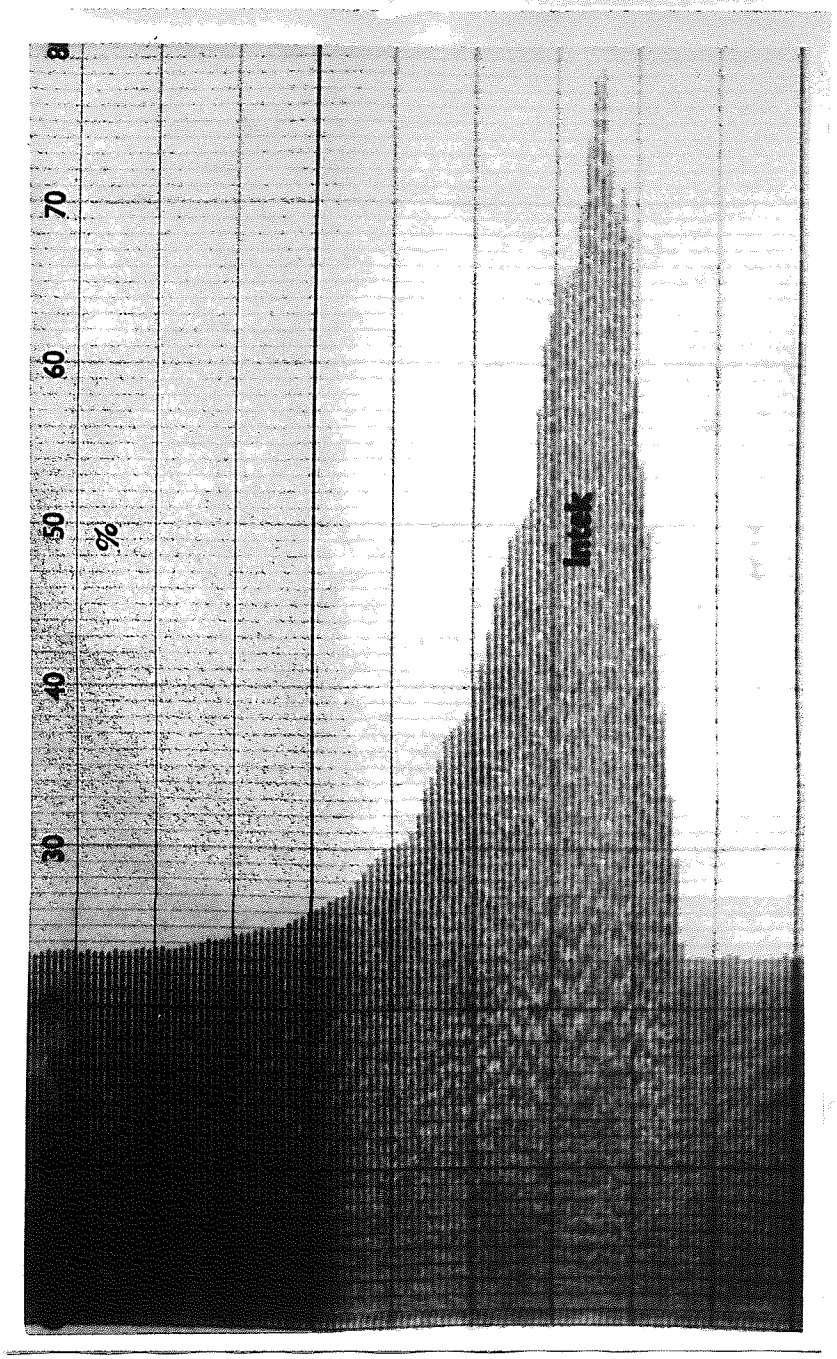

Plate 5.6 A typical Pilot Plant Spray Drier Tracer Output Concentration Profile: Experiment No. SD 22.

The data collected from these experiments, together with the residence time distribution parameters are used extensively in the derivation of Design Parameters for Spray Driers to be developed in the next chapter.

5.3.2 Analysis of Tracer Experimental Results

The Tracer Experiments were carried out as explained in Section 4.4.3, both on the laboratory pilot plant spray drier and the Humber spray drying unit. Plates 5.5 and 5.6 are typical of the tracer exit concentration profiles of argon mapped out by the mass spectrometer recorder. These profiles constitute the data used to evaluate the parameters derived in equations (3.28) to (3.48) in Section 3.4. An ICL Fortran IV program was written and compiled to normalise the raw experimental response data and a Basic 16 program was compiled to simulate the response in order to evaluate the parameters. The listing of both programs are presented in Appendix F. The program included 'GRASP' (Graphics Aston Simulation Package) a departmental package compiled on the 'Honeywell 316" computer. GRASP can develop graphical simulations and in the case of the differential equations being treated, it employs a 4th-order Runge-Kutta subroutine for solution.

The Honeywell 16 printouts are presented in Tables F1 to F7 in Appendix F. These show the time, the experimental tracer concentration and the simulated response in dimensionless terms. The graphical printouts corresponding to these response values are presented in Figures 5.12 to 5.18. The evaluated parameters,

FIGURE 5.12

EXPERIMENT NUMBER: SD21

A = 0.60 B = 0.2075 J = 0.056

K = 0.125 M = 0.3 N = 0.15 L = 0.17

$\sum_{i=1}^{N_1} (e_i)^2 = 0.2018$

Variance, $\sigma = 2.127 \times 10^{-3}$

Mean Residence Time = 16.7879s

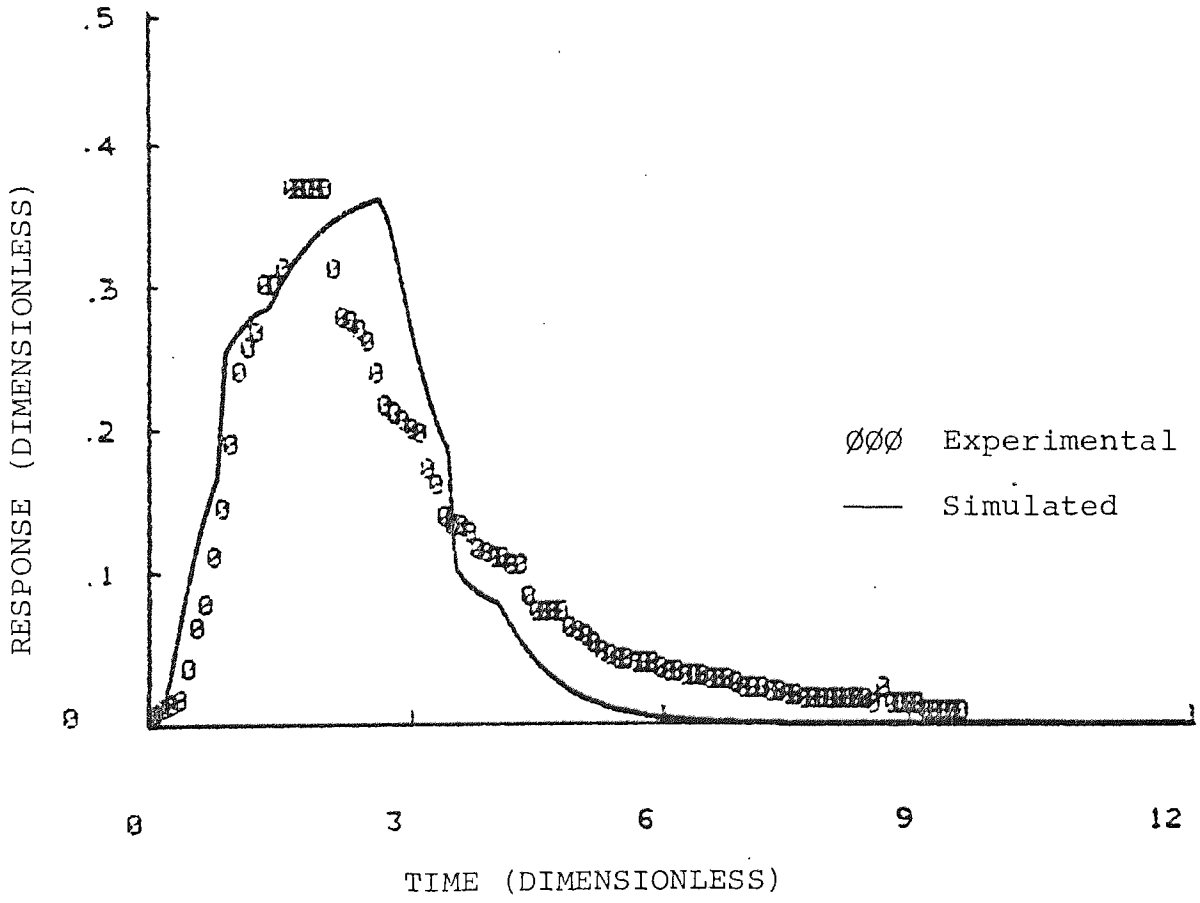

FIGURE 5.13

EXPERIMENT NUMBER: SD22

A = 0.60 B = 0.215 J = 0.065

K = 0.125 M = 0.30 N = 0.15 L = 0.145

$$\sum_{i=1}^{N_1} (e_i)^2 = 0.2332$$

$$\sigma = 2.454 \times 10^{-3}$$

Mean Residence Time = 14.0468s

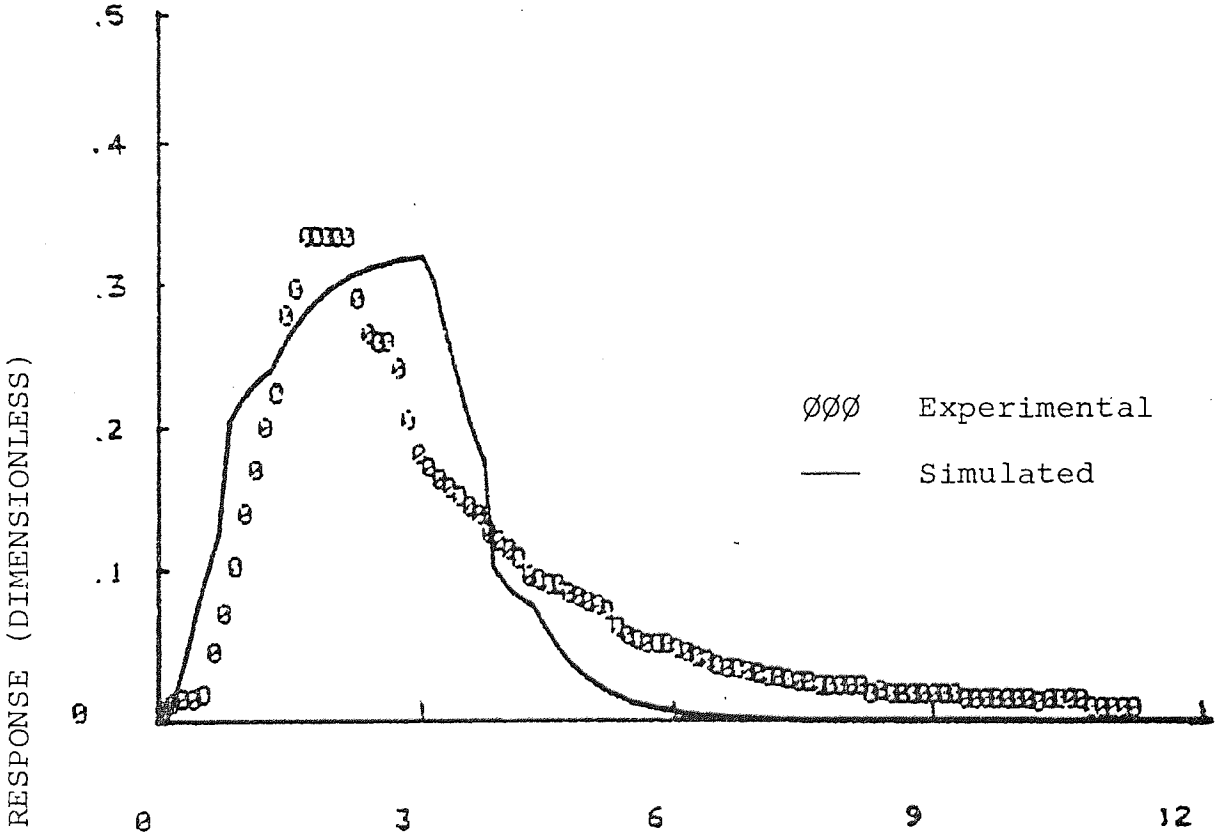

FIGURE 5.14

EXPERIMENT NUMBER: SD23

A = 0.60 B = 0.250 J = 0.09

K = 0.125 M = 0.225 N = 0.15 L = 0.12

$\sum_{i=1}^{N_1} (e_i)^2 = 0.1568$

$\sigma = 1.889 \times 10^{-3}$

Mean Residence Time = 12.1426s

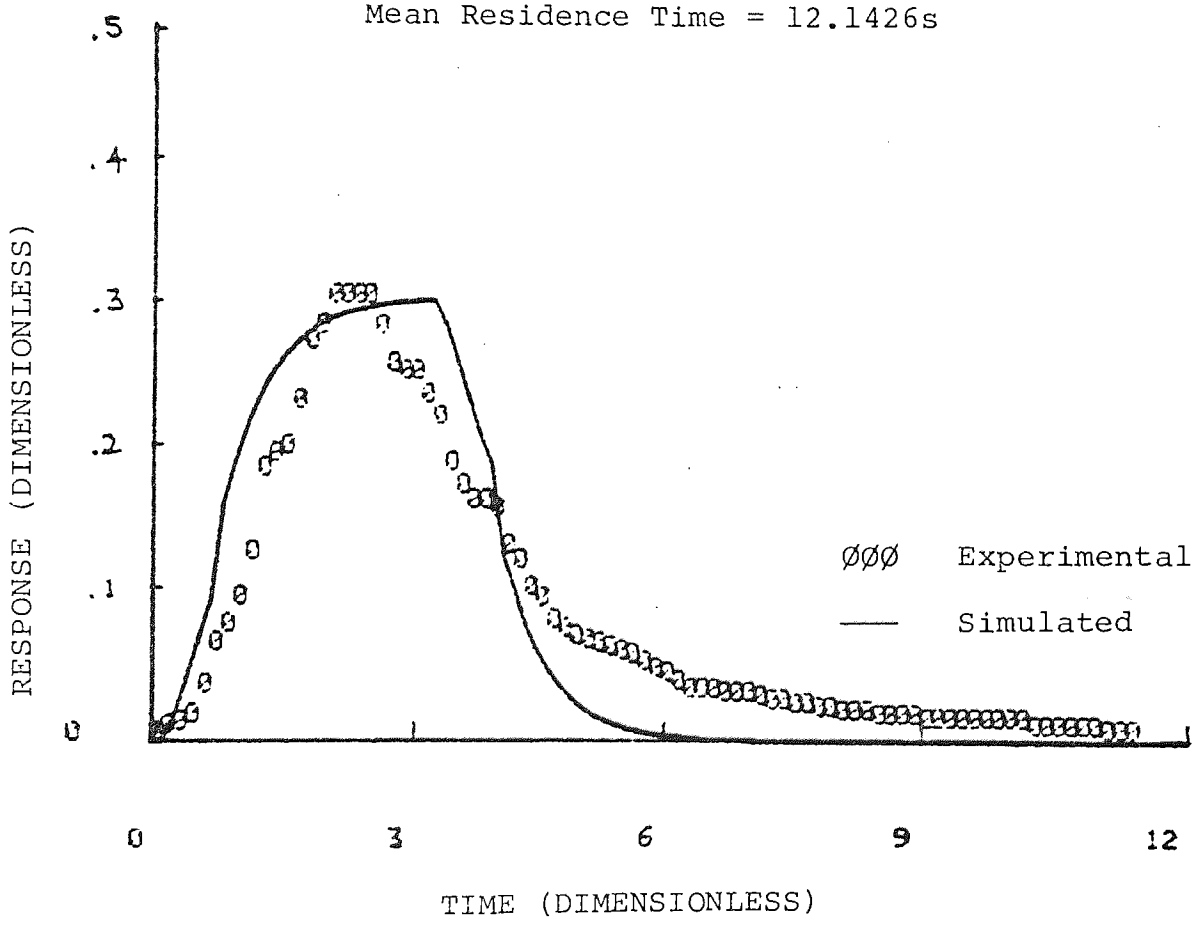

FIGURE 5.15

EXPERIMENT NUMBER: SD24

A = 0.60 B = 0.220 J = 0.09

K = 0.12 M = 0.20 N = 0.13 L = 0.12

$\sum_{i=1}^{N_1} (e_i)^2 = 0.2454$

$\sigma = 2.956 \times 10^{-3}$

Mean Residence Time = 11.1453s

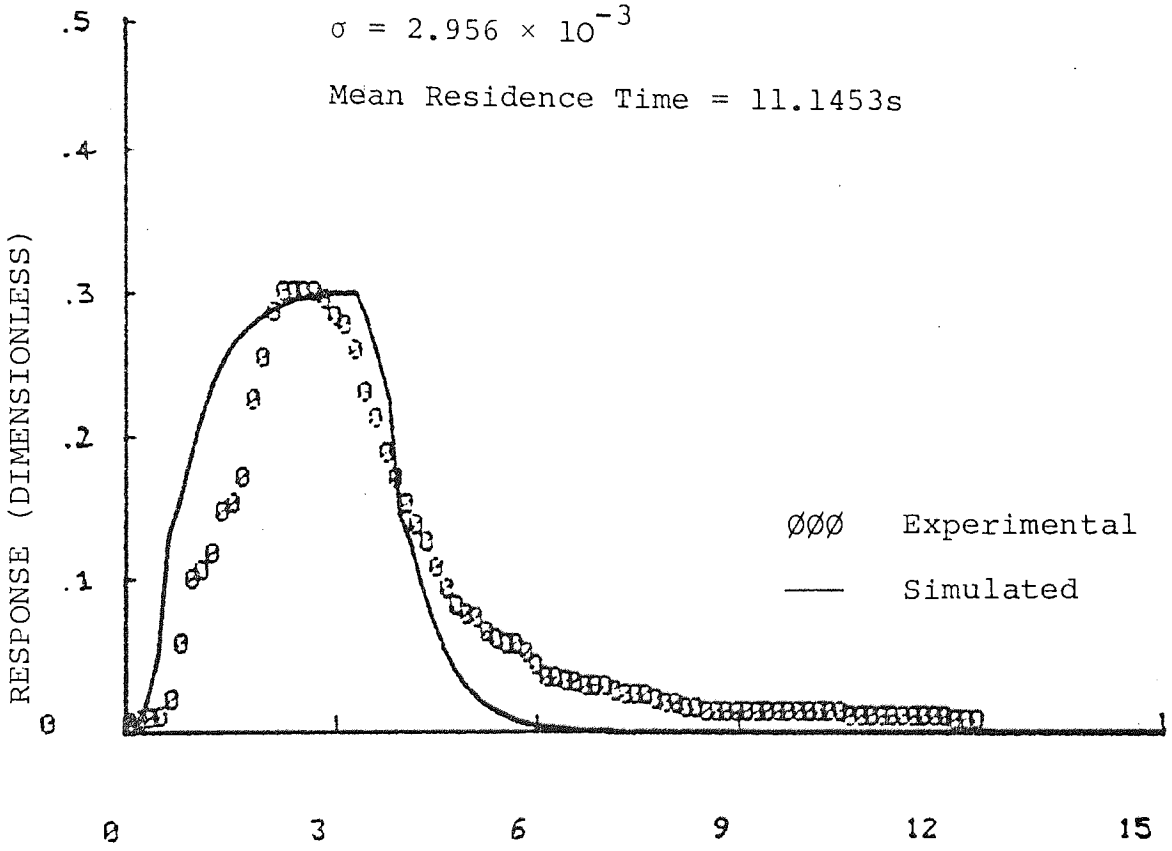

FIGURE 5.16

EXPERIMENT NUMBER: SD25

A = 0.60 B = 0.2905 J = 0.0125

K = 0.07 M = 0.26 N = 0.13 L = 0.1

$\sum_{i=1}^{N_1} (e_i)^2 = 0.1488$

$\sigma = 2.011 \times 10^{-3}$

Mean Residence Time = 10.348s

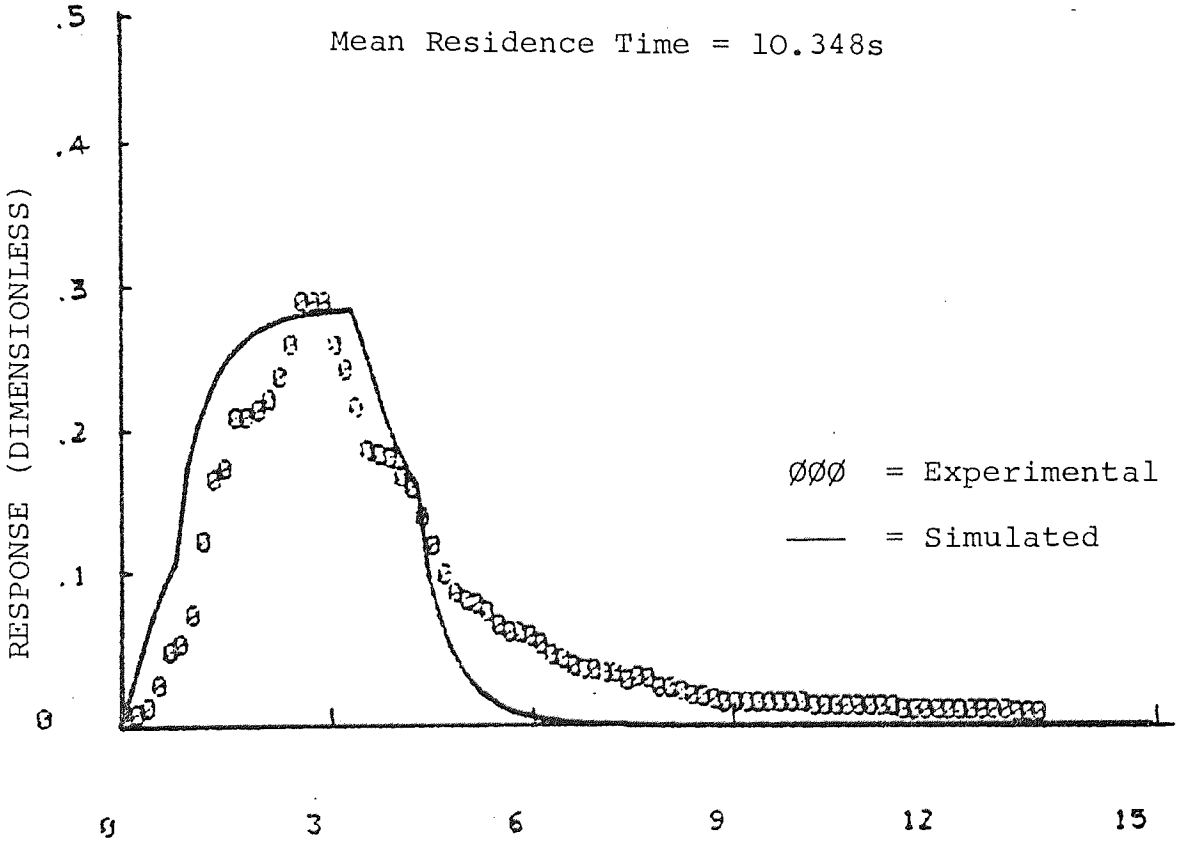

FIGURE 5.18

EXPERIMENT NUMBER: H5

A = 0.39 B = 0.48 M = 0.225

J = 0.015 K = 0.0125 N = 0.15 L = 0.1

Sum of Squared Errors = 0.1627

Variance = 1.933×10^{-3}

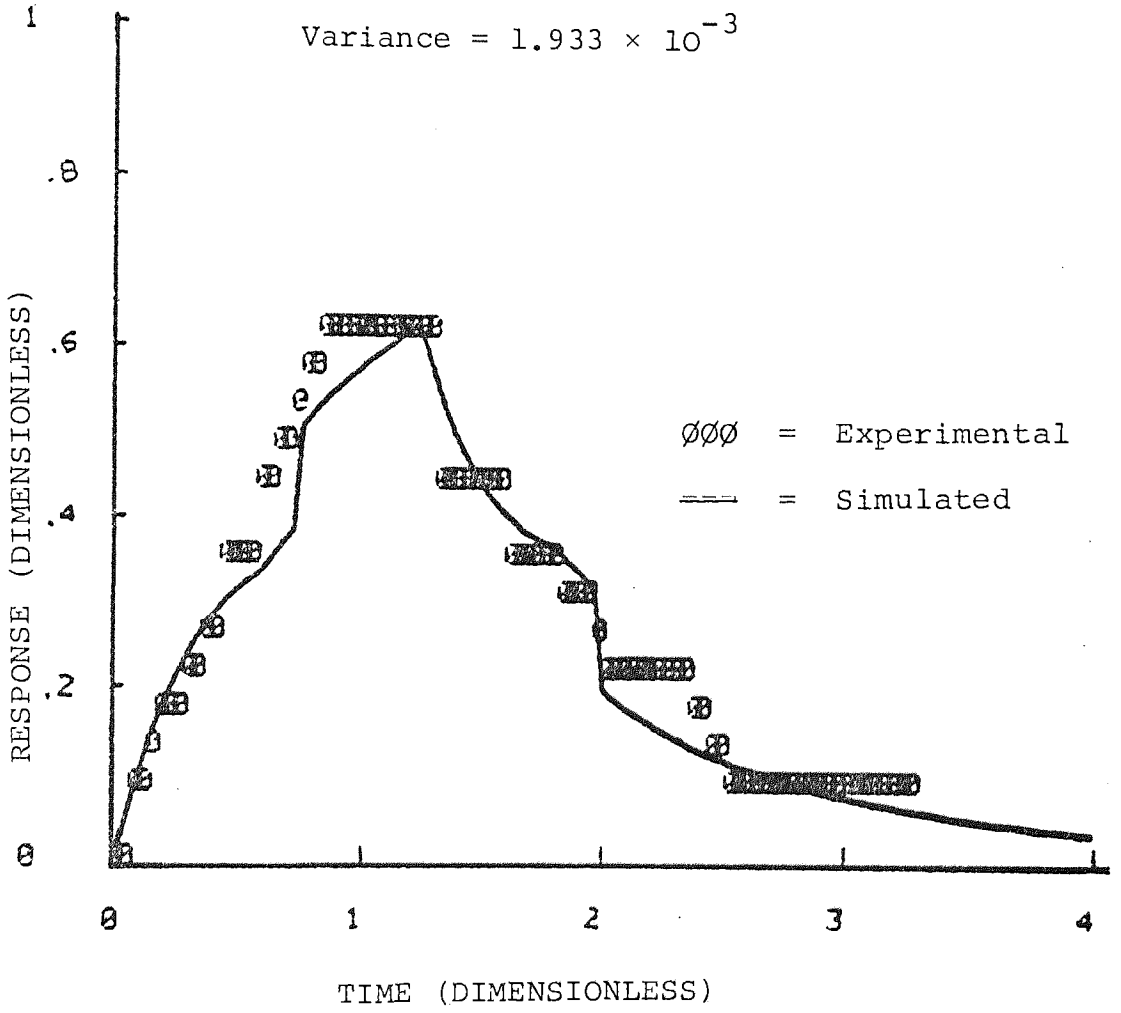

the 'sum of squared erros' and the variance between experimental and simulated response values are presented on the graphs. The last two factors were used as the criteria to determine the degree of fit between experimental and simulated response.

The graphs on Figure 5.12 to 5.16 show the various responses as the drying air flowrate increase from 0.13 kgs^{-1} to 0.23 kgs^{-1}. They show that the mean residence time decreased correspondingly from 16.787 seconds to 10.348 seconds. The volumes of the zones in the proposed air flow network are presented in Table 5.5. The trend in the parameters for the zones display different trends. Of particular interest is the trend in the three parallel streams in the air flow pattern. Stream A remained constant throughout at 0.6, while stream B increased from 0.2075 to 0.2905 as shown in Figure 5.16. The third stream, found by difference, decreased with increasing air flowrate, and varied from 0.1925 at air flowrate of 0.13 kgs^{-1} to 0.1095 at 0.23 kgs^{-1}. Correspondingly the proportion of zone C1 decreased from 0.175 at 0.13 kgs^{-1} to 0.12 at 0.23 kgs^{-1}. This phenomenon indicated that, as the air flowrate increased, more and more of it is 'active' in the drying process.

The first well-mixed zone in stream A was found by difference. Thus from the fractions of volumes presented in Figures 5.12 to 5.16, these were found to increase from 0.194 to 0.4075 at the highest experimental air flowrate. It was also observed that the plug flow zones A2 and B1 decreased

correspondingly as the drying air flowrate increased, thus J the fraction of the plug flow in stream B varied from 0.056 to 0.0125 and similarly M, in stream B from 0.30 to 0.20.

The whole response results indicate that higher air flowrates in the spray drier favour the predominance of well mixed zones. They also support previous works[86,90] that suggested that plug flow within a counter-current spray drier tends to decrease as air flowrate increases. The response curves exhibit a close degree of fit as evidenced by the sum of the squared errors which ranged closely between 0.142 and 0.245 while the variance from 1.716×10^{-3} to 2.956×10^{-3}.

The Humber Tracer Experiment computer printouts are presented in Figures 5.17 and 5.18. The experiments involved sampling the two exit ports from the spray chamber at the Number 1 and Number 2 cyclones. The response curves obtained from the Number 1 cyclone were not very sensitive and, as such, did not lend themselves much to analysis. Efforts were therefore concentrated on the response data from Number 2 cyclone. The various parameters are also shown in the curves, and once again there is a good degree of fit between the experimental and simulated responses, with the sum of squared errors on the average being about 0.18 and a variance of about 2.15×10^{-3}.

The evaluated parameters indicate that about 13.88% of the air into the spray drier passed through the by-pass suggesting that this proportion of the hot air into the drier was wasted. The general shape of the response curves show

a predominance of well mixed zones. An example is the first well mixed zone in stream A which was evaluated at 0.435 in Figure 5.17 and 0.4975 in Figure 5.18.

TABLE 5.5

ESTIMATED ZONES VOLUMES IN THE SPRAY DRIER AIR DISTRIBUTION NETWORK

EXPERIMENT NUMBER	STREAM A			STREAM B		STREAM C	TOTAL VOLUME V_T (m^3)
	A1	A2	A3	B1	B2		
SD 21	0.6372	0.1793	0.9606	0.4803	0.4003	0.5443	3.202
SD 22	0.6884	0.2081	0.9606	0.4803	0.4003	0.4643	3.202
SD 23	0.9286	0.2882	0.7205	0.4803	0.4003	0.3842	3.202
SD 24	1.0887	0.2882	0.6404	0.4163	0.3842	0.3842	3.202
SD 25	1.3689	0.0400	0.8325	0.4163	0.2241	0.3202	3.202
H 1	170.868	5.8920	29.4600	88.3800	51.0640	47.1360	392.80
H 5	195.4180	5.8920	4.9100	88.3800	58.9200	39.2800	392.80

DESIGN MODEL FOR SPRAY DRIER

6.1 INTRODUCTION

As was pointed out in Section 2.4, the development of a unified design model for spray drier performance has hitherto been empirical because of the complexity and diversity of parameters involved. It has been recognised that one of the salient aspects of spray drier design is the prediction of the spray droplets trajectories. The studies were initiated by Bailey, Slater and Eisenklam[110] who predicted droplet trajectories for some simple cases in a vortex flow and considered the relationship between heat and mass transfer at elevated temperatures. In addition Domingos and Roriz[111] in 1974 and Fabian[112] also in 1974 reported their work on droplet trajectories in swirling flows.

Fabian suggested an analytical approach by computing the flow pattern of the droplets spray for both laminar and turbulent boundary layers from a conical convergent nozzle with swirling throughput. Paris et al.[87] developed the mathematical model of the air flow pattern in a counter current spray drier by Tracer Analysis. Sen[113], on the other hand, used both the distributed parameters and the lumped parameters model to predict drier performance and concluded that the steady state temperature distribution within a spray drier lie between those predicted by the distributed parameters and lumped parameters models.

A more exhaustive attempt is the recent work by Gauvin

and Katta[109], and Ade John[86]. Gauvin's approach was basically Lagrangian. They identified the major design parameters as:

(a) Physical properties and the drying characteristics of the feed solution.

(b) The Droplet Size Distribution (DSD) and the largest drop diameter.

(c) Atomizer type and the drying air flow pattern.

(d) The heat and mass transfer rates in the drier.

The Guavin design method was based on the criterion that the size of the spray drier will be such the largest drop in the feed sprayed will be dry. They later tried to relax this restraint but this tended to impose a very rigorous guideline on the design method.

The Ade-John method was more experimental in that the various volumes in the proposed air flow pattern were measured and correlated in terms of the flow characteristics and he was able to predict the spray drier performance very closely

In the present work the approach is semi-empirical and numerical. The drying air flow pattern had been established by experimental and numerical method, and the drying characteristics was established by presentation of the mathematical model. The spray drying experimental data for experiment number SD20 shall be used as an example to develop the design model.

6.2 AIR RESIDENCE TIME DISTRIBUTION

From Table 5.5, the residence time of the air in the individual zones of the distribution network could be evaluated. Thus for the tracer analysis experiment number SD25:-

In zone A2:-

$$\theta_J = V_J/Q_T \qquad (6.1)$$

$$= \frac{0.0400}{0.3094}$$

$$= \underline{0.129s}$$

In zone A3:-

$$\theta_K = V_K/Q_T \qquad (6.2)$$

$$= \frac{0.8325}{0.3094}$$

$$= \underline{2.691s}$$

In zone B1:-

$$\theta_M = V_M/Q_T \qquad (6.3)$$

$$= \frac{0.4163}{0.3094}$$

$$= \underline{1.346s}$$

In zone B2:-

$$\theta_N = V_N/Q_T \qquad (6.4)$$

$$= \frac{0.2241}{0.3094}$$

$$= \underline{0.724s}$$

In zone C:-

$$\theta_L = V_L/Q_T \qquad (6.5)$$

$$= \frac{0.3202}{0.3094}$$

$$= \underline{1.035s}$$

The residence time in zone A3 can then be evaluated by difference and was found to be 4.42s.

The total residence time of air in the tower could then be evaluated as

$$\theta_T = \sum_{i=1}^{7} \theta_i$$

where i represents the individual seven zones in the network. Thus θ_T was 10.345 seconds.

6.3 DROP SIZE DISTRIBUTION

The drop size distribution was not measured directly in this study, but Ashton's[114], investigation on spray droplets dispersion at swirl nozzles in a spray drier has been helpful. He studied five formulations of Chalk slurry using five different pressure nozzles and sprayed them into the chamber of a transparent perspex spray drier and he used a high speed photographic technique to predict the drop size distribution in the ensuing spray. Essentially Ashton proposed that the drop size could be predicted in terms of the slurry flowrate, nozzle diameter, and other physical quantities of the system. Using Dimensional Analysis he established the sheet length as:-

$$L_s = 1871.35\ d_o (Re)^{-0.117} (We)^{-0.449} (D_G)^{-0.934} (\theta_c)^{-0.434} \quad (6.6)$$

He obtained a correlation coefficient of 0.9 for the above equation. From the knowledge of the sheet length and the predicted sheet velocity, (V_s), he predicted the drop size as follows:-

$$D_p = 0.524 \left(\frac{Q_S}{V_s^3 L_s \text{ Sin } \theta_c}\right)^{0.5} \quad (6.7)$$

He compared the predicted drop size to the experimentally measured volume surface mean diameter, and a regression analysis resulted in the following equation

$$D_{VS} = 0.547\ D_p + 76.8 \quad (6.8)$$

where D_{VS} is the surface mean diameter in microns. A correlation coefficient of 0.93 was obtained for equation (6.8).

Thus applying equations (6.6) to (6.8) for the similar conditions of the present work yield:

$$V_s = 15.20\ ms^{-1}$$
$$L_s = 22.3 \quad 10^{-3} m$$
$$\theta_c = 34.0^o$$
$$Q_S = 1.862 \times 10^{-2}/1405$$
$$= 1.3253 \times 10^{-5}\ m^3 s^{-1}$$

Therefore:

$$D_p = 0.524 \left|\frac{1.3253 \times 10^{-5}}{(15.2)^3 \times 22.3 \times 10^{-3} \text{ Sin } 34}\right|^{0.5}$$

$$= 2.883 \times 10^{-4} \text{ m.}$$

Thus $D_{VS} = \underline{2.325 \times 10^{-4} \text{m}}$

6.3.1 Number of Drops

Having calculated the drop size, it is now possible to predict the number of drops in the spray drying chamber.

Recall $Q_S = 1.3253 \times 10^{-5} \text{ m}^3\text{s}^{-1}$

$$\text{Volume of a drop} = \frac{\pi D_{VS}^3}{6}$$

$$= \frac{\pi (2.325 \times 10^{-4})^3}{6}$$

Then number of drops

$$= \frac{6. \times 1.3253 \times 10^{-5}}{\pi \times (2.325 \times 10^{-4})^3}$$

$$= \underline{2.0140 \times 10^6}$$

6.3.2 Droplets Residence Time

An overall heat balance over the spray drier during the residence of the droplets in the spray drier yields

$$\theta_D G_S \Delta C\lambda = G_a S(t_i - t_o)\bar{t} - G_s C_p (T_i - T_o) \qquad (6.9)$$

From experimental data and steam tables the following values were collected:

$G_a = 0.23\ kgs^{-1}$

$t_i = 205.0^{o}C$

$t_o = 140.0^{o}C$

$\bar{t} = 10.3475\ s$

$G_s = 1.862 \times 10^{-2}\ kgs^{-1}$

$T_i = 92.0^{o}C$

$T_o = 45^{o}C$

$\lambda = 2148.0\ KJ/KG$

$S = 1.0295\ kJ\ KG^{-1}\ {}^{o}K^{-1}$

$C_p = 0.7787\ KJ\ KG^{-1}\ {}^{o}K^{-1}$

Therefore

$$\theta_D = \frac{|(0.23\times1.0295\times10.3475\times65)-(1.862\times10^{-2}\times0.7787\times47)|}{1.862\times10^{-2}\times2148.0\times0.7787\times0.2}$$

$$= \underline{25.48\ s}$$

6.4 DRYING RATE

The mass transfer rate to a size range of droplets could be given as:

$$\frac{dm_i}{d\theta_i} = \pi D_v\ \rho_a d_i Sh\ n_i (H_s - H_i) \qquad (6.10)$$

The drying rate N_D over the whole droplets spectrum can be evaluated from the following equations

$$N_D = \pi\ D_V\ \rho_a D_{VS} NSh \Delta H_s \qquad (6.11)$$

The Sherwood Number is calculated from the Ranz-Marshall[29] equation:

$$Sh = 2.0 + 0.6Re^{0.5} Sc^{0.33} \qquad (2.16)$$

Using the experimental data and also data from International Critical Tables, the following parameters were evaluated:-

$$\rho_a = 7.4326 \times 10^{-1} \text{ kgm}^{-3}$$

$$\mu_a = 2.9571 \times 10^{-5} \text{ Nms}^{-2}$$

$$D_V = 5.8611 \times 10^{-5} \text{ m}^2\text{s}^{-1}$$

Then

$$Sh = 2.6590$$

and equation (6.11) yields

$$N_D = \pi 5.8611\times10^{-5}\times7.4326\times10^{-1}\times2.6590\times10^{-5}\times2.325\times10^{-4}\times2.0140\times10^{6}\times2.4744\times10^{-2}$$

$$= \underline{4.2164 \times 10^{-3} \text{ kgs}^{-1}}$$

6.5 FINAL PRODUCT MOISTURE CONTENT

The amount of moisture evaporated during the residence time of the droplets in the drier

$$= 4.2164 \times 10^{-4} \times 25.48$$

$$= 0.1075 \text{ kg.}$$

Slurry Flowrate

$$= 1.862 \times 10^{-2} \text{ kgs}^{-1}$$

Moisture in Slurry $= 0.335 \times 1.862 \times 10^{-2} \times 25.48$

$= 0.1590$ kg

Then dry powder in product

$= (1-0.335) \times 1.862 \times 10^{-2} \times 25.48$

$= 0.3156$ kg

The amount of unevaporated moisture

$= 0.1590-0.1075$

$= 5.15 \times 10^{-2}$ kg

Thus total powder and moisture

$= 0.3671$ kg

Therefore the final product moisture content

$$= \frac{5.15 \times 10^{-2}}{0.3671} \quad 100\%$$

$= \underline{14.029\%, \text{ wt/wt}}$

This compares favourably with the experimental moisture content of 13.50.

6.6 DRYING EFFICIENCY

The efficiency of the spray drying operation could be defined as the ratio of the heat used in evaporation to the total heat input[44,109]. That is

$$\eta_{Drying} = \frac{\text{Heat used in Evaporation}}{\text{Heat Input}}$$

$$= \frac{N_e \lambda}{G_a S(t_i - t_{\omega b}) + G_s C_p (T_i - T_{\omega b})} \qquad (6.12)$$

where N_e is the evaporative capacity of the evaporative capacity of the drier.

$T_{\omega b}$ is the wet bulb temperature of the drying air.

From psychometry, $T_{\omega b}$ was estimated at $76.67^{o}C$.

From the preliminary experiments carried out on the spray drier and refering to the results presented on Table 5.3, the average evaporative capacity of the drier during experiments number SD9 and SD10, the conditions of which are analogous to SD20, yields

$$N_e = 5.6486 \times 10^{-2} \text{ kgs}^{-1}$$

Using the other parameters in equation for efficiency yields

$$\eta_{\text{Drying}} = \underline{33.36\%}$$

Comments on the spray drier design model shall be offered in the next chapter.

CHAPTER SEVEN

DISCUSSION

DISCUSSION

7.1 SINGLE DROP EXPERIMENTS

The results obtained from the Thermal Conductivity experiments proved to be reliable and they compare favourably with published values [30, 115]. Values found in literature however do not relate the variation of the thermal conductivity with temperature as evaluated in the present work. Thus, apart from the use of the thermal conductivity data for heat balance on the crust, they present valuable data for future applications.

Audu[23,24] made the proposition that crust thickness was the controlling factor in a drying drop. His work however, was limited to low mass transfer rates and the drying phenomenon in his theory was by diffusion through the pores. There is yet to be published work at high mass transfer rates as attempted in this investigation.

The use of stereoscan analysis has been helpful in justifying the proposals put forward in this project as it had shown that the major controlling factors in the drop drying are crust thickness and the porosity of the material being dried and at high rates revealed crack formation justifyi pressure build up in accordance with the basis for the model proposed. The porosity of the slurries remained near constant at 0.3 throughout the experimental programme independent of temperatur and moisture content. This value also compares favourably with published values[116] and as such acceptable. Another

factor which could be considered is the chemical composition and chemical reactions in the different types of slurry handled. The data on the chemical composition of the slurries [104] show they are all similar with the exception of the Humber slurry which contained 5.0% Ferric Oxide (Fe_2O_3) as opposed to 1.9% in others. The peculiarity of the Humber slurry is because it is used in making "Sulphate Resisting" cement. These types of cement slurry by their composition and processing resist sulphates better than any other type of slurry.

In cement manufacture, the chemical reactions, i.e. crystallisation of amorphous dehydration products of clay, evolution of carbon dioxide from clay etc., take place at temperatures of 500°C and above [117] and it will be recalled that all efforts to produce a stable drop at temperatures above 400°C were abortive. Hence it can then be concluded that chemical composition and reactions do not affect the Drying Characteristics of the slurries except the porosity and crust thickness.

7.2 SPRAY DRYING AND RESIDENCE TIME DISTRIBUTION EXPERIMENTS

The RTD experiments established the distribution of drying air in the pilot plant and Humber spray driers; and this gave an indication of the air residence times in the various zones of the flow pattern network. The results obtained in these experiments concerning the predominance of well mixed zones at high flowrates together with the corresponding diminishing of plug flow zones were supported by similar findings by Ade-John [8]

and Paris et al.[87]. The numerical method used in simulating the tracer response is an iterative one using a digital computer. A search through literature shows that while there have been various attempts to simulate tracer response, none has yet been attempted by this approach. Paris et al.[87] tried to simulate the response analysis by a system of differential equations, but they used a TR-48EA1 Analogue computer for the solution.

The spray drying experiments yielded some facts concerning spray drier performance. They showed that the evaporative capacity of the drier increases with increasing air flowrates, which is not unusual since the high air flow ensures that more moisture be evaporated from the slurry feed. The thermal efficiency evaluated was between 0.6 and 0.8 shows a good drier performance at the particular drying air and slurry feed flowrates. The actual spray drying experiments however did not yield as low a final product moisture content as desired. This is evidenced by the final moisture content of between 20.0% and 12% and shown in the experimental results presented in the Appendix. The two feed flowrates experimented on show that the lower feed flow yield better drier performance than the higher one under the same set of conditions. These findings agree with those of Masters[44] who concluded that high inlet air temperature, low feed flowrates among other factors enhance the performance of a spray drier.

The proposed Design model worked remarkably well in predicting the performance of the spray drier. This is

evidenced by the deviation error of 3.91%. This gives credence to the theory that the drying performance of the drier could be predicted by that of the 'largest' drop in the drop size distribution. The overall drying efficiency of 33.36% reported by the deisgn model is not unexpected, as it gives support to the rather high final product moisture content reported in the experiments; and to the accuracy of the model. The reported drying efficiency indicated that the slurry flowrate is probably too high. Thus the spray drier had operated to its full capacity in removing as much moisture as it can from the slurry feed. The drying efficiency calculated by the design model is thus not a reflection on the model but on the drying parameters. It is not too low however considering that the reported efficiency values are between 40.0 and 50.0%[44,109].

CHAPTER EIGHT

CONCLUSIONS AND RECOMMENDATIONS

CONCLUSIONS AND RECOMMENDATIONS

8.1 CONCLUSIONS

The conclusions drawn from the investigations are presented in two parts: (i) Single Drop Experiments and (ii) Spray Drying Experiments.

8.1.1 Single Drop Experiments

1. The Thermal Conductivity of the crust was experimentally determined by a modified Lee's Disc method. The experimental data for each sample were well correlated by the polynomial:

$$k + A + BT + CT^2 + DT^3 + ... \qquad (5.1)$$

The variance ranged from 5.877×10^{-3} for Mason slurry to 1.124×10^{-3} for Shoreham slurry.

2. The Mass Tansfer Coefficient of the crust was predicted as a function of vapour pressure, vapour velocity through the pores, pore length and crust thickness. Thus:

$$K_c = \frac{\varepsilon^3 \rho}{5(1-\varepsilon)^2 \mu S^2 \beta} \qquad (3.20)$$

3. The crust thickness increases with increasing drying air temperatures and initial moisture content of the slurry drop.

4. The crust mass transfer coefficient decreases with increasing drying air temperature and initial moisture content of the drop.

5. The overall mass transfer coefficient and consequently the drying rate decreases with increasing drying air temperature and initial moisture content of the slurry.

6. There was good agreement between the experimental mass transfer coefficient and the proposed momentum transfer coefficient. A linear regression was carried out yielding a typical correlation coefficient of 0.9960 for Humber slurry at a standard deviation of 5.481×10^{-3}.

7. The structure of both internal and the external surface of the drops, as drying proceeds, confirmed the theory that steam is ejected from the drops during the drying process.

8.1.2 Spray Drying and Residence Time Distribution Experiments

8. The residence time distribution of the drying air in the spray drier was simulated and the model solved numerically and there was a favourable agreement between experimental and simulated responses. The degree of fit determined by the value of "sum of squared errors" which ranged between 0.145 and 0.245 while the variance from 1.716×10^{-3} to 2.956×10^{-3}.

9. The air flow pattern was determined by Tracer Analysis and showed that high flowrates favour well mixed zones in the spray drier with the plug flow zones tending to decrease proportionally.

10. The evaporative capicity of the pilot plant spray drier was determined and experiments prove that high air flowrates and temperature enhances the evaporative capacity of the drier.

11. The spray drying experiments carried out on the pilot plant spray drier established that high air temperature and low slurry flowrates enhances the spray drying operation.

12. The proposed design model was applied to the pilot plant spray drier and it predicted the spray drier performance with a 3.91% error deviation.

8.2 RECOMMENDATIONS FOR FURTHER WORK

1. The Single Drop Experiments should be extended to another drying medium such as steam.

2. The tracer response simulation program could be improved. Two suggestions are offered, (i) The response from each zone could be traced out individually and this will offer greater insight into the air flow pattern in the spray drier.
(ii) The method of evaluating the parameters is repetitive and very tedious. This could be minimised by evaluating initial values for the parameters by an adequate optimisation model.

3. Efforts should be directed at operating the spray drier under more varied conditions of air temperatures, slurry feed flowrate and slurry feed temperature at the nozzle. This would help to establish the maximum, minimum and optimum drying conditions of the drier.

4. A great deal of difficulty was encountered with the blocking of the nozzle by extraenous matter in the slurry. A filter system should be incorporated in future work. The use of centrifugal nozzles should be considered.

5. The possibility of pre-heating the slurry should be considered as this could improve the drying efficiency of the drier.

6. The dust recovery unit should be improved to include a valve system to control powder flow in the recovery chute.

7. The effect of noxious fumes like NO_x,SO_x on the drying characteristics and spray drying of cement slurries should be investigated.

8. A controller system could be incorporated into the spray drying unit such that a specified product moisture content could be achieved by controlling, say, the inlet and outlet air temperatures, feed flowrate, etc..

9. Finally, the spray drying experiments should be extended to other products such as chemicals, foodstuffs, etc..

APPENDICES

APPENDIX A

1. Tables A1-A5, Experimental measurements for the determination of the thermal conductivity of the various slurries.

2. Tables A6-A10, Results from the Fortran IV computer program to evaluate the thermal conductivity of the slurries.

3. Program Listing for the calculation of thermal conductivity of slurry samples by the modified Lee's disc experiment.

TABLE A1

SAMPLE:- WESTBURY SLURRY

CURRENT, I (amps)	VOLTAGE, V (volts)	ROOM (^{o}C) TEMPERATURE	DISC 1 (^{o}C) TEMPERATURE	DISC 2 (^{o}C) TEMPERATURE	HOT PLATE (^{o}C) TEMPERATURE
1.0	30.0	20.0	50.0	95.0	105.0
1.5	50.0	20.0	99.0	189.0	195.0
2.0	70.0	20.0	133.0	265.0	270.0
2.5	95.0	20.0	155.0	330.0	335.0
3.0	115.0	20.0	190.0	418.0	420.0
3.5	140.0	20.0	220.0	485.0	515.0
4.0	155.0	20.0	229.0	550.0	560.0
4.5	175.0	20.0	241.0	595.0	600.0
5.0	195.0	20.0	250.0	600.0	660.0

TABLE A2

SAMPLE:- NORTHFLEET SLURRY

CURRENT, I (amps)	VOLTAGE, V (volts)	ROOM (^{o}C) TEMPERATURE	DISC 1 (^{o}C) TEMPERATURE	DISC 2 (^{o}C) TEMPERATURE	HOT PLATE (^{o}C) TEMPERATURE
1.0	30.0	20.0	80.0	115.0	120.0
1.5	50.0	20.0	108.0	190.0	195.0
2.0	70.0	20.0	150.0	260.0	265.0
2.5	95.0	20.0	165.0	313.0	320.0
3.0	115.0	20.0	195.0	385.0	390.0
3.5	140.0	20.0	225.0	480.0	500.0
4.0	155.0	20.0	235.0	525.0	530.0
4.5	175.0	20.0	265.0	600.0	620.0
5.0	198.0	20.0	275.0	650.0	660.0

TABLE A3

SAMPLE:- SHOREHAM SLURRY

CURRENT, I (amps)	VOLTAGE, V (volts)	ROOM (^{O}C) TEMPERATURE	DISC 1 (^{O}C) TEMPERATURE	DISC 2 (^{O}C) TEMPERATURE	HOT PLATE (^{O}C) TEMPERATURE
1.0	30.0	25.0	68.0	117.0	125.0
1.5	50.0	25.0	88.0	166.0	175.0
2.0	70.0	23.0	118.0	265.0	270.0
2.5	95.0	23.0	136.0	340.0	350.0
3.0	115.0	24.0	174.0	413.0	425.0
3.5	140.0	23.0	183.0	495.0	498.0
4.0	155.0	23.0	200.0	530.0	550.0
4.5	175.0	23.0	255.0	620.0	630.0
5.0	195.0	23.0	270.0	655.0	660.0

TABLE A4

SAMPLE:- MASON SLURRY

CURRENT, I (amps)	VOLTAGE, V (volts)	ROOM (^{o}C) TEMPERATURE	DISC 1 (^{o}C) TEMPERATURE	DISC 2 (^{o}C) TEMPERATURE	HOT PLATE (^{o}C) TEMPERATURE
1.0	30.0	20.0	62.0	100.0	120.0
1.5	50.0	20.0	100.0	195.0	195.0
2.0	70.0	20.0	120.0	260.0	260.0
2.5	95.0	20.0	150.0	330.0	335.0
3.0	115.0	22.0	180.0	404.0	410.0
3.5	140.0	20.0	225.0	508.0	515.0
4.0	155.0	20.0	235.0	560.0	560.0
4.5	175.0	20.0	258.0	600.0	600.0
5.0	195.0	20.0	280.0	660.0	660.0

TABLE A5

SAMPLE:- HUMBER (S/R) SLURRY

CURRENT, I (amps)	VOLTAGE, V (volts)	ROOM (°C) TEMPERATURE	DISC 1 (°C) TEMPERATURE	DISC 2 (°C) TEMPERATURE	HOT PLATE (°C) TEMPERATURE
1.0	30.0	18.0	53.0	122.0	125.0
1.5	50.0	18.0	74.0	185.0	190.0
2.0	70.0	18.0	95.0	245.0	255.0
2.5	95.0	18.0	118.0	320.0	337.0
3.0	115.0	18.0	140.0	405.0	415.0
3.5	140.0	18.0	172.0	475.0	485.0
4.0	155.0	18.0	196.0	530.0	565.0
4.5	175.0	18.0	208.0	590.0	610.0
5.0	195.0	18.0	270.0	630.0	680.0

TABLE A6

SLURRY SAMPLE FROM: MASON

Temperature (^{o}C)	Thermal Conductivity ($W/M/^{o}C$)	
	Experimental	Calculated
55.0	0.1164	0.1360
87.0	0.2941	0.2073
120.0	0.1909	0.2911
195.0	0.5427	0.4949
260.0	0.6372	0.6612
335.0	0.8331	0.8218
410.0	0.9678	0.9503
515.0	1.0965	1.1259
560.0	1.1715	1.2295
600.0	1.4491	1.3539
660.0	1.6016	1.6285

TABLE A7

SAMPLE OF SLURRY FROM: NORTHFLEET

Temperature (^{o}C)	Thermal Conductivity (W/M/^{o}C)	
	Experimental	Calculated
62.0	0.4880	0.5339
120.0	0.7357	0.6059
195.0	0.6787	0.7985
265.0	0.9879	0.9951
320.0	1.1528	1.1244
390.0	1.2823	1.2366
500.0	1.2449	1.3174
530.0	1.3742	1.3363
620.0	1.4690	1.4747
660.0	1.6198	1.6178

TABLE A8

SLURRY SAMPLE FROM: WESTBURY

Temperature (°C)	Thermal Conductivity (W/M/°C)	
	Experimental	Calculated
105.0	0.3318	0.3263
195.0	0.5521	0.5641
270.0	0.7124	0.7239
335.0	0.8744	0.8420
420.0	0.9685	0.9787
515.0	1.1285	1.1232
560.0	1.1488	1.1938
600.0	1.3051	1.2603
660.0	1.3601	1.3692

TABLE A9

SLURRY SAMPLE FROM: SHOREHAM

Temperature (^{o}C)	Thermal Conductivity (W/M/^{o}C)	
	Experimental	Calculated
125.0	0.3975	0.4364
175.0	0.6134	0.5282
270.0	0.5676	0.6273
350.0	0.6356	0.6805
425.0	0.8402	0.7481
498.0	0.8424	0.8666
550.0	1.0017	1.0018
630.0	1.2797	1.3242
660.0	1.5210	1.4887

TABLE A10

SLURRY SAMPLE FORM: HUMBER

Temperature (^{o}C)	Thermal Conductivity (W/M/^{o}C)	
	Experimental	Calculated
60.0	0.2181	0.2209
95.0	0.2228	0.2202
117.0	0.2504	0.2367
125.0	0.2272	0.2453
190.0	0.3518	0.3467
255.0	0.4843	0.4694
337.0	0.5921	0.6043
415.0	0.6476	0.6991
485.0	0.8513	0.7815
565.0	0.9619	0.9454
610.0	1.0604	1.1149
680.0	1.5917	1.5744

Program Listing for the calculation of thermal conductivity of slurry samples by the Modified Lee's disc experiment.

```
      MASTER CON
       PROGRAM TO EVALUATE THE THERMAL CONDUCTIVITY OF SPECIMEN USING
       THE DATA COLLECTED FROM LEE'S DISC  EXPERIMENT.


       DIMENSION  TEMP1(50),TEMP2(50),TEMP3(50),RTEMP(50),EMIS(50)
       DIMENSION AMP(50),VOLT(50),CONDTY(50),BETA(50),X1(20),X2(20)
       DIMENSION Y1(20),AR(10,10),XR(10),Y3(50),XM(10),BC(10)
       CALL OPENINOGPH
       DIAM=5.06E-2
       PIE=3.1412
       PORSTY=.450
       AREA1=4.01E-3
       AREA11=3.33E-2
       AREA2=2.00E-3
       AREA3=4.01E-3
       SUM1=0.0
       SUM2=0.0
       SUM3=0.0
       SUM4=0.0
       SUM5=0.0
       SUM6=0.0

       READ(1,100)N
       READ(1,110)(TEMP1(I),I=1,N)
       READ(1,110)(TEMP2(I),I=1,N)
       READ(1,110)(TEMP3(I),I=1,N)
       READ(1,110)(RTEMP(I),I=1,N)
       READ(1,110)(AMP(I),I=1,N)
       READ(1,110)(VOLT(I),I=1,N)
       READ(1,110)(BETA(I),I=1,N)
       READ(1,120)N4,(XM(I),I=1,N4)
  100  FORMAT(I2)
  110  FORMAT(12F0.0)
  120  FORMAT(I2,6E0.0)
       XF=750.0
       X2(1)=50.0
       N2=(XF-X2(1))/50.

       AREA22=AREA2*(1-PORSTY)
       DO 10 I=1,N
       AREAS=(1-PORSTY)*PIE*DIAM*BETA(I)
       IF(VOLT(I)-20.0)20,20,30
   20  AREAE=(1-PORSTY)*2.01E-3
       GO TO 31
   30  AREA1=AREA11
       AREA2=AREA22
       AREAE=PIE*(DIAM**2)*(1-PORSTY)/4.00
       GO TO 31
   31  A=AREA1*(TEMP1(I)-RTEMP(I))
       B=AREA2*(TEMP2(I)-RTEMP(I))
       D=AREA3*(TEMP3(I)-RTEMP(I))
       TEMP=(TEMP2(I)+TEMP3(I))/2.0
```

```
      C=AREAS*(TEMP-RTEMP(I))
      EMIS(I)=(AMP(I)*VOLT(I))/(A+B+C+D)
      X=AREAS*(TEMP2(I)+TEMP3(I)-(2*RTEMP(I)))/4.0
      Y=AREA3*(TEMP3(I)-RTEMP(I))
      CONDTY(I)=EMIS(I)*BETA(I)*(C+2*D)/(2.*AREAE*(TEMP2(I)
   10 CONTINUE
      M=2
      M1=M+1
      M2=M+2
      DO 11 J=1,M1
      DO 12 I=1,N
      SUM1=SUM1+TEMP1(I)**(J-1)
      SUM2=SUM2+TEMP1(I)**J
      SUM3=SUM3+TEMP1(I)**(J+1)
      SUM5=SUM5+CONDTY(I)*TEMP1(I)**(J-1)
   12 CONTINUE
      AR(J,1)=SUM1
      AR(J,2)=SUM2
      AR(J,3)=SUM3
      AR(J,M2)=SUM5
   11 CONTINUE
      CALL GAUSS(AR,M1,XR)
      DO 14 I=1,N2
      X2(I+1)=X2(I)+50.0
      DO 13 L=1,N4
      SUM6=SUM6+XM(L)*(X2(I)**(L-1))
   13 CONTINUE
      Y1(I)=SUM6
      SUM6=0.0
   14 CONTINUE
      DO 15 I=1,N
      DO 16 MU=1,N4
      SUM4=SUM4+XM(MU)*(TEMP1(I)**(MU-1))
   16 CONTINUE
      Y3(I)=SUM4
      SUM4=0.0
   15 CONTINUE
      CALL SHIFT2(100.,100.)
      CALL CHASIZ(2.6,2.3)
      NPTI=N2
      NPTS=N
      NSYM=7
      NSYM1=5
      NSPACE=0
      AC=AMAX1(Y1(N2),CONDTY(N))
      AC1=AC+0.10
      CALL AXIPOS(1,0.,0.,125.,1)
      CALL AXIPOS(1,0.,0.,150.,2)
      CALL AXISCA(3,5,0.,800.,1)
      CALL AXISCA(3,5,0.0,AC1,2)
      CALL AXIDRA(1,1,1)
      CALL AXIDRA(-1,-1,2)
      CALL MOVTO2(50.0,200.0)
```

```
      CALL CHARJL(12HFIGURE 5.1*.)
      CALL MJVTJ2(15.0,190.0)
      CALL CHARJL(33HCJRRELATED THERMAL CJNDUCTIVITY*.)
      CALL MJVTJ2(15.0,180.0)
      CALL CHARJL(33HFJR SLURRY SAMPLE FRJM WESTBURY*.)
      CALL CHAANG(90.0)
      CALL MJVTJ2(-15.0,20.0)
      CALL CHARJL(47HTHERMAL CJNDUCTIVITY (WATTS/METERS/DEG.C
      CALL CHAANG(0.0)
      CALL MJVTJ2(30.0,-15.0)
      CALL CHARJL(30HTEMPERATURE(DEG. CENTIGRADE)*.)
      CALL MJVTJ2(80.0,40.0)
      CALL SYMBJL(NSYM)
      CALL MJVTJ2(85.0,40.0)
      CALL CHARJL(16HE*LXPERIMENTAL*.)
      CALL GRASYM(TEMP1,CJNDTY,NPTS,NSYM,NSPACE)
      CALL GRACUR(X2,Y1,NPT1)
      CALL MJVTJ2(-50.0,-40.0)
      CALL LINTJ2(-50.0,250.0)
      CALL LINTJ2(160.0,250.0)
      CALL LINTJ2(160.0,-40.0)
      CALL LINTJ2(-50.,-40.)
      CALL DEVEND
      STJP
      END

      SUBRJUTINE GAUSS(A,N,X)
      DIMENSIJN A(10,10), X(10)
      NA=N+1
      DJ 10 J=1,N-1
      KB=J+1
      KA=J
      C=ABS(A(J,J))
      DJ 20 I=KB,N
      IF(C-ABS(A(I,J)))30,20,20
   30 C=ABS(A(I,J))
      KA=I
   20 CJNTINUE
      DJ 40 K=J,N+1
      B=A(J,K)
      A(J,K)=A(KA,K)
   40 A(KA,K)=B
      DJ 10 I=KB,N
      B=A(I,J)/A(J,J)
      DJ 10 K=J,N+1
   10 A(I,K)=A(I,K)-A(J,K)*B
      DJ 50 I=1,N-1
      NII=NA-I
      B=A(NII,NA)/A(NII,NII)
      L=1+I
      DJ 60 K=L,N
      J=NA-K
   60 A(J,NA)=A(J,NA)-A(J,NII)*B
      A(NII,NII)=1.
   50 A(NII,NA)=B
```

```
      A(I,NA)=A(I,NA)/A(I,I)
      A(I,I)=1.
      DO 105 J=1,N
      X(J)=A(J,NA)
  105 CONTINUE
      RETURN
      END
      FINISH
```

APPENDIX B

1. Tables B1 - B75, Data from the Single Drop Experiments.

2. Fortran IV program listing for calculating drying characteristics of slurry samples.

Table B1

Sample: NORTHFLEET SLURRY

Drying Air Temperature: 200^{o}C

Initial Drop Moisture Content: 30%, wt/wt

Initial Drop Size: 5.0×10^{-3}m

Air Flowrate: 1.0×10^{-3} kgs^{-1}

DRYING TIME (MIN)	HUMIDITIES (KG/KG)	
	UPSTREAM $\times 10^{-3}$	DOWNSTREAM $\times 10^{-3}$
0	0.8253	1.1312
1	0.8253	1.3923
2	0.8253	1.2821
3	0.8253	1.2821
4	0.8253	1.2821
5	0.8253	1.2821
6	0.8253	1.1797
7	0.8253	1.1797
8	0.8253	1.1797
9	0.8253	1.1797
10	0.8253	1.1797
15	0.8253	1.1312
20	0.8253	1.1312
25	0.8253	1.1312
30	0.8253	1.1312

Table B2

Sample: NORTHFLEET SLURRY

Drying Air Temperature : 300^{o}C

Initial Drop Moisture Content: 30% wt/wt

Initial Drop Size: 3.8×10^{-3} m

Air Flowrate: 1.0×10^{-3} kgs^{-1}

DRYING TIME (MIN)	HUMIDITIES (KG/KG)	
	UPSTREAM $\times 10^{-3}$	DOWNSTREAM $\times 10^{-3}$
0	0.8253	0.9960
1	0.8253	1.1312
2	0.8253	1.7742
3	0.8253	1.8461
4	0.8253	1.5731
5	0.8253	1.5731
6	0.8253	1.6378
7	0.8253	1.6378
8	0.8253	1.2821
9	0.8253	1.1312
10	0.8253	1.1312
15	0.8253	1.0394
20	0.8253	1.0394
25	0.8253	1.0394
30	0.8253	1.0394

Table B3

Sample: NORTHFLEET SLURRY

Drying Air Temperature: 400°C

Initial Drop Moisture Content: 30% wt/wt

Initial Drop Size: 3.0×10^{-3} m

Air Flowrate: 1.0×10^{-3} kgs^{-1}

DRYING TIME (MIN)	HUMIDITIES (KG/KG)	
	UPSTREAM $\times 10^{-3}$	DOWNSTREAM $\times 10^{-3}$
0	0.8253	0.9960
1	0.8253	0.9960
2	0.8253	2.6174
3	0.8253	2.0773
4	0.8253	1.8461
5	0.8253	1.7742
6	0.8253	1.7048
7	0.8253	1.6378
8	0.8253	1.6378
9	0.8253	1.6378
10	0.8253	1.6378
15	0.8253	1.5107
20	0.8253	1.5107
25	0.8253	1.5107
30	0.8253	1.5107

Table B4

Sample: NORTHFLEET SLURRY

Drying Air Temperature: 200°C

Initial Drop Moisture Content: 35% wt/wt

Initial Drop Size: 4.5×10^{-3} m

Air Flowrate: 1.0×10^{-3} kgs^{-1}

DRYING TIME (MIN)	HUMIDITIES (KG/KG)	
	UPSTREAM $\times 10^{-3}$	DOWNSTREAM $\times 10^{-3}$
0	0.8253	2.0773
1	0.8253	3.0431
2	0.8253	2.6174
3	0.8253	2.3336
4	0.8253	2.2452
5	0.8253	2.2452
6	0.8253	2.2452
7	0.8253	2.2452
8	0.8253	2.2452
9	0.8253	2.2452
10	0.8253	2.2452
15	0.8253	2.2452
20	0.8253	2.2452
25	0.8253	2.2452
30	0.8253	2.2452

Table B5

Sample: NORTHFLEET SLURRY

Drying Air Temperature: 300°C

Initial Drop Moisture Content: 35% wt/wt

Initial Drop Size: 3.0×10^{-3}

Air Flowrate: 1.0×10^{-3} kgs^{-1}

DRYING TIME (MIN)	HUMIDITIES (KG/KG)	
	UPSTREAM $\times 10^{-3}$	DOWNSTREAM $\times 10^{-3}$
0	0.8253	0.9542
1	0.8253	0.9960
2	0.8253	1.0394
3	0.8253	1.2300
4	0.8253	1.3923
5	0.8253	1.5107
6	0.8253	1.5107
7	0.8253	1.2300
8	0.8253	1.1797
9	0.8253	1.1312
10	0.8253	1.1312
15	0.8253	1.0844
20	0.8253	0.9960
30	0.8253	0.9960

Table B6

Sample: NORTHFLEET SLURRY

Drying Air Temperature: 400°C

Initial Drop Moisture Content: 35% wt/wt

Initial Drop Size: 2.2×10^{-3} m

Air Flowrate: 1.0×10^{-3} kgs^{-1}

DRYING TIME (MIN)	HUMIDITIES (KG/KG)	
	UPSTREAM $\times 10^{-3}$	DOWNSTREAM $\times 10^{-3}$
0	0.7673	0.8019
1	0.7673	0.8019
2	0.7673	1.1312
3	0.7673	1.3923
4	0.7673	1.4504
5	0.7673	1.3923
6	0.7673	1.5107
7	0.7673	1.7048
8	0.7673	1.1312
9	0.7673	1.0844
10	0.7673	0.9960
15	0.7673	0.9960
20	0.7673	0.9960
30	0.7673	0.9960

Table B7

Sample: NORTHFLEET SLURRY

Drying Air Temperature: 200°C

Initial Drop Moisture Content: 45%, wt/wt

Initial Drop Size: 4.0×10^{-3} m

Air Flowrate: 1.0×10^{-3} kgs^{-1}

DRYING TIME (MIN)	HUMIDITIES (KG/KG)	
	UPSTREAM $\times 10^{-3}$	DOWNSTREAM $\times 10^{-3}$
0	0.8253	1.7742
1	0.8253	1.9205
2	0.8253	1.9205
3	0.8253	1.9205
4	0.8253	1.9205
5	0.8253	1.9975
6	0.8253	2.0773
7	0.8253	2.0773
8	0.8253	1.9975
9	0.8253	1.9975
10	0.8253	1.9975
15	0.8253	1.8461
30	0.8253	1.7742

Table B8

Sample: NORTHFLEET SLURRY

Drying Air Temperature: 300°C

Initial Drop Moisture Content: 45% wt/wt

Initial Drop Size: 3.0×10^{-3} m

Air Flowrate: 1.0×10^{-3} kgs^{-1}

DRYING TIME (MIN)	HUMIDITIES (KG/KG)	
	UPSTREAM $\times 10^{-3}$	DOWNSTREAM $\times 10^{-3}$
0	0.8253	2.1598
1	0.8253	2.6174
2	0.8253	2.8231
3	0.8253	2.8231
4	0.8253	2.8231
5	0.8253	2.8231
6	0.8253	2.9313
7	0.8253	2.8231
8	0.8253	2.8231
9	0.8253	2.8231
10	0.8253	2.6174
15	0.8253	2.6174
20	0.8253	2.6174
30	0.8253	2.1598

TABLE B9

Sample: NORTHFLEET SLURRY

Drying Air Temperature: 400^{o}C

Initial Drop Moisture Content: 45% wt/wt

Initial Drop Size: 2.2×10^{-3} m

Air Flowrate: 1.0×10^{-3} kgs^{-1}

DRYING TIME (MIN)	HUMIDITIES (KG/KG)	
	UPSTREAM $\times 10^{-3}$	DOWNSTREAM $\times 10^{-3}$
0	0.8253	3.1586
1	0.8253	3.4015
2	0.8253	4.2333
3	0.8253	3.7970
4	0.8253	3.5290
5	0.8253	3.4647
6	0.8253	3.4267
7	0.8253	3.4015
8	0.8253	3.4015
9	0.8253	3.4015
10	0.8253	3.4015
15	0.8253	3.2781
20	0.8253	3.2781
30	0.8253	3.1586

TABLE B10

Sample: NORTHFLEET SLURRY

Drying Air Temperature: 200°C

Initial Drop Moisture Content: 50% wt/wt

Initial Drop Size: 4.0×10^{-3} m

Air Flowrate: 1.0×10^{-3} kgs^{-1}

DRYING TIME (MIN)	HUMIDITIES (KG/KG)	
	UPSTREAM $\times 10^{-3}$	DOWNSTREAM $\times 10^{-3}$
0	0.8253	1.6378
1	0.8253	1.7742
2	0.8253	1.9205
3	0.8253	1.9975
4	0.8253	1.9975
5	0.8253	1.9205
6	0.8253	1.9205
7	0.8253	1.9205
8	0.8253	1.9205
9	0.8253	1.9205
10	0.8253	1.9205
15	0.8253	1.6378
20	0.8253	1.6378
30	0.8253	1.6378

TABLE B11

Sample: NORTHFLEET SLURRY

Drying Air Temperature: 300°C

Initial Drop Moisture Content: 50% wt/wt

Initial Drop Size: 3.0×10^{-3} m

Air Flowrate: 1.0×10^{-3} kgs^{-1}

DRYING TIME (MIN)	HUMIDITIES (KG/KG)	
	UPSTREAM $\times 10^{-3}$	DOWNSTREAM $\times 10^{-3}$
0	0.8253	3.1586
1	0.8253	3.4015
2	0.8253	3.4015
3	0.8253	3.4015
4	0.8253	3.4015
5	0.8253	3.4015
6	0.8253	3.4015
7	0.8253	3.4015
8	0.8253	3.4015
9	0.8253	3.4015
10	0.8253	3.4015
15	0.8253	3.2781
20	0.8253	3.2781
30	0.8253	3.2781

TABLE B12

Sample: NORTHFLEET SLURRY

Drying Air Temperature: 400^{o}C

Initial Drop Moisture Content: 50% wt/wt

Initial Drop Size: 2.6×10^{-3} m

Air Flowrate: 1.0×10^{-3} kgs^{-1}

DRYING TIME (MIN)	HUMIDITIES (KG/KG)	
	UPSTREAM $\times 10^{-3}$	DOWNSTREAM $\times 10^{-3}$
0	0.8253	3.1586
1	0.8253	4.0832
2	0.8253	4.2333
3	0.8253	4.2333
4	0.8253	4.2333
5	0.8253	3.5290
6	0.8253	3.4015
7	0.8253	3.4015
8	0.8253	3.4015
9	0.8253	3.4015
10	0.8253	3.1586
15	0.8253	3.1586
20	0.8253	3.1586
30	0.8253	3.1586

TABLE B13

Sample: NORTHFLEET SLURRY

Drying Air Temperature: 200°C

Initial Drop Moisture Content: 55% wt/wt

Initital Drop Size: 3.0×10^{-3} m

Air Flowrate: 1.0×10^{-3} kgs^{-1}

DRYING TIME (MIN)	HUMIDITIES (KG/KG)	
	UPSTREAM $\times 10^{-3}$	DOWNSTREAM $\times 10^{-3}$
0	0.8253	3.2781
1	0.8253	3.3147
2	0.8253	3.4015
3	0.8253	3.4267
4	0.8253	3.4267
5	0.8253	3.4015
6	0.8253	3.4015
7	0.8253	3.4015
8	0.8253	3.3765
9	0.8253	3.3765
10	0.8253	3.3765
15	0.8253	3.3147
20	0.8253	3.2781
30	0.8253	3.2781

TABLE B14

Sample: NORTHFLEET SLURRY

Drying Air Temperature: 200°C

Initial Drop Moisture Content: 55% wt/wt

Initial Drop Size: 2.5×10^{-3} m

Air Flowrate: 1.0×10^{-3} kgs^{-1}

DRYING TIME (MIN)	HUMIDITIES (KG/KG)	
	UPSTREAM $\times 10^{-3}$	DOWNSTREAM $\times 10^{-3}$
0	0.8253	3.5290
1	0.8253	3.5290
2	0.8253	3.7970
3	0.8253	3.7970
4	0.8253	3.5290
5	0.8253	3.5290
6	0.8253	3.5290
7	0.8253	3.5290
8	0.8253	3.5290
9	0.8253	3.5290
10	0.8253	3.5290
15	0.8253	3.5290
20	0.8253	3.5290
30	0.8253	3.5290

TABLE B15

Sample: NORTHFLEET SLURRY

Drying Air Temperature: 400°C

Initial Drop Moisture Content: 55% wt/wt

Initial Drop Size: 2.0×10^{-3} m

Air Flowrate: 1.0×10^{-3} kgs^{-1}

DRYING TIME (MIN)	HUMIDITIES (KG/KG)	
	UPSTREAM $\times 10^{-3}$	DOWNSTREAM $\times 10^{-3}$
0	0.8253	3.4015
1	0.8253	4.0823
2	0.8253	4.2333
3	0.8253	6.4652
4	0.8253	7.6768
5	0.8253	4.2333
6	0.8253	4.2333
7	0.8253	3.5290
8	0.8253	3.5290
9	0.8253	3.5920
10	0.8253	3.5920
15	0.8253	3.5920
20	0.8253	3.5920
30	0.8253	3.5920

TABLE B16

Sample: MASON SLURRY

Drying Air Temperature: 200°C

Initial Drop Moisture Content: 30% wt/wt

Initial Drop Size: 5.0×10^{-3} m

Air Flowrate: 1.0×10^{-3} kgs^{-1}

DRYING TIME (MIN)	HUMIDITIES (KG/KG)	
	UPSTREAM $\times 10^{-3}$	DOWNSTREAM $\times 10^{-3}$
0	0.9542	3.0659
1	0.9542	3.1586
2	0.9542	3.1704
3	0.9542	3.1704
4	0.9542	3.1586
5	0.9542	3.1586
6	0.9542	3.1586
7	0.9542	3.1586
8	0.9542	3.1586
9	0.9542	3.1586
10	0.9542	3.0431
15	0.9542	3.0431
20	0.9542	3.0431
25	0.9542	3.0431
30	0.9542	3.0431

TABLE B17

Sample: MASON SLURRY

Drying Air Temperature: 300°C

Initial Drop Moisture Content: 30% wt/wt

Initial Drop Size: 5.0×10^{-3} m

Air Flowrate: 1.0×10^{-3} kgs^{-1}

DRYING TIME (MIN)	HUMIDITIES (KG/KG)	
	UPSTREAM $\times 10^{-3}$	DOWNSTREAM $\times 10^{-3}$
0	0.9542	3.0431
1	0.9542	3.4015
2	0.9542	3.4015
3	0.9542	3.2781
4	0.9542	3.1586
5	0.9542	3.1586
6	0.9542	3.1352
7	0.9542	3.1352
8	0.9542	3.1352
9	0.9542	2.9313
10	0.9542	2.9313
15	0.9542	2.9313
20	0.9542	2.9313
25	0.9542	2.9313
30	0.9542	2.9313

TABLE B18

Sample: MASON SLURRY

Drying Air Temperature: 400^{o}C

Initial Drop Moisture Content: 30% wt/wt

Initial Drop Size: 5.0×10^{-3}m

Air Flowrate: 1.0×10^{-3} kgs^{-1}

DRYING TIME (MIN)	HUMIDITIES (KG/KG)	
	UPSTREAM $\times 10^{-3}$	DOWNSTREAM $\times 10^{-3}$
0	0.9542	2.9313
1	0.9542	3.5290
2	0.9542	3.5290
3	0.9542	3.4015
4	0.9542	3.2781
5	0.9542	3.2781
6	0.9542	3.1586
7	0.9542	3.1586
8	0.9542	2.8231
9	0.9542	2.8231
10	0.9542	2.8231
15	0.9542	2.8231
20	0.9542	2.8231
25	0.9542	2.8231
30	0.9542	2.8231

TABLE B19

Sample: MASON SLURRY

Drying Air Temperature: 200°C

Initial Drop Moisture Content: 35% wt/wt

Initial Drop Size: 4.0×10^{-3} m

Air Flowrate: 1.0×10^{-3} kgs^{-1}

DRYING TIME (MIN)	HUMIDITIES (KG/KG)	
	UPSTREAM $\times 10^{-3}$	DOWNSTREAM $\times 10^{-3}$
0	0.9542	3.0659
1	0.9542	3.1586
2	0.9542	3.1586
3	0.9542	3.1352
4	0.9542	3.1352
5	0.9542	3.1352
6	0.9542	3.0431
7	0.9542	3.0431
8	0.9542	3.0431
9	0.9542	3.0431
10	0.9542	3.0431
15	0.9542	3.0431
20	0.9542	3.0431
30	0.9542	3.0431

TABLE B20

Sample: MASON SLURRY

Drying Air Temperature: 300°C

Initial Drop Moisture Content: 35% wt/wt

Initial Drop Size: 4.0×10^{-3} m

Air Flowrate: 1.0×10^{-3} kgs^{-1}

DRYING TIME (MIN)	HUMIDITIES (KG/KG)	
	UPSTREAM $\times 10^{-3}$	DOWNSTREAM $\times 10^{-3}$
0	0.9542	3.0431
1	0.9542	3.2781
2	0.9542	3.2298
3	0.9542	3.2298
4	0.9542	3.1586
5	0.9542	3.1586
6	0.9542	3.1586
7	0.9542	2.9313
8	0.9542	2.9313
9	0.9542	2.9313
10	0.9542	2.9313
15	0.9542	2.9313
20	0.9542	2.9313
30	0.9542	2.9313

TABLE B21

Sample: MASON SLURRY

Drying Air Temperature: 400°C

Initial Drop Moisture Content: 35% wt/wt

Initial Drop Size: 3.5×10^{-3} m

Air Flowrate: 1.0×10^{-3} kgs^{-1}

DRYING TIME (MIN)	HUMIDITIES (KG/KG)	
	UPSTREAM $\times 10^{-3}$	DOWNSTREAM $\times 10^{-3}$
0	0.9542	2.9313
1	0.9542	3.5290
2	0.9542	3.2781
3	0.9542	3.2298
4	0.9542	3.2298
5	0.9542	3.1586
6	0.9542	3.1586
7	0.9542	2.8231
8	0.9542	2.8231
9	0.9542	2.8231
10	0.9542	2.8231
15	0.9542	2.8231
20	0.9542	2.8231
30	0.9542	2.8231

TABLE B22

Sample: MASON SLURRY

Drying Air Temperature: 200°C

Initial Drop Moisture Content: 45% wt/wt

Initial Drop Size: 4.0×10^{-3} m

Air Flowrate: 1.0×10^{-3} kgs^{-1}

DRYING TIME (MIN)	HUMIDITIES (KG/KG)	
	UPSTREAM $\times 10^{-3}$	DOWNSTREAM $\times 10^{-3}$
0	0.9542	3.1004
1	0.9542	3.1586
2	0.9542	3.2781
3	0.9542	3.1586
4	0.9542	3.1586
5	0.9542	3.1586
6	0.9542	3.1586
7	0.9542	3.0431
8	0.9542	3.0431
9	0.9542	3.0431
10	0.9542	3.0431
15	0.9542	3.0431
20	0.9542	3.0431
25	0.9542	3.0431
30	0.9542	3.0431

TABLE B23

Sample: MASON SLURRY

Drying Air Temperature: 300°C

Initial Drop Moisture Content: 45% wt/wt

Initial Drop Size: 3.5×10^{-3} m

Air Flowrate: 1.0×10^{-3} kgs^{-1}

DRYING TIME (MIN)	HUMIDITIES (KG/KG)	
	UPSTREAM $\times 10^{-3}$	DOWNSTREAM $\times 10^{-3}$
0	0.9542	2.9867
1	0.9542	3.5290
2	0.9542	3.5290
3	0.9542	3.4015
4	0.9542	3.2781
5	0.9542	3.1586
6	0.9542	3.1586
7	0.9542	3.1586
8	0.9542	2.9313
9	0.9542	2.9313
10	0.9542	2.9313
15	0.9542	2.9313
20	0.9542	2.9313
25	0.9542	2.9313
30	0.9542	2.9313

TABLE B24

Sample: MASON SLURRY

Drying Air Temperature: 400°C

Initial Drop Moisture Content: 45% wt/wt

Initial Drop Size: 4.30×10^{-3} m

Air Flowrate: 1.0×10^{-3} kgs^{-1}

DRYING TIME (MIN)	HUMIDITIES (KG/KG)	
	UPSTREAM $\times 10^{-3}$	DOWNSTREAM $\times 10^{-3}$
0	0.9542	2.8767
1	0.9542	4.0832
2	0.9542	4.2333
3	0.9542	3.7970
4	0.9542	3.5290
5	0.9542	3.2781
6	0.9542	3.1586
7	0.9542	3.1586
8	0.9542	2.8231
9	0.9542	2.8231
10	0.9542	2.8231
15	0.9542	2.8231
20	0.9542	2.8231
25	0.9542	2.8231
30	0.9542	2.8231

TABLE B25

Sample: MASON SLURRY

Drying Air Temperature: 200°C

Initial Drop Moisture Content: 50% wt/wt

Initial Drop Size: 3.5×10^{-3} m

Air Flowrate: 1.0×10^{-3} kgs^{-1}

DRYING TIME (MIN)	HUMIDITIES (KG/KG)	
	UPSTREAM $\times 10^{-3}$	DOWNSTREAM $\times 10^{-3}$
0	0.9542	3.1004
1	0.9542	3.2781
2	0.9542	3.2781
3	0.9542	3.1586
4	0.9542	3.1004
5	0.9542	3.1004
6	0.9542	3.0888
7	0.9542	3.0888
8	0.9542	3.0431
9	0.9542	3.0431
10	0.9542	3.0431
15	0.9542	3.0431
20	0.9542	3.0431
25	0.9542	3.0431
30	0.9542	3.0431

TABLE B26

Sample: MASON SLURRY

Drying Air Temperature: 300°C

Initial Drop Moisture Content: 50% wt/wt

Initial Drop Size: 4.8×10^{-3} m

Air Flowrate: 1.0×10^{-3} kgs^{-1}

DRYING TIME (MIN)	HUMIDITIES (KG/KG)	
	UPSTREAM $\times 10^{-3}$	DOWNSTREAM $\times 10^{-3}$
0	0.9542	2.9867
1	0.9542	3.7970
2	0.9542	4.7138
3	0.9542	5.0608
4	0.9542	4.0832
5	0.9542	3.7970
6	0.9542	3.5290
7	0.9542	3.2781
8	0.9542	2.9313
9	0.9542	2.9313
10	0.9542	2.9313
15	0.9542	2.9313
20	0.9542	2.9313
25	0.9542	2.9313
30	0.9542	2.9313

TABLE B27

Sample: MASON SLURRY

Drying Air Temperature: 400°C

Initial Drop Moisture Content: 50% wt/wt

Initial Drop Size: 4.5×10^{-3} m

Air Flowrate: 1.0×10^{-3} kgs^{-1}

DRYING TIME (MIN)	HUMIDITIES (KG/KG)	
	UPSTREAM $\times 10^{-3}$	DOWNSTREAM $\times 10^{-3}$
0	0.9542	2.8767
1	0.9542	5.0608
2	0.9542	4.7138
3	0.9542	4.0832
4	0.9542	3.7920
5	0.9542	3.2781
6	0.9542	3.4015
7	0.9542	3.4015
8	0.9542	2.8231
9	0.9542	2.8231
10	0.9542	2.8231
15	0.9542	2.8231
20	0.9542	2.8231
30	0.9542	2.8231

TABLE B28

Sample: MASON SLURRY

Drying Air Temperature: 300°C

Initial Drop Moisture Content: 55% wt/wt

Initial Drop Size: 4.0×10^{-3} m

Air Flowrate: 1.0×10^{-3} kgs^{-1}

DRYING TIME (MIN)	HUMIDITIES (KG/KG)	
	UPSTREAM $\times 10^{-3}$	DOWNSTREAM $\times 10^{-3}$
0	0.9542	2.9867
1	0.9542	4.0832
2	0.9542	4.0832
3	0.9542	3.7970
4	0.9542	3.7930
5	0.9542	3.5290
6	0.9542	3.5290
7	0.9542	3.5290
8	0.9542	2.9313
9	0.9542	2.9313
10	0.9542	2.9313
15	0.9542	2.9313
20	0.9542	2.9313
30	0.9542	2.9313

TABLE B29

Sample: MASON SLURRY

Drying Air Temperature: 200°C

Initial Drop Moisture Content: 55% wt/wt

Initial Drop Size: 4.0×10^{-3} m

Air Flowrate: 1.0×10^{-3} kgs^{-1}

DRYING TIME (MIN)	HUMIDITIES (KG/KG)	
	UPSTREAM $\times 10^{-3}$	DOWNSTREAM $\times 10^{-3}$
0	0.9542	3.1004
1	0.9542	3.2781
2	0.9542	3.2781
3	0.9542	3.4015
4	0.9542	3.2781
5	0.9542	3.0888
6	0.9542	3.0888
7	0.9542	3.0888
8	0.9542	3.0888
9	0.9542	3.0431
10	0.9542	3.0431
15	0.9542	3.0431
20	0.9542	3.0431
30	0.9542	3.0431

TABLE B30

Sample: MASON SLURRY

Drying Air Temperature: 400°C

Initial Drop Moisture Content: 55% wt/wt

Initial Drop Size: 4.0×10^{-3} m

Air Flowrate: 1.0×10^{-3} kgs^{-1}

DRYING TIME (MIN)	HUMIDITIES (KG/KG)	
	UPSTREAM $\times 10^{-3}$	DOWNSTREAM $\times 10^{-3}$
0	0.9542	2.8767
1	0.9542	5.4307
2	0.9542	4.7138
3	0.9542	4.0832
4	0.9542	3.5290
5	0.9542	3.5290
6	0.9542	3.5290
7	0.9542	3.5290
8	0.9542	3.5290
9	0.9542	3.5290
10	0.9542	3.5290
15	0.9542	3.5290
20	0.9542	3.5290
30	0.9542	3.5290

TABLE B31

Sample: HUMBER (S/R) SLURRY

Drying Air Temperature: 200^{o}C

Initial Drop Moisture Content: 30% wt/wt

Initial Drop Size: 3.0×10^{-3} m

Air Flowrate: 1.0×10^{-3} kgs^{-1}

DRYING TIME (MIN)	HUMIDITIES (KG/KG)	
	UPSTREAM $\times 10^{-3}$	DOWNSTREAM $\times 10^{-3}$
0	1.4504	2.7185
1	1.4504	3.1586
2	1.4504	3.2781
3	1.4504	3.4015
4	1.4504	3.4015
5	1.4504	3.1586
6	1.4504	3.1586
7	1.4504	3.1586
8	1.4504	3.0431
9	1.4504	3.0431
10	1.4504	3.0431
15	1.4504	3.0431
20	1.4504	3.0431
30	1.4504	3.0431

TABLE B32

Sample: HUMBER (S/R) SLURRY

Drying Air Temperature: 300^{o}C

Initial Drop Moisture Content: 30% wt/wt

Iniital Drop Size: 3.5×10^{-3}m

Air Flowrate: 1.0×10^{-3} kgs^{-1}

DRYING TIME (MIN)	HUMIDITIES (KG/KG)	
	UPSTREAM $\times 10^{-3}$	DOWNSTREAM $\times 10^{-3}$
0	1.1797	2.7185
1	1.1797	3.7970
2	1.1797	3.6609
3	1.1797	3.5290
4	1.1797	3.4015
5	1.1797	3.1586
6	1.1797	3.1586
7	1.1797	3.1586
8	1.1797	3.0091
9	1.1797	3.0091
10	1.1797	3.0091
15	1.1797	3.0091
20	1.1797	3.0091
30	1.1797	3.0091

TABLE B33

Sample: HUMBER (S/R) SLURRY

Drying Air Temperature: 400^{o}C

Initial Drop Moisture Content: 30% wt/wt

Initial Drop Size: 3.5×10^{-3} m

Air Flowrate: 1.0×10^{-3} kgs^{-1}

DRYING TIME (MIN)	HUMIDITIES (KG/KG)	
	UPSTREAM $\times 10^{-3}$	DOWNSTREAM $\times 10^{-3}$
0	1.1797	2.7185
1	1.1797	4.0832
2	1.1797	4.0832
3	1.1797	3.7970
4	1.1797	3.7970
5	1.1797	3.7970
6	1.1797	3.1586
7	1.1797	3.1586
8	1.1797	2.9979
9	1.1797	2.9979
10	1.1797	2.9979
15	1.1797	2.9979
20	1.1797	2.9979
30	1.1797	2.9979

TABLE B34

Sample: HUMBER (S/R) SLURRY

Drying Air Temperature: 200°C

Initial Drop Moisture Content: 35% wt/wt

Initial Drop Size: 3.3×10^{-3} m

Air Flowrate: 1.0×10^{-3} kgs^{-1}

DRYING TIME (MIN)	HUMIDITIES (KG/KG)	
	UPSTREAM $\times 10^{-3}$	DOWNSTREAM $\times 10^{-3}$
0	1.1312	2.7185
1	1.1312	3.1586
2	1.1312	3.4015
3	1.1312	3.4015
4	1.1312	3.5290
5	1.1312	3.1586
6	1.1312	3.1586
7	1.1312	3.0431
8	1.1312	3.0431
9	1.1312	3.0431
10	1.1312	3.0431
15	1.1312	3.0431
20	1.1312	3.0431
30	1.1312	3.0431

TABLE B35

Sample: HUMBER (S/R) SLURRY

Drying Air Temperature: 300^{o}C

Initial Drop Moisture Content: 35% wt/wt

Initial Drop Size: 3.00×10^{-3} m

Air Flowrate: 1.0×10^{-3} kgs^{-1}

DRYING TIME (MIN)	HUMIDITIES (KG/KG)	
	UPSTREAM $\times 10^{-3}$	DOWNSTREAM $\times 10^{-3}$
0	1.3923	2.7185
1	1.3923	3.7970
2	1.3923	3.5944
3	1.3923	3.6609
4	1.3293	3.5290
5	1.3293	3.1586
6	1.3293	3.1586
7	1.3293	3.0091
8	1.3293	3.0091
9	1.3293	3.0091
10	1.3293	3.0091
15	1.3293	3.0091
20	1.3293	3.0091
30	1.3293	3.0091

TABLE B36

Sample: HUMBER (S/R) SLURRY

Drying Air Temperature: 400°C

Initial Drop Moisture Content: 35% wt/wt

Initial Drop Size: 3.0×10^{-3} m

Air Flowrate: 1.0×10^{-3} kgs^{-1}

DRYING TIME (MIN)	HUMIDITIES (KG/KG)	
	UPSTREAM $\times 10^{-3}$	DOWNSTREAM $\times 10^{-3}$
0	1.4504	2.7185
1	1.4504	4.2333
2	1.4504	4.2333
3	1.4504	3.7970
4	1.4504	3.7970
5	1.4504	3.7970
6	1.4504	3.1586
7	1.4504	3.1586
8	1.4504	2.9867
9	1.4504	2.9867
10	1.4504	2.9867
15	1.4504	2.9867
20	1.4504	2.9867
30	1.4504	2.9867

TABLE B37

Sample: HUMBER (S/R) SLURRY

Drying Air Temperature: 200°C

Initial Drop Moisture Content: 45% wt/wt

Initial Drop Size: 3.5×10^{-3} m

Air Flowrate: 1.0×10^{-3} kgs^{-1}

DRYING TIME (MIN)	HUMIDITIES (KG/KG)	
	UPSTREAM $\times 10^{-3}$	DOWNSTREAM $\times 10^{-3}$
0	1.4504	2.7185
1	1.4504	3.2781
2	1.4504	3.2781
3	1.4504	3.3393
4	1.4504	3.3393
5	1.4504	3.4015
6	1.4504	3.0431
7	1.4504	3.0431
8	1.4504	3.0431
9	1.4504	3.0431
10	1.4504	3.0431
15	1.4504	3.0431
20	1.4504	3.0431
30	1.4504	3.0431

TABLE B38

Sample: HUMBER (S/R) SLURRY

Drying Air Temperature: 300^{o}C

Initial Drop Moisture Content: 45% wt/wt

Initial Drop Size: 3.0×10^{-3} m

Air Flowrate: 1.0×10^{-3} kgs^{-1}

DRYING TIME (MIN)	HUMIDITIES (KG/KG)	
	UPSTREAM $\times 10^{-3}$	DOWNSTREAM $\times 10^{-3}$
0	1.2300	2.7185
1	1.2300	3.1586
2	1.2300	3.1586
3	1.2300	3.1586
4	1.2300	3.1586
5	1.2300	3.1586
6	1.2300	3.0091
7	1.2300	3.0091
8	1.2300	3.0091
9	1.2300	3.0091
10	1.2300	3.0091
15	1.2300	3.0091
20	1.2300	3.0091
30	1.2300	3.0091

TABLE B39

Sample: HUMBER (S/R) SLURRY

Drying Air Temperature: 400°C

Initial Drop Moisture Content: 45% wt/wt

Initial Drop Size: 3.0×10^{-3} m

Air Flowrate: 1.0×10^{-3} kgs^{-1}

DRYING TIME (MIN)	HUMIDITIES (KG/KG)	
	UPSTREAM $\times 10^{-3}$	DOWNSTREAM $\times 10^{-3}$
0	1.2300	2.7185
1	1.2300	4.3102
2	1.2300	4.3102
3	1.2300	3.7970
4	1.2300	3.7970
5	1.2300	3.1586
6	1.2300	3.1586
7	1.2300	2.9867
8	1.2300	2.9867
9	1.2300	2.9867
10	1.2300	2.9867
15	1.2300	2.9867
20	1.2300	2.9867
30	1.2300	2.9867

TABLE B40

Sample: HUMBER (S/R) SLURRY

Drying Air Temperature: 200°C

Initial Drop Moisture Content: 50% wt/wt

Initial Drop Size: 3.5×10^{-3} m

Air Flowrate: 1.0×10^{-3} kgs^{-1}

DRYING TIME (MIN)	HUMIDITIES (KG/KG)	
	UPSTREAM $\times 10^{-3}$	DOWNSTREAM $\times 10^{-3}$
0	1.1513	2.7185
1	1.1513	3.2781
2	1.1513	3.2781
3	1.1513	3.4015
4	1.1513	3.4015
5	1.1513	3.4015
6	1.1513	3.0431
7	1.1513	3.0431
8	1.1513	3.0431
9	1.1513	3.0431
10	1.1513	3.0431
15	1.1513	3.0431
20	1.1513	3.0431
30	1.1513	3.0431

TABLE B41

Sample: HUMBER (S/R) SLURRY

Drying Air Temperature: 300^{o}C

Initial Drop Moisture Content: 50% wt/wt

Initial Drop Size: 3.0×10^{-3} m

Air Flowrate: 1.0×10^{-3} kgs^{-1}

DRYING TIME (MIN)	HUMIDITIES (KG/KG)	
	UPSTREAM $\times 10^{-3}$	DOWNSTREAM $\times 10^{-3}$
0	1.1513	2.7185
1	1.1513	3.1586
2	1.1513	3.1586
3	1.1513	3.5290
4	1.1513	3.5290
5	1.1513	3.5290
6	1.1513	2.9644
7	1.1513	2.9313
8	1.1513	2.9313
9	1.1513	2.9313
10	1.1513	2.9313
15	1.1513	2.9313
20	1.1513	2.9313
30	1.1513	2.9313

TABLE B42

Sample: HUMBER (S/R) SLURRY

Drying Air Temperature: 400°C

Initial Drop Moisture Content: 50% wt/wt

Initial Drop Size: 3.0×10^{-3} m

Air Flowrate: 1.0×10^{-3} kgs^{-1}

DRYING TIME (MIN)	HUMIDITIES (KG/KG)	
	UPSTREAM $\times 10^{-3}$	DOWNSTREAM $\times 10^{-3}$
0	1.1513	2.7185
1	1.1513	4.3883
2	1.1513	4.3883
3	1.1513	3.7970
4	1.1513	3.7970
5	1.1513	3.7970
6	1.1513	3.5290
7	1.1513	3.1586
8	1.1513	2.8767
9	1.1513	2.8767
10	1.1513	2.8767
15	1.1513	2.8767
20	1.1513	2.8767
30	1.1513	2.8767

TABLE B43

Sample: HUMBER (S/R) SLURRY

Drying Air Temperature: 200°C

Initial Drop Moisture Content: 55% wt/wt

Initial Drop Size: 3.0×10^{-3} m

Air Flowrate: 1.0×10^{-3} kgs^{-1}

DRYING TIME (MIN)	HUMIDITIES (KG/KG)	
	UPSTREAM $\times 10^{-3}$	DOWNSTREAM $\times 10^{-3}$
0	0.9960	2.7185
1	0.9960	3.2781
2	0.9960	3.5290
3	0.9960	3.5290
4	0.9960	3.5290
5	0.9960	3.5290
6	0.9960	3.5290
7	0.9960	2.9313
8	0.9960	2.9313
9	0.9960	2.9313
10	0.9960	2.9313
15	0.9960	2.9313
20	0.9960	2.9313
30	0.9960	2.9313

TABLE B44

Sample: HUMBER (S/R) SLURRY

Drying Air Temperature: 300°C

Initial Drop Moisture Content: 55% wt/wt

Initial Drop Size: 3.5×10^{-3} m

Air Flowrate: 1.0×10^{-3} kgs^{-1}

DRYING TIME (MIN)	HUMIDITIES (KG/KG)	
	UPSTREAM $\times 10^{-3}$	DOWNSTREAM $\times 10^{-3}$
0	0.9960	2.7185
1	0.9960	4.5484
2	0.9960	4.5484
3	0.9960	3.7970
4	0.9960	3.7970
5	0.9960	3.5290
6	0.9960	3.5290
7	0.9960	2.8767
8	0.9960	2.8767
9	0.9960	2.8767
10	0.9960	2.8767
15	0.9960	2.8767
20	0.9960	2.8767
30	0.9960	2.8767

TABLE B45

Sample: HUMBER (S/R) SLURRY

Drying Air Temperature: 400°C

Initial Drop Moisture Content: 55% wt/wt

Initial Drop Size: 3.0×10^{3} m

Air Flowrate: 1.0×10^{-3} kgs^{-1}

DRYING TIME (MIN)	HUMIDITIES (KG/KG)	
	UPSTREAM $\times 10^{-3}$	DOWNSTREAM $\times 10^{-3}$
0	1.0844	2.7185
1	1.0844	5.0608
2	1.0844	4.7138
3	1.0844	4.3883
4	1.0844	4.0832
5	1.0844	3.7970
6	1.0844	3.2781
7	1.0844	2.8231
8	1.0844	2.8231
9	1.0844	2.8231
10	1.0844	2.8231
15	1.0844	2.8231
20	1.0844	2.8231
30	1.0844	2.8231

TABLE B46

Sample: WESTBURY SLURRY

Drying Air Temperature: 200°C

Initial Drop Moisture Content: 30% wt/wt

Initial Drop Size: 4.5×10^{-3} m

Air Flowrate: 1.0×10^{-3} kgs^{-1}

DRYING TIME (MIN)	HUMIDITIES (KG/KG)	
	UPSTREAM $\times 10^{-3}$	DOWNSTREAM $\times 10^{-3}$
0	0.7673	2.9313
1	0.7673	3.5290
2	0.7673	3.5290
3	0.7673	3.4015
4	0.7673	3.3393
5	0.7673	3.2781
6	0.7673	3.1586
7	0.7673	2.8231
8	0.7673	2.8231
9	0.7673	2.8231
10	0.7673	2.8231
15	0.7673	2.8231
20	0.7673	2.8231
30	0.7673	2.8231

TABLE B47

Sample: WESTBURY SLURRY

Drying Air Temperature: 300°C

Initial Drop Moisture Content: 30% wt/wt

Initial Drop Size: 3.5×10^{-3} m

Air Flowrate: 1.0×10^{-3} kgs^{-1}

DRYING TIME (MIN)	HUMIDITIES (KG/KG)	
	UPSTREAM $\times 10^{-3}$	DOWNSTREAM $\times 10^{-3}$
0	0.7673	2.9313
1	0.7673	3.1586
2	0.7673	3.2178
3	0.7673	3.2781
4	0.7673	3.7970
5	0.7673	3.3393
6	0.7673	3.1586
7	0.7673	2.8231
8	0.7673	2.7185
9	0.7673	2.7185
10	0.7673	2.7185
15	0.7673	2.7185
20	0.7673	2.7185
30	0.7673	2.7185

TABLE B48

Sample: WESTBURY SLURRY

Drying Air Temperature: 400°C

Initial Drop Moisture Content: 30% wt/wt

Initial Drop Size: 3.0×10^{-3} m

Air Flowrate: 1.0×10^{-3} kgs^{-1}

DRYING TIME (MIN)	HUMIDITIES (KG/KG)	
	UPSTREAM $\times 10^{-3}$	DOWNSTREAM $\times 10^{-3}$
0	0.7673	2.9313
1	0.7673	3.2781
2	0.7673	3.4015
3	0.7673	3.5290
4	0.7673	4.0832
5	0.7673	3.9379
6	0.7673	3.4015
7	0.7673	2.9313
8	0.7673	2.6174
9	0.7673	2.6174
10	0.7673	2.6174
15	0.7673	2.6174
20	0.7673	2.6174
30	0.7673	2.6174

TABLE B49

Sample: WESTBURY SLURRY

Drying Air Temperature: 200°C

Initial Drop Moisture Content: 35% wt/wt

Initial Drop Size: 5.0×10^{-3}

Air Flowrate: 1.0×10^{-3} kgs^{-1}

DRYING TIME (MIN)	HUMIDITIES (KG/KG)	
	UPSTREAM $\times 10^{-3}$	DOWNSTREAM $\times 10^{-3}$
0	0.7673	2.9313
1	0.7673	3.0431
2	0.7673	3.1586
3	0.7673	3.2781
4	0.7673	3.5290
5	0.7673	3.7970
6	0.7673	3.5290
7	0.7673	3.1586
8	0.7673	2.8231
9	0.7673	2.8231
10	0.7673	2.8231
15	0.7673	2.8231
20	0.7673	2.8231
30	0.7673	2.8231

TABLE B50

Sample: WESTBURY SLURRY

Drying Air Temperature: 300°C

Initial Drop Moisture Content: 35% wt/wt

Initial Drop Size: 3.5×10^{-3} m

Air Flowrate: 1.0×10^{-3} kgs^{-1}

DRYING TIME (MIN)	HUMIDITIES (KG/KG)	
	UPSTREAM $\times 10^{-3}$	DOWNSTREAM $\times 10^{-3}$
0	0.7673	2.9313
1	0.7673	3.9379
2	0.7673	4.3883
3	0.7673	4.2333
4	0.7673	3.9379
5	0.7673	3.9146
6	0.7673	3.7970
7	0.7673	3.2781
8	0.7673	2.9313
9	0.7673	2.7185
10	0.7673	2.7185
15	0.7673	2.7185
20	0.7673	2.7185
30	0.7673	2.7185

TABLE B51

Sample: WESTBURY SLURRY

Drying Air Temperature: 400°C

Initial Drop Moisture Content: 35% wt/wt

Initial Drop Size: 3.0×10^{-3} m

Air Flowrate: 1.0×10^{-3} kgs^{-1}

DRYING TIME (MIN)	HUMIDITIES (KG/KG)	
	UPSTREAM $\times 10^{-3}$	DOWNSTREAM $\times 10^{-3}$
0	0.7673	2.9313
1	0.7673	4.8845
2	0.7673	4.7138
3	0.7673	4.3883
4	0.7673	3.0832
5	0.7673	3.9146
6	0.7673	3.4015
7	0.7673	3.0431
8	0.7673	2.6174
9	0.7673	2.6174
10	0.7673	2.6174
15	0.7673	2.6174
20	0.7673	2.6174
30	0.7673	2.6174

TABLE B52

Sample: WESTBURY SLURRY

Drying Air Temperature: 200°C

Initial Drop Moisture Content: 45% wt/wt

Initial Drop Size: 4.0×10^{-3} m

Air Flowrate: 1.0×10^{-3} kgs^{-1}

DRYING TIME (MIN)	HUMIDITIES (KG/KG)	
	UPSTREAM $\times 10^{-3}$	DOWNSTREAM $\times 10^{-3}$
0	0.7673	2.9313
1	0.7673	3.0431
2	0.7673	3.2781
3	0.7673	3.4015
4	0.7673	3.7970
5	0.7673	3.1586
6	0.7673	3.0431
7	0.7673	2.9313
8	0.7673	2.8231
9	0.7673	2.8231
10	0.7673	2.8231
15	0.7673	2.8231
20	0.7673	2.8231
30	0.7673	2.8231

TABLE B53

Sample: WESTBURY SLURRY

Drying Air Temperature: 300°C

Initial Drop Moisture Content: 45% wt/wt

Initial Drop Size: 3.0×10^{-3} m

Air Flowrate: 1.0×10^{-3} kgs^{-1}

DRYING TIME (MIN)	HUMIDITIES (KG/KG)	
	UPSTREAM $\times 10^{-3}$	DOWNSTREAM $\times 10^{-3}$
0	0.7673	2.9313
1	0.7673	3.2781
2	0.7673	3.4015
3	0.7673	3.4015
4	0.7673	3.7970
5	0.7673	4.3883
6	0.7673	4.2333
7	0.7673	3.4015
8	0.7673	2.7185
9	0.7673	2.7185
10	0.7673	2.7185
15	0.7673	2.7185
20	0.7673	2.7185
30	0.7673	2.7185

TABLE B54

Sample: WESTBURY SLURRY

Drying Air Temperature: 400 ^{o}C

Initial Drop Moisture Content: 45% wt/wt

Initial Drop Size: 2.5×10^{-3} m

Air Flowrate: 1.0×10^{-3} kgs^{-1}

DRYING TIME (MIN)	HUMIDITIES (KG/KG)	
	UPSTREAM $\times 10^{-3}$	DOWNSTREAM $\times 10^{-3}$
0	0.7673	2.9313
1	0.7673	4.0832
2	0.7673	4.3883
3	0.7673	5.0608
4	0.7673	4.7138
5	0.7673	4.0832
6	0.7673	3.5290
7	0.7673	3.1586
8	0.7673	2.6174
9	0.7673	2.6174
10	0.7673	2.6174
15	0.7673	2.6174
20	0.7673	2.6174
30	0.7673	2.6174

TABLE B55

Sample: WESTBURY SLURRY

Drying Air Temperature: 200°C

Initial Drop Moisture Content: 50% wt/wt

Initial Drop Size: 3.5×10^{-3} m

Air Flowrate: 1.0×10^{-3} kgs^{-1}

DRYING TIME (MIN)	HUMIDITIES (KG/KG)	
	UPSTREAM $\times 10^{-3}$	DOWNSTREAM $\times 10^{-3}$
0	0.7673	2.9313
1	0.7673	3.0431
2	0.7673	3.2781
3	0.7673	3.4015
4	0.7673	3.7970
5	0.7673	3.1586
6	0.7673	3.0431
7	0.7673	2.8231
8	0.7673	2.8231
9	0.7673	2.8231
10	0.7673	2.8231
15	0.7673	2.8231
20	0.7673	2.8231
30	0.7673	2.8231

TABLE B56

Sample: WESTBURY SLURRY

Drying Air Temperature: 300°C

Initial Drop Moisture Content: 50% wt/wt

Initial Drop Size: 3.0×10^{-3} m

Air Flowrate: 1.0×10^{-3} kgs^{-1}

DRYING TIME (MIN)	HUMIDITIES (KG/KG)	
	UPSTREAM $\times 10^{-3}$	DOWNSTREAM $\times 10^{-3}$
0	0.7673	2.9313
1	0.7673	4.5484
2	0.7673	4.3883
3	0.7673	4.0832
4	0.7673	3.7970
5	0.7673	3.2781
6	0.7673	3.0431
7	0.7673	2.9313
8	0.7673	2.7185
9	0.7673	2.7185
10	0.7673	2.7185
11	0.7673	2.7185
15	0.7673	2.7185
20	0.7673	2.7185
30	0.7673	2.7185

TABLE B57

Sample: WESTBURY SLURRY

Drying Air Temperature: 400°C

Initial Drop Moisture Content: 50% wt/wt

Initial Drop Size: 2.0×10^{-3} m

Air Flowrate: 1.0×10^{-3} kgs^{-1}

DRYING TIME (MIN)	HUMIDITIES (KG/KG)	
	UPSTREAM $\times 10^{-3}$	DOWNSTREAM $\times 10^{-3}$
0	0.7673	2.9313
1	0.7673	5.2428
2	0.7673	5.0608
3	0.7673	4.7138
4	0.7673	4.3883
5	0.7673	4.2333
6	0.7673	4.0832
7	0.7673	3.7970
8	0.7673	2.6174
9	0.7673	2.6174
10	0.7673	2.6174
15	0.7673	2.6174
20	0.7673	2.6174
30	0.7673	2.6174

TABLE B58

Sample: WESTBURY SLURRY

Drying Air Temperature: 200°C

Initial Drop Moisture Content: 55% wt/wt

Initial Drop Size: 3.0×10^{-3} m

Air Flowrate: 1.0×10^{-3} kgs^{-1}

DRYING TIME (MIN)	HUMIDITIES (KG/KG)	
	UPSTREAM $\times 10^{-3}$	DOWNSTREAM $\times 10^{-3}$
0	0.7673	2.9313
1	0.7673	4.2333
2	0.7673	4.0832
3	0.7673	3.7970
4	0.7673	3.2781
5	0.7673	3.1586
6	0.7673	2.1586
7	0.7673	2.9313
8	0.7673	2.8231
9	0.7673	2.8231
10	0.7673	2.8231
15	0.7673	2.8231
20	0.7673	2.8231
30	0.7673	2.8231

TABLE B59

Sample: WESTBURY SLURRY

Drying Air Temperature: 300°C

Initial Drop Moisture Content: 55% wt/wt

Initial Drop Size: 2.0×10^{-3} m

Air Flowrate: 1.0×10^{-3} kgs^{-1}

DRYING TIME (MIN)	HUMIDITIES (KG/KG)	
	UPSTREAM $\times 10^{-3}$	DOWNSTREAM $\times 10^{-3}$
0	0.7673	2.9313
1	0.7673	4.8845
2	0.7673	4.5848
3	0.7673	4.3883
4	0.7673	3.7970
5	0.7673	3.1586
6	0.7673	3.0431
7	0.7673	2.9313
8	0.7673	2.7185
9	0.7673	2.7185
10	0.7673	2.7185
15	0.7673	2.7185
20	0.7673	2.7185
30	0.7673	2.7185

TABLE B60

Sample: WESTBURY SLURRY

Drying Air Temperature: 400°C

Initial Drop Moisture Content: 55% wt/wt

Initial Drop Size: 2.0×10^{-3} m

Air Flowrate: 1.0×10^{-3} kgs^{-1}

DRYING TIME (MIN)	HUMIDITIES (KG/KG)	
	UPSTREAM $\times 10^{-3}$	DOWNSTREAM $\times 10^{-3}$
0	0.7673	2.9313
1	0.7673	5.4307
2	0.7673	5.2428
3	0.7673	5.0608
4	0.7673	4.7138
5	0.7673	3.7970
6	0.7673	3.4015
7	0.7673	3.1586
8	0.7673	2.6174
9	0.7673	2.6174
10	0.7673	2.6174
15	0.7673	2.6174
20	0.7673	2.6174
30	0.7673	2.6174

TABLE B61

Sample: SHOREHAM SLURRY

Drying Air Temperature: 200°C

Initial Drop Moisture Content: 30% wt/wt

Initial Drop Size: 5.0×10^{-3} m

Air Flowrate: 1.0×10^{-3} kgs^{-1}

DRYING TIME (MIN)	HUMIDITIES (KG/KG)	
	UPSTREAM $\times 10^{-3}$	DOWNSTREAM $\times 10^{-3}$
0	1.0844	2.6574
1	1.0844	2.7185
2	1.0844	2.8131
3	1.0844	2.8659
4	1.0844	2.8659
5	1.0844	2.8767
6	1.0844	2.8767
7	1.0844	3.0431
8	1.0844	2.8231
9	1.0844	2.8231
10	1.0844	2.8231
15	1.0844	2.8231
20	1.0844	2.8231
30	1.0844	2.8231

TABLE B62

Sample: SHOREHAM SLURRY

Drying Air Temperature: 300°C

Initial Drop Moisture Content: 30% wt/wt

Initial Drop Size: 4.5×10^{-3} m

Air Flowrate: 1.0×10^{-3} kgs^{-1}

DRYING TIME (MIN)	HUMIDITIES (KG/KG)	
	UPSTREAM $\times 10^{-3}$	DOWNSTREAM $\times 10^{-3}$
0	1.0844	2.8231
1	1.0844	3.1586
2	1.0844	3.1586
3	1.0844	3.1586
4	1.0844	2.8231
5	1.0844	2.8659
6	1.0844	2.8767
7	1.0844	2.8767
8	1.0844	2.8659
9	1.0844	2.8659
10	1.0844	2.8659
15	1.0844	2.8659
20	1.0844	2.8569
30	1.0844	2.8569

TABLE B63

Sample: SHOREHAM SLURRY

Drying Air Temperature: 400°C

Initial Drop Moisture Content: 30% wt/wt

Initial Drop Size: 5.0×10^{-3} m

Air Flowrate: 1.0×10^{-3} kgs^{-1}

DRYING TIME (MIN)	HUMIDITIES (KG/KG)	
	UPSTREAM $\times 10^{-3}$	DOWNSTREAM $\times 10^{-3}$
0	1.0844	2.8231
1	1.0844	3.4015
2	1.0844	3.2781
3	1.0844	3.0431
4	1.0844	2.9867
5	1.0844	2.9313
6	1.0844	2.8767
7	1.0844	2.8231
8	1.0844	2.8231
9	1.0844	2.8231
10	1.0844	2.8231
15	1.0844	2.8231
20	1.0844	2.8231
30	1.0844	2.8231

TABLE B64

Sample: SHOREHAM SLURRY

Drying Air Temperature: 200°C

Initial Drop Moisture Content: 35% wt/wt

Initial Drop Size: 4.0×10^{-3} m

Air Flowrate: 1.0×10^{-3} kgs^{-1}

DRYING TIME (MIN)	HUMIDITIES (KG/KG)	
	UPSTREAM $\times 10^{-3}$	DOWNSTREAM $\times 10^{-3}$
0	1.0844	2.7185
1	1.0844	3.0431
2	1.0844	2.9313
3	1.0844	2.9313
4	1.0844	2.9867
5	1.0844	2.9867
6	1.0844	3.0431
7	1.0844	3.0431
8	1.0844	2.9313
9	1.0844	2.9313
10	1.0844	2.9313
15	1.0844	2.9313
20	1.0844	2.9313
30	1.0844	2.9313

TABLE B65

Sample: SHOREHAM SLURRY

Drying Air Temperature: 300°C

Initial Drop Moisture Content: 35% wt/wt

Initial Drop Size; 4.5×10^{-3} m

Air Flowrate: 1.0×10^{-3} kgs^{-1}

DRYING TIME (MIN)	HUMIDITIES (KG/KG)	
	UPSTREAM $\times 10^{-3}$	DOWNSTREAM $\times 10^{-3}$
0	1.0844	2.7185
1	1.0844	3.1586
2	1.0844	3.2781
3	1.0844	3.2781
4	1.0844	3.1586
5	1.0844	3.0431
6	1.0844	3.0431
7	1.0844	2.9313
8	1.0844	2.9313
9	1.0844	2.9313
10	1.0844	2.9313
15	1.0844	2.9313
20	1.0844	2.9313
30	1.0844	2.9313

TABLE B66

Sample: SHOREHAM SLURRY

Drying Air Temperature: 400°C

Initial Drop Moisture Content: 35% wt/wt

Initial Drop Size: 4.0×10^{-3} m

Air Flowrate: 1.0×10^{-3} kgs^{-1}

DRYING TIME (MIN)	HUMIDITIES (KG/KG)	
	UPSTREAM $\times 10^{-3}$	DOWNSTREAM $\times 10^{-3}$
0	1.0844	2.8231
1	1.0844	3.4015
2	1.0844	3.5290
3	1.0844	3.4015
4	1.0844	3.2781
5	1.0844	3.1586
6	1.0844	3.0431
7	1.0844	2.8767
8	1.0844	2.8231
9	1.0844	2.8231
10	1.0844	2.8231
15	1.0844	2.8231
20	1.0844	2.8231
30	1.0844	2.8231

TABLE B67

Sample: SHOREHAM SLURRY

Drying Air Temperature: 200°C

Initial Drop Moisture Content: 45% wt/wt

Initial Drop Size: 3.5×10^{-3} m

Air Flowrate: 1.0×10^{-3} kgs^{-1}

DRYING TIME (MIN)	HUMIDITIES (KG/KG)	
	UPSTREAM $\times 10^{-3}$	DOWNSTREAM $\times 10^{-3}$
0	1.0844	2.7185
1	1.0844	3.1586
2	1.0844	3.1586
3	1.0844	2.9867
4	1.0844	2.9867
5	1.0844	2.9867
6	1.0844	2.8231
7	1.0844	2.8231
8	1.0844	2.8231
9	1.0844	2.8231
10	1.0844	2.8231
15	1.0844	2.8231
20	1.0844	2.8231
30	1.0844	2.8231

TABLE B68

Sample: SHOREHAM SLURRY

Drying Air Temperature: 300°C

Initial Drop Moisture Content: 45% wt/wt

Initial Drop Size: 4.0×10^{-3} m

Air Flowrate: 1.0×10^{-3} kgs^{-1}

DRYING TIME (MIN)	HUMIDITIES (KG/KG)	
	UPSTREAM $\times 10^{-3}$	DOWNSTREAM $\times 10^{-3}$
0	1.0844	2.8231
1	1.0844	3.4015
2	1.0844	3.2781
3	1.0844	3.1586
4	1.0844	3.1586
5	1.0844	3.1004
6	1.0844	3.0431
7	1.0844	2.9313
8	1.0844	2.9313
9	1.0844	2.9313
10	1.0844	2.9313
15	1.0844	2.9313
20	1.0844	2.9313
30	1.0844	2.9313

TABLE B69

Sample: SHOREHAM SLURRY

Drying Air Temperature: 400°C

Initial Drop Moisture Content: 45% wt/wt

Initial Drop Size: 4.5×10^{-3} m

Air Flowrate: 1.0×10^{-3} kgs^{-1}

DRYING TIME (MIN)	HUMIDITIES (KG/KG)	
	UPSTREAM $\times 10^{-3}$	DOWNSTREAM $\times 10^{-3}$
0	1.0844	2.8231
1	1.0844	3.5290
2	1.0844	3.7970
3	1.0844	3.5290
4	1.0844	3.4015
5	1.0844	3.2781
6	1.0844	3.0431
7	1.0844	2.8767
8	1.0844	2.8767
9	1.0844	2.8767
10	1.0844	2.8767
15	1.0844	2.8767
20	1.0844	2.8767
30	1.0844	2.8767

TABLE B70

Sample: SHOREHAM SLURRY

Drying Air Temperature: 200°C

Initial Drop Moisture Content: 50% wt/wt

Initial Drop Size; 3.5×10^{-3} m

Air Flowrate; 1.0×10^{-3} kgs^{-1}

DRYING TIME (MIN)	HUMIDITIES (KG/KG)	
	UPSTREAM $\times 10^{-3}$	DOWNSTREAM $\times 10^{-3}$
0	1.0844	2.6675
1	1.0844	2.7185
2	1.0844	3.5290
3	1.0844	3.7970
4	1.0844	3.5290
5	1.0844	3.2781
6	1.0844	3.1586
7	1.0844	3.1586
8	1.0844	3.0431
9	1.0844	3.0431
10	1.0844	3.0431
15	1.0844	3.0431
20	1.0844	3.0431
30	1.0844	3.0431

TABLE B71

Sample: SHOREHAM SLURRY

Drying Air Temperature: 300°C

Initial Drop Moisture Content: 50% wt/wt

Initial Drop Size: 4.0×10^{-3} m

Air Flowrate: 1.0×10^{-3} kgs^{-1}

DRYING TIME (MIN)	HUMIDITIES (KG/KG)	
	UPSTREAM $\times 10^{-3}$	DOWNSTREAM $\times 10^{-3}$
0	1.0844	2.7185
1	1.0844	2.8231
2	1.0844	4.0832
3	1.0844	3.7970
4	1.0844	3.5290
5	1.0844	3.4015
6	1.0844	3.2781
7	1.0844	3.1586
8	1.0844	2.9313
9	1.0844	2.9313
10	1.0844	2.9313
15	1.0844	2.9313
20	1.0844	2.9313
30	1.0844	2.9313

TABLE B72

Sample: SHOREHAM SLURRY

Drying Air Temperature: 400%

Initial Drop Moisture Content: 50% wt/wt

Initial Drop Size: 3.5×10^{-3} m

Air Flowrate: 1.0×10^{-3} kgs^{-1}

DRYING TIME (MIN)	HUMIDITIES (KG/KG)	
	UPSTREAM $\times 10^{-3}$	DOWNSTREAM $\times 10^{-3}$
0	1.0844	2.9313
1	1.0844	3.0431
2	1.0844	4.2333
3	1.0844	4.0832
4	1.0844	3.7970
5	1.0844	3.5290
6	1.0844	3.2781
7	1.0844	3.1586
8	1.0844	2.8231
9	1.0844	2.8231
10	1.0844	2.8231
15	1.0844	2.8231
20	1.0844	2.8231
30	1.0844	2.8231

TABLE B73

Sample: SHOREHAM SLURRY

Drying Air Temperature: 200°C

Initial Drop Moisture Content: 55% wt/wt

Initial Drop Size: 3.0×10^{-3} m

Air Flowrate: 1.0×10^{-3} kgs^{-1}

DRYING TIME (MIN)	HUMIDITIES (KG/KG)	
	UPSTREAM $\times 10^{-3}$	DOWNSTREAM $\times 10^{-3}$
0	1.0844	2.6675
1	1.0844	2.8231
2	1.0844	3.7970
3	1.0844	3.5290
4	1.0844	3.1586
5	1.0844	3.0431
6	1.0844	2.9867
7	1.0844	2.9313
8	1.0844	2.8231
9	1.0844	2.8231
10	1.0844	2.8231
15	1.0844	2.8231
20	1.0844	2.8231
30	1.0844	2.8231

TABLE B74

Sample: SHOREHAM SLURRY

Drying Air Temperature; 300°C

Initial Drop Moisture Content : 55% wt/wt

Initial Drop Size: 4.0×10^{-3} m

Air Flowrate; 1.0×10^{-3} kgs^{-1}

DRYING TIME (MIN)	HUMIDITIES (KG/KG)	
	UPSTREAM $\times 10^{-3}$	DOWNSTREAM $\times 10^{-3}$
0	1.0844	2.7185
1	1.0844	4.3883
2	1.0844	4.2333
3	1.0844	4.0832
4	1.0844	3.7970
5	1.0844	3.4015
6	1.0844	3.1586
7	1.0844	3.1586
8	1.0844	2.8231
9	1.0844	2.8231
10	1.0844	2.8231
15	1.0844	2.8231
20	1.0844	2.8231
30	1.0844	2.8231

TABLE B75

Sample: SHOREHAM SLURRY

Drying Air Temperature: 400^{o}C

Initial Drop Moisture Content: 55% wt/wt

Initial Drop Size: 4.5×10^{-3}m

Air Flowrate: 1.0×10^{-3} kgs^{-1}

DRYING TIME (MIN)	HUMIDITIES (KG/KG)	
	UPSTREAM $\times 10^{-3}$	DOWNSTREAM $\times 10^{-3}$
0	1.0844	2.9313
1	1.0844	4.7138
2	1.0844	4.4677
3	1.0844	4.0832
4	1.0844	3.7970
5	1.0844	3.2781
6	1.0844	3.1586
7	1.0844	2.9313
8	1.0844	2.8231
9	1.0844	2.8231
10	1.0844	2.8231
15	1.0844	2.8231
20	1.0844	2.8231
30	1.0844	2.8231

```
      MASTER CRUST
      PRJGRAM FJR THE EVALUATIJN JF DRYING CHARACTERISTICS JF A
     SLURRY SAMPLE

      CJMMJN TIME,KC,K1,KE,KC2,B,I,J,CJ,TC,RN,S2
      CJMMJN/BLJCK1/H1,H2,H3,H4
      REAL LAMDA,MIU,KC,K1,KI1,KC1,KC2,KE,KG,KT,KE1,K
      DIMENSIJN DM(10),DR(40,10),RH(40,10),RH1(40,10),PRS(40),RE(10)
      DIMENSIJN DFC(40,10),B(40,10),A(40,10),KC(40,10),TC(10),TK(10)
      DIMENSIJN HU(40,10),HD(40,10),RAD(10),TIME(40),DH(40,10),C1(10)
      DIMENSIJN TCJ(10),SC(10),VIS(10),TCK(10),KE(40,10),KE1(40,10)
      DIMENSIJN HS(40,10),DHS(40,10),AA(10),T(10),KG(40,10),KT(40,10)
      DIMENSIJN MIU(10),RHJ(10),DEN(10),DF(10),K(40,10),K1(40,10)
      DIMENSIJN KC1(40,10),AM(5),BM(5),X1(50),Y1(50),KT1(40,10)
      DIMENSIJN X2(50),Y2(50),AN(5),BN(5),S1(5),S2(5),RN(5),ST1(70)
      DIMENSIJN KC2(40,10),RM(10),RE1(5),DM1(5),ST2(70)
      DIMENSIJN TIME1(40)
      CALL JPENGINJGPW
      CALL DEVPAP(2000.0,720.0,IK)

      INPUT ALL CJNSTANTS,AIR AND SLURRY PRJPERTIES

      TIME(1)=60.0
      E=0.395
      TC(1)=200.0
      TC(2)=300.0
      TC(3)=400.0
      GC=9.81
      TA=293.16
      RC=8.3143
      PIE=3.1416
      R7=2.54E-2
      G=1.0E-03
      LAMDA=2256.7
      R=5.0E-3
      H1=-0.35053E-1
      H2=0.39491E-2
      H3=-0.52239E-5
      H4=0.37338E-8

      INPUT THE AIR HUMIDITY READING,DENSITY,VISCJSITY,ETC

      READ(1,102) CJ
      READ(1,100) ((RH(I,J),I=1,8),J=1,3)
      READ(1,101)(RAD(J),J=1,3)
      READ(1,100)(TCJ(J),J=1,3)
      READ(5,102)(RHJ(J),J=1,3)
  100 FJRMAT(8F0.0)
  101 FJRMAT(6E0.0)
  102 FJRMAT(3F0.0)
      DJ 10 L=9,32
      RH(L,1)=-4.00
      RH(L,2)=-4.50
      RH(L,3)=-5.0
   10 CJNTINUE
```

```
DO 25 J=1,3
DO 20 I=1,32

EVALUATION OF UPSTREAM AND DOWNSTREAM HUMIDITY VALUES

T2=TCO(J)
T1=RH(I,J)
RH1(I,J)=-20.0
T3=RH1(I,J)
CALL TINU(T3,PR)
CALL TINU(T2,P1)
CALL TINU(T1,PR1)
HU(I,J)=HUM(PR)
HS(I,J)=HUM(P1)
HD(I,J)=HUM(PR1)
TK(J)=TC(J)+273.16
TCK(J)=TCO(J)+273.16
FLO=G/(1.0+HD(I,J))
AD=0.22E-4
DM(J)=AD*(TK(J)/273.16)**1.75
DM1(J)=AD*(TCK(J)/273.16)**1.75
DH(I,J)=ABS(HD(I,J)-HU(I,J))
DHS(I,J)=ABS(HS(I,J)-HU(I,J))
AB=ABS(DHS(I,J)-DH(I,J))
C1(J)=COND(T2)
T(J)=TK(J)-TCK(J)
AA(J)=DM1(J)*(E**2.5)*LAMDA*AB/(C1(J)*(1.0-E))

 PREDICTING CRUST GROWTH RATE

FD=3*FLO*DH(I,J)*TIME(I)/(2.0E3*PIE*CO)
AFD=ABS(RAD(J)**3-FD)
B(I,J)=RAD(J)-(AFD)**0.333


TIME(I+1)=TIME(I)+60.0
CORRELATION OF GAS PHASE TRANSFER COEFFICIENT FROM
THE SYSTEM REYNOLD'S AND SCHMIDT'S NUMBERS

DEN(J)=1.2929*273.16/TK(J)
MIU(J)=8.8E-6*(9.232E2/(TCK(J)+6.5E2))*((TCK(J)/273.16)**1.5)
VIS(J)=1.7E-5*TK(J)/273.16
RE(J)=G*RAD(J)/(VIS(J)*PIE*(R7**2))
RE1(J)=G*RAD(J)/MIU(J)*PIE*(R7**2)
SC(J)=VIS(J)/(DEN(J)*DM(J))

EVALUATION OF THE CRUST MASS TRANSFER COEFFICIENT
FROM THE PROPOSED MOMENTUM - TRANSFER MODEL

AL=0.72*B(I,J)*(1.-(2*RAD(J)-B(I,J)))**0.5
G1=AL*GC
S=3.0*AL*B(I,J)/(RAD(J)**3-(RAD(J)-B(I,J))**3)
A(I,J)=2*PIE*(RAD(J)**2.-(RAD(J)-B(I,J))**2.)/E
KC(I,J)=(E**3)*RHO(J)*G1/(5.0*((1.0-E)**2)*(S**2)*MIU(J)*B(I,
KC2(I,J)=FLO*DH(I,J)/A(I,J)
```

```
      EXPERIMENTAL MASS TRANSFER COEFFICIENT

      KE(I,J)=FLO*DH(I,J)/(A(I,J)*AB)
      A1=T(J)/TA
      A2=-0.008
      B1=0.44*(A1**A2)
      B2=KE(J)**0.5
      B3=SC(J)**0.333
      B4=DM(J)/RAD(J)
      KG(I,J)=B4*(2.0+B1*B2*B3)
      KT(I,J)=KC(I,J)*KG(I,J)/(KC(I,J)+KG(I,J))
      DFC(I,J)=KC2(I,J)/KC(I,J)
   20 CONTINUE
   25 CONTINUE
      DO 37 J=1,3
      DO 36 I=1,32
      X2(I)=KT(I,J)
      Y2(I)=KE(I,J)
   36 CONTINUE
      CALL APPLE(X2,Y2,32,BC,AC,R2,SS)
      AN(J)=AC
      BN(J)=BC
      RN(J)=R2
      S2(J)=SS
   37 CONTINUE
      DO 35 J=1,3
      WRITE(2,95)
   95 FORMAT(1H1,////,20X,'SAMPLE - WESTBURY SLURRY',/)
      WRITE(2,99) TCO(J),C1(J)
   99 FORMAT(/,20X,'MEAN SAT. DROP TEMPURATURE=',F10.2,2X,'DEG.C',//
     1,'CRUST THERMAL CONDUCTIVITY=',2X,F5.4,' W/M/DEG. C'/)
      WRITE(2,200) TC(J),RAD(J),CO,KG(1,J)
  200 FORMAT(20X,'AIR TEMPERATURE = ',F10.2,2X,'DEG. C',//,20X,'DROP
     3ERNAL DIAMETER = ',F10.4,2X,'METERS',//,20X,'INITIAL MOISTURE
     2CONTENT = ',F10.3,'KG/KG',//,20X,'GAS FILM TRANSFER COEFFIENT=
     15X,1PE10.4,2X,'M/S',/)
      WRITE(2,96)
   96 FORMAT(/,13X,'DRYING TIME(SEC)',5X,'KC',10X,'KT',10X,'KE')
      WRITE(2,205)(TIME(I),KC(I,J),KT(I,J),KE(I,J),I=1,20)
  205 FORMAT(15X,1PE10.4,5X,1PE10.4,2X,1PE10.4,2X,1PE10.4,/)
      WRITE(6,206)(TIME(I),B(I,J),KC(I,J),KE(I,J),KC2(I,J),
     1I=1,30)
  206 FORMAT(10X,5(5X,1PE10.4))
      WRITE(6,97)
   97 FORMAT(1H1,///)
   35 CONTINUE
      WRITE(2,1)(T(J),AA(J),RE(J),BM(J),RE1(J),J=1,3)
    1 FORMAT(1H1,20X,5(5X,1PE10.4))
      CALL PLOT
      STOP
      END
```

```
      SUBPRJGRAM TJ CJRRELATE THE PARTIAL VAPJUR PRESSURE JF THE AIR
      SUBRJUTINE TINU(TI,VP)
      TK=TI+273.16
      AA=-2445.5646/TK+(8.2312*ALJG10(TK))-(0.01677006*TK)+(1.20514E
     A-5*(TK**2))-6.757169
      PR=EXP10(AA)
      BB=-(1.1489*TI)/TK-1.33E-5*(TI**2)+9.084*10E-8*(TI**3)
      VPRES=PR*(EXP10(BB))
      IF(TK-273.16) 20,20,30
20    DELP=VPRES/(5*TK)
      GJ TJ 40
30    DELP=VPRES*(0.0775-(3.13E-4*TI))/100
40    VP=VPRES+DELP
      RETURN
      END

      FUNCTIJN HUM(A)

      FUNCTIJN EVALUATES THE HUMIDITY JF DRYING AIR FRJM
      THE KNJWN PARTIAL VAPJUR PRESSURE CALCULATED IN
      SEGMENT TINU

      HUM=18.0*A/((760.0-A)*28.9)
      RETURN
      END
      FUNCTIJN CJND(T)


       FUNTIJN CJRRELATES THE THERMAL CJNDUCTIVITY JF THE
      CRUST FRJM THE PRJPJSED PJLYNJMIAL WITH THE PRE -
      DETERMINED CJEFFICIENTS SUPPLIED FRJM THE MAIN SEGMENT

      CJMMJN/BLJCK1/A,B,C,D
      CJND=A+(B*T)+(C*(T**2))+(D*(T**3))
      RETURN
      END

    THE GRAPHICS SEGMENT FJR PLJTTING JUT THE DRYING

    CHARACTERISTICS EVALUATED IN THE MAIN SEGMENT

      SUBRJUTINE PLJT
      CJMMJN TIME,RC,RT,RE,RC2,B,I,J,CJ,TC,RN,S2
      REAL RC,RT,RE,RC2
      DIMENSIJN TIME(40),RC(40,10),RE(40,10),RC2(40,10),B(40,10)
      DIMENSIJN D6(50),A1(50),A2(50),A3(50),A4(50),TC(10),RN(5)
      NSYM(1)=8
      NSYM(2)=2
      NSYM(3)=7
      NSPACE=0
      NPJINT=20
      A3 1)=0.0
      AJB=AMAX1(B(30,1),B(30,2),B(30,3))
```

```
      PLOT  THE CRUST GROWTH AT VARIOUS DRYING
     TIME AND AIR TEMPERATURES

      CALL SHIFT2(100.0,100.0)
      CALL CHASIZ(3.5,3.75)
      CALL GRABOX(-30.0,-40.0,CO)
      CALL SHIFT2(40.0,50.0)
      C@LL AXISPLOT(120.0,150.0,2.0E3,AJB)
      CALL CHASIZ(2.5,2.5)
      DO 10 J=1,3
      MS=NSYM(J)
      DO 2 I=1,30
      A1(I)=B(I,J)
    2 CONTINUE
      CALL GRASYM(TIME,A1,30,MS,1)
   10 CONTINUE

      ROUTINE PLOTS CRUST MASS TRANSFER COEFFICIENTS
      EVALUATED BY PROPOSED MODEL

      CALL SHIFT2(0.0,225.0)
      CALL CHASIZ(3.5,3.75)
      AC=AMAX1(KC(1,1),KC(1,2),KC(1,3))
      AKC=1.25*AC
      CALL AXISPLOT(120.0,150.0,1.5E3,AKC)
      DO 11 J=1,3
      MS=NSYM(J)
      DO 3 I=1,NPOINT
      A2(I)=KC(I,J)
    3 CONTINUE
      CALL CHASIZ(2.5,2.5)
      CALL GRASYM(TIME,A2,NPOINT,MS,NSPACE)
   11 CONTINUE

       ROUTINE PLOTS THE OVERALL EXPERIMENTAL MASS
       TRANSFER COEFFIENTS AT VARIOUS DRYING AIR
       TEMPERATURE AND TIME

      CALL SHIFT2(190.0,0.0)
      CALL CHASIZ(3.5,3.75)
      AE=AMAX1(KE(1,1),KE(1,2),KE(1,3))
      AKE=1.25*AE
      CALL AXISPLOT(120.0,150.0,1.5E3,AKE)
      DO 13 J=1,3
      MS=NSYM(J)
      DO 5 I=1,NPOINT
      A4(I)=KE(I,J)
    5 CONTINUE
      CALL CHASIZ((2.5,2.5)
```

```
      CALL GRASYM(TIME,A4,NPJINT,MS,NSPACE)
   13 CJNTINUE
      CALL SHIFT2(0.0,-225.0)
      CALL CHASIZ(3.5,3.75)
      DF=AMAX1(KC2(1,2),KC2(1,1),KC2(1,3))
      ADF=1.25*DF
      CALL AXISPLJT(120.0,150.0,1.5E3,ADF)
      DJ 14 J=1,3
      MS=NSYM(J)
      DJ 6 I=1,NPJINT
      D3(I)=KC2(I,J)
    6 CJNTINUE
      CALL CHASIZ(2.6,2.7)
      CALL GRASYM(TIME,D3,NPJINT,MS,NSPACE)
   14 CJNTINUE
      DJ 15 J=1,3
      MS=NSYM(J)
      TI=TC(J)
      R=RN(J)
      S=S2(J)
      DJ 7 I=1,NPJINT
      D1(I)=KT(I,J)
      D2(I)=KE(I,J)
    7 CJNTINUE
      AK=AMAX1(KC(1,J),KE(1,J))
      AJK=1.25*AK
      CALL SHIFT2(300.0,0.0)
      CALL AXISPLJT(130.0,130.0,AJK,AJK)
      CALL GRAPJL(D2,D2,NPJINT)
      CALL GRASYM(D1,D2,NPJINT,MS,1)
      CALL GRABJX1(-50.0,-40.0,CJ,TI,R,S)
   15 CJNTINUE
      CALL DEVEND
      RETURN
      END
      SUBRJUTINE TJ SET UP AXES FJR GRAPH PLJTTING

      SUBRJUTINE AXISPLJT(R,X,Y,Z)
      CALL AXIPJS(1,0.0,0.0,R,1)
      CALL AXIPJS(1,0.0,0.0,X,2)
      CALL AXISCA(3,5,0.0,Y,1)
      CALL AXISCA(3,5,0.0,Z,2)
      CALL AXIDRA(1,1,1)
      CALL AXIDRA(-1,-1,2)
      RETURN
      END
```

```
SUBROUTINE FOR A LINEAR REGRESSION ANALYSIS ON EXPERIMENTAL DATA


      SUBROUTINE APPLE(X,Y,N,B,A,R,S)
      DIMENSION X(50),Y(50)
      SUMX=0.0
      SUMY=0.0
      SUMX2=0.0
      SUMY2=0.0
      SUMXY=0.0
      DO 10 I=1,N
      SUMX=SUMX+X(I)
      SUMY=SUMY+Y(I)
      SUMX2=SUMX2+X(I)**2.
      SUMY2=SUMY2+Y(I)**2.
      SUMXY=SUMXY+X(I)*Y(I)
   10 CONTINUE
      AN=N
      XM=SUMX/AN
      YM=SUMY/AN
      B=(SUMXY-AN*XM*YM)/(SUMX2-AN*XM**2.)
      A=YM-B*XM
      R1=(SUMXY-SUMX*SUMY/AN)**2
      R2=SUMX2-SUMX**2/AN
      R3=SUMY2-SUMY**2/AN
      R=R1/(R2*R3)
      S=SQRT((SUMY2-A*SUMY-B*SUMXY)/(AN-2))
      RETURN
      END

      SUBROUTINE TO LABEL AXES AND SET UP A FRAME
      AROUND THE AXES

      SUBROUTINE GRABOX(X,Y,CO)
      C=100.0*CO
      CALL MOVTO2(X,Y)
      CALL LINTO2(X,540.0)
      CALL LINTO2(390.0,540.0)
      CALL LINTO2(390.0,Y)
      CALL LINTO2(X,Y)
      CALL MOVTO2(50.0,480.0)
      CALL CHAHOL(43HDRYING CHARACTERISTICS OF WESTBURY SLURRY*.)
      CALL MOVTO2(200.0,480.0)
      CALL CHAHOL(33HSAMPLE WITH AN INITIAL M. C. OF*.)
      CALL MOVTO2(315.0,480.0)
      CALL CHAFIX(C,6,2)
      CALL MOVTO2(340.0,480.0)
      CALL CHAHOL(10HPER CENT*.)
      CALL MOVTO2(X,Y)
      CALL MOVTO2(60.0,210.0)
      CALL CHAHOL(27HEFFECT OF AIR TEMPERATURE*.)
```

```
CALL MOVTO2(60.0,200.0)
CALL CHAHOL(17HON CRUST GROWTH*.)
CALL MOVTO2(60.0,440.0)
CALL CHAHOL(33HCRUST MASS TRANSFER COEFFICIENT*.)
CALL MOVTO2(60.0,430.0)
CALL CHAHOL(38HAT ALL EXPERIMENTAL AIR TEMPERATURES*.)
CALL MOVTO2(250.0,440.0)
CALL CHAHOL(35HOVERALL MASS TRANSFER COEFFICIENT*.)
CALL MOVTO2(250.0,430.0)
CALL CHAHOL(38HAT ALL EXPERIMENTAL AIR TEMPERATURES*.)
CALL MOVTO2(250.0,210.0)
CALL CHAHOL(27HEFFECT OF AIR TEMPERATURE*.)
CALL MOVTO2(250.0,200.0)
CALL CHAHOL(16HON DRYING RATE*.)
CALL MOVTO2(60.0,30.0)
CALL CHAHOL(22HDRYING TIME(SECONDS)*.)
CALL MOVTO2(60.0,260.0)
CALL CHAHOL(22HDRYING TIME(SECONDS)*.)
CALL MOVTO2(255.0,260.0)
CALL CHAHOL(22HDRYING TIME(SECONDS)*.)
CALL MOVTO2(20.0,80.0)
CALL CHAANG(90.0)
CALL CHAHOL(25HCRUST THICKNESS(METERS)*.)
CALL MOVTO2(20.0,290.0)
CALL CHAANG(90.0)
CALL CHAHOL(38HCRUST MASS TRANSFER COEFFICIENT(M/S)*.)
CALL MOVTO2(210.0,290.0)
CALL CHAANG(90.0)
CALL CHAHOL(40HOVERALL MASS TRANSFER COEFFICIENT(M/S)*.)
CALL MOVTO2(210.0,75.0)
CALL CHAANG(90.0)
CALL CHAHOL(33HDRYING RATE(KG/SQ.METER-SECOND)*.)
CALL CHAANG(0.0)
CALL MOVTO2(255.0,30.0)
CALL CHAHOL(22HDRYING TIME(SECONDS)*.)
CALL MOVTO2(X,Y)
RETURN
END
SUBROUTINE GRABOX1(X1,Y1,CO,T1,K,S)
C=100.0*CO
CALL MOVTO2(X1,Y1)
CALL LINTO2(X1,250.0)
CALL LINTO2(160.0,250.0)
CALL LINTO2(160.0,Y1)
CALL LINTO2(X1,Y1)
CALL MOVTO2(35.0,220.0)
CALL CHAHOL(33HEXPERIMENTAL VERSUS THEORETICAL*.)
CALL MOVTO2(35.0,210.0)
CALL CHAHOL(31HMASS TRANSFER COEFFICIENT FOR*.)
CALL MOVTO2(35.0,200.0)
CALL CHAHOL(24HWESTBURY SLURRY SAMPLE*.)
CALL MOVTO2(45.0,150.0)
```

```
      CALL CHAHOL(31HA*LIR *UT*LEMPERATURE(DEG.C)=*.)
      CALL MOVTO2(105.0,150.0)
      CALL CHAFIX(T1,6,2)
      CALL MOVTO2(45.0,145.0)
      CALL CHAHOL(35HM*LOISTURE *UC*LONTENT(PER CENT)=*.)
      CALL MOVTO2(115.0,145.0)
      CALL CHAFIX(C,6,2)
      CALL MOVTO2(45.0,140.0)
      CALL CHAHOL(27HS*LTANDARD *UD*LEVIATION=*.)
      CALL MOVTO2(100.0,140.0)
      CALL CHAFLO(S,10)
      CALL MOVTO2(45.0,135.0)
      CALL CHAHOL(30HC*LORRELATION *UC*LOEFFIENT=*.)
      CALL MOVTO2(112.0,135.0)
      CALL CHAFIX(R,6,4)
      CALL CHAANG(90.0)
      CALL MOVTO2(-15.0,10.0)
      CALL CHAHOL(45HEXPERIMENTAL MASS TRANSFER COEFFICIENT(M/S)*.)
      CALL CHAANG(0.0)
      CALL MOVTO2(30.0,-15.0)
      CALL CHAHOL(44HTHEORETICAL MASS TRANSFER COEFFICIENT(M/S)*.)
      CALL MOVTO2(X1,Y1)
      RETURN
      END
      SUBROUTINE LINTER(X,Y,N,XIN,YOUT)

      PROGRAM FOR INTERPOLATION FOR WATER VAPOUR DENSITY
      BY THE LANGRANGIAN INTERPOLATION METHOD
      DIMENSION X(70),Y(70)
      YOUT=0.0
      DO 20 I=1,N
      TERM=Y(I)
      DO 10 J=1,N
      IF(I-J) 9,10,9
    9 TERM=TERM*(XIN-X(J))/(X(I)-X(J))
   10 CONTINUE
   20 YOUT=YOUT+TERM
      RETURN
      END
      FINISH
```

APPENDIX C

1. Figures C1-C10, Graphical plots of the effect of drying air temperature on the Drying Characteristics of the slurry samples.

2. Figures C11-C26, Graphical plots of the effect of the initial moisture content of slurry samples on their Drying Characteristics.

FIGURE C1

DRYING CHARACTERISTICS OF NORTHFLEET SLURRY SAMPLE WITH AN INITIAL M. C. OF 45.00 PER CE T

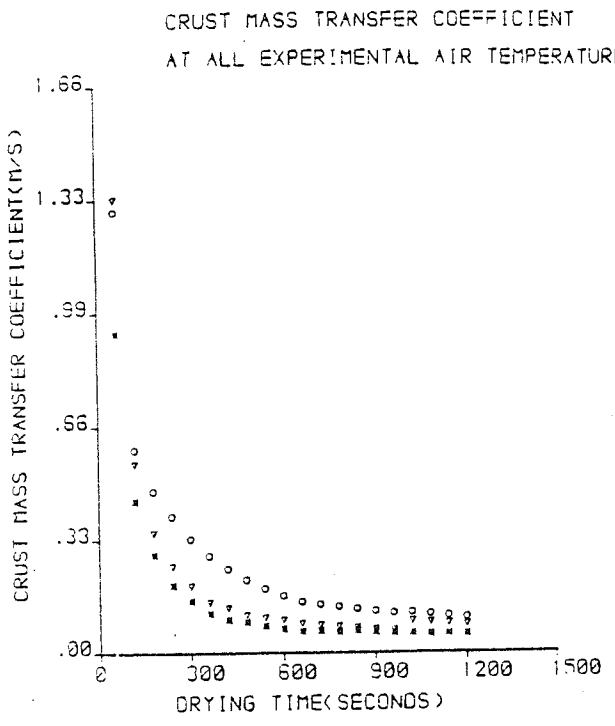

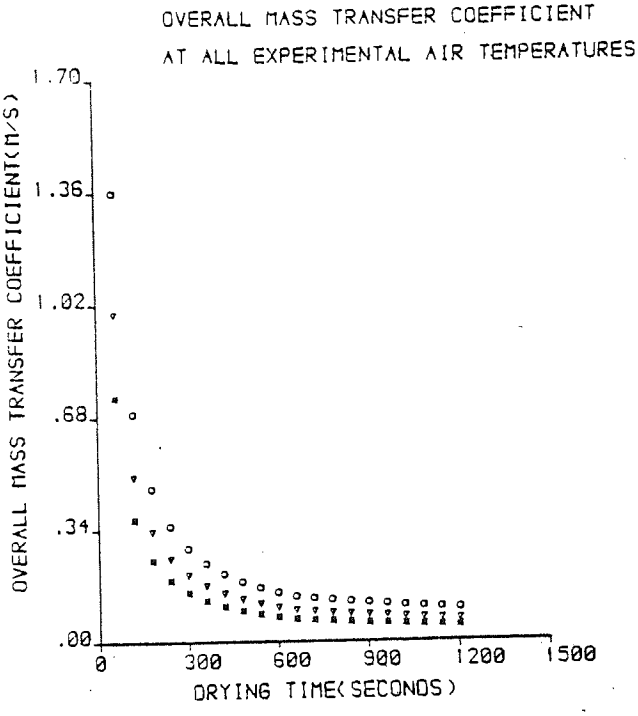

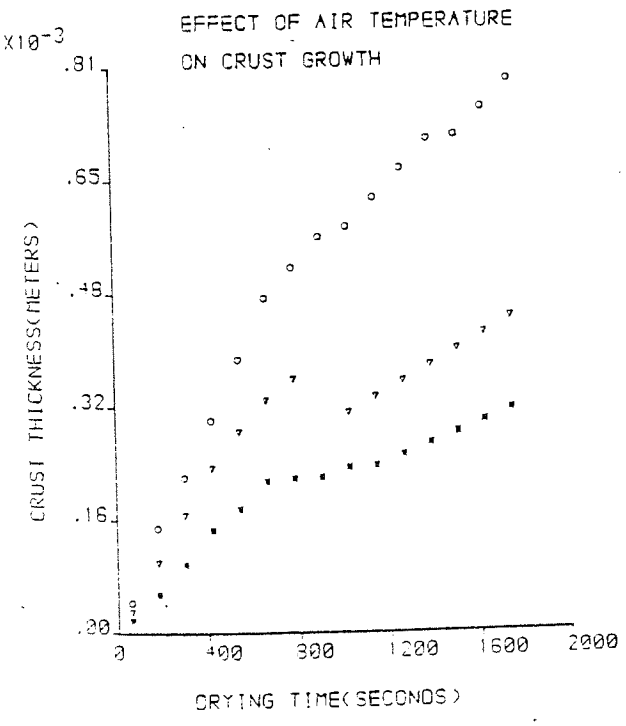

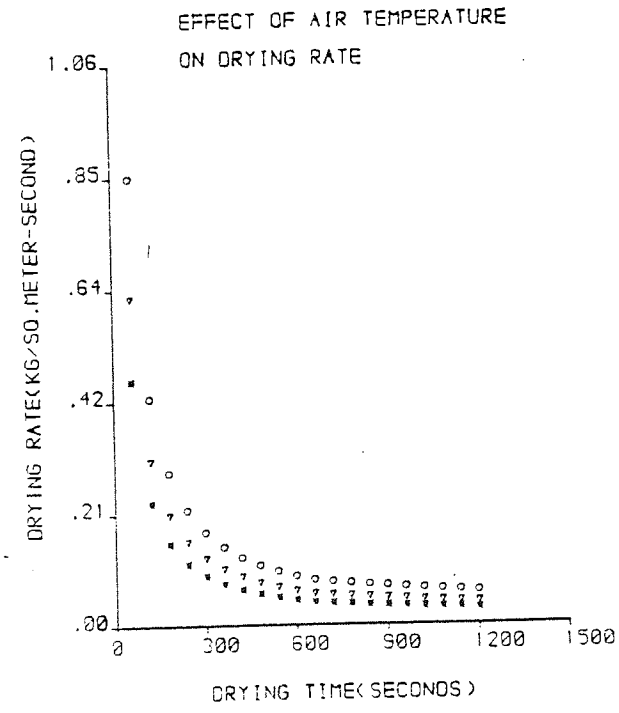

FIGURE C2

DRYING CHARACTERISTICS OF NORTHFLEET SLURRY SAMPLE WITH AN INITIAL M. C. OF 50.00 PER CENT

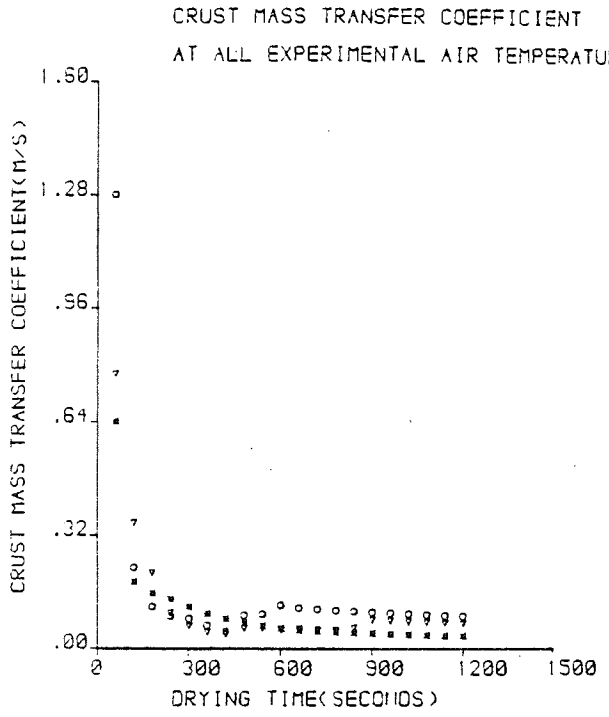

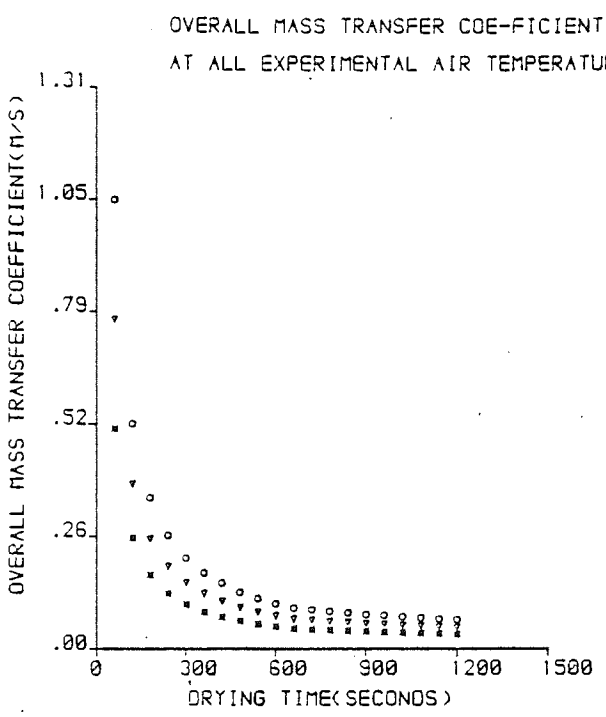

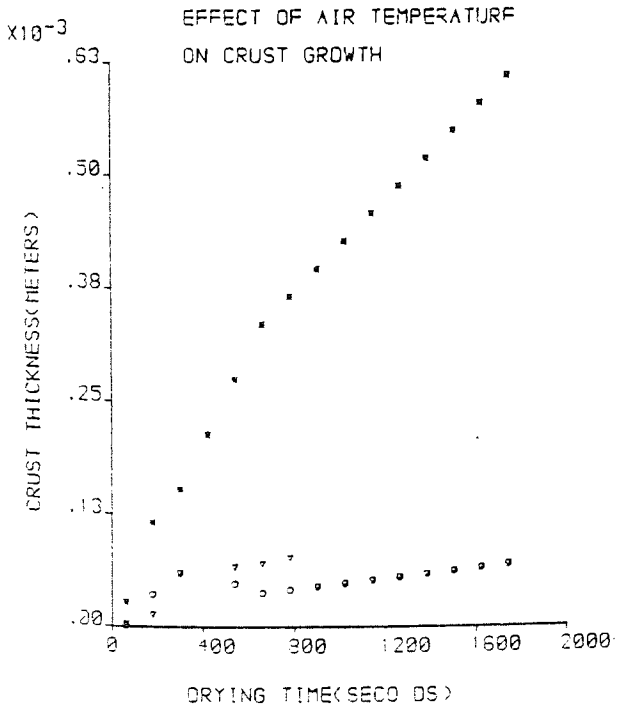

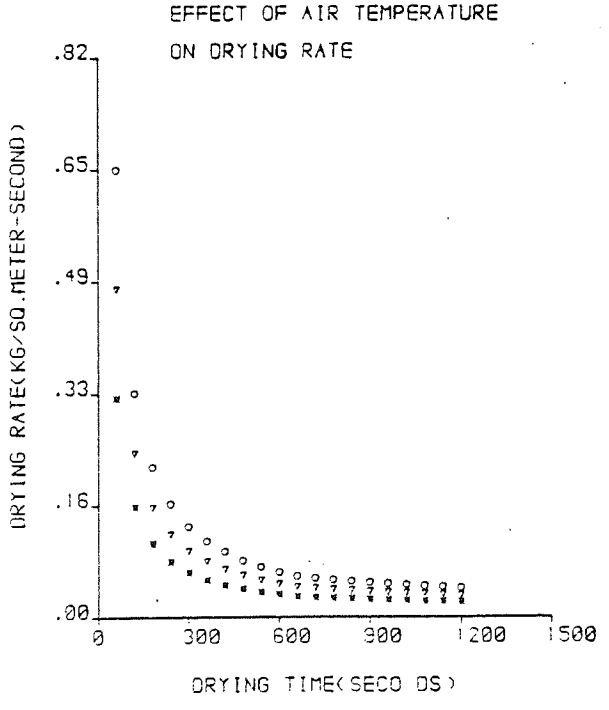

FIGURE C3

DRYING CHARACTERISTICS OF HUMBER SLURRY SAMPLE WITH AN INITIAL M. C. OF 45.00 PER CENT

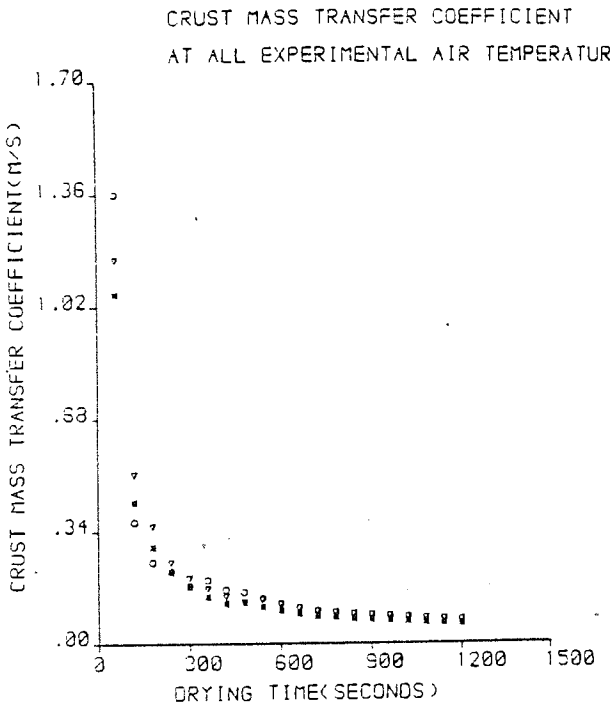

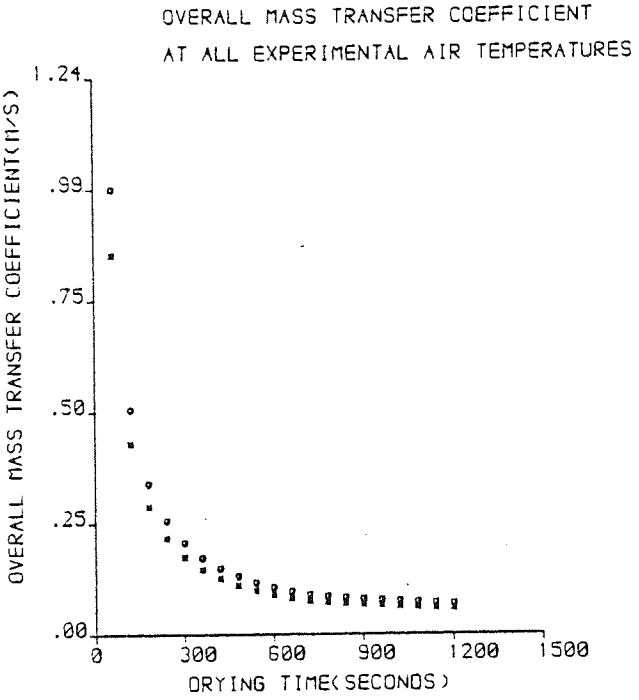

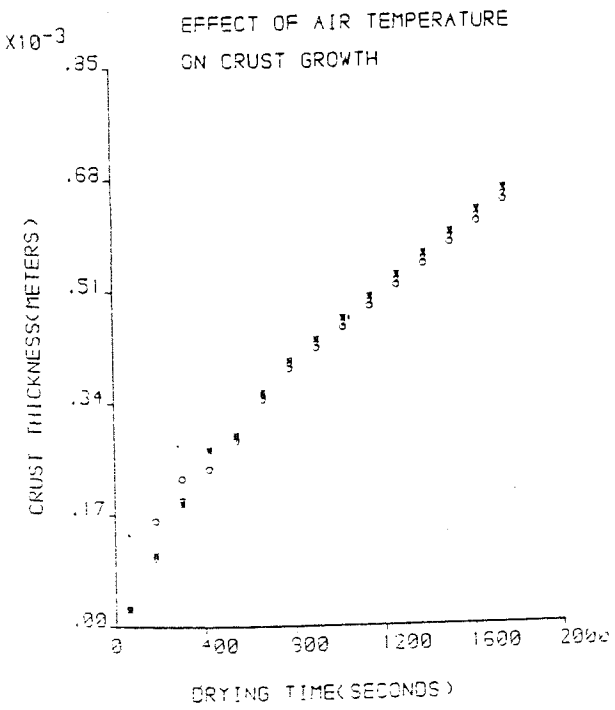

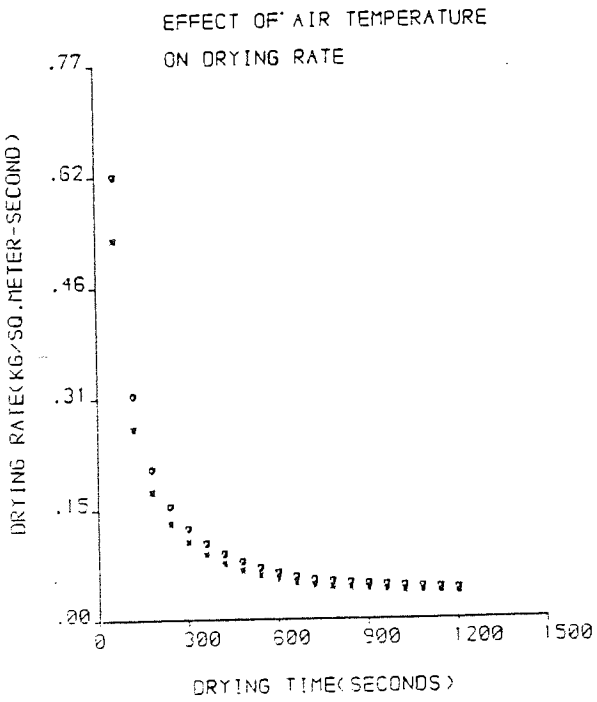

FIGURE C4

DRYING CHARACTERISTI S OF MASON SLURRY SAMPLE WITH AN INITIAL M. C. OF 35.00 PER CENT

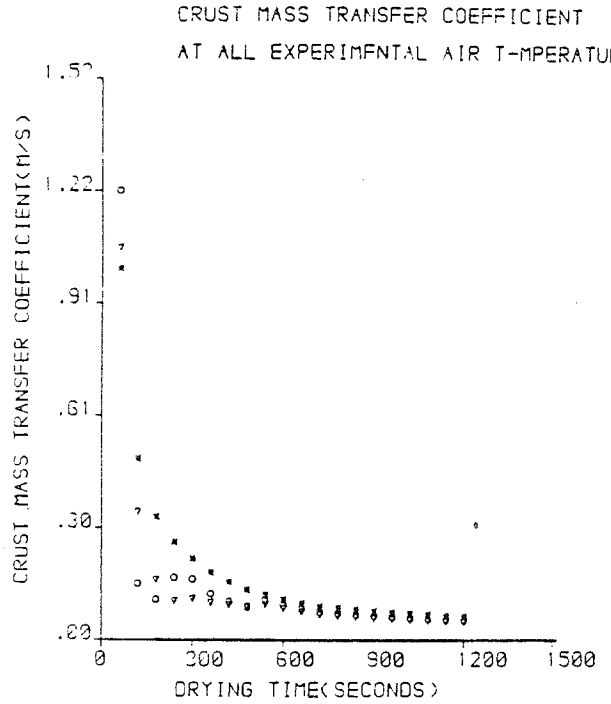

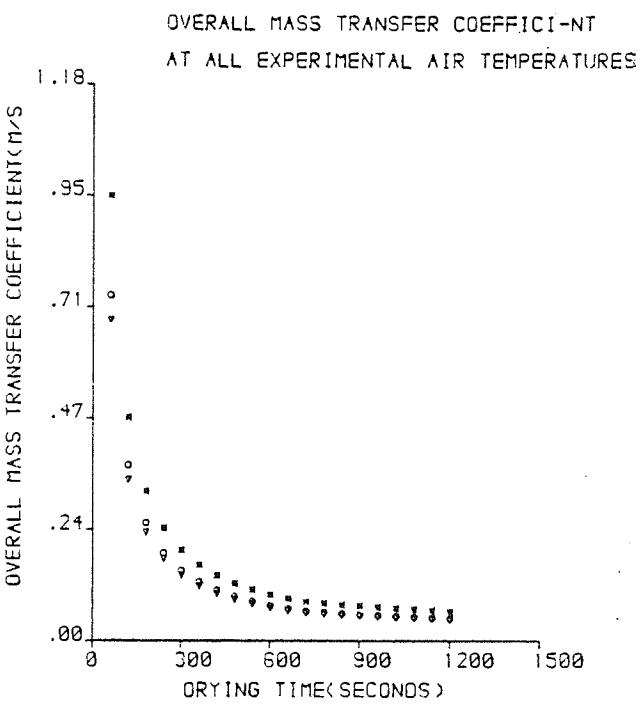

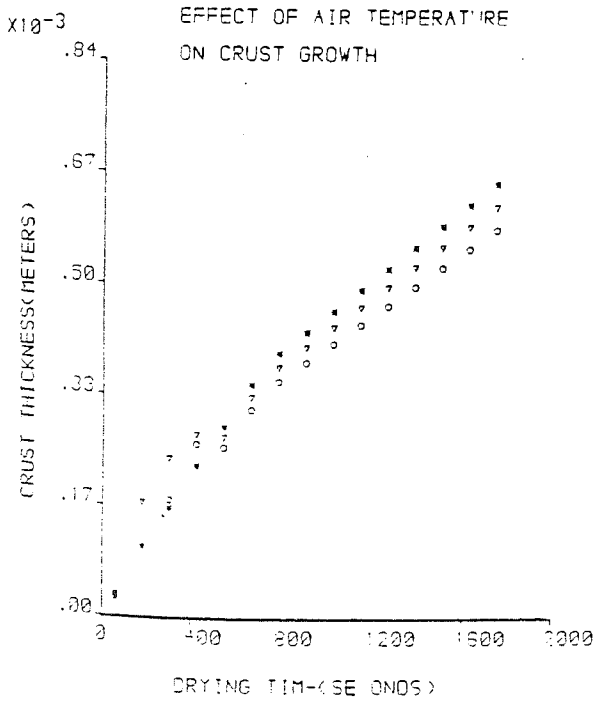

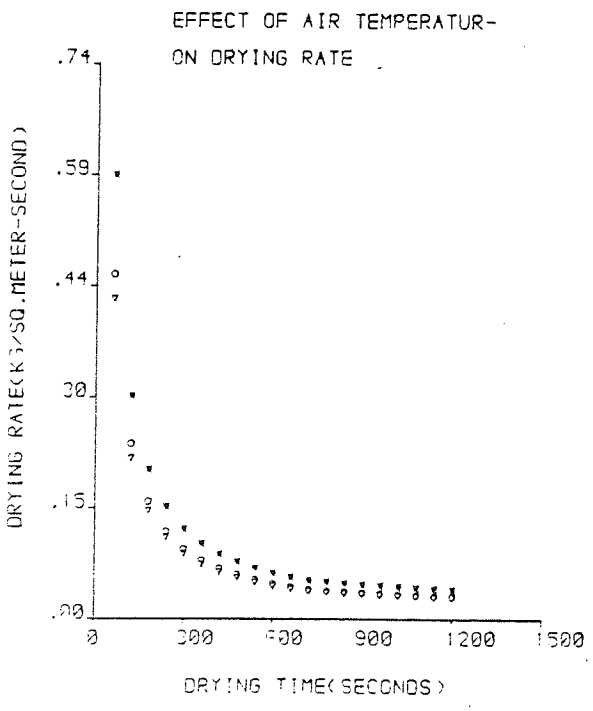

FIGURE C5

DRYING CHARACTERISTI S OF MASON SLURRY SAMPLE WITH AN INITIAL M. C. OF 45.00 PER CENT

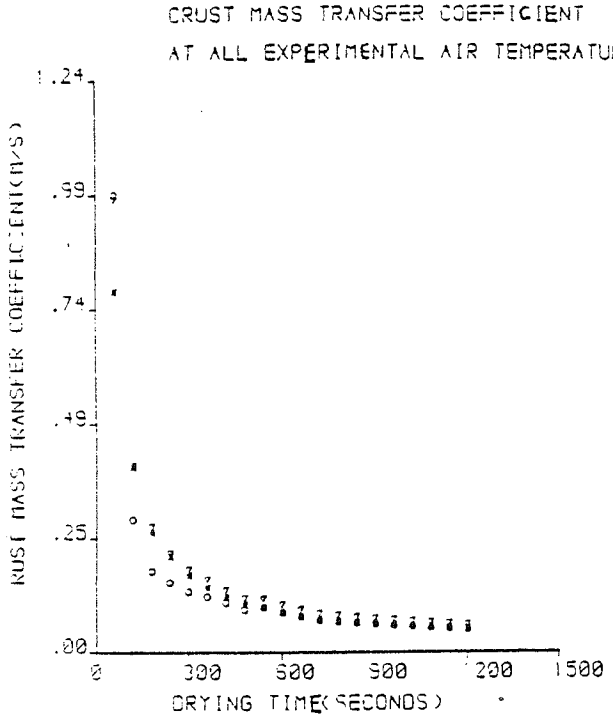

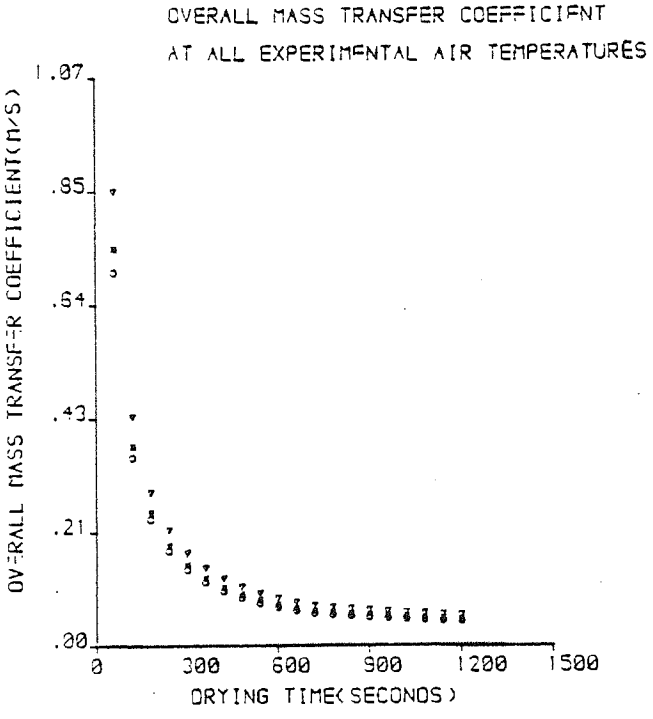

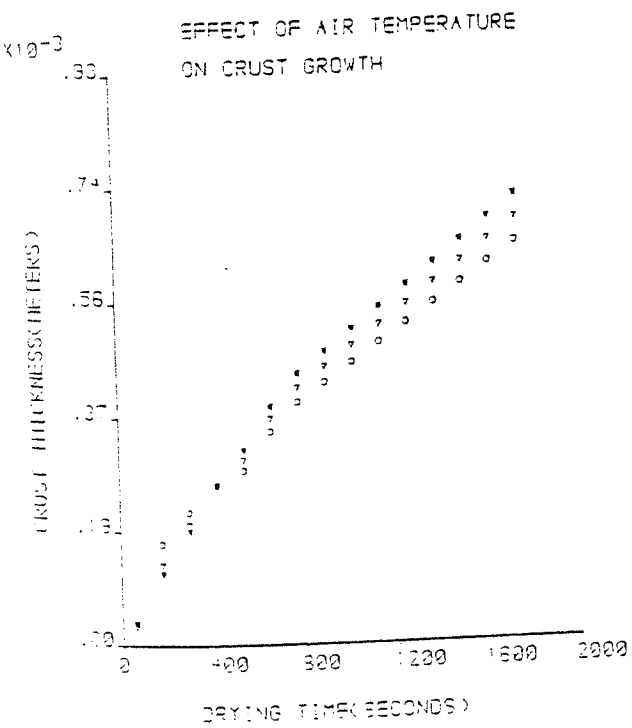

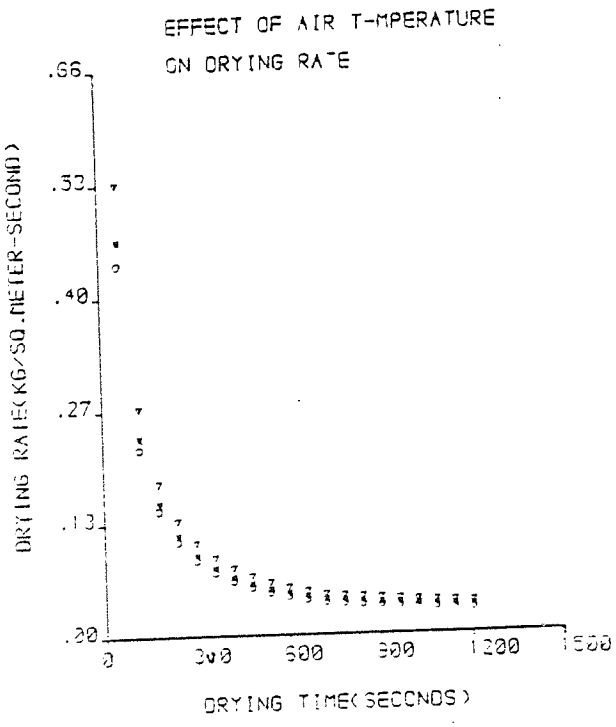

FIGURE C6

DRYING CHARACTERISTICS OF SHOREHAM SLURRY SAMPLE WITH AN INITIAL M. C. OF 30.00 PER CENT

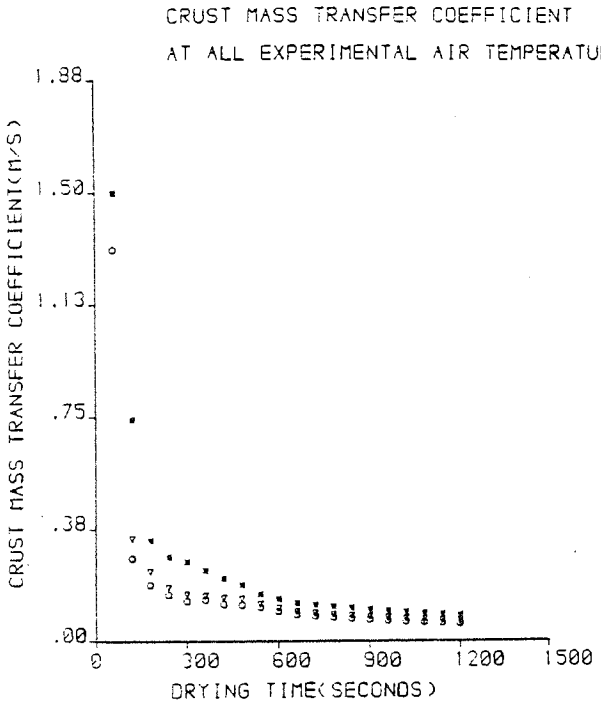

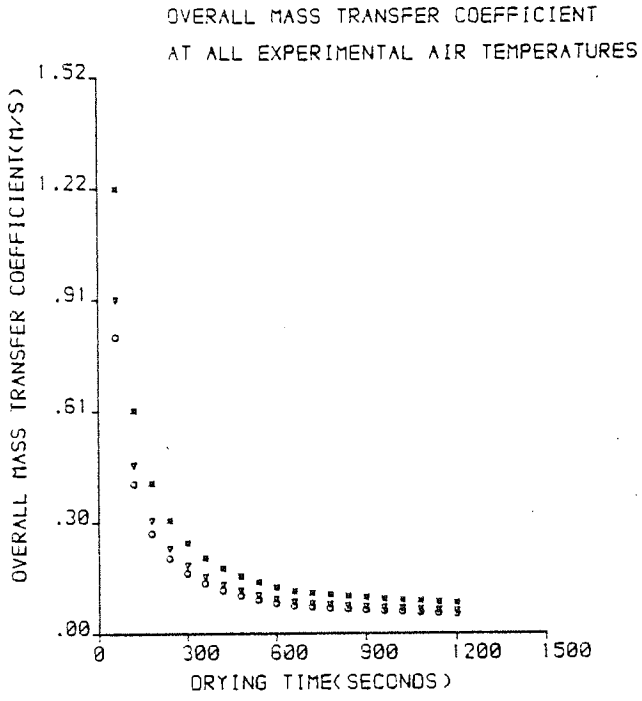

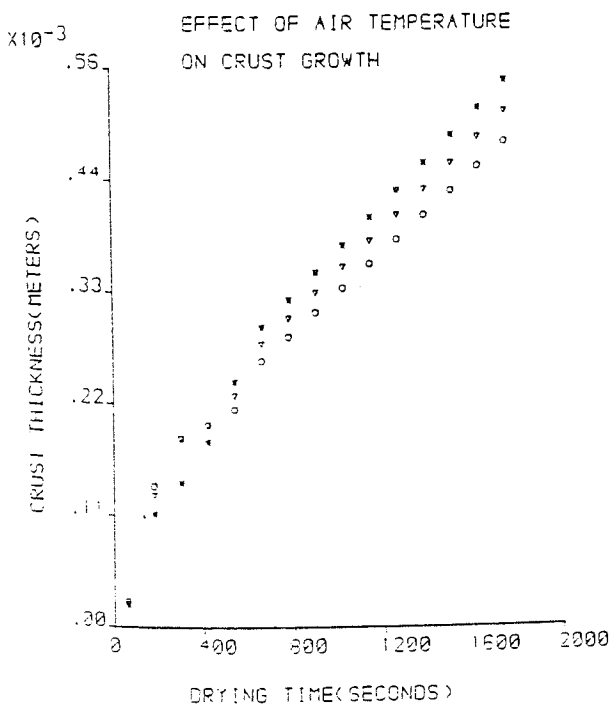

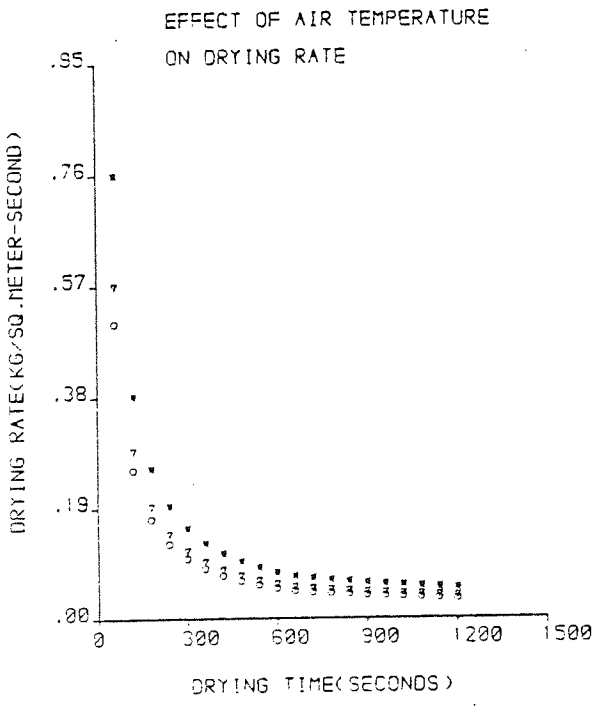

FIGURE C7

DRYING CHARACTERISTICS OF WESTBURY SLURRY SAMPLE WITH AN INITIAL M. C. OF 30.00 PER CENT

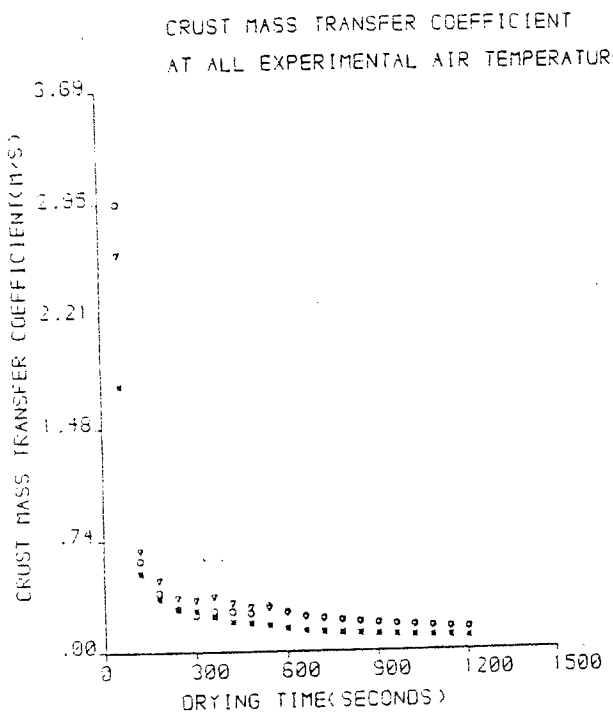

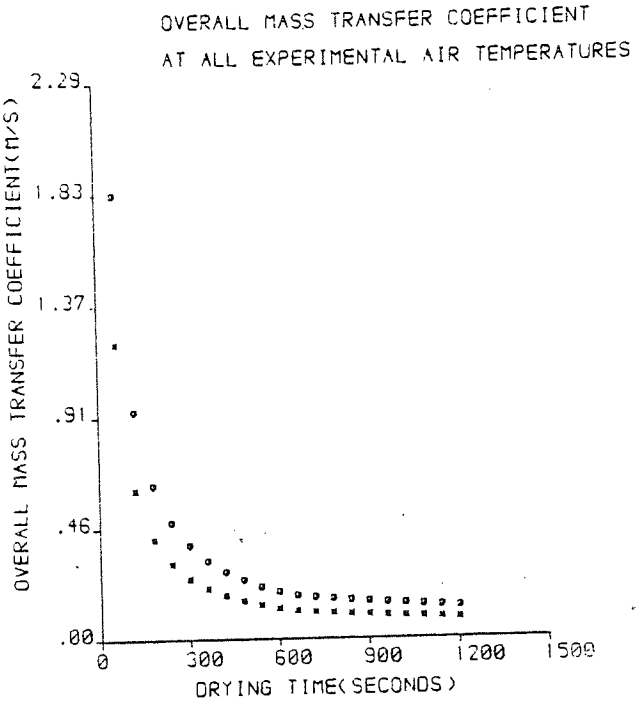

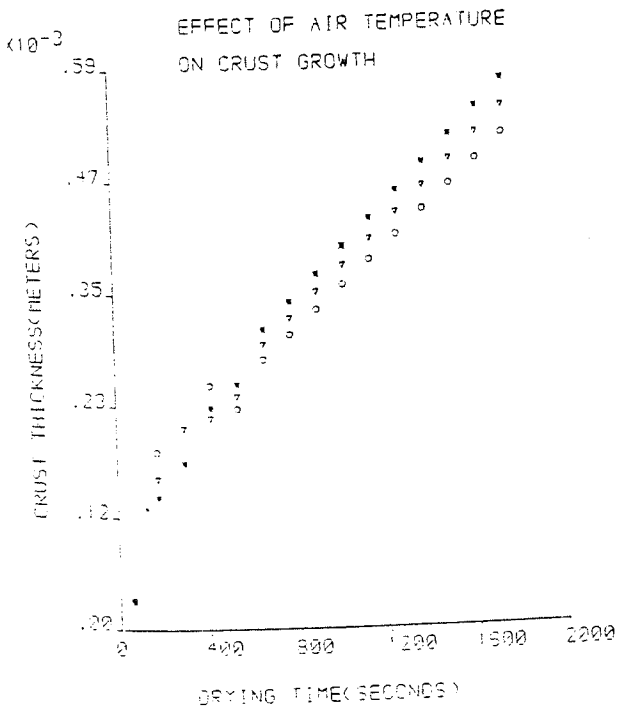

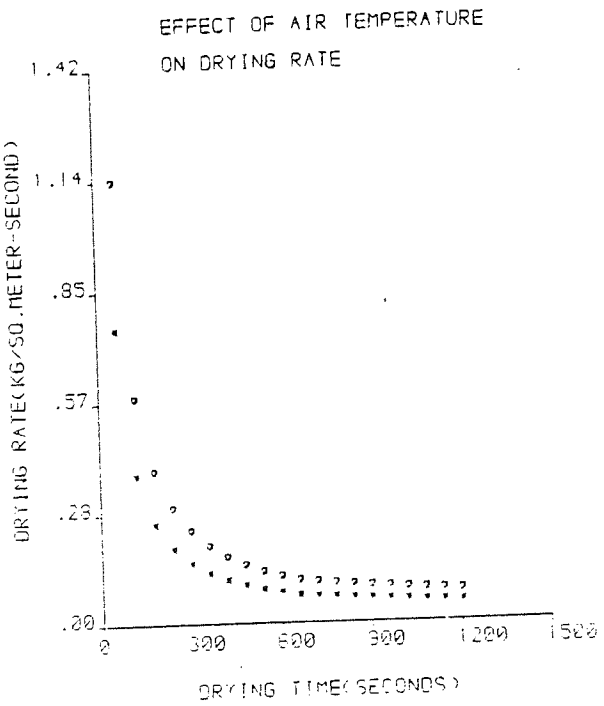

FIGURE C8

DRYING CHARACTERISTICS OF WESTBURY SLURRY SAMPLE WITH AN INITIAL M. C. OF 35.00 PER CENT

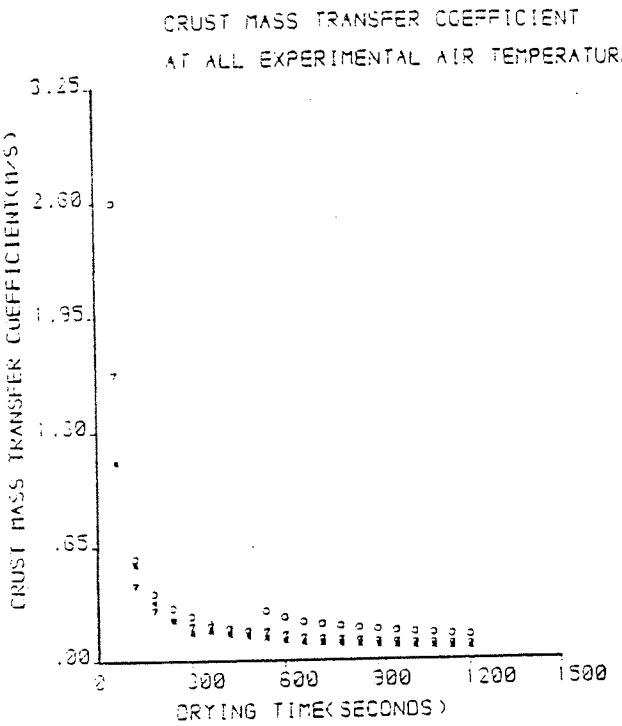

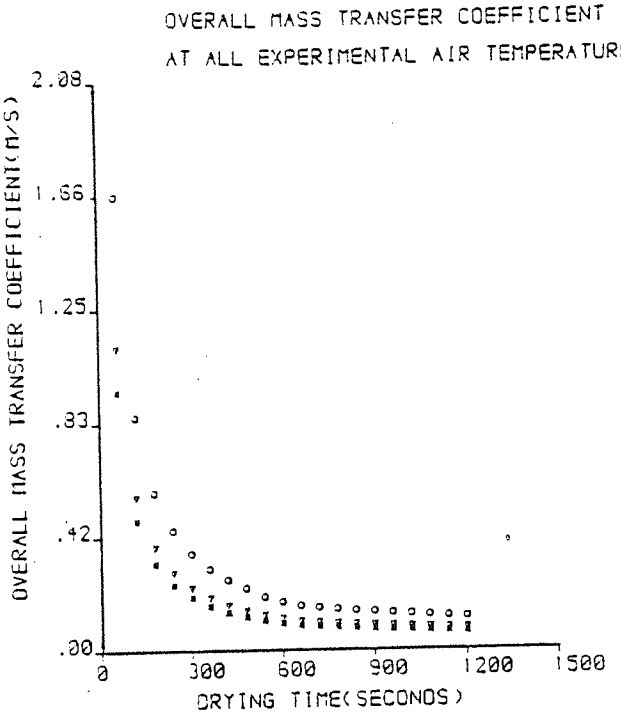

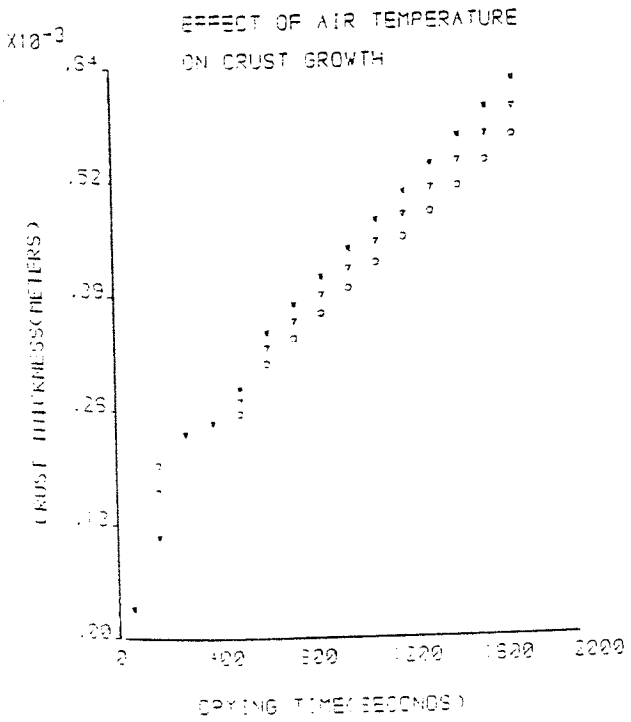

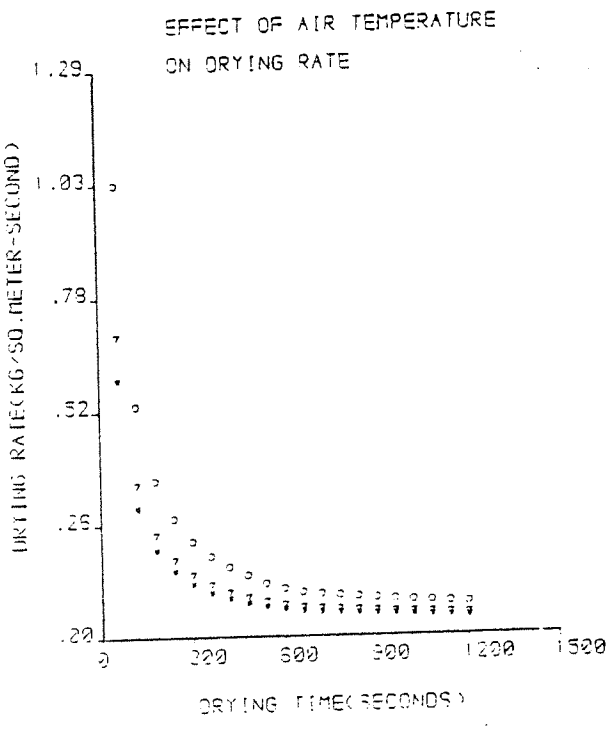

FIGURE C9

DRYING CHARACTERISTICS OF WESTBURY SLURRY SAMPLE WITH AN INITIAL M. C. OF 45.00 PER CENT

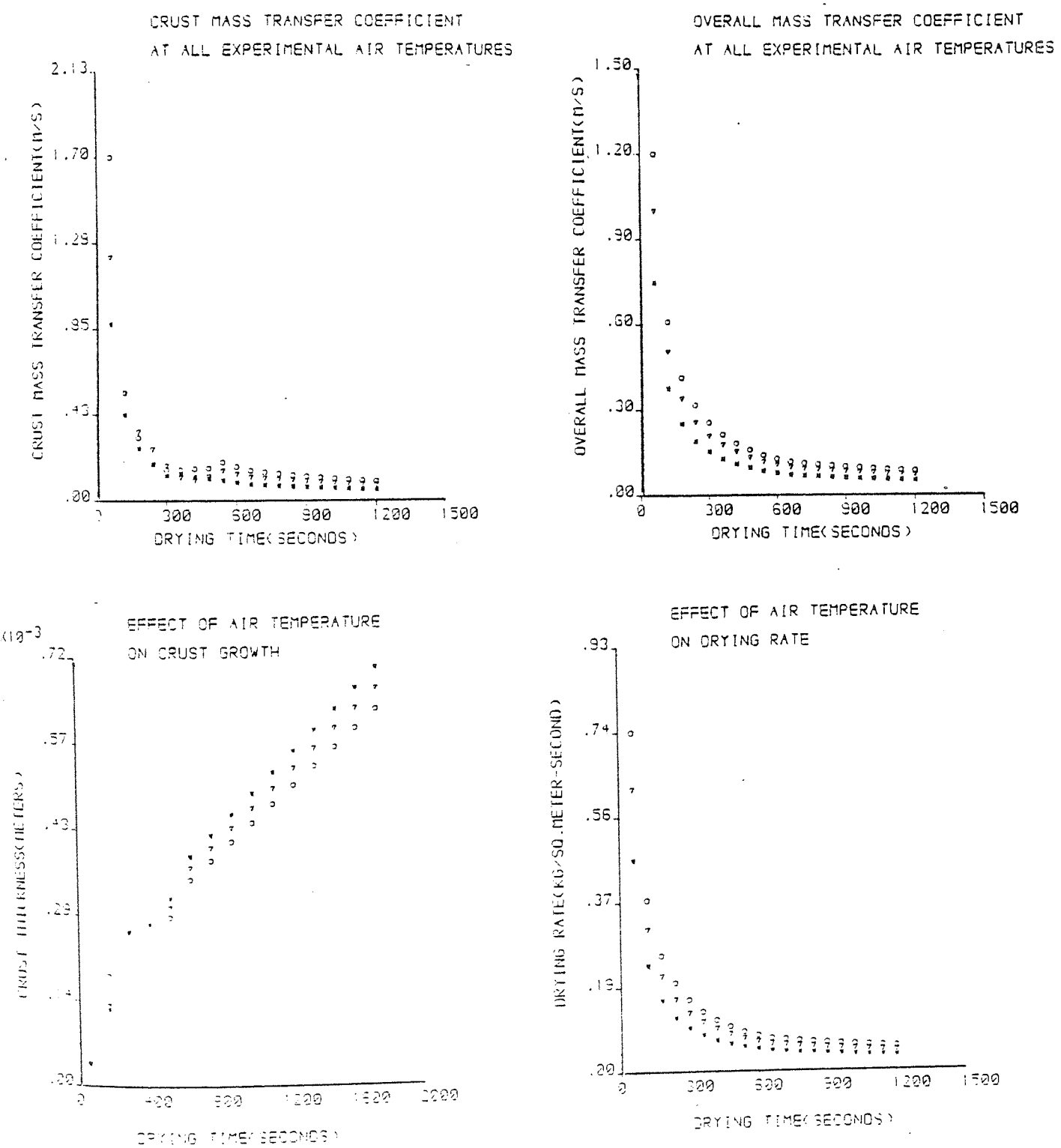

FIGURE C10

DRYING CHARACTERISTICS OF WESTBURY SLURRY SAMPLE WITH AN INITIAL M. C. OF 55.00 PER CENT

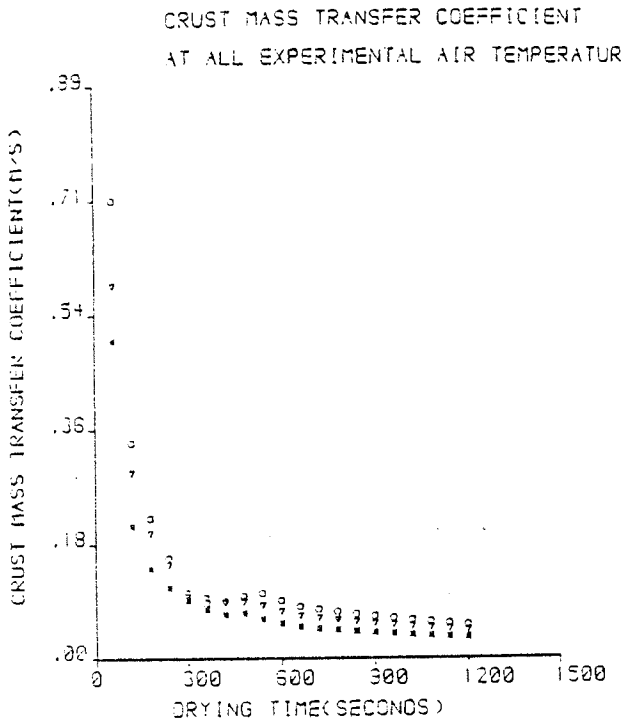

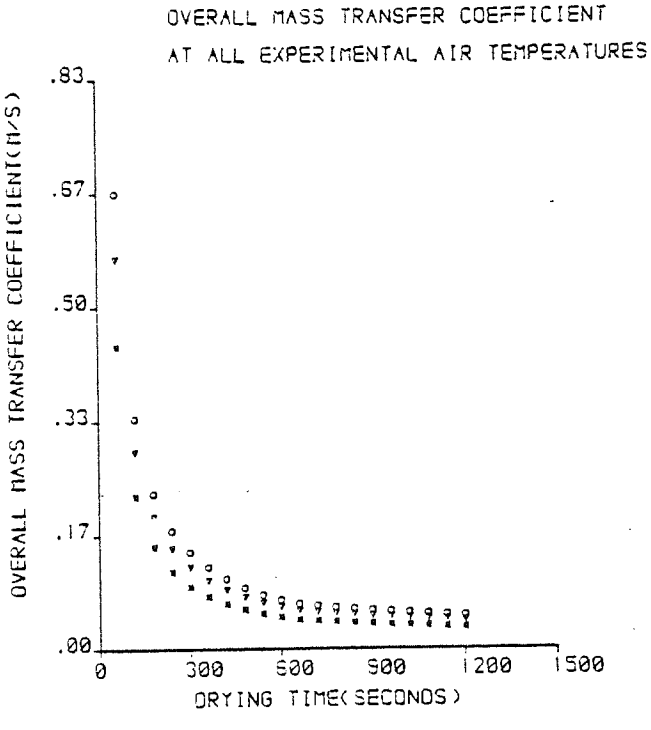

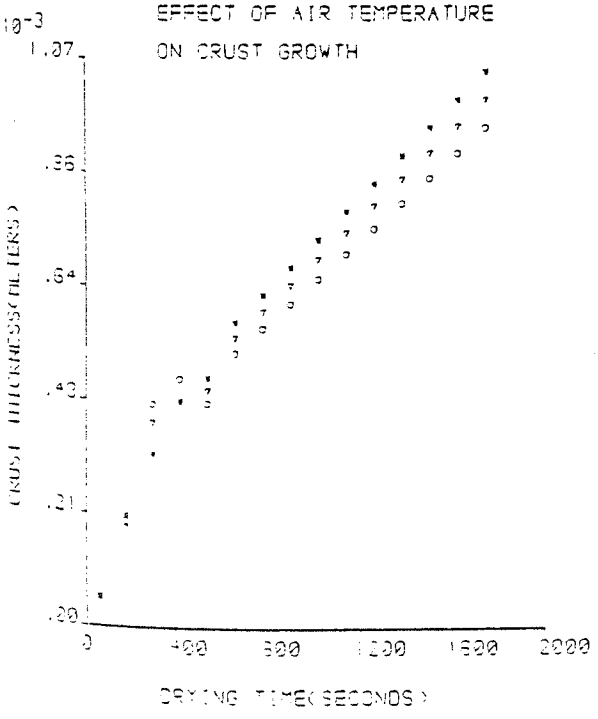

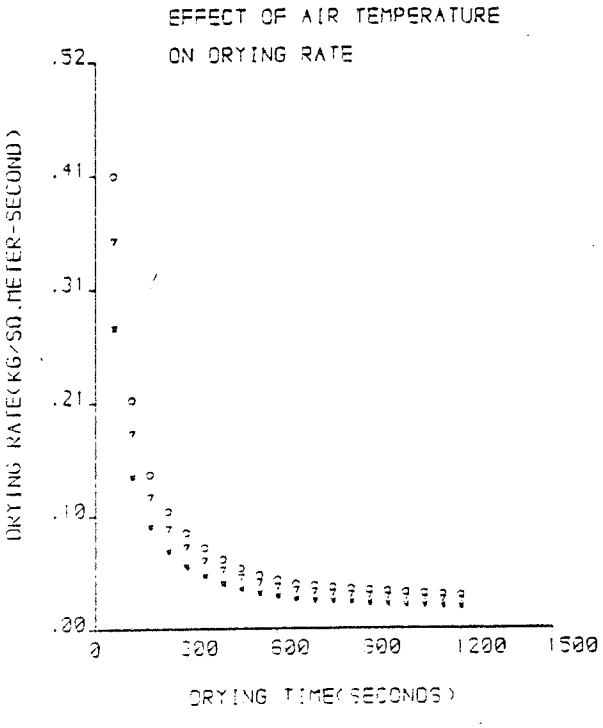

FIGURE C11

EFFECT OF INITIAL MOISTURE CONTENT ON CRUST GROWTH RATE FOR SHOREHAM SLURRY

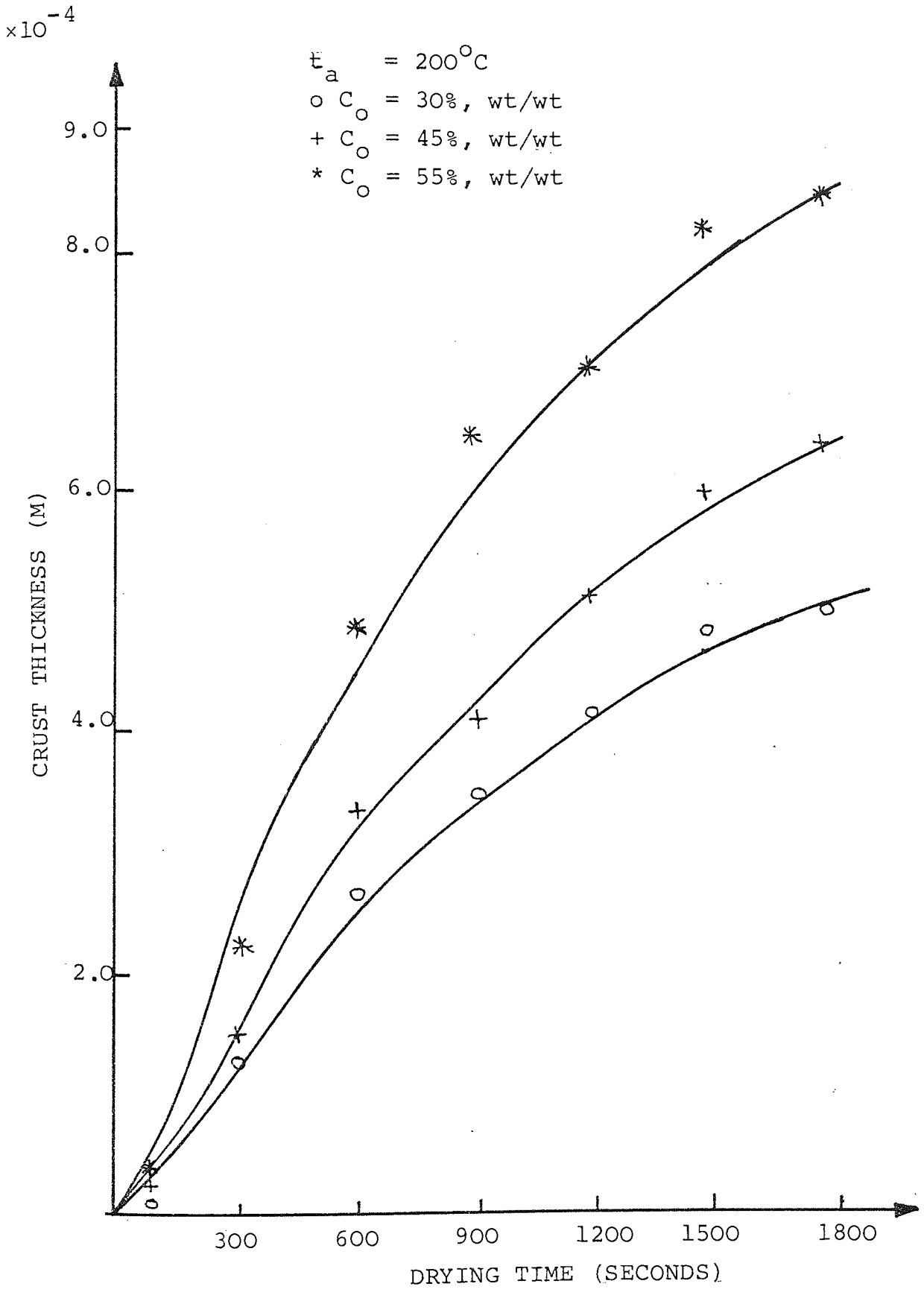

FIGURE C12

EFFECT ON INITIAL SLURRY M.C. ON CRUST GROWTH RATE FOR NORTHFLEET SLURRY

t_a = 200°C
o C_o = 45%, wt/wt
+ C_o = 45%, wt/wt
* C_o = 55%, wt/wt

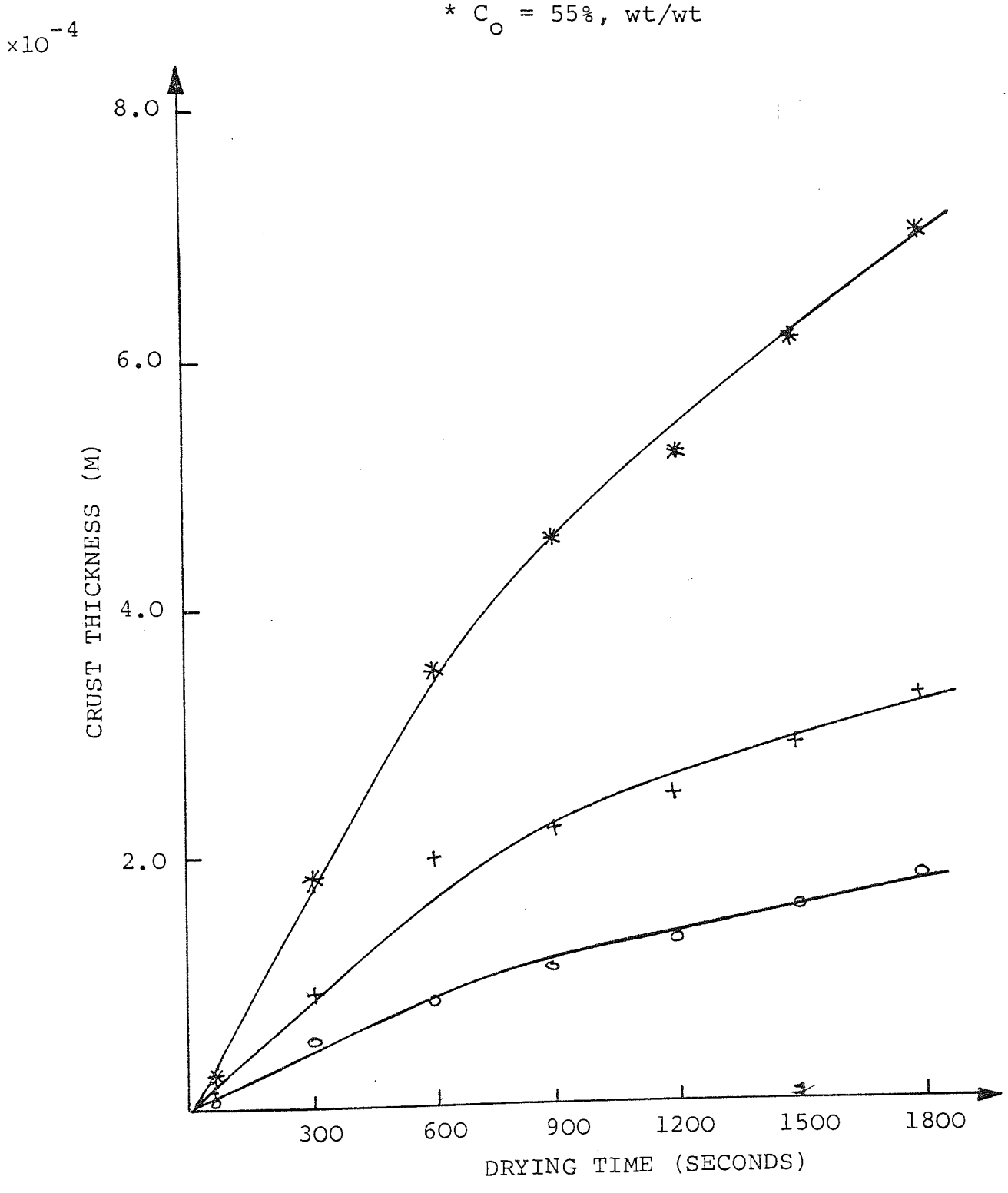

FIGURE C13

EFFECT OF INITIAL MOISTURE CONTENT ON THE CRUST GROWTH RATE FOR MASON SLURRY

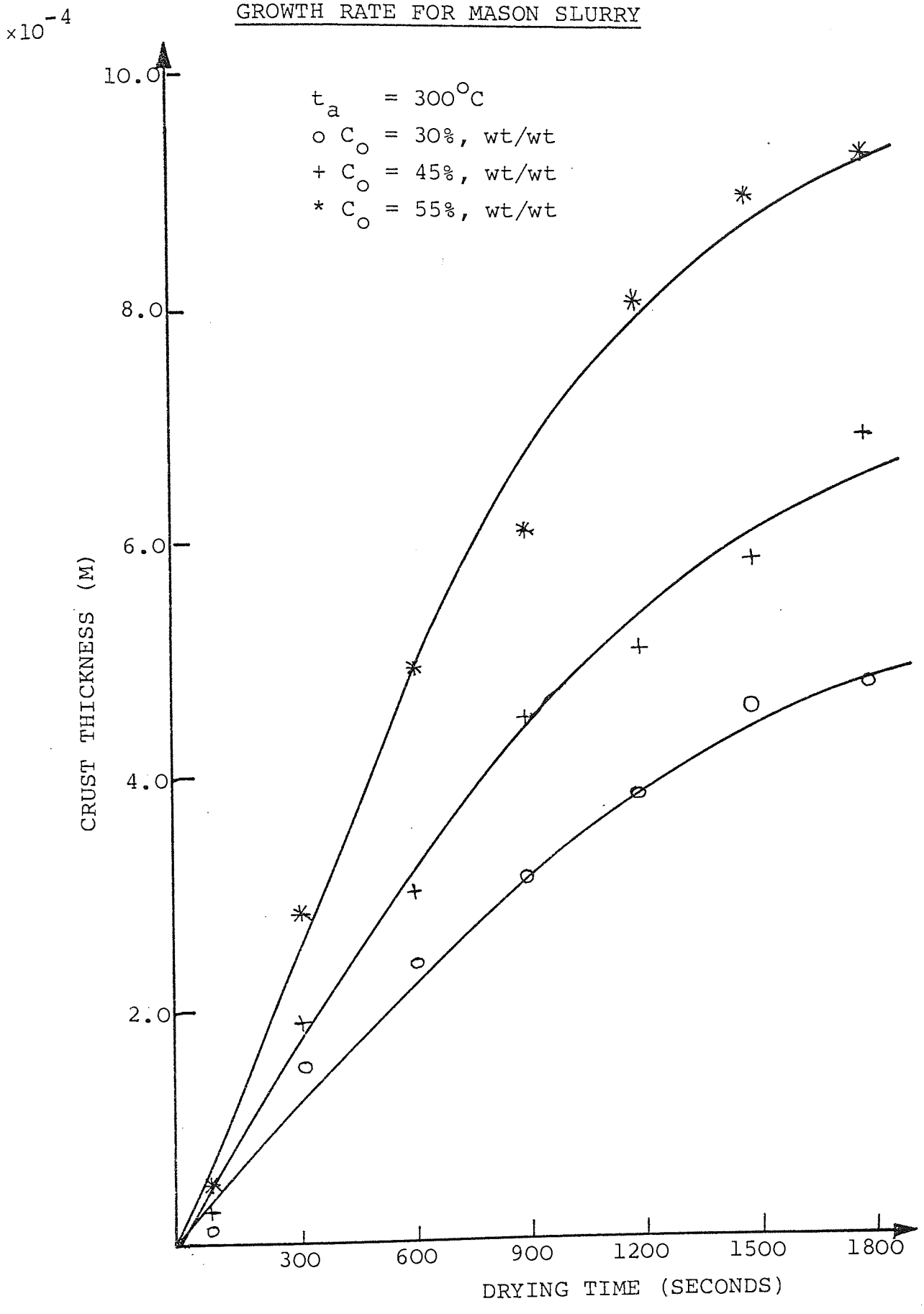

FIGURE C14

EFFECT OF INITIAL MOISTURE CONTENT ON THE CRUST GROWTH RATE FOR HUMBER SLURRY

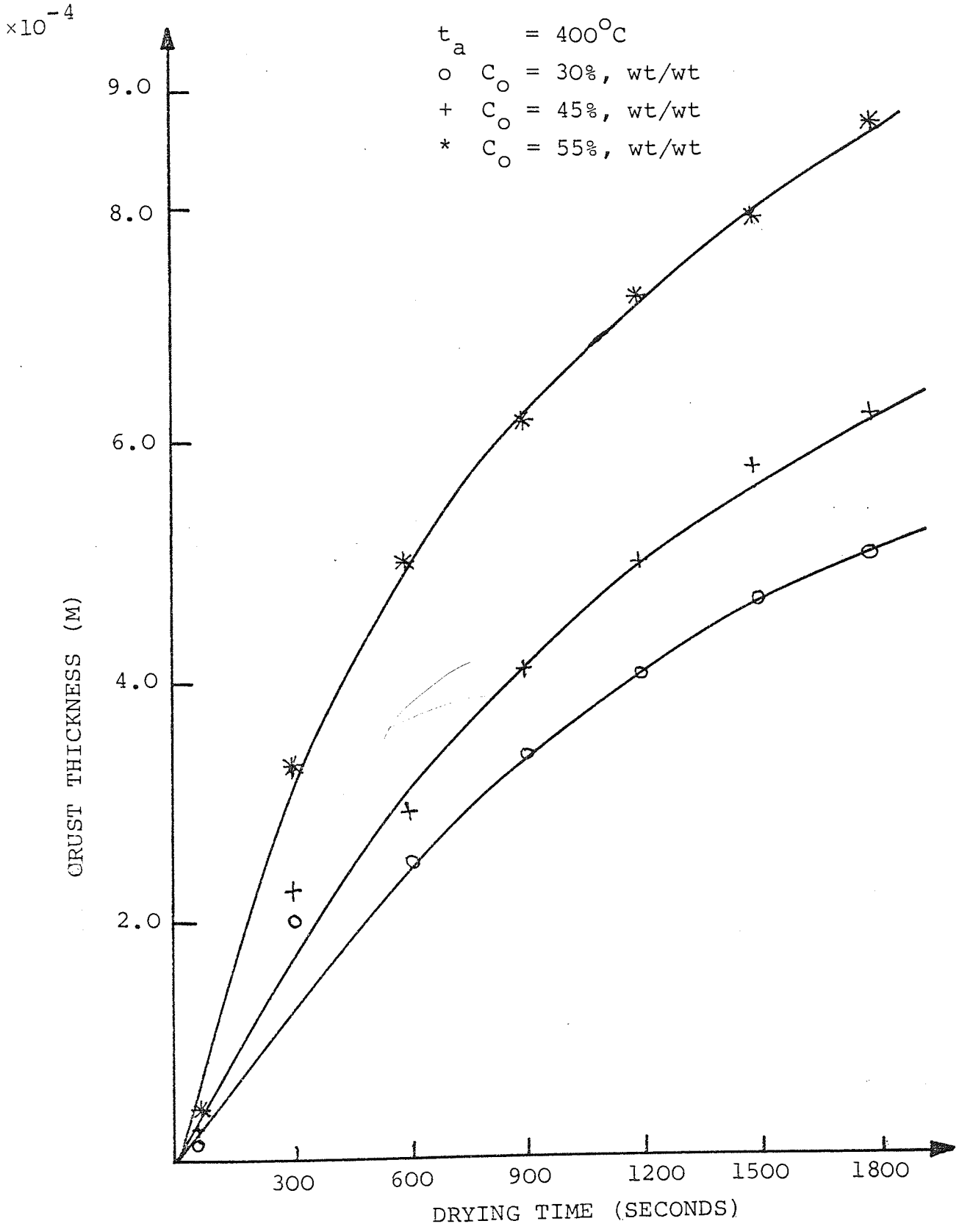

FIGURE C15

EFFECT OF INITIAL MOISTURE CONTENT ON CRUST MASS TRANSFER COEFFICIENT FOR SHOREHAM SLURRY

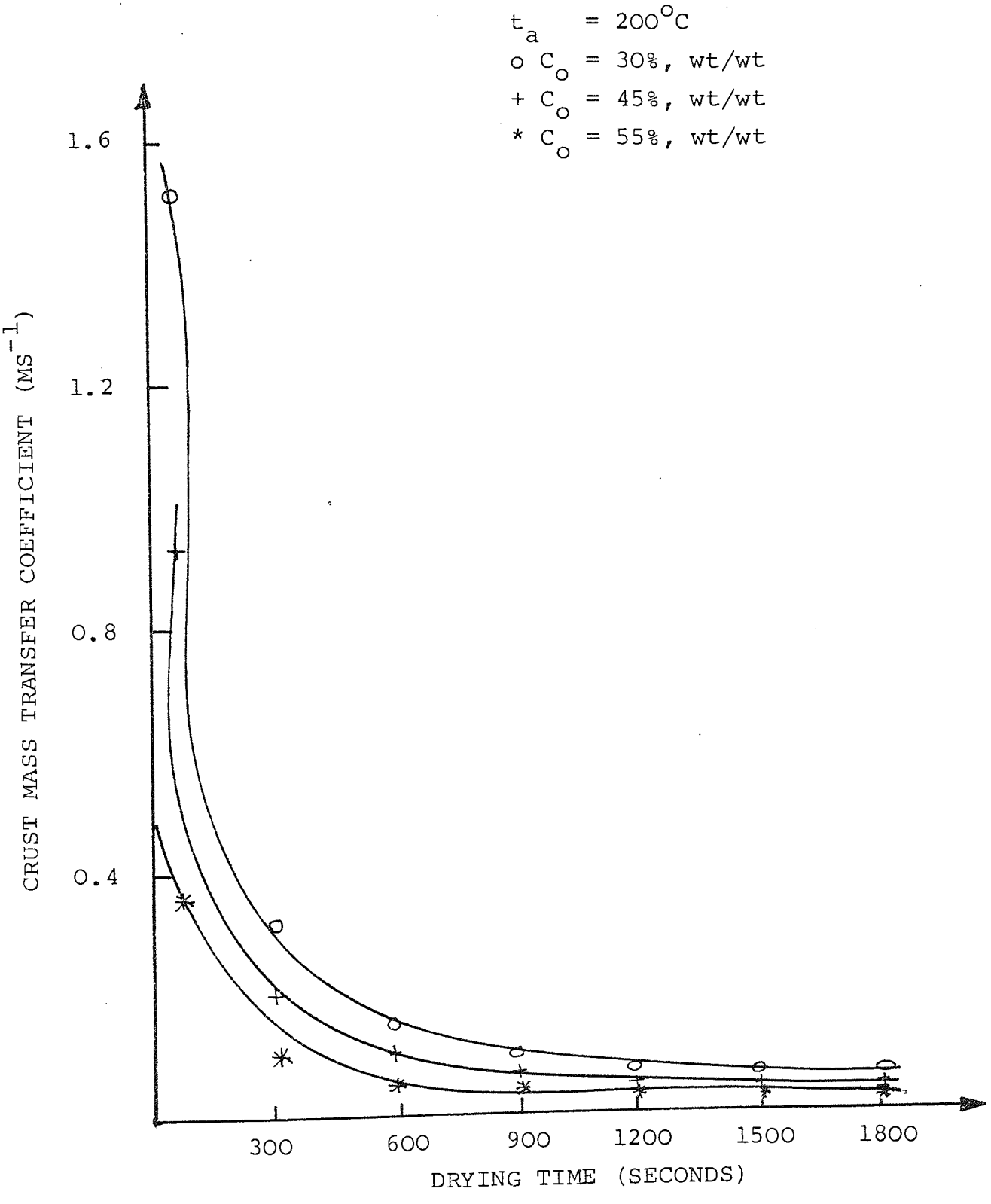

FIGURE C16

EFFECT OF INITIAL MOISTURE CONTENT ON CRUST MASS TRANSFER COEFFICIENT FOR NORTHFLEET SLURRY

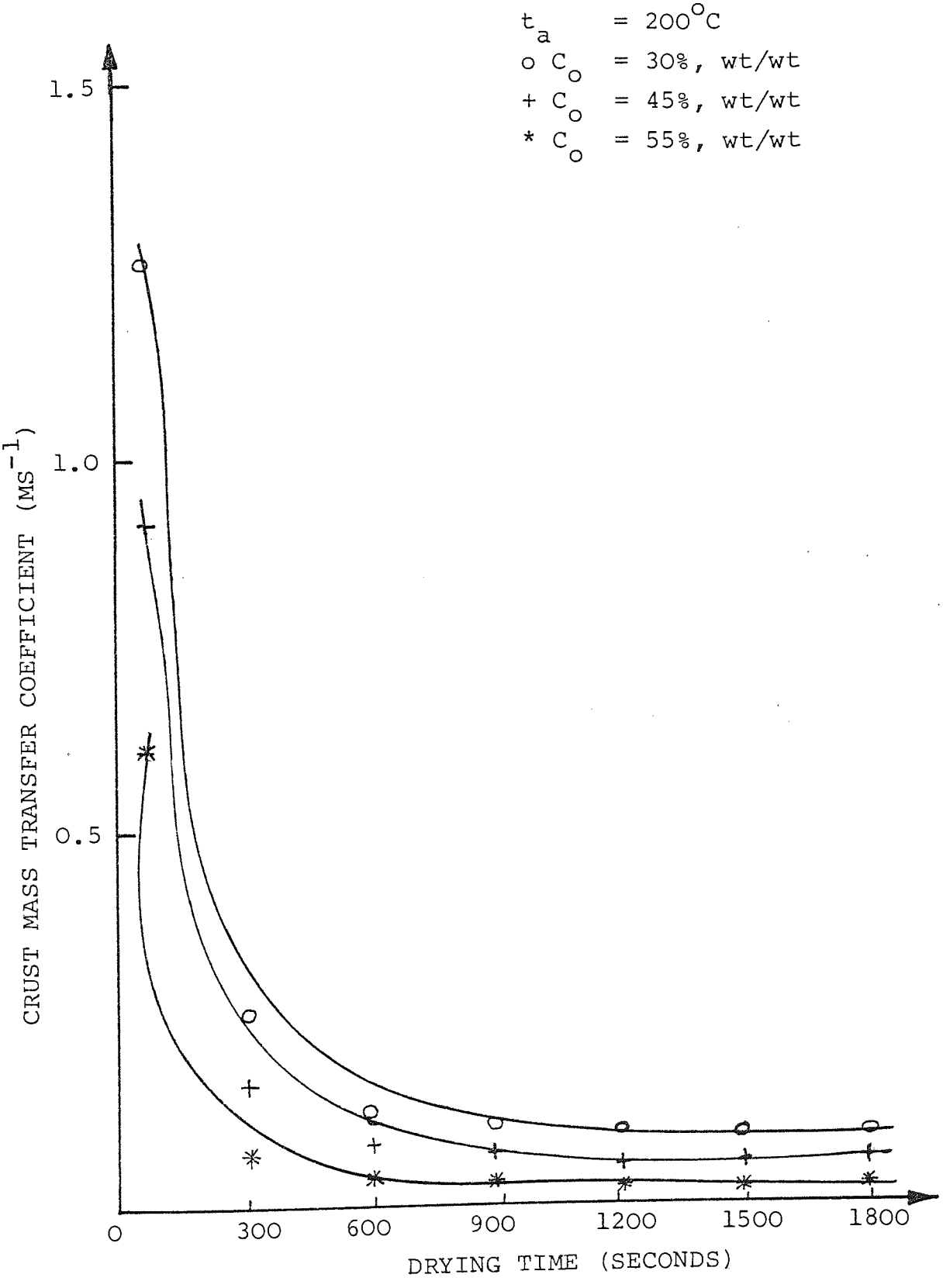

FIGURE C17

EFFECT OF INITIAL MOISTURE CONTENT ON CRUST MASS TRANSFER COEFFICIENT FOR MASON SLURRY

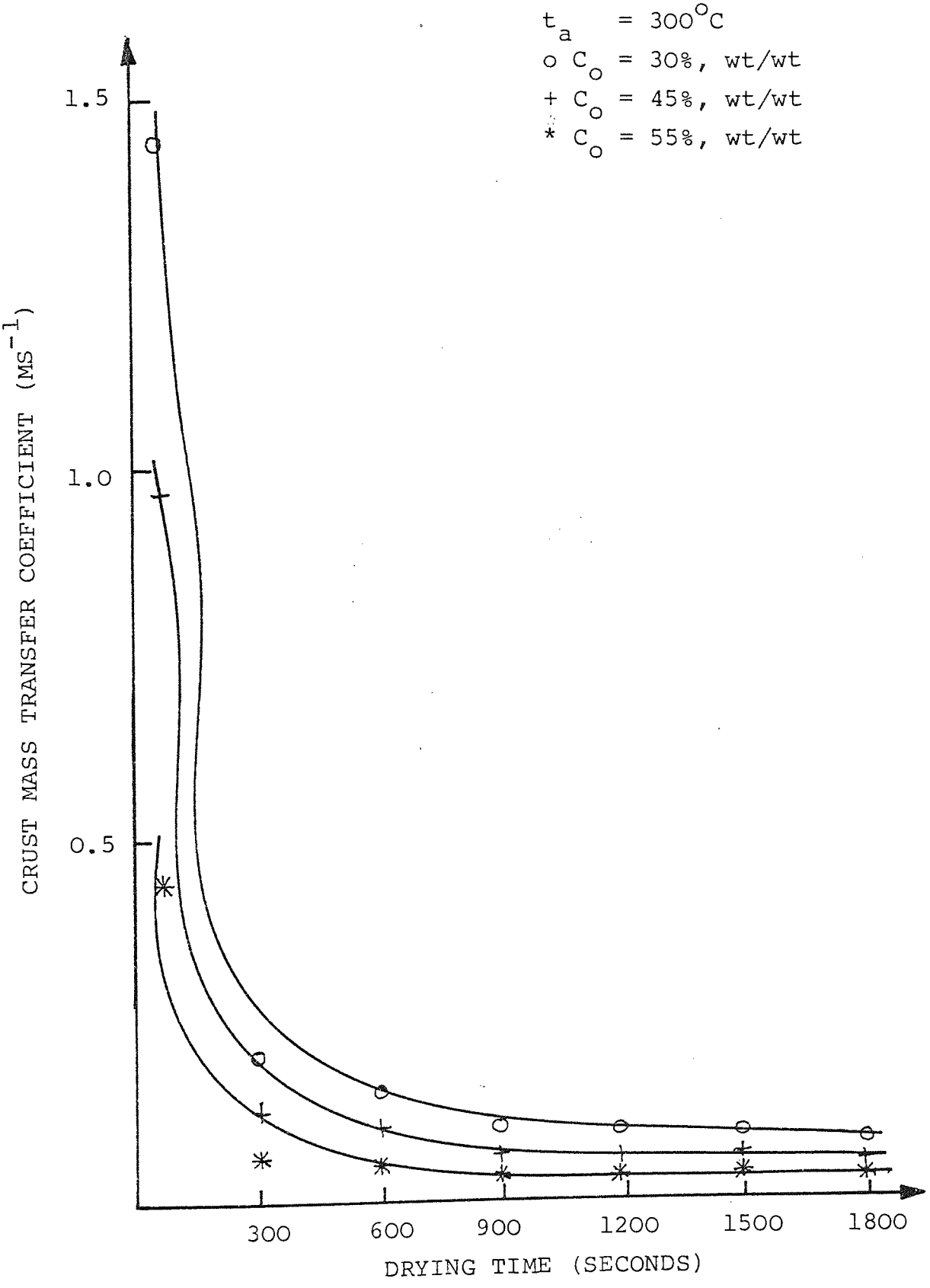

FIGURE C18

EFFECT OF INITIAL MOISTURE CONTENT OF CRUST MASS TRANSFER COEFFICIENT FOR HUMBER SLURRY

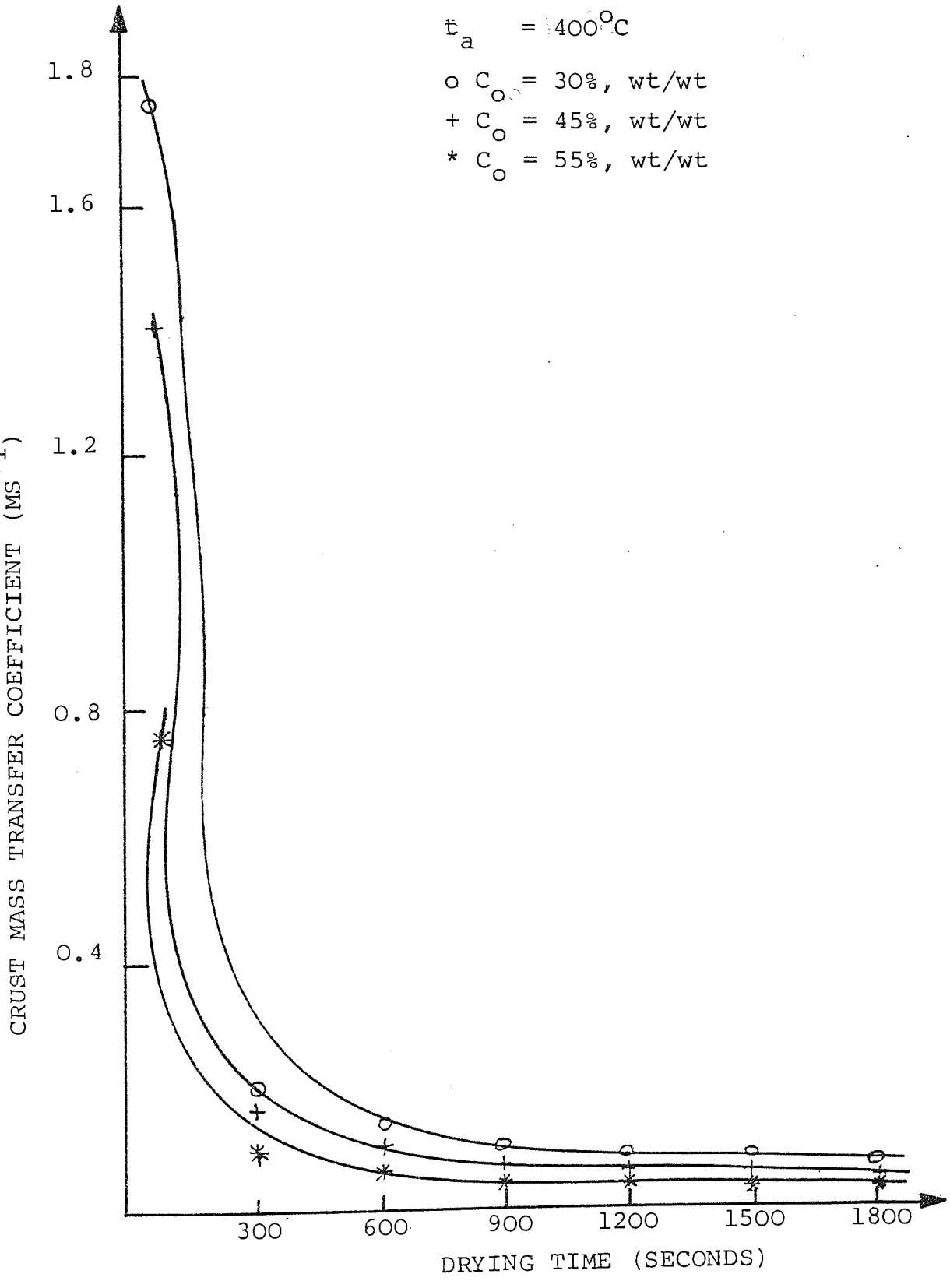

FIGURE C19

EFFECT OF INITIAL MOISTURE CONTENT ON EXPERIMENTAL MASS TRANSFER COEFFICIENT FOR SHOREHAM SLURRY

t_a = 200°C

o C_o = 30%, wt/wt

\+ C_o = 45%, wt/wt

* C_o = 55%, wt/wt

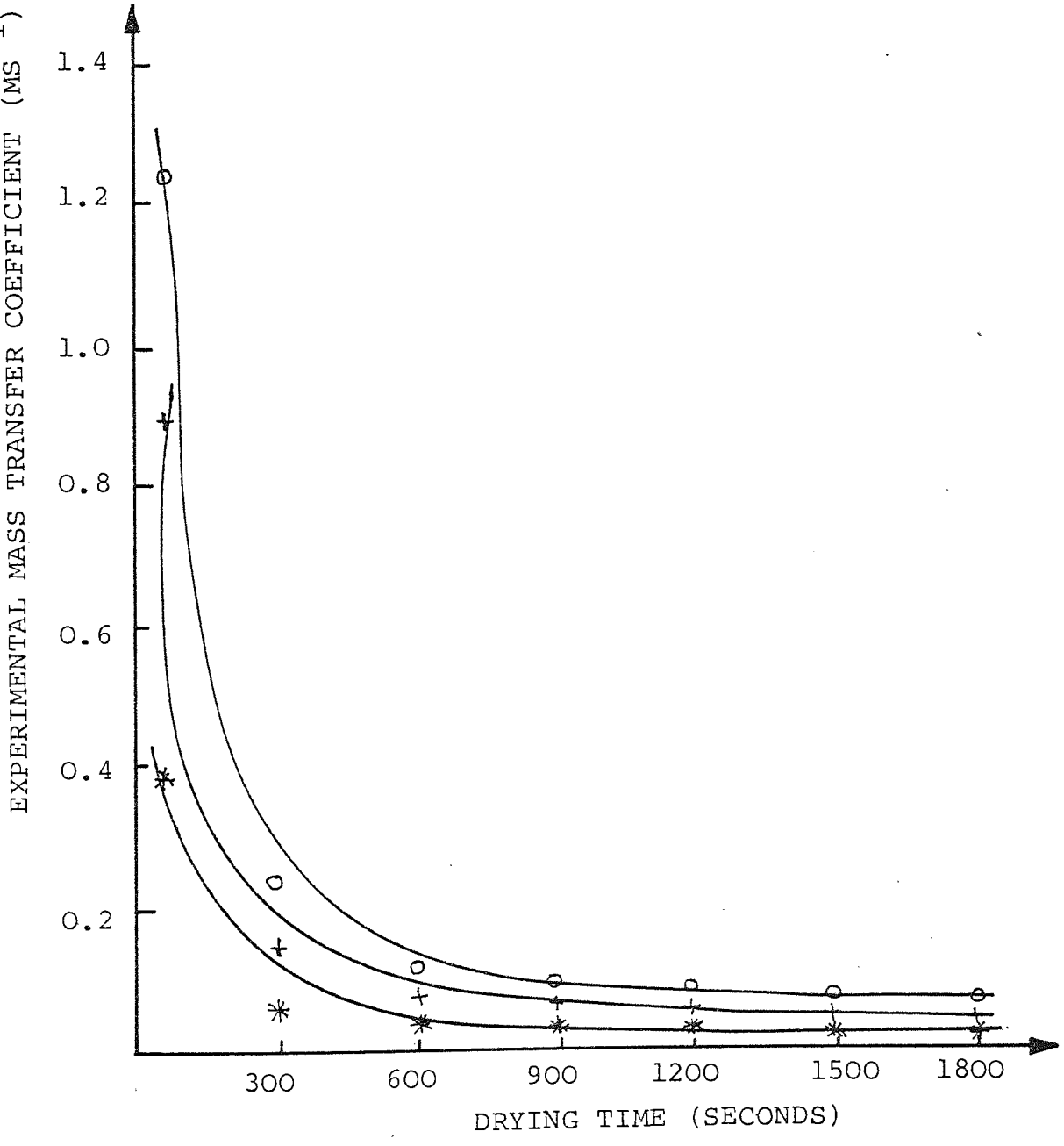

FIGURE C20

EFFECT OF INITIAL MOISTURE CONTENT ON EXPERIMENTAL MASS TRANSFER FOR NORTHFLEET SLURRY

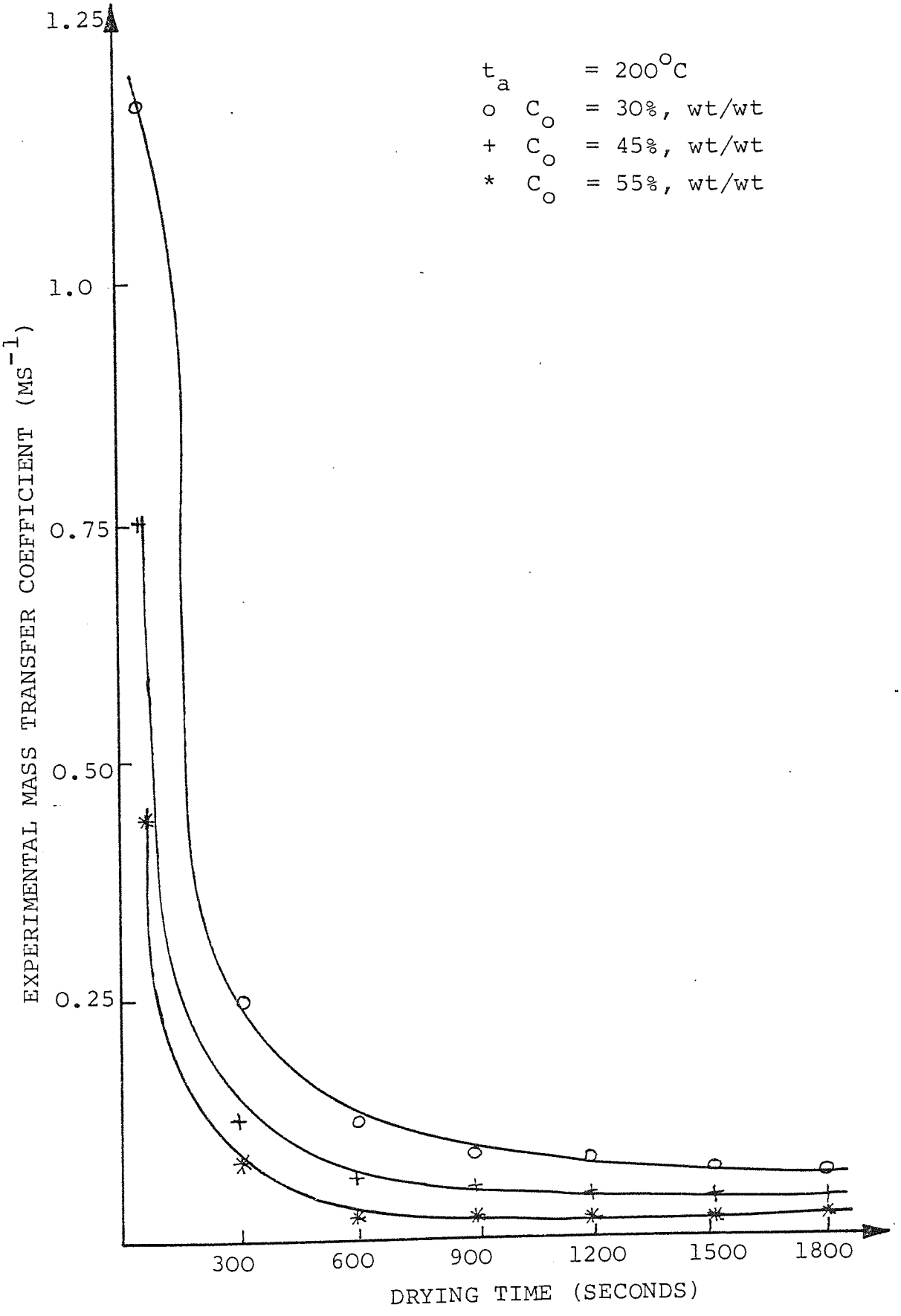

FIGURE C21

EFFECT OF INITIAL MOISTURE CONTENT ON EXPERIMENTAL MASS TRANSFER COEFFICIENT FOR MASON SLURRY

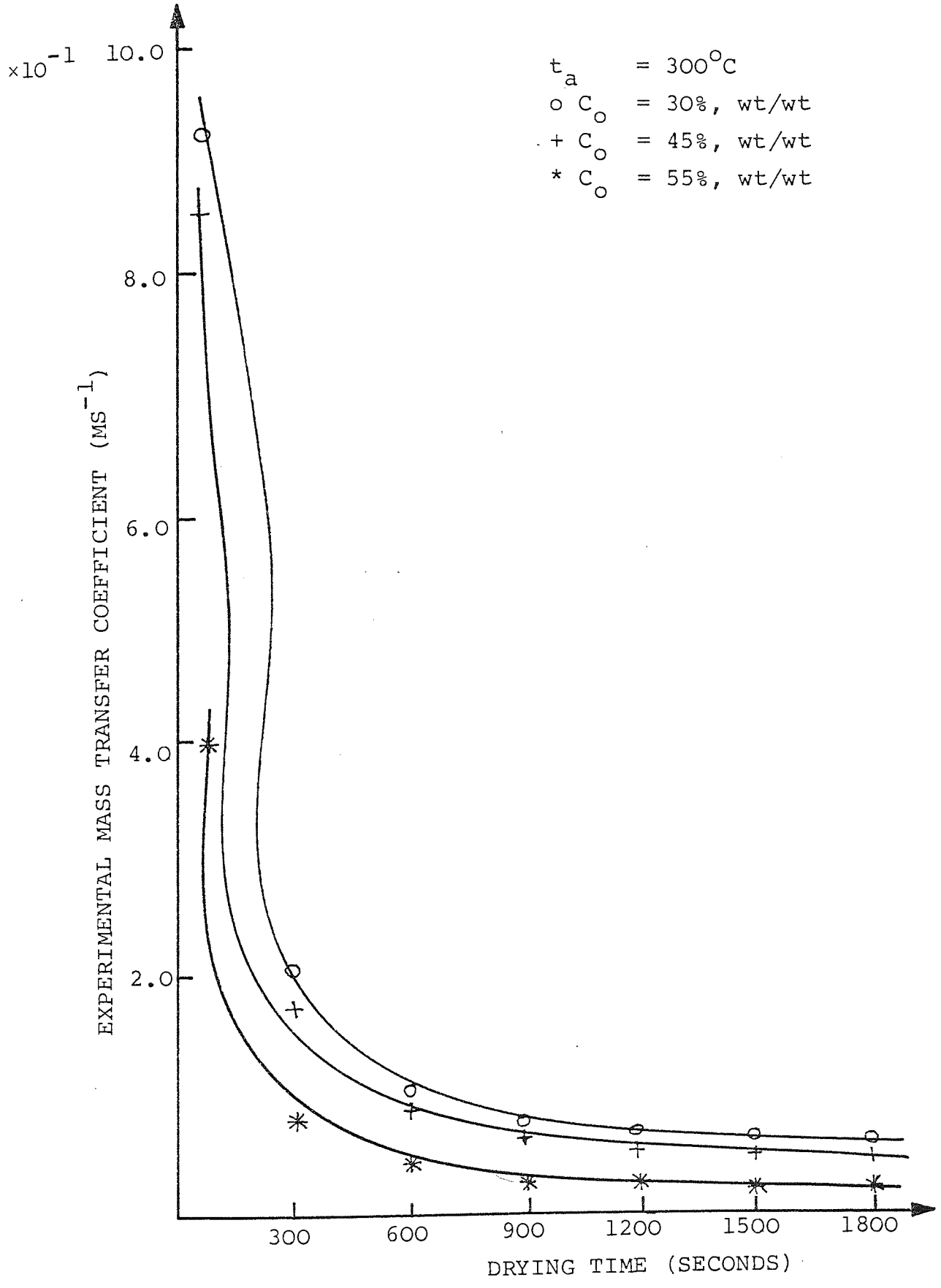

FIGURE C22

EFFECT OF INITIAL MOISTURE CONTENT ON EXPERIMENTAL MASS TRANSFER COEFFICIENT FOR HUMBER SLURRY

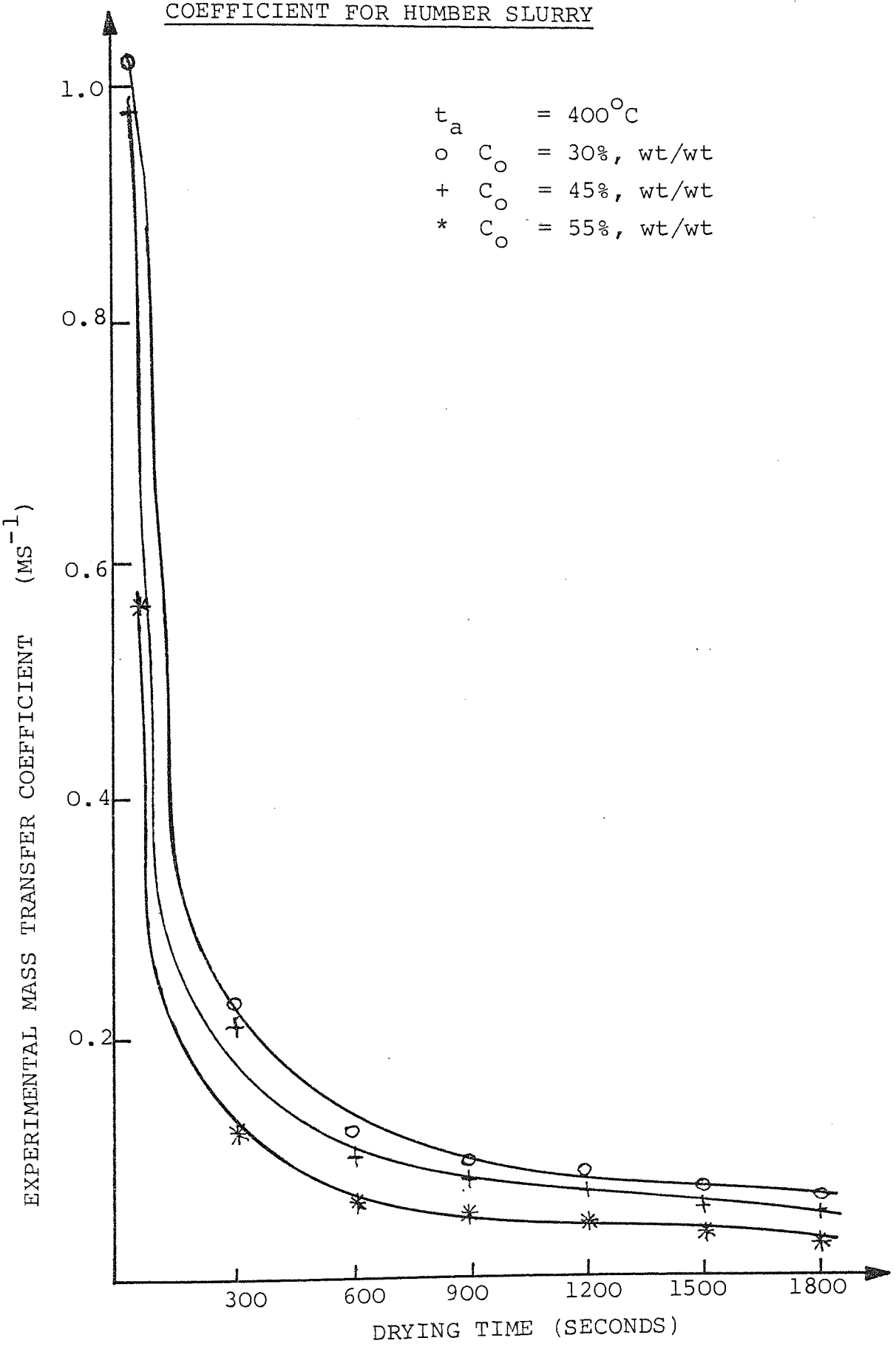

FIGURE C23

EFFECT OF INITIAL MOISTURE CONTENT ON THE DRYING RATE FOR SHOREHAM SLURRY

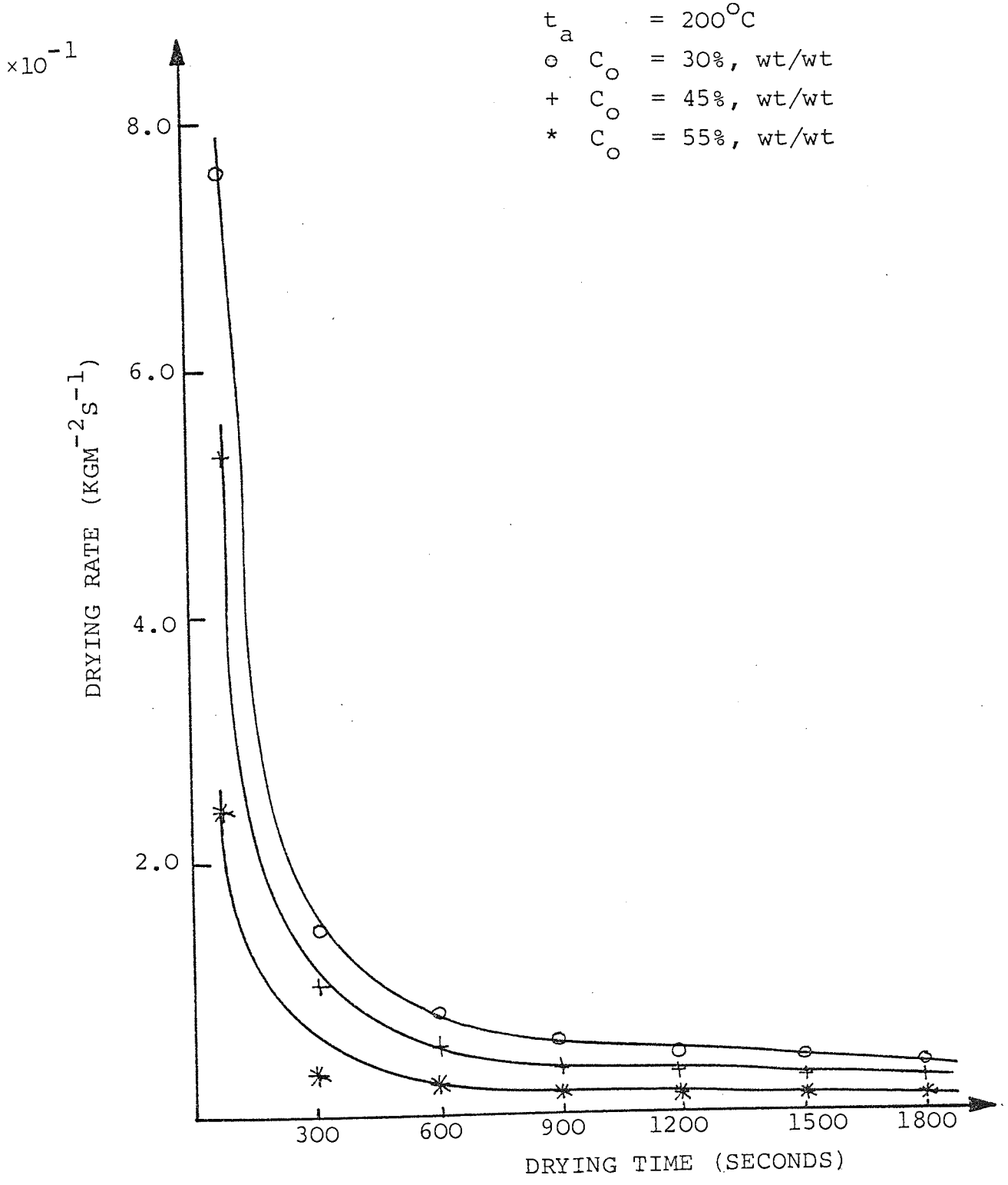

FIGURE C24

EFFECT OF INITIAL MOISTURE CONTENT ON THE DRYING RATE FOR NORTHFLEET SLURRY

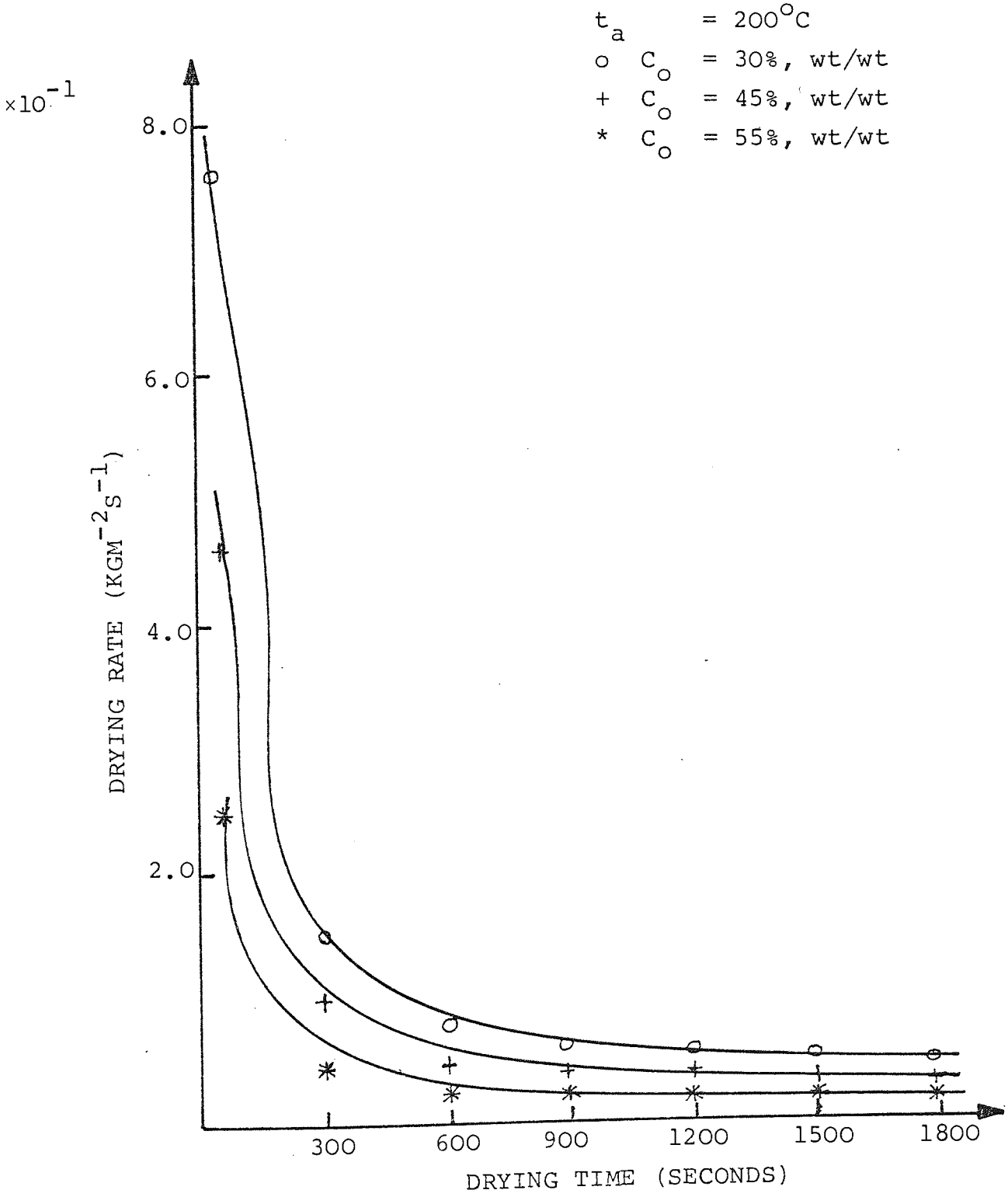

FIGURE C25

EFFECT ON INITIAL MOISTURE CONTENT ON THE DRYING RATE FOR MASON SLURRY

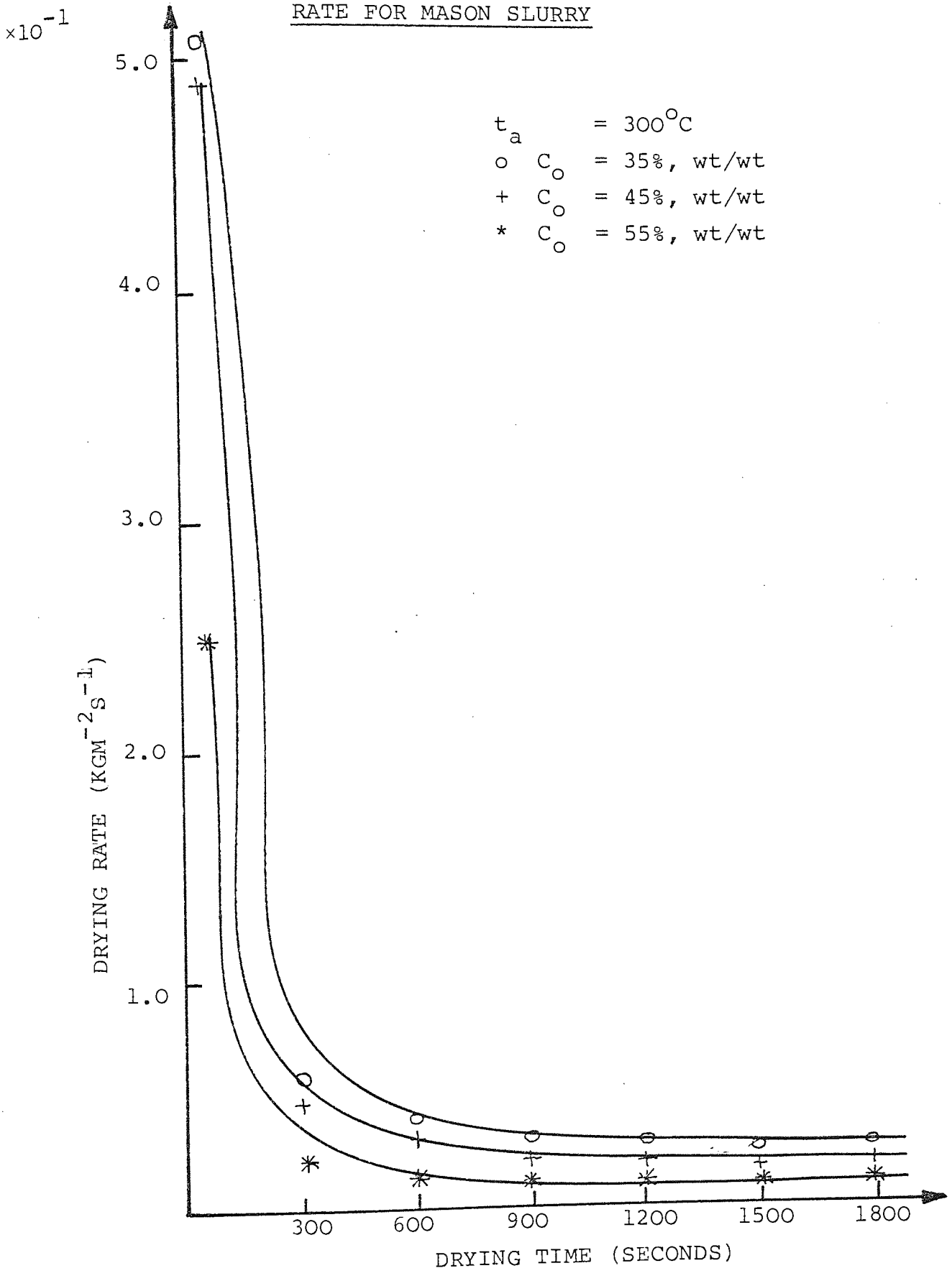

FIGURE C26

EFFECT OF INITIAL MOISTURE CONTENT ON THE DRYING RATE FOR HUMBER SLURRY

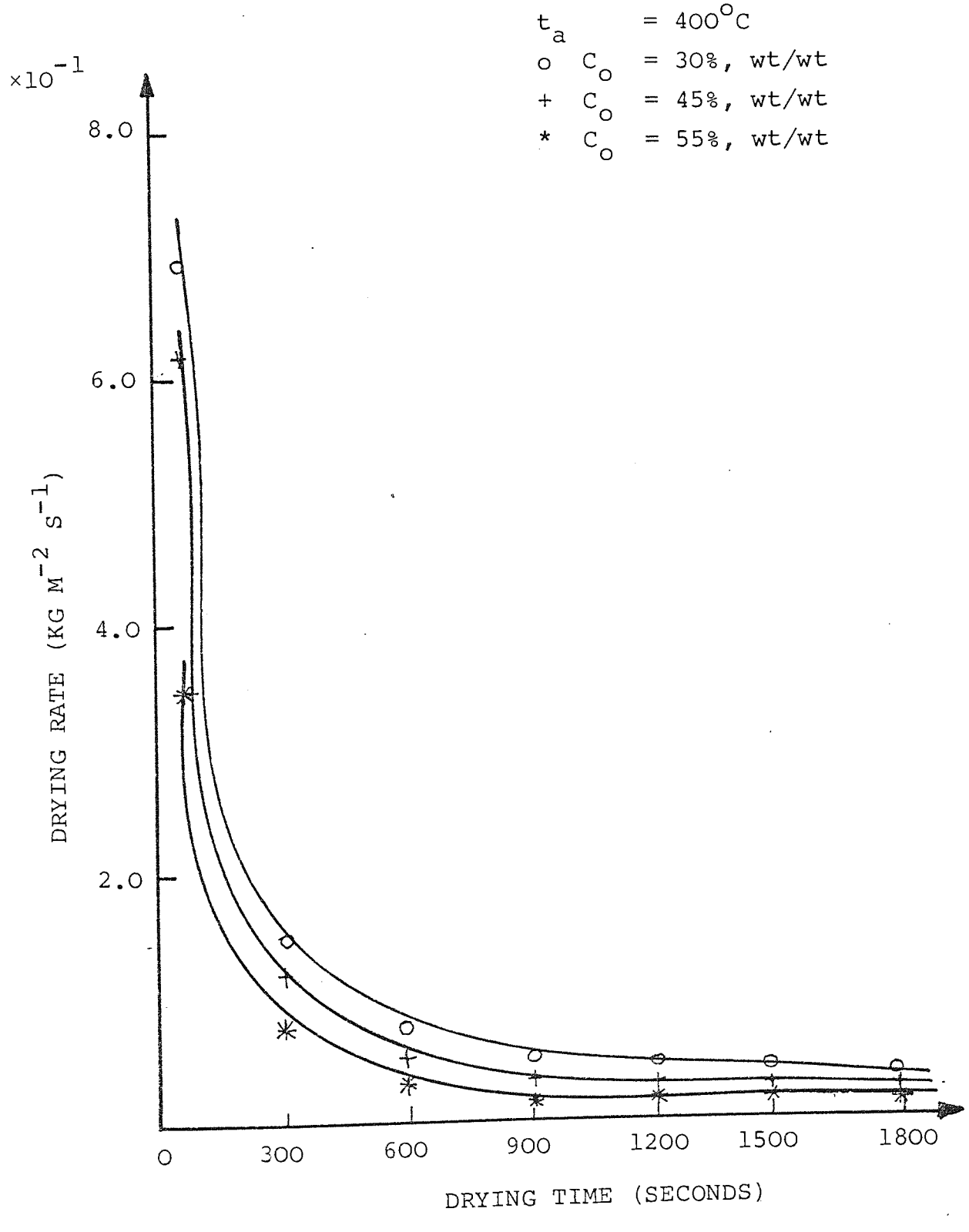

APPENDIX D

1. Tables D1-D44, The computer printout from the comparison of the Crust Mass Transfer Coefficient, Experimental Mass Transfer Coefficient and the Theoretical Mass Transfer Coefficient.

2. Figures D1-D15, Graphical Plots of Linear Regression for drops dried at 200^{o}C.

3. Figures D16-D30, Graphical Plots of Linear Regression for drops dried at 300^{o}C.

4. Figures D31-D44, Graphical Plots of Linear Regression for drops dried at 400^{o}C.

TABLE D1

SAMPLE - MASON SLURRY

MEAN SAT. DROP TEMPERATURE= 178.00 DEG.C

CRUST THERMAL CONDUCTIVITY= .4487 W/M/DEG. C

AIR TEMPERATURE = 200.00 DEG. C.

INITIAL MOISTURE CONTENT = 0.300 KG/KG

GAS FILM TRANSFER COEFFIENT = 3.8835 M/S

DRYING TIME(SEC)	KC	KT	KE
6.0000E 01	1.0446E 00	8.2320E-01	9.1034E-01
1.2000E 02	4.9197E-01	4.3666E-01	4.5716E-01
1.8000E 02	3.2902E-01	3.0332E-01	3.0601E-01
2.4000E 02	2.3353E-01	2.2029E-01	2.3065E-01
3.0000E 02	1.9581E-01	1.8641E-01	1.8511E-01
3.6000E 02	1.7695E-01	1.6924E-01	1.5459E-01
4.2000E 02	1.5052E-01	1.4490E-01	1.3301E-01
4.8000E 02	1.3056E-01	1.2632E-01	1.1682E-01
5.4000E 02	1.1770E-01	1.1423E-01	1.0416E-01
6.0000E 02	1.0490E-01	1.0214E-01	9.4098E-02
6.6000E 02	9.4384E-02	9.2145E-02	8.5866E-02
7.2000E 02	8.5596E-02	8.3750E-02	7.9008E-02
7.8000E 02	8.1722E-02	8.0037E-02	7.5991E-02
8.4000E 02	7.8141E-02	7.6600E-02	7.3207E-02
9.0000E 02	7.4822E-02	7.3407E-02	7.0630E-02
9.6000E 02	7.1736E-02	7.0435E-02	6.8237E-02
1.0200E 03	6.8862E-02	6.7662E-02	6.6010E-02
1.0800E 03	6.6176E-02	6.5068E-02	6.3931E-02
1.1400E 03	6.3663E-02	6.2636E-02	6.1988E-02
1.2000E 03	6.1304E-02	6.0352E-02	6.0166E-02

TABLE D2

SAMPLE - MASON SLURRY

MEAN SAT. DROP TEMPERATURE= 280.50 DEG.C

CRUST THERMAL CONDUCTIVITY= .7086 W/M/DEG. C

AIR TEMPERATURE = 300.00 DEG. C.

INITIAL MOISTURE CONTENT = 0.300 KG/KG

GAS FILM TRANSFER COEFFIENT = 5.3250 M/S

DRYING TIME(SEC)	KC	KT	KE
6.0000E 01	1.3586E 00	1.0824E 00	9.1016E-01
1.2000E 02	4.0846E-01	3.7936E-01	4.5844E-01
1.8000E 02	2.6176E-01	2.4950E-01	3.0731E-01
2.4000E 02	2.1126E-01	2.0320E-01	2.3129E-01
3.0000E 02	1.6406E-01	1.5916E-01	1.8596E-01
3.6000E 02	1.4905E-01	1.4499E-01	1.5531E-01
4.2000E 02	1.2462E-01	1.2177E-01	1.3374E-01
4.8000E 02	1.0645E-01	1.0436E-01	1.1756E-01
5.4000E 02	1.2642E-01	1.2349E-01	1.0398E-01
6.0000E 02	1.1168E-01	1.0939E-01	9.3910E-02
6.6000E 02	9.9701E-02	9.7869E-02	8.5677E-02
7.2000E 02	8.9776E-02	8.8287E-02	7.8817E-02
7.8000E 02	8.5428E-02	8.4079E-02	7.5800E-02
8.4000E 02	8.1426E-02	8.0199E-02	7.3015E-02
9.0000E 02	7.7731E-02	7.6612E-02	7.0437E-02
9.6000E 02	7.4309E-02	7.3286E-02	6.8043E-02
1.0200E 03	7.1132E-02	7.0195E-02	6.5815E-02
1.0800E 03	6.8175E-02	6.7313E-02	6.3736E-02
1.1400E 03	6.5416E-02	6.4623E-02	6.1792E-02
1.2000E 03	6.2837E-02	6.2104E-02	5.9969E-02

TABLE D3

SAMPLE - MASON SLURRY

MEAN SAT. DROP TEMPERATURE= 319.00 DEG.C

CRUST THERMAL CONDUCTIVITY= .7905 W/M/DEG. C

AIR TEMPERATURE = 400.00 DEG. C.

INITIAL MOISTURE CONTENT = 0.300 KG/KG

GAS FILM TRANSFER COEFFIENT = 6.9257 M/S

DRYING TIME(SEC)	KC	KT	KE
6.0000E 01	1.7122E 00	1.3728E 00	9.0999E-01
1.2000E 02	1.8443E-01	1.7965E-01	4.6424E-01
1.8000E 02	1.3645E-01	1.3382E-01	3.1157E-01
2.4000E 02	1.2980E-01	1.2741E-01	2.3398E-01
3.0000E 02	1.2212E-01	1.2000E-01	1.8748E-01
3.6000E 02	1.5515E-01	1.5175E-01	1.5531E-01
4.2000E 02	1.2845E-01	1.2611E-01	1.3374E-01
4.8000E 02	1.0880E-01	1.0711E-01	1.1756E-01
5.4000E 02	1.3973E-01	1.3697E-01	1.0380E-01
6.0000E 02	1.2271E-01	1.2058E-01	9.3729E-02
6.6000E 02	1.0897E-01	1.0728E-01	8.5494E-02
7.2000E 02	9.7657E-02	9.6299E-02	7.8633E-02
7.8000E 02	9.2723E-02	9.1498E-02	7.5615E-02
8.4000E 02	8.8194E-02	8.7085E-02	7.2830E-02
9.0000E 02	8.4023E-02	8.3016E-02	7.0251E-02
9.6000E 02	8.0171E-02	7.9253E-02	6.7857E-02
1.0200E 03	7.6603E-02	7.5765E-02	6.5628E-02
1.0800E 03	7.3289E-02	7.2522E-02	6.3549E-02
1.1400E 03	7.0205E-02	6.9500E-02	6.1603E-02
1.2000E 03	6.7328E-02	6.6679E-02	5.9780E-02

TABLE D4

SAMPLE - MASON SLURRY

MEAN SAT. DROP TEMPERATURE= 180.00 DEG.C

CRUST THERMAL CONDUCTIVITY= .4542 W/M/DEG. C

AIR TEMPERATURE = 200.00 DEG. C.

INITIAL MOISTURE CONTENT = 0.450 KG/KG

GAS FILM TRANSFER COEFFIENT = 3.8843 M/S

DRYING TIME(SEC)	KC	KT	KE
6.0000E 01	7.8030E-01	6.4977E-01	7.4544E-01
1.2000E 02	4.0160E-01	3.6397E-01	3.7452E-01
1.8000E 02	2.6063E-01	2.4425E-01	2.5106E-01
2.4000E 02	2.0783E-01	1.9727E-01	1.8904E-01
3.0000E 02	1.6698E-01	1.6009E-01	1.5195E-01
3.6000E 02	1.3914E-01	1.3433E-01	1.2724E-01
4.2000E 02	1.1891E-01	1.1538E-01	1.0959E-01
4.8000E 02	1.0350E-01	1.0082E-01	9.6352E-02
5.4000E 02	9.6745E-02	9.4394E-02	8.5866E-02
6.0000E 02	8.6443E-02	8.4561E-02	7.7637E-02
6.6000E 02	7.7933E-02	7.6400E-02	7.0907E-02
7.2000E 02	7.0782E-02	6.9515E-02	6.5301E-02
7.8000E 02	6.7617E-02	6.6460E-02	6.2836E-02
8.4000E 02	6.4686E-02	6.3626E-02	6.0561E-02
9.0000E 02	6.1963E-02	6.0990E-02	5.8455E-02
9.6000E 02	5.9427E-02	5.8532E-02	5.6500E-02
1.0200E 03	5.7059E-02	5.6233E-02	5.4680E-02
1.0800E 03	5.4844E-02	5.4080E-02	5.2983E-02
1.1400E 03	5.2766E-02	5.2059E-02	5.1395E-02
1.2000E 03	5.0814E-02	5.0158E-02	4.9908E-02

TABLE D5

SAMPLE - MASON SLURRY

MEAN SAT. DROP TEMPERATURE= 281.00 DEG.C

CRUST THERMAL CONDUCTIVITY= .7098 W/M/DEG. C

AIR TEMPERATURE = 300.00 DEG. C.

INITIAL MOISTURE CONTENT = 0.450 KG/KG

GAS FILM TRANSFER COEFFIENT = 5.9899 M/S

DRYING TIME(SEC)	KC	KT	KE
6.0000E 01	9.7781E-01	8.4059E-01	8.5226E-01
1.2000E 02	4.0458E-01	3.7898E-01	4.2938E-01
1.8000E 02	2.7200E-01	2.6019E-01	2.8807E-01
2.4000E 02	2.1447E-01	2.0706E-01	2.1716E-01
3.0000E 02	1.7998E-01	1.7473E-01	1.7452E-01
3.6000E 02	1.5728E-01	1.5326E-01	1.4601E-01
4.2000E 02	1.3360E-01	1.3068E-01	1.2585E-01
4.8000E 02	1.1564E-01	1.1345E-01	1.1073E-01
5.4000E 02	1.1449E-01	1.1234E-01	9.8467E-02
6.0000E 02	1.0191E-01	1.0021E-01	8.9065E-02
6.6000E 02	9.1552E-02	9.0174E-02	8.1377E-02
7.2000E 02	8.2870E-02	8.1739E-02	7.4974E-02
7.8000E 02	7.9035E-02	7.8005E-02	7.2158E-02
8.4000E 02	7.5487E-02	7.4547E-02	6.9559E-02
9.0000E 02	7.2195E-02	7.1336E-02	6.7154E-02
9.6000E 02	6.9133E-02	6.8344E-02	6.4922E-02
1.0200E 03	6.6277E-02	6.5552E-02	6.2844E-02
1.0800E 03	6.3608E-02	6.2940E-02	6.0906E-02
1.1400E 03	6.1108E-02	6.0491E-02	5.9093E-02
1.2000E 03	5.8761E-02	5.8190E-02	5.7395E-02

TABLE D6

SAMPLE - MASON SLURRY

MEAN SAT. DROP TEMPERATURE= 320.00 DEG.C

CRUST THERMAL CONDUCTIVITY= .7925 W/M/DEG. C

AIR TEMPERATURE = 400.00 DEG. C.

INITIAL MOISTURE CONTENT = 0.450 KG/KG

GAS FILM TRANSFER COEFFIENT = 6.5646 M/S

DRYING TIME(SEC)	KC	KT	KE
6.0000E 01	9.8886E-01	8.5940E-01	7.0109E-01
1.2000E 02	2.8774E-01	2.7566E-01	3.5361E-01
1.8000E 02	1.7646E-01	1.7184E-01	2.3745E-01
2.4000E 02	1.5032E-01	1.4696E-01	1.7864E-01
3.0000E 02	1.3084E-01	1.2828E-01	1.4335E-01
3.6000E 02	1.1957E-01	1.1743E-01	1.1972E-01
4.2000E 02	1.0653E-01	1.0483E-01	1.0294E-01
4.8000E 02	9.1343E-02	9.0089E-02	9.0478E-02
5.4000E 02	9.6450E-02	9.5054E-02	8.0291E-02
6.0000E 02	8.5332E-02	8.4237E-02	7.2541E-02
6.6000E 02	7.6269E-02	7.5394E-02	6.6202E-02
7.2000E 02	6.8745E-02	6.8032E-02	6.0922E-02
7.8000E 02	6.5443E-02	6.4797E-02	5.8599E-02
8.4000E 02	6.2401E-02	6.1813E-02	5.6456E-02
9.0000E 02	5.9589E-02	5.9053E-02	5.4471E-02
9.6000E 02	5.6984E-02	5.6493E-02	5.2629E-02
1.0200E 03	5.4562E-02	5.4112E-02	5.0914E-02
1.0800E 03	5.2306E-02	5.1893E-02	4.9314E-02
1.1400E 03	5.0200E-02	4.9819E-02	4.7817E-02
1.2000E 03	4.8229E-02	4.7877E-02	4.6415E-02

TABLE D7

SAMPLE - MASON SLURRY

MEAN SAT. DROP TEMPERATURE= 170.00 DEG.C

CRUST THERMAL CONDUCTIVITY= .4268 W/M/DEG. C

AIR TEMPERATURE = 200.00 DEG. C.

INITIAL MOISTURE CONTENT = 0.550 KG/KG

GAS FILM TRANSFER COEFFIENT = 3.1997 M/S

DRYING TIME(SEC)	KC	KT	KE
6.0000E 01	3.8317E-01	3.4219E-01	3.9790E-01
1.2000E 02	2.0232E-01	1.9029E-01	2.0012E-01
1.8000E 02	1.4027E-01	1.3438E-01	1.3419E-01
2.4000E 02	1.0780E-01	1.0429E-01	1.0122E-01
3.0000E 02	8.7880E-02	8.5531E-02	8.1431E-02
3.6000E 02	7.3753E-02	7.2092E-02	6.8252E-02
4.2000E 02	6.3367E-02	6.2136E-02	5.8842E-02
4.8000E 02	5.5385E-02	5.4443E-02	5.1789E-02
5.4000E 02	5.1860E-02	5.1033E-02	4.6178E-02
6.0000E 02	4.6458E-02	4.5793E-02	4.1793E-02
6.6000E 02	4.1967E-02	4.1423E-02	3.8207E-02
7.2000E 02	3.8170E-02	3.7720E-02	3.5222E-02
7.8000E 02	3.6484E-02	3.6072E-02	3.3909E-02
8.4000E 02	3.4918E-02	3.4541E-02	3.2697E-02
9.0000E 02	3.3460E-02	3.3113E-02	3.1576E-02
9.6000E 02	3.2099E-02	3.1780E-02	3.0536E-02
1.0200E 03	3.0825E-02	3.0531E-02	2.9568E-02
1.0800E 03	2.9631E-02	2.9360E-02	2.8664E-02
1.1400E 03	2.8510E-02	2.8258E-02	2.7820E-02
1.2000E 03	2.7454E-02	2.7220E-02	2.7029E-02

TABLE D8

SAMPLE - MASON SLURRY

MEAN SAT. DROP TEMPERATURE= 270.50 DEG.C

CRUST THERMAL CONDUCTIVITY= .6858 W/M/DEG. C

AIR TEMPERATURE = 300.00 DEG. C.

INITIAL MOISTURE CONTENT = 0.550 KG/KG

GAS FILM TRANSFER COEFFIENT = 4.3790 M/S

DRYING TIME(SEC)	KC	KT	KE
6.0000E 01	4.1069E-01	3.7548E-01	3.9788E-01
1.2000E 02	1.8827E-01	1.8051E-01	2.0037E-01
1.8000E 02	1.2836E-01	1.2470E-01	1.3443E-01
2.4000E 02	1.0214E-01	9.9810E-02	1.0133E-01
3.0000E 02	8.6312E-02	8.4643E-02	8.1431E-02
3.6000E 02	7.1820E-02	7.0661E-02	6.8252E-02
4.2000E 02	6.1945E-02	6.1081E-02	5.8817E-02
4.8000E 02	5.3818E-02	5.3164E-02	5.1763E-02
5.4000E 02	5.2692E-02	5.2065E-02	4.6055E-02
6.0000E 02	4.7027E-02	4.6527E-02	4.1668E-02
6.6000E 02	4.2342E-02	4.1936E-02	3.8081E-02
7.2000E 02	3.8402E-02	3.8068E-02	3.5094E-02
7.8000E 02	3.6657E-02	3.6353E-02	3.3781E-02
8.4000E 02	3.5041E-02	3.4762E-02	3.2569E-02
9.0000E 02	3.3539E-02	3.3284E-02	3.1447E-02
9.6000E 02	3.2140E-02	3.1905E-02	3.0406E-02
1.0200E 03	3.0833E-02	3.0617E-02	2.9437E-02
1.0800E 03	2.9610E-02	2.9411E-02	2.8533E-02
1.1400E 03	2.8463E-02	2.8279E-02	2.7688E-02
1.2000E 03	2.7386E-02	2.7215E-02	2.6896E-02

TABLE D9

SAMPLE - MASON SLURRY

MEAN SAT. DROP TEMPERATURE= 325.00 DEG.C

CRUST THERMAL CONDUCTIVITY= .8024 W/M/DEG. C

AIR TEMPERATURE = 400.00 DEG. C.

INITIAL MOISTURE CONTENT = 0.550 KG/KG

GAS FILM TRANSFER COEFFIENT = 5.6920 M/S

DRYING TIME(SEC)	KC	KT	KE
6.0000E 01	4.5369E-01	4.2020E-01	3.9776E-01
1.2000E 02	1.8133E-01	1.7573E-01	2.0050E-01
1.8000E 02	1.2138E-01	1.1885E-01	1.3456E-01
2.4000E 02	9.5440E-02	9.3866E-02	1.0146E-01
3.0000E 02	7.9914E-02	7.8808E-02	8.1558E-02
3.6000E 02	6.5906E-02	6.5152E-02	6.8381E-02
4.2000E 02	5.9078E-02	5.8471E-02	5.8843E-02
4.8000E 02	5.1027E-02	5.0573E-02	5.1789E-02
5.4000E 02	5.3745E-02	5.3243E-02	4.5936E-02
6.0000E 02	4.7811E-02	4.7413E-02	4.1548E-02
6.6000E 02	4.2926E-02	4.2605E-02	3.7960E-02
7.2000E 02	3.8836E-02	3.8572E-02	3.4972E-02
7.8000E 02	3.7030E-02	3.6790E-02	3.3658E-02
8.4000E 02	3.5360E-02	3.5141E-02	3.2445E-02
9.0000E 02	3.3811E-02	3.3611E-02	3.1323E-02
9.6000E 02	3.2370E-02	3.2187E-02	3.0281E-02
1.0200E 03	3.1027E-02	3.0859E-02	2.9311E-02
1.0800E 03	2.9772E-02	2.9617E-02	2.8407E-02
1.1400E 03	2.8597E-02	2.8454E-02	2.7561E-02
1.2000E 03	2.7494E-02	2.7362E-02	2.6768E-02

TABLE D10

SAMPLE - SHUREHAM SLURRY

MEAN SAT. DROP TEMPERATURE= 174.00 DEG.C

CRUST THERMAL CONDUCTIVITY= .5267 W/M/DEG. C

AIR TEMPERATURE = 200.00 DEG. C.

INITIAL MOISTURE CONTENT = 0.300 KG/KG

GAS FILM TRANSFER COEFFIENT = 4.9967 M/S

DRYING TIME(SEC)	KC	KT	KE
6.0000E 01	1.5046E 00	1.1564E 00	1.2165E 00
1.2000E 02	7.4269E-01	6.4658E-01	6.1111E-01
1.8000E 02	3.3823E-01	3.1679E-01	4.1251E-01
2.4000E 02	2.8355E-01	2.6832E-01	3.1045E-01
3.0000E 02	2.6774E-01	2.5412E-01	2.4856E-01
3.6000E 02	2.3687E-01	2.2615E-01	2.0777E-01
4.2000E 02	2.0922E-01	2.0081E-01	1.7874E-01
4.8000E 02	1.8841E-01	1.8156E-01	1.5693E-01
5.4000E 02	1.5715E-01	1.5236E-01	1.4047E-01
6.0000E 02	1.4067E-01	1.3682E-01	1.2703E-01
6.6000E 02	1.2702E-01	1.2387E-01	1.1603E-01
7.2000E 02	1.2103E-01	1.1817E-01	1.1125E-01
7.8000E 02	1.1552E-01	1.1291E-01	1.0687E-01
8.4000E 02	1.1043E-01	1.0804E-01	1.0284E-01
9.0000E 02	1.0570E-01	1.0351E-01	9.9120E-02
9.6000E 02	1.0131E-01	9.9300E-02	9.5678E-02
1.0200E 03	9.7219E-02	9.5364E-02	9.2484E-02
1.0800E 03	9.3394E-02	9.1681E-02	8.9511E-02
1.1400E 03	8.9812E-02	8.8226E-02	8.6737E-02
1.2000E 03	8.6450E-02	8.4979E-02	8.4143E-02

TABLE D11

SAMPLE - SHIREHAM SLURRY

MEAN SAT. DROP TEMPERATURE= 275.00 DEG.C

CRUST THERMAL CONDUCTIVITY= .6309 W/M/DEG. C

AIR TEMPERATURE = 300.00 DEG. C.

INITIAL MOISTURE CONTENT = 0.300 KG/KG

GAS FILM TRANSFER COEFFIENT = 5.3224 M/S

DRYING TIME(SEC)	KC	KT	KE
6.0000E 01	1.5004E 00	1.1704E 00	9.1173E-01
1.2000E 02	3.4362E-01	3.2278E-01	4.6107E-01
1.8000E 02	2.3297E-01	2.2320E-01	3.0883E-01
2.4000E 02	1.7885E-01	1.7303E-01	2.3261E-01
3.0000E 02	1.5579E-01	1.5136E-01	1.8652E-01
3.6000E 02	1.5143E-01	1.4724E-01	1.5543E-01
4.2000E 02	1.4413E-01	1.4033E-01	1.3332E-01
4.8000E 02	1.4128E-01	1.3762E-01	1.1667E-01
5.4000E 02	1.2349E-01	1.2069E-01	1.0405E-01
6.0000E 02	1.0934E-01	1.0714E-01	9.3950E-02
6.6000E 02	9.7814E-02	9.6048E-02	8.5692E-02
7.2000E 02	9.2820E-02	9.1229E-02	8.2103E-02
7.8000E 02	8.8253E-02	8.6813E-02	7.8812E-02
8.4000E 02	8.4060E-02	8.2753E-02	7.5786E-02
9.0000E 02	8.0198E-02	7.9008E-02	7.2993E-02
9.6000E 02	7.6630E-02	7.5543E-02	7.0407E-02
1.0200E 03	7.3325E-02	7.2328E-02	6.8006E-02
1.0800E 03	7.0253E-02	6.9338E-02	6.5771E-02
1.1400E 03	6.7393E-02	6.6550E-02	6.3685E-02
1.2000E 03	6.4723E-02	6.3945E-02	6.1734E-02

TABLE D12

SAMPLE - SHREHAM SLURRY

MEAN SAT. DROP TEMPERATURE= 320.50 DEG.C

CRUST THERMAL CONDUCTIVITY= .6609 W/M/DEG. C

AIR TEMPERATURE = 400.00 DEG. C.

INITIAL MOISTURE CONTENT = 0.300 KG/KG

GAS FILM TRANSFER COEFFIENT = 6.2424 M/S

DRYING TIME(SEC)	KC	KT	KE
6.0000E 01	1.3125E 00	1.0845E 00	8.1072E-01
1.2000E 02	2.7827E-01	2.6640E-01	4.0994E-01
1.8000E 02	1.8832E-01	1.8280E-01	2.7442E-01
2.4000E 02	1.5459E-01	1.5085E-01	2.0628E-01
3.0000E 02	1.3352E-01	1.3072E-01	1.6536E-01
3.6000E 02	1.3831E-01	1.3531E-01	1.3760E-01
4.2000E 02	1.2296E-01	1.2058E-01	1.1817E-01
4.8000E 02	1.2038E-01	1.1810E-01	1.0340E-01
5.4000E 02	1.1231E-01	1.1032E-01	9.2024E-02
6.0000E 02	9.8827E-02	9.7287E-02	8.3050E-02
6.6000E 02	8.7938E-02	8.6717E-02	7.5708E-02
7.2000E 02	8.3247E-02	8.2152E-02	7.2516E-02
7.8000E 02	7.8972E-02	7.7986E-02	6.9591E-02
8.4000E 02	7.5061E-02	7.4169E-02	6.6899E-02
9.0000E 02	7.1470E-02	7.0661E-02	6.4416E-02
9.6000E 02	6.8162E-02	6.7426E-02	6.2116E-02
1.0200E 03	6.5106E-02	6.4434E-02	5.9981E-02
1.0800E 03	6.2275E-02	6.1660E-02	5.7993E-02
1.1400E 03	5.9646E-02	5.9081E-02	5.6138E-02
1.2000E 03	5.7198E-02	5.6679E-02	5.4403E-02

TABLE D13

SAMPLE - SHREHAM SLURRY

MEAN SAT. DROP TEMPERATURE= 172.50 DEG.C

CRUST THERMAL CONDUCTIVITY= .5244 W/M/DEG. C

AIR TEMPERATURE = 200.00 DEG. C.

INITIAL MOISTURE CONTENT = 0.450 KG/KG

GAS FILM TRANSFER COEFFIENT = 4.3621 M/S

DRYING TIME(SEC)	KC	KT	KE
6.0000E 01	9.3890E-01	7.7261E-01	8.5349E-01
1.2000E 02	4.1791E-01	3.8138E-01	4.2967E-01
1.8000E 02	2.9097E-01	2.7278E-01	2.8790E-01
2.4000E 02	2.3584E-01	2.2374E-01	2.1675E-01
3.0000E 02	1.9699E-01	1.8848E-01	1.7410E-01
3.6000E 02	1.6579E-01	1.5972E-01	1.4577E-01
4.2000E 02	1.4704E-01	1.4224E-01	1.2541E-01
4.8000E 02	1.2900E-01	1.2530E-01	1.1024E-01
5.4000E 02	1.0807E-01	1.0546E-01	9.8714E-02
6.0000E 02	9.6973E-02	9.4865E-02	8.9284E-02
6.6000E 02	8.7751E-02	8.6021E-02	8.1573E-02
7.2000E 02	8.3698E-02	8.2122E-02	7.8222E-02
7.8000E 02	7.9959E-02	7.8519E-02	7.5151E-02
8.4000E 02	7.6497E-02	7.5179E-02	7.2326E-02
9.0000E 02	7.3283E-02	7.2072E-02	6.9720E-02
9.6000E 02	7.0291E-02	6.9176E-02	6.7307E-02
1.0200E 03	6.7498E-02	6.6469E-02	6.5068E-02
1.0800E 03	6.4884E-02	6.3933E-02	6.2984E-02
1.1400E 03	6.2434E-02	6.1553E-02	6.1040E-02
1.2000E 03	6.0132E-02	5.9314E-02	5.9222E-02

TABLE D14

SAMPLE - SHJREHAM SLURRY

MEAN SAT. DRJP TEMPERATURE= 270.00 DEG.C

CRUST THERMAL CJNDUCTIVITY= .6273 W/M/DEG. C

AIR TEMPERATURE = 300.00 DEG. C.

INITIAL MJISTURE CJNTENT = 0.450 KG/KG

GAS FILM TRANSFER CJEFFIENT = 5.3205 M/S

DRYING TIME(SEC)	KC	KT	KE
6.0000E 01	8.7081E-01	7.4833E-01	7.4673E-01
1.2000E 02	3.4412E-01	3.2321E-01	3.7602E-01
1.8000E 02	2.4486E-01	2.3409E-01	2.5168E-01
2.4000E 02	1.9483E-01	1.8795E-01	1.8942E-01
3.0000E 02	1.5579E-01	1.5136E-01	1.5222E-01
3.6000E 02	1.3318E-01	1.2993E-01	1.2731E-01
4.2000E 02	1.1699E-01	1.1447E-01	1.0950E-01
4.8000E 02	1.0818E-01	1.0603E-01	9.6015E-02
5.4000E 02	9.5503E-02	9.3819E-02	8.5692E-02
6.0000E 02	8.5279E-02	8.3934E-02	7.7437E-02
6.6000E 02	7.6856E-02	7.5761E-02	7.0684E-02
7.2000E 02	7.3176E-02	7.2184E-02	6.7750E-02
7.8000E 02	6.9794E-02	6.8890E-02	6.5060E-02
8.4000E 02	6.6674E-02	6.5849E-02	6.2586E-02
9.0000E 02	6.3787E-02	6.3032E-02	6.0302E-02
9.6000E 02	6.1108E-02	6.0414E-02	5.8189E-02
1.0200E 03	5.8615E-02	5.7976E-02	5.6227E-02
1.0800E 03	5.6290E-02	5.5700E-02	5.4400E-02
1.1400E 03	5.4115E-02	5.3570E-02	5.2696E-02
1.2000E 03	5.2077E-02	5.1573E-02	5.1102E-02

TABLE D15

SAMPLE - SHREHAM SLURRY

MEAN SAT. DROP TEMPERATURE= 315.00 DEG.C

CRUST THERMAL CONDUCTIVITY= .6574 W/M/DEG. C

AIR TEMPERATURE = 400.00 DEG. C.

INITIAL MOISTURE CONTENT = 0.450 KG/KG

GAS FILM TRANSFER COEFFIENT = 6.2416 M/S

DRYING TIME(SEC)	KC	KT	KE
6.0000E 01	8.5404E-01	7.5124E-01	6.6373E-01
1.2000E 02	3.1065E-01	2.9593E-01	3.3410E-01
1.8000E 02	1.8069E-01	1.7561E-01	2.2421E-01
2.4000E 02	1.4804E-01	1.4461E-01	1.6862E-01
3.0000E 02	1.2289E-01	1.2052E-01	1.3533E-01
3.6000E 02	1.0665E-01	1.0486E-01	1.1310E-01
4.2000E 02	1.0186E-01	1.0022E-01	9.7008E-02
4.8000E 02	9.6843E-02	9.5363E-02	8.4963E-02
5.4000E 02	8.7724E-02	8.6508E-02	7.5708E-02
6.0000E 02	7.7774E-02	7.6817E-02	6.8367E-02
6.6000E 02	6.9658E-02	6.8889E-02	6.2363E-02
7.2000E 02	6.6137E-02	6.5444E-02	5.9753E-02
7.8000E 02	6.2915E-02	6.2287E-02	5.7361E-02
8.4000E 02	5.9955E-02	5.9385E-02	5.5160E-02
9.0000E 02	5.7227E-02	5.6707E-02	5.3129E-02
9.6000E 02	5.4705E-02	5.4230E-02	5.1249E-02
1.0200E 03	5.2367E-02	5.1931E-02	4.9503E-02
1.0800E 03	5.0193E-02	4.9793E-02	4.7878E-02
1.1400E 03	4.8168E-02	4.7799E-02	4.6362E-02
1.2000E 03	4.6276E-02	4.5935E-02	4.4944E-02

TABLE D16

SAMPLE - SHREHAM SLURRY

MEAN SAT. DROP TEMPERATURE= 175.50 DEG.C

CRUST THERMAL CONDUCTIVITY= .5289 W/M/DEG. C

AIR TEMPERATURE = 200.00 DEG. C.

INITIAL MOISTURE CONTENT = 0.550 KG/KG

GAS FILM TRANSFER COEFFIENT = 3.2011 M/S

DRYING TIME(SEC)	KC	KT	KE
6.0000E 01	3.7068E-01	3.3221E-01	3.9827E-01
1.2000E 02	2.0729E-01	1.9468E-01	2.0002E-01
1.8000E 02	1.4169E-01	1.3569E-01	1.3404E-01
2.4000E 02	1.0923E-01	1.0562E-01	1.0103E-01
3.0000E 02	9.0285E-02	8.7809E-02	8.1200E-02
3.6000E 02	7.6602E-02	7.4812E-02	6.7994E-02
4.2000E 02	6.6763E-02	6.5399E-02	5.8554E-02
4.8000E 02	5.8144E-02	5.7107E-02	5.1515E-02
5.4000E 02	4.8718E-02	4.7988E-02	4.6169E-02
6.0000E 02	4.4003E-02	4.3406E-02	4.1770E-02
6.6000E 02	4.0050E-02	3.9555E-02	3.8172E-02
7.2000E 02	3.8303E-02	3.7850E-02	3.6609E-02
7.8000E 02	3.6685E-02	3.6269E-02	3.5176E-02
8.4000E 02	3.5181E-02	3.4799E-02	3.3859E-02
9.0000E 02	3.3781E-02	3.3428E-02	3.2643E-02
9.6000E 02	3.2472E-02	3.2146E-02	3.1518E-02
1.0200E 03	3.1247E-02	3.0945E-02	3.0473E-02
1.0800E 03	3.0098E-02	2.9817E-02	2.9501E-02
1.1400E 03	2.9016E-02	2.8756E-02	2.8595E-02
1.2000E 03	2.7998E-02	2.7755E-02	2.7747E-02

TABLE D17

SAMPLE - SHOREHAM SLURRY

MEAN SAT. DROP TEMPERATURE= 250.00 DEG.C

CRUST THERMAL CONDUCTIVITY= .6119 W/M/DEG. C

AIR TEMPERATURE = 300.00 DEG. C.

INITIAL MOISTURE CONTENT = 0.550 KG/KG

GAS FILM TRANSFER COEFFIENT = 4.7943 M/S

DRYING TIME(SEC)	KC	KT	KE
6.0000E 01	4.3170E-01	3.9604E-01	4.4305E-01
1.2000E 02	2.0494E-01	1.9654E-01	2.2317E-01
1.8000E 02	1.4321E-01	1.3905E-01	1.4966E-01
2.4000E 02	1.1028E-01	1.0780E-01	1.1292E-01
3.0000E 02	1.0559E-01	1.0332E-01	9.0392E-02
3.6000E 02	8.7012E-02	8.5461E-02	7.5769E-02
4.2000E 02	7.4617E-02	7.3473E-02	6.5299E-02
4.8000E 02	6.5455E-02	6.4573E-02	5.7438E-02
5.4000E 02	5.6423E-02	5.5767E-02	5.1405E-02
6.0000E 02	5.0620E-02	5.0091E-02	4.6519E-02
6.6000E 02	4.5789E-02	4.5355E-02	4.2524E-02
7.2000E 02	4.3663E-02	4.3269E-02	4.0788E-02
7.8000E 02	4.1700E-02	4.1341E-02	3.9197E-02
8.4000E 02	3.9882E-02	3.9553E-02	3.7734E-02
9.0000E 02	3.8193E-02	3.7891E-02	3.6384E-02
9.6000E 02	3.6620E-02	3.6342E-02	3.5134E-02
1.0200E 03	3.5150E-02	3.4894E-02	3.3975E-02
1.0800E 03	3.3775E-02	3.3539E-02	3.2896E-02
1.1400E 03	3.2485E-02	3.2266E-02	3.1889E-02
1.2000E 03	3.1272E-02	3.1069E-02	3.0948E-02

TABLE D18

SAMPLE - SHJREHAM SLURRY

MEAN SAT. DRJP TEMPERATURE= 320.50 DEG.C

CRUST THERMAL CJNDUCTIVITY= .6609 W/M/DEG. C

AIR TEMPERATURE = 400.00 DEG. C.

INITIAL MJISTURE CJNTENT = 0.550 KG/KG

GAS FILM TRANSFER CJEFFIENT = 5.6913 M/S

DRYING TIME(SEC)	KC	KT	KE
6.0000E 01	4.2533E-01	3.9576E-01	3.9855E-01
1.2000E 02	1.7122E-01	1.6622E-01	2.0094E-01
1.8000E 02	1.2246E-01	1.1988E-01	1.3461E-01
2.4000E 02	1.0333E-01	1.0149E-01	1.0125E-01
3.0000E 02	8.5313E-02	8.4053E-02	8.1343E-02
3.6000E 02	7.3169E-02	7.2241E-02	6.8058E-02
4.2000E 02	6.4453E-02	6.3732E-02	5.8554E-02
4.8000E 02	5.6110E-02	5.5562E-02	5.1477E-02
5.4000E 02	5.1165E-02	5.0710E-02	4.5912E-02
6.0000E 02	4.5706E-02	4.5341E-02	4.1512E-02
6.6000E 02	4.1197E-02	4.0900E-02	3.7913E-02
7.2000E 02	3.9224E-02	3.8955E-02	3.6349E-02
7.8000E 02	3.7408E-02	3.7164E-02	3.4916E-02
8.4000E 02	3.5732E-02	3.5509E-02	3.3597E-02
9.0000E 02	3.4180E-02	3.3976E-02	3.2381E-02
9.6000E 02	3.2738E-02	3.2551E-02	3.1255E-02
1.0200E 03	3.1396E-02	3.1224E-02	3.0209E-02
1.0800E 03	3.0142E-02	2.9984E-02	2.9236E-02
1.1400E 03	2.8970E-02	2.8823E-02	2.8329E-02
1.2000E 03	2.7870E-02	2.7734E-02	2.7480E-02

TABLE D19

SAMPLE - HUMBER SLURRY

MEAN SAT. DROP TEMPERATURE= 131.50 DEG.C

CRUST THERMAL CONDUCTIVITY= .2530 W/M/DEG. C

AIR TEMPERATURE = 200.00 DEG. C

INITIAL MOISTURE CONTENT= 0.450 KG/KG

GAS FILM TRANSFER COEFFICIENT = 4.3543 M/S

DRYING TIME(SEC)	KC	KT	KE
6.0000E 01	1.0584E 00	8.5144E-01	8.4792E-01
1.2000E 02	4.2950E-01	3.9094E-01	4.2676E-01
1.8000E 02	2.9433E-01	2.7569E-01	2.8601E-01
2.4000E 02	2.1774E-01	2.0737E-01	2.1577E-01
3.0000E 02	1.7506E-01	1.6830E-01	1.7357E-01
3.6000E 02	1.4185E-01	1.3737E-01	1.4557E-01
4.2000E 02	1.2109E-01	1.1781E-01	1.2549E-01
4.8000E 02	1.2594E-01	1.2240E-01	1.0964E-01
5.4000E 02	1.1140E-01	1.0862E-01	9.7926E-02
6.0000E 02	9.9616E-02	9.7388E-02	8.8561E-02
6.6000E 02	8.9865E-02	8.8048E-02	8.0902E-02
7.2000E 02	8.1659E-02	8.0155E-02	7.4523E-02
7.8000E 02	7.8023E-02	7.6650E-02	7.1717E-02
8.4000E 02	7.4654E-02	7.3396E-02	6.9129E-02
9.0000E 02	7.1522E-02	7.0366E-02	6.6732E-02
9.6000E 02	6.8604E-02	6.7540E-02	6.4508E-02
1.0200E 03	6.5877E-02	6.4896E-02	6.2438E-02
1.0800E 03	6.3325E-02	6.2417E-02	6.0507E-02
1.1400E 03	6.0930E-02	6.0089E-02	5.8701E-02
1.2000E 03	5.8679E-02	5.7898E-02	5.7008E-02

TABLE D20

SAMPLE - RUMBER SLURRY

MEAN SAT. DROP TEMPERATURE= 225.00 DEG.C

CRUST THERMAL CONDUCTIVITY= .4128 W/M/DEG. C

AIR TEMPERATURE = 300.00 DEG. C

INITIAL MOISTURE CONTENT= 0.450 KG/KG

GAS FILM TRANSFER COEFFICIENT = 6.8514 M/S

DRYING TIME(SEC)	KC	KT	KE
6.0000E 01	1.1621E 00	9.9356E-01	9.9358E-01
1.2000E 02	5.1245E-01	4.7679E-01	5.0029E-01
1.8000E 02	3.5569E-01	3.3814E-01	3.3547E-01
2.4000E 02	2.4514E-01	2.3667E-01	2.5378E-01
3.0000E 02	1.9784E-01	1.9229E-01	2.0437E-01
3.6000E 02	1.6525E-01	1.6136E-01	1.7144E-01
4.2000E 02	1.4133E-01	1.3847E-01	1.4793E-01
4.8000E 02	1.2298E-01	1.2081E-01	1.3032E-01
5.4000E 02	1.3255E-01	1.3004E-01	1.1541E-01
6.0000E 02	1.1865E-01	1.1663E-01	1.0445E-01
6.6000E 02	1.0710E-01	1.0546E-01	9.5485E-02
7.2000E 02	9.7353E-02	9.5989E-02	8.8023E-02
7.8000E 02	9.3023E-02	9.1777E-02	8.4742E-02
8.4000E 02	8.9005E-02	8.7863E-02	8.1715E-02
9.0000E 02	8.5264E-02	8.4216E-02	7.8913E-02
9.6000E 02	8.1774E-02	8.0810E-02	7.6312E-02
1.0200E 03	7.8510E-02	7.7621E-02	7.3892E-02
1.0800E 03	7.5451E-02	7.4629E-02	7.1635E-02
1.1400E 03	7.2578E-02	7.1817E-02	6.9524E-02
1.2000E 03	6.9874E-02	6.9168E-02	6.7546E-02

TABLE D21

SAMPLE - HUMBER SLURRY

MEAN SAT. DROP TEMPERATURE= 308.00 DEG.C

CRUST THERMAL CONDUCTIVITY= .5610 W/M/DEG. C

AIR TEMPERATURE = 400.00 DEG. C

INITIAL MOISTURE CONTENT= 0.450 KG/KG

GAS FILM TRANSFER COEFFICIENT = 8.9477 M/S

DRYING TIME(SEC)	KC	KT	KE
6.0000E 01	1.3605E 00	1.1810E 00	9.9358E-01
1.2000E 02	3.6920E-01	3.5457E-01	5.0359E-01
1.8000E 02	2.4697E-01	2.4033E-01	3.3881E-01
2.4000E 02	2.2032E-01	2.1503E-01	2.5495E-01
3.0000E 02	1.7470E-01	1.7136E-01	2.0555E-01
3.6000E 02	1.9216E-01	1.8812E-01	1.7071E-01
4.2000E 02	1.6334E-01	1.6041E-01	1.4720E-01
4.8000E 02	1.5564E-01	1.5298E-01	1.2905E-01
5.4000E 02	1.3697E-01	1.3491E-01	1.1534E-01
6.0000E 02	1.2189E-01	1.2025E-01	1.0438E-01
6.6000E 02	1.0944E-01	1.0812E-01	9.5415E-02
7.2000E 02	9.9003E-02	9.7920E-02	8.7952E-02
7.8000E 02	9.4388E-02	9.3402E-02	8.4671E-02
8.4000E 02	9.0116E-02	8.9217E-02	8.1643E-02
9.0000E 02	8.6151E-02	8.5329E-02	7.8840E-02
9.6000E 02	8.2461E-02	8.1708E-02	7.6239E-02
1.0200E 03	7.9018E-02	7.8327E-02	7.3819E-02
1.0800E 03	7.5800E-02	7.5163E-02	7.1561E-02
1.1400E 03	7.2784E-02	7.2196E-02	6.9450E-02
1.2000E 03	6.9952E-02	6.9409E-02	6.7472E-02

TABLE D22

SAMPLE - RUMBER SLURRY

MEAN SAT. DROP TEMPERATURE= 125.00 DEG.C

CRUST THERMAL CONDUCTIVITY= .2453 W/M/DEG. C

AIR TEMPERATURE = 200.00 DEG. C

INITIAL MOISTURE CONTENT= 0.550 KG/KG

GAS FILM TRANSFER COEFFICIENT = 4.9869 M/S

DRYING TIME(SEC)	KC	KT	KE
6.0000E 01	6.6962E-01	5.9035E-01	6.5793E-01
1.2000E 02	3.2530E-01	3.0538E-01	3.3239E-01
1.8000E 02	2.2366E-01	2.1406E-01	2.2384E-01
2.4000E 02	1.6680E-01	1.6140E-01	1.6979E-01
3.0000E 02	1.3663E-01	1.3299E-01	1.3718E-01
3.6000E 02	1.2847E-01	1.2524E-01	1.1470E-01
4.2000E 02	1.1104E-01	1.0862E-01	9.9192E-02
4.8000E 02	9.7386E-02	9.5520E-02	8.7571E-02
5.4000E 02	9.1872E-02	9.0210E-02	7.8175E-02
6.0000E 02	8.2378E-02	8.1040E-02	7.0960E-02
6.6000E 02	7.4391E-02	7.3297E-02	6.5066E-02
7.2000E 02	6.7570E-02	6.6666E-02	6.0163E-02
7.8000E 02	6.4518E-02	6.3694E-02	5.8009E-02
8.4000E 02	6.1674E-02	6.0920E-02	5.6023E-02
9.0000E 02	5.9015E-02	5.8325E-02	5.4186E-02
9.6000E 02	5.6524E-02	5.5891E-02	5.2482E-02
1.0200E 03	5.4187E-02	5.3604E-02	5.0898E-02
1.0800E 03	5.1989E-02	5.1452E-02	4.9421E-02
1.1400E 03	4.9918E-02	4.9423E-02	4.8042E-02
1.2000E 03	4.7963E-02	4.7506E-02	4.6751E-02

TABLE D23

SAMPLE - HUMBER SLURRY

MEAN SAT. DROP TEMPERATURE= 235.00 DEG.C

CRUST THERMAL CONDUCTIVITY= .4319 W/M/DEG. C

AIR TEMPERATURE = 300.00 DEG. C

INITIAL MOISTURE CONTENT= 0.550 KG/KG

GAS FILM TRANSFER COEFFICIENT = 5.9763 M/S

DRYING TIME(SEC)	KC	KT	KE
6.0000E 01	6.5808E-01	5.9281E-01	5.6835E-01
1.2000E 02	2.3318E-01	2.2443E-01	2.8805E-01
1.8000E 02	1.7006E-01	1.6535E-01	1.9362E-01
2.4000E 02	1.3696E-01	1.3389E-01	1.4628E-01
3.0000E 02	1.1669E-01	1.1446E-01	1.1778E-01
3.6000E 02	1.0933E-01	1.0737E-01	9.8434E-02
4.2000E 02	9.3769E-02	9.2320E-02	8.5010E-02
4.8000E 02	8.1754E-02	8.0651E-02	7.4950E-02
5.4000E 02	7.8449E-02	7.7433E-02	6.6785E-02
6.0000E 02	7.0110E-02	6.9297E-02	6.0534E-02
6.6000E 02	6.3158E-02	6.2498E-02	5.5425E-02
7.2000E 02	5.7271E-02	5.6727E-02	5.1172E-02
7.8000E 02	5.4651E-02	5.4156E-02	4.9303E-02
8.4000E 02	5.2217E-02	5.1765E-02	4.7579E-02
9.0000E 02	4.9950E-02	4.9536E-02	4.5984E-02
9.6000E 02	4.7832E-02	4.7452E-02	4.4504E-02
1.0200E 03	4.5850E-02	4.5501E-02	4.3127E-02
1.0800E 03	4.3991E-02	4.3670E-02	4.1843E-02
1.1400E 03	4.2244E-02	4.1947E-02	4.0643E-02
1.2000E 03	4.0599E-02	4.0325E-02	3.9519E-02

TABLE D24

SAMPLE - HUMBER SLURRY

MEAN SAT. DROP TEMPERATURE= 305.00 DEG.C

CRUST THERMAL CONDUCTIVITY= .5562 W/M/DEG. C

AIR TEMPERATURE = 400.00 DEG. C

INITIAL MOISTURE CONTENT= 0.550 KG/KG

GAS FILM TRANSFER COEFFICIENT = 7.7953 M/S

DRYING TIME(SEC)	KC	KT	KE
6.0000E 01	7.5802E-01	6.9085E-01	5.6835E-01
1.2000E 02	2.3193E-01	2.2523E-01	2.8866E-01
1.8000E 02	1.5770E-01	1.5457E-01	1.9453E-01
2.4000E 02	1.3147E-01	1.2929E-01	1.4687E-01
3.0000E 02	1.0469E-01	1.0331E-01	1.1866E-01
3.6000E 02	8.6278E-02	8.5334E-02	9.9880E-02
4.2000E 02	7.2799E-02	7.2125E-02	8.6481E-02
4.8000E 02	8.5467E-02	8.4540E-02	7.4950E-02
5.4000E 02	7.5086E-02	7.4370E-02	6.7133E-02
6.0000E 02	6.6654E-02	6.6089E-02	6.0887E-02
6.6000E 02	6.5835E-02	6.5284E-02	5.5398E-02
7.2000E 02	5.9493E-02	5.9042E-02	5.1145E-02
7.8000E 02	5.6680E-02	5.6271E-02	4.9276E-02
8.4000E 02	5.4073E-02	5.3700E-02	4.7552E-02
9.0000E 02	5.1648E-02	5.1308E-02	4.5956E-02
9.6000E 02	4.9388E-02	4.9077E-02	4.4476E-02
1.0200E 03	4.7277E-02	4.6992E-02	4.3099E-02
1.0800E 03	4.5300E-02	4.5039E-02	4.1815E-02
1.1400E 03	4.3446E-02	4.3205E-02	4.0614E-02
1.2000E 03	4.1703E-02	4.1481E-02	3.9490E-02

TABLE D25

SAMPLE - HUMBER SLURRY

MEAN SAT. DROP TEMPERATURE= 135.00 DEG.C

CRUST THERMAL CONDUCTIVITY= .2575 W/M/DEG. C

AIR TEMPERATURE = 200.00 DEG. C

INITIAL MOISTURE CONTENT= 0.300 KG KG

GAS FILM TRANSFER COEFFICIENT = 4.9882 M/S

DRYING TIME(SEC)	KC	KT	KE
6.0000E 01	1.6872E 00	1.2608E 00	1.2112E 00
1.2000E 02	6.5774E-01	5.8111E-01	6.0963E-01
1.8000E 02	3.9600E-01	3.6687E-01	4.0931E-01
2.4000E 02	2.9507E-01	2.7859E-01	3.0882E-01
3.0000E 02	2.3360E-01	2.2315E-01	2.4854E-01
3.6000E 02	1.9215E-01	1.8502E-01	2.0837E-01
4.2000E 02	1.6228E-01	1.5717E-01	1.7969E-01
4.8000E 02	1.8821E-01	1.8136E-01	1.5639E-01
5.4000E 02	1.6542E-01	1.6011E-01	1.3966E-01
6.0000E 02	1.4709E-01	1.4287E-01	1.2628E-01
6.6000E 02	1.3202E-01	1.2862E-01	1.1534E-01
7.2000E 02	1.1942E-01	1.1663E-01	1.0623E-01
7.8000E 02	1.1386E-01	1.1132E-01	1.0222E-01
8.4000E 02	1.0873E-01	1.0641E-01	9.8522E-02
9.0000E 02	1.0397E-01	1.0184E-01	9.5099E-02
9.6000E 02	9.9542E-02	9.7594E-02	9.1921E-02
1.0200E 03	9.5418E-02	9.3627E-02	8.8963E-02
1.0800E 03	9.1566E-02	8.9916E-02	8.6204E-02
1.1400E 03	8.7960E-02	8.6436E-02	8.3623E-02
1.2000E 03	8.4578E-02	8.3168E-02	8.1205E-02

TABLE D26

SAMPLE - RUBBER SLURRY

MEAN SAT. DROP TEMPERATURE= 241.50 DEG.C

CRUST THERMAL CONDUCTIVITY= .4442 W/M/DEG. C

AIR TEMPERATURE = 300.00 DEG. C

INITIAL MOISTURE CONTENT= 0.300 KG/KG

GAS FILM TRANSFER COEFFICIENT = 5.9775 M/S

DRYING TIME(SEC)	KC	KT	KE
6.0000E 01	1.7169E 00	1.3338E 00	1.0400E 00
1.2000E 02	3.8524E-01	3.6191E-01	5.2561E-01
1.8000E 02	2.4703E-01	2.3723E-01	3.5292E-01
2.4000E 02	2.3345E-01	2.2468E-01	2.6498E-01
3.0000E 02	1.8155E-01	1.7620E-01	2.1319E-01
3.6000E 02	1.6530E-01	1.6085E-01	1.7810E-01
4.2000E 02	1.3826E-01	1.3513E-01	1.5345E-01
4.8000E 02	1.6709E-01	1.6255E-01	1.3353E-01
5.4000E 02	1.4584E-01	1.4237E-01	1.1915E-01
6.0000E 02	1.2892E-01	1.2620E-01	1.0765E-01
6.6000E 02	1.1514E-01	1.1296E-01	9.8245E-02
7.2000E 02	1.0371E-01	1.0194E-01	9.0409E-02
7.8000E 02	9.8693E-02	9.7090E-02	8.6962E-02
8.4000E 02	9.4076E-02	9.2618E-02	8.3781E-02
9.0000E 02	8.9810E-02	8.8480E-02	8.0836E-02
9.6000E 02	8.5857E-02	8.4641E-02	7.8102E-02
1.0200E 03	8.2185E-02	8.1071E-02	7.5557E-02
1.0800E 03	7.8766E-02	7.7742E-02	7.3182E-02
1.1400E 03	7.5574E-02	7.4631E-02	7.0961E-02
1.2000E 03	7.2589E-02	7.1718E-02	6.8880E-02

TABLE D27

SAMPLE - HUMBER SLURRY

MEAN SAT. DROP TEMPERATURE= 310.00 DEG.C

CRUST THERMAL CONDUCTIVITY= .5642 W/M/DEG. C

AIR TEMPERATURE = 400.00 DEG. C

INITIAL MOISTURE CONTENT= 0.300 KG/KG

GAS FILM TRANSFER COEFFICIENT = 8.9480 M/S

DRYING TIME(SEC)	KC	KT	KE
6.0000E 01	2.1297E 00	1.7203E 00	1.2140E 00
1.2000E 02	4.0388E-01	3.8644E-01	6.1614E-01
1.8000E 02	2.8294E-01	2.7427E-01	4.1370E-01
2.4000E 02	2.2572E-01	2.2016E-01	3.1206E-01
3.0000E 02	1.9402E-01	1.8990E-01	2.5076E-01
3.6000E 02	1.7533E-01	1.7196E-01	2.0966E-01
4.2000E 02	1.4556E-01	1.4323E-01	1.8092E-01
4.8000E 02	1.5864E-01	1.5588E-01	1.5780E-01
5.4000E 02	1.7973E-01	1.7619E-01	1.3966E-01
6.0000E 02	1.5840E-01	1.5564E-01	1.2625E-01
6.6000E 02	1.4105E-01	1.3886E-01	1.1528E-01
7.2000E 02	1.2668E-01	1.2491E-01	1.0614E-01
7.8000E 02	1.2038E-01	1.1879E-01	1.0212E-01
8.4000E 02	1.1459E-01	1.1314E-01	9.8412E-02
9.0000E 02	1.0924E-01	1.0792E-01	9.4979E-02
9.6000E 02	1.0429E-01	1.0309E-01	9.1792E-02
1.0200E 03	9.9691E-02	9.8592E-02	8.8826E-02
1.0800E 03	9.5412E-02	9.4405E-02	8.6058E-02
1.1400E 03	9.1421E-02	9.0496E-02	8.3470E-02
1.2000E 03	8.7690E-02	8.6839E-02	8.1044E-02

TABLE D28

SAMPLE - WESTBURY SLURRY

MEAN SAT. DROP TEMPERATURE= 163.50 DEG.C

CRUST THERMAL CONDUCTIVITY= .4873 W/M/DEG. C

AIR TEMPERATURE = 200.00 DEG. C.

INITIAL MOISTURE CONTENT = 0.300 KG/KG

GAS FILM TRANSFER COEFFIENT = 4.9935 M/S

DRYING TIME(SEC)	KC	KT	KE
6.0000E 01	1.7526E 00	1.2973E 00	1.2164E 00
1.2000E 02	5.1788E-01	4.6922E-01	6.1550E-01
1.8000E 02	3.4968E-01	3.2680E-01	4.1323E-01
2.4000E 02	2.8072E-01	2.6578E-01	3.1147E-01
3.0000E 02	2.6980E-01	2.5597E-01	2.4935E-01
3.6000E 02	2.3182E-01	2.2153E-01	2.0867E-01
4.2000E 02	1.9398E-01	1.8672E-01	1.7989E-01
4.8000E 02	1.8649E-01	1.7977E-01	1.5760E-01
5.4000E 02	1.7242E-01	1.6666E-01	1.4048E-01
6.0000E 02	1.5202E-01	1.4753E-01	1.2707E-01
6.6000E 02	1.3539E-01	1.3182E-01	1.1610E-01
7.2000E 02	1.2818E-01	1.2497E-01	1.1133E-01
7.8000E 02	1.2159E-01	1.1870E-01	1.0696E-01
8.4000E 02	1.1553E-01	1.1292E-01	1.0294E-01
9.0000E 02	1.0995E-01	1.0759E-01	9.9232E-02
9.6000E 02	1.0480E-01	1.0265E-01	9.5800E-02
1.0200E 03	1.0003E-01	9.8062E-02	9.2614E-02
1.0800E 03	9.5591E-02	9.3795E-02	8.9649E-02
1.1400E 03	9.1460E-02	8.9815E-02	8.6882E-02
1.2000E 03	8.7605E-02	8.6095E-02	8.4296E-02

TABLE D29

SAMPLE - WESTBURY SLURRY

MEAN SAT. DROP TEMPERATURE= 268.50 DEG.C

CRUST THERMAL CONDUCTIVITY= .7210 W/M/DEG. C

AIR TEMPERATURE = 300.00 DEG. C.

INITIAL MOISTURE CONTENT = 0.300 KG/KG

GAS FILM TRANSFER COEFFIENT = 9.8807 M/S

DRYING TIME(SEC)	KC	KT	KE
6.0000E 01	2.6174E 00	2.0692E 00	1.8292E 00
1.2000E 02	6.6550E-01	6.2351E-01	9.3558E-01
1.8000E 02	4.6806E-01	4.4689E-01	6.3060E-01
2.4000E 02	3.5383E-01	3.4160E-01	4.7833E-01
3.0000E 02	3.3569E-01	3.2466E-01	3.8346E-01
3.6000E 02	3.5776E-01	3.4526E-01	3.1849E-01
4.2000E 02	3.1627E-01	3.0646E-01	2.7456E-01
4.8000E 02	2.8622E-01	2.7816E-01	2.4145E-01
5.4000E 02	2.8130E-01	2.7351E-01	2.1479E-01
6.0000E 02	2.4713E-01	2.4110E-01	1.9472E-01
6.6000E 02	2.1919E-01	2.1443E-01	1.7831E-01
7.2000E 02	2.0706E-01	2.0281E-01	1.7118E-01
7.8000E 02	1.9594E-01	1.9213E-01	1.6466E-01
8.4000E 02	1.8573E-01	1.8231E-01	1.5866E-01
9.0000E 02	1.7632E-01	1.7323E-01	1.5312E-01
9.6000E 02	1.6762E-01	1.6482E-01	1.4800E-01
1.0200E 03	1.5955E-01	1.5701E-01	1.4325E-01
1.0800E 03	1.5205E-01	1.4975E-01	1.3883E-01
1.1400E 03	1.4507E-01	1.4297E-01	1.3471E-01
1.2000E 03	1.3855E-01	1.3663E-01	1.3085E-01

TABLE D30

SAMPLE - WESTBURY SLURRY

MEAN SAT. DROP TEMPERATURE= 321.50 DEG.C

CRUST THERMAL CONDUCTIVITY= .8187 W/M/DEG. C

AIR TEMPERATURE = 400.00 DEG. C.

INITIAL MOISTURE CONTENT = 0.300 KG/KG

GAS FILM TRANSFER COEFFIENT = 12.9183 M/S

DRYING TIME(SEC)	KC	KT	KE
6.0000E 01	2.9528E 00	2.4034E 00	1.8292E 00
1.2000E 02	6.0112E-01	5.7440E-01	9.3956E-01
1.8000E 02	3.9094E-01	3.7945E-01	6.3565E-01
2.4000E 02	2.8814E-01	2.8185E-01	4.8328E-01
3.0000E 02	2.4097E-01	2.3656E-01	3.9023E-01
3.6000E 02	2.6798E-01	2.6254E-01	3.2314E-01
4.2000E 02	2.6312E-01	2.5787E-01	2.7717E-01
4.8000E 02	2.5089E-01	2.4611E-01	2.4311E-01
5.4000E 02	2.9964E-01	2.9285E-01	2.1406E-01
6.0000E 02	2.6199E-01	2.5679E-01	1.9397E-01
6.6000E 02	2.3141E-01	2.2734E-01	1.7756E-01
7.2000E 02	2.1819E-01	2.1457E-01	1.7043E-01
7.8000E 02	2.0612E-01	2.0288E-01	1.6389E-01
8.4000E 02	1.9505E-01	1.9215E-01	1.5789E-01
9.0000E 02	1.8488E-01	1.8227E-01	1.5235E-01
9.6000E 02	1.7550E-01	1.7314E-01	1.4722E-01
1.0200E 03	1.6682E-01	1.6469E-01	1.4246E-01
1.0800E 03	1.5877E-01	1.5684E-01	1.3804E-01
1.1400E 03	1.5129E-01	1.4954E-01	1.3391E-01
1.2000E 03	1.4433E-01	1.4273E-01	1.3005E-01

TABLE D31

SAMPLE - WESTBURY SLURRY

MEAN SAT. DROP TEMPERATURE= 158.50 DEG.C

CRUST THERMAL CONDUCTIVITY= .4745 W/M/DEG. C

AIR TEMPERATURE = 200.00 DEG. C.

INITIAL MOISTURE CONTENT = 0.450 KG/KG

GAS FILM TRANSFER COEFFIENT = 3.8785 M/S

DRYING TIME(SEC)	KC	KT	KE
6.0000E 01	8.7575E-01	7.1443E-01	7.4607E-01
1.2000E 02	4.2457E-01	3.8268E-01	3.7497E-01
1.8000E 02	2.5693E-01	2.4097E-01	2.5162E-01
2.4000E 02	1.8223E-01	1.7406E-01	1.8996E-01
3.0000E 02	1.2419E-01	1.2034E-01	1.5354E-01
3.6000E 02	1.3165E-01	1.2733E-01	1.2768E-01
4.2000E 02	1.1762E-01	1.1416E-01	1.0981E-01
4.8000E 02	1.0742E-01	1.0452E-01	9.6371E-02
5.4000E 02	9.9823E-02	9.7319E-02	8.5883E-02
6.0000E 02	8.8743E-02	8.6758E-02	7.7647E-02
6.6000E 02	7.9643E-02	7.8040E-02	7.0912E-02
7.2000E 02	7.5676E-02	7.4228E-02	6.7985E-02
7.8000E 02	7.2035E-02	7.0722E-02	6.5302E-02
8.4000E 02	6.8682E-02	6.7487E-02	6.2834E-02
9.0000E 02	6.5583E-02	6.4492E-02	6.0557E-02
9.6000E 02	6.2710E-02	6.1713E-02	5.8450E-02
1.0200E 03	6.0041E-02	5.9126E-02	5.6493E-02
1.0800E 03	5.7554E-02	5.6713E-02	5.4672E-02
1.1400E 03	5.5232E-02	5.4456E-02	5.2973E-02
1.2000E 03	5.3058E-02	5.2342E-02	5.1384E-02

TABLE D32

SAMPLE - WESTBURY SLURRY

MEAN SAT. DROP TEMPERATURE= 260.00 DEG.C

CRUST THERMAL CONDUCTIVITY= .7042 W/M/DEG. C

AIR TEMPERATURE = 300.00 DEG. C.

INITIAL MOISTURE CONTENT = 0.450 KG/KG

GAS FILM TRANSFER COEFFIENT = 6.8589 M/S

DRYING TIME(SEC)	KC	KT	KE
6.0000E 01	1.2056E 00	1.0254E 00	9.9635E-01
1.2000E 02	5.3451E-01	4.9586E-01	5.0237E-01
1.8000E 02	3.3958E-01	3.2356E-01	3.3773E-01
2.4000E 02	2.5228E-01	2.4333E-01	2.5524E-01
3.0000E 02	1.7077E-01	1.6662E-01	2.0703E-01
3.6000E 02	1.1315E-01	1.1132E-01	1.7601E-01
4.2000E 02	9.9127E-02	9.7715E-02	1.5201E-01
4.8000E 02	1.1730E-01	1.1533E-01	1.3167E-01
5.4000E 02	1.4476E-01	1.4177E-01	1.1577E-01
6.0000E 02	1.2832E-01	1.2596E-01	1.0480E-01
6.6000E 02	1.1479E-01	1.1290E-01	9.5831E-02
7.2000E 02	1.0890E-01	1.0720E-01	9.1935E-02
7.8000E 02	1.0348E-01	1.0194E-01	8.8364E-02
8.4000E 02	9.8494E-02	9.7100E-02	8.5081E-02
9.0000E 02	9.3883E-02	9.2616E-02	8.2052E-02
9.6000E 02	8.9610E-02	8.8454E-02	7.9249E-02
1.0200E 03	8.5638E-02	8.4582E-02	7.6647E-02
1.0800E 03	8.1937E-02	8.0970E-02	7.4226E-02
1.1400E 03	7.8482E-02	7.7594E-02	7.1968E-02
1.2000E 03	7.5248E-02	7.4432E-02	6.9857E-02

TABLE D33

SAMPLE - WESTBURY SLURRY

MEAN SAT. DROP TEMPERATURE= 308.50 DEG.C

CRUST THERMAL CONDUCTIVITY= .7957 W/M/DEG. C

AIR TEMPERATURE = 400.00 DEG. C.

INITIAL MOISTURE CONTENT = 0.450 KG/KG

GAS FILM TRANSFER COEFFIENT = 10.5451 M/S

DRYING TIME(SEC)	KC	KT	KE
6.0000E 01	1.7050E 00	1.4677E 00	1.1971E 00
1.2000E 02	5.3547E-01	5.0960E-01	6.0827E-01
1.8000E 02	3.1144E-01	3.0250E-01	4.1164E-01
2.4000E 02	1.8203E-01	1.7894E-01	3.1589E-01
3.0000E 02	1.5323E-01	1.5104E-01	2.5501E-01
3.6000E 02	1.5165E-01	1.4950E-01	2.1255E-01
4.2000E 02	1.5723E-01	1.5492E-01	1.8175E-01
4.8000E 02	1.5931E-01	1.5693E-01	1.5888E-01
5.4000E 02	1.8902E-01	1.8569E-01	1.3992E-01
6.0000E 02	1.6609E-01	1.6351E-01	1.2677E-01
6.6000E 02	1.4737E-01	1.4534E-01	1.1602E-01
7.2000E 02	1.3925E-01	1.3743E-01	1.1135E-01
7.8000E 02	1.3181E-01	1.3019E-01	1.0708E-01
8.4000E 02	1.2499E-01	1.2352E-01	1.0314E-01
9.0000E 02	1.1869E-01	1.1737E-01	9.9517E-02
9.6000E 02	1.1288E-01	1.1168E-01	9.6160E-02
1.0200E 03	1.0749E-01	1.0641E-01	9.3045E-02
1.0800E 03	1.0249E-01	1.0150E-01	9.0147E-02
1.1400E 03	9.7828E-02	9.6929E-02	8.7444E-02
1.2000E 03	9.3479E-02	9.2658E-02	8.4918E-02

TABLE D34

SAMPLE - WESTBURY SLURRY

MEAN SAT. DROP TEMPERATURE= 160.00 DEG.C

CRUST THERMAL CONDUCTIVITY= .4784 W/M/DEG. C

AIR TEMPERATURE = 200.00 DEG. C.

INITIAL MOISTURE CONTENT = 0.550 KG/KG

GAS FILM TRANSFER COEFFIENT = 3.5018 M/S

DRYING TIME(SEC)	KC	KT	KE
6.0000E 01	4.9571E-01	4.3424E-01	4.4280E-01
1.2000E 02	2.0741E-01	1.9581E-01	2.2362E-01
1.8000E 02	1.4013E-01	1.3474E-01	1.5027E-01
2.4000E 02	1.1027E-01	1.0690E-01	1.1344E-01
3.0000E 02	8.9919E-02	8.7667E-02	9.1365E-02
3.6000E 02	7.6143E-02	7.4523E-02	7.6631E-02
4.2000E 02	6.7991E-02	6.6696E-02	6.6005E-02
4.8000E 02	6.9302E-02	6.7957E-02	5.7693E-02
5.4000E 02	6.0929E-02	5.9887E-02	5.1597E-02
6.0000E 02	5.4158E-02	5.3333E-02	4.6724E-02
6.6000E 02	4.8567E-02	4.7903E-02	4.2741E-02
7.2000E 02	4.6122E-02	4.5522E-02	4.1010E-02
7.8000E 02	4.3872E-02	4.3329E-02	3.9424E-02
8.4000E 02	4.1796E-02	4.1303E-02	3.7966E-02
9.0000E 02	3.9874E-02	3.9425E-02	3.6620E-02
9.6000E 02	3.8089E-02	3.7679E-02	3.5375E-02
1.0200E 03	3.6428E-02	3.6053E-02	3.4220E-02
1.0800E 03	3.4878E-02	3.4535E-02	3.3145E-02
1.1400E 03	3.3429E-02	3.3113E-02	3.2142E-02
1.2000E 03	3.2071E-02	3.1780E-02	3.1205E-02

TABLE D35

SAMPLE - WESTBURY SLURRY

MEAN SAT. DROP TEMPERATURE= 309.00 DEG.C

CRUST THERMAL CONDUCTIVITY= .7966 W/M/DEG. C

AIR TEMPERATURE = 400.00 DEG. C.

INITIAL MOISTURE CONTENT = 0.550 KG/KG

GAS FILM TRANSFER COEFFIENT = 8.9478 M/S

DRYING TIME(SEC)	KC	KT	KE
6.0000E 01	7.1386E-01	6.6112E-01	6.6629E-01
1.2000E 02	3.3631E-01	3.2413E-01	3.3734E-01
1.8000E 02	2.1902E-01	2.1379E-01	2.2776E-01
2.4000E 02	1.5670E-01	1.5400E-01	1.7322E-01
3.0000E 02	1.0122E-01	1.0009E-01	1.4213E-01
3.6000E 02	8.6382E-02	8.5556E-02	1.1977E-01
4.2000E 02	8.9594E-02	8.8706E-02	1.0235E-01
4.8000E 02	9.6366E-02	9.5340E-02	8.9065E-02
5.4000E 02	1.0073E-01	9.9610E-02	7.8915E-02
6.0000E 02	8.9248E-02	8.8366E-02	7.1628E-02
6.6000E 02	7.9727E-02	7.9023E-02	6.5676E-02
7.2000E 02	7.5552E-02	7.4920E-02	6.3092E-02
7.8000E 02	7.1707E-02	7.1137E-02	6.0725E-02
8.4000E 02	6.8153E-02	6.7638E-02	5.8550E-02
9.0000E 02	6.4860E-02	6.4393E-02	5.6544E-02
9.6000E 02	6.1799E-02	6.1376E-02	5.4689E-02
1.0200E 03	5.8949E-02	5.8563E-02	5.2968E-02
1.0800E 03	5.6288E-02	5.5936E-02	5.1369E-02
1.1400E 03	5.3798E-02	5.3477E-02	4.9877E-02
1.2000E 03	5.1465E-02	5.1170E-02	4.8484E-02

TABLE D36

SAMPLE - NORTHFLEET SLURRY

MEAN SAT. DROP TEMPERATURE= 150.00 DEG.C

CRUST THERMAL CONDUCTIVITY= .6768 W/M/DEG. C

AIR TEMPERATURE = 200.00 DEG. C

INITIAL MOISTURE CONTENT = 0.450 KG/KG

GAS FILM TRANSFER COEFFICIENT= 3.8770 M/S

DRYING TIME(SEC)	KC	KT	KE
6.0000E 01	9.3538E-01	7.5357E-01	7.4360E-01
1.2000E 02	4.4565E-01	3.9970E-01	3.7266E-01
1.8000E 02	2.8772E-01	2.6784E-01	2.4901E-01
2.4000E 02	1.9804E-01	1.8841E-01	1.8730E-01
3.0000E 02	1.5262E-01	1.4684E-01	1.5023E-01
3.6000E 02	1.1571E-01	1.1235E-01	1.2564E-01
4.2000E 02	9.7278E-02	9.4896E-02	1.0798E-01
4.8000E 02	9.0160E-02	8.8111E-02	9.4603E-02
5.4000E 02	7.8820E-02	7.7250E-02	8.4303E-02
6.0000E 02	6.9816E-02	6.8581E-02	7.6064E-02
6.6000E 02	6.2500E-02	6.1508E-02	6.9324E-02
7.2000E 02	6.4294E-02	6.3245E-02	6.6263E-02
7.8000E 02	6.1180E-02	6.0230E-02	6.3577E-02
8.4000E 02	6.3389E-02	6.2369E-02	6.0979E-02
9.0000E 02	6.0551E-02	5.9620E-02	5.8698E-02
9.6000E 02	5.7932E-02	5.7079E-02	5.6587E-02
1.0200E 03	5.6465E-02	5.5655E-02	5.4601E-02
1.0800E 03	5.4177E-02	5.3430E-02	5.2775E-02
1.1400E 03	5.5830E-02	5.5038E-02	5.0974E-02
1.2000E 03	5.3711E-02	5.2977E-02	4.9380E-02

TABLE D37

SAMPLE - NORTHFLEET SLURRY

MEAN SAT. DROP TEMPERATURE= 238.00 DEG.C

CRUST THERMAL CONDUCTIVITY= .9258 W/M/DEG. C

AIR TEMPERATURE = 300.00 DEG. C

INITIAL MOISTURE CONTENT = 0.450 KG/KG

GAS FILM TRANSFER COEFFICIENT= 6.8537 M/S

DRYING TIME(SEC)	KC	KT	KE
6.0000E 01	1.3260E 00	1.1110E 00	9.9485E-01
1.2000E 02	5.5226E-01	5.1108E-01	5.0061E-01
1.8000E 02	3.5123E-01	3.3410E-01	3.3564E-01
2.4000E 02	2.5306E-01	2.4405E-01	2.5318E-01
3.0000E 02	1.9523E-01	1.8982E-01	2.0371E-01
3.6000E 02	1.4755E-01	1.4444E-01	1.7108E-01
4.2000E 02	1.3051E-01	1.2807E-01	1.4721E-01
4.8000E 02	1.1069E-01	1.0893E-01	1.2957E-01
5.4000E 02	1.0221E-01	1.0071E-01	1.1552E-01
6.0000E 02	9.5948E-02	9.4623E-02	1.0423E-01
6.6000E 02	8.4935E-02	8.3896E-02	9.5261E-02
7.2000E 02	8.0182E-02	7.9255E-02	9.1363E-02
7.8000E 02	7.5846E-02	7.5016E-02	8.7791E-02
8.4000E 02	7.1876E-02	7.1130E-02	8.4506E-02
9.0000E 02	6.8227E-02	6.7555E-02	8.1474E-02
9.6000E 02	6.4865E-02	6.4257E-02	7.8669E-02
1.0200E 03	9.1273E-02	9.0073E-02	7.4589E-02
1.0800E 03	8.7260E-02	8.6163E-02	7.2159E-02
1.1400E 03	8.3529E-02	8.2523E-02	6.9892E-02
1.2000E 03	8.0050E-02	7.9126E-02	6.7772E-02

TABLE D38

SAMPLE - NORTHFLEET SLURRY

MEAN SAT. DROP TEMPERATURE= 305.00 DEG.C

CRUST THERMAL CONDUCTIVITY= *1.0994 W/M/DEG. C

AIR TEMPERATURE = 400.00 DEG. C

INITIAL MOISTURE CONTENT = 0.450 KG/KG

GAS FILM TRANSFER COEFFICIENT= 11.8406 M/S

DRYING TIME(SEC)	KC	KT	KE
6.0000E 01	1.2900E 00	1.1633E 00	1.3639E 00
1.2000E 02	5.9452E-01	5.6609E-01	6.9374E-01
1.8000E 02	4.7342E-01	4.5522E-01	4.6622E-01
2.4000E 02	3.9937E-01	3.8634E-01	3.5226E-01
3.0000E 02	3.3277E-01	3.2367E-01	2.8451E-01
3.6000E 02	2.8345E-01	2.7683E-01	2.3942E-01
4.2000E 02	2.4547E-01	2.4049E-01	2.0727E-01
4.8000E 02	2.1369E-01	2.0990E-01	1.8331E-01
5.4000E 02	1.8812E-01	1.8518E-01	1.6471E-01
6.0000E 02	1.6707E-01	1.6474E-01	1.4987E-01
6.6000E 02	1.4942E-01	1.4756E-01	1.3775E-01
7.2000E 02	1.4163E-01	1.3996E-01	1.3250E-01
7.8000E 02	1.3442E-01	1.3291E-01	1.2769E-01
8.4000E 02	1.2773E-01	1.2637E-01	1.2328E-01
9.0000E 02	1.2151E-01	1.2027E-01	1.1921E-01
9.6000E 02	1.1571E-01	1.1459E-01	1.1545E-01
1.0200E 03	1.1768E-01	1.1652E-01	1.1110E-01
1.0800E 03	1.1239E-01	1.1133E-01	1.0785E-01
1.1400E 03	1.0743E-01	1.0646E-01	1.0483E-01
1.2000E 03	1.0276E-01	1.0187E-01	1.0200E-01

TABLE D39

SAMPLE - NORTHFLEET SLURRY

MEAN SAT. DROP TEMPERATURE= 155.50 DEG.C

CRUST THERMAL CONDUCTIVITY= .6910 W/M/DEG. C

AIR TEMPERATURE = 200.00 DEG. C

INITIAL MOISTURE CONTENT = 0.550 KG/KG

GAS FILM TRANSFER COEFFICIENT= 3.1968 M/S

DRYING TIME(SEC)	KC	KT	KE
6.0000E 01	5.9085E-01	4.9868E-01	3.9584E-01
1.2000E 02	1.4399E-01	1.3778E-01	1.9836E-01
1.8000E 02	1.1831E-01	1.1409E-01	1.3231E-01
2.4000E 02	8.6934E-02	8.4633E-02	9.9344E-02
3.0000E 02	6.8381E-02	6.6949E-02	7.9565E-02
3.6000E 02	7.4525E-02	7.2828E-02	6.6271E-02
4.2000E 02	6.3114E-02	6.1893E-02	5.6854E-02
4.8000E 02	5.4627E-02	5.3709E-02	4.9791E-02
5.4000E 02	4.8073E-02	4.7360E-02	4.4297E-02
6.0000E 02	4.2863E-02	4.2296E-02	3.9903E-02
6.6000E 02	3.8625E-02	3.8164E-02	3.6307E-02
7.2000E 02	3.6791E-02	3.6372E-02	3.4744E-02
7.8000E 02	3.5113E-02	3.4732E-02	3.3311E-02
8.4000E 02	3.3573E-02	3.3224E-02	3.1992E-02
9.0000E 02	3.2156E-02	3.1835E-02	3.0775E-02
9.6000E 02	3.0846E-02	3.0551E-02	2.9649E-02
1.0200E 03	2.9632E-02	2.9360E-02	2.8602E-02
1.0800E 03	2.8505E-02	2.8253E-02	2.7628E-02
1.1400E 03	2.7454E-02	2.7221E-02	2.6719E-02
1.2000E 03	2.6474E-02	2.6257E-02	2.5869E-02

TABLE D40

SAMPLE - NORTHFLEET SLURRY

MEAN SAT. DROP TEMPERATURE= 225.00 DEG.C

CRUST THERMAL CONDUCTIVITY= .8886 W/M/DEG. C

AIR TEMPERATURE = 300.00 DEG. C

INITIAL MOISTURE CONTENT = 0.550 KG/KG

GAS FILM TRANSFER COEFFICIENT= 5.5563 M/S

DRYING TIME(SEC)	KC	KT	KE
6.0000E 01	4.9183E-01	4.5184E-01	5.2073E-01
1.2000E 02	1.8124E-01	1.7552E-01	2.6076E-01
1.8000E 02	5.3733E-02	5.3218E-02	1.7522E-01
2.4000E 02	4.0192E-02	3.9903E-02	1.3196E-01
3.0000E 02	4.3318E-02	4.2983E-02	1.0543E-01
3.6000E 02	3.7359E-02	3.7109E-02	8.8075E-02
4.2000E 02	3.0689E-02	3.0520E-02	7.5802E-02
4.8000E 02	2.7438E-02	2.7303E-02	6.6508E-02
5.4000E 02	4.0472E-02	4.0179E-02	5.8624E-02
6.0000E 02	5.1914E-02	5.1434E-02	5.2566E-02
6.6000E 02	4.8109E-02	4.7696E-02	4.7835E-02
7.2000E 02	4.6425E-02	4.6040E-02	4.5778E-02
7.8000E 02	4.4863E-02	4.4504E-02	4.3892E-02
8.4000E 02	4.3412E-02	4.3075E-02	4.2158E-02
9.0000E 02	5.6787E-02	5.6212E-02	4.0391E-02
9.6000E 02	5.5112E-02	5.4571E-02	3.8908E-02
1.0200E 03	5.3542E-02	5.3031E-02	3.7531E-02
1.0800E 03	5.2068E-02	5.1584E-02	3.6249E-02
1.1400E 03	5.0679E-02	5.0221E-02	3.5053E-02
1.2000E 03	4.9369E-02	4.8934E-02	3.3934E-02

TABLE D41

SAMPLE - NORTHFLEET SLURRY

MEAN SAT. DROP TEMPERATURE= 299.50 DEG.C

CRUST THERMAL CONDUCTIVITY= *1.0868 W/M/DEG. C

AIR TEMPERATURE = 400.00 DEG. C

INITIAL MOISTURE CONTENT = 0.550 KG/KG

GAS FILM TRANSFER COEFFICIENT= 8.9464 M/S

DRYING TIME(SEC)	KC	KT	KE
6.0000E 01	8.3479E-01	7.6354E-01	6.5969E-01
1.2000E 02	5.3927E-01	5.0861E-01	3.3006E-01
1.8000E 02	8.4240E-02	8.3455E-02	2.2506E-01
2.4000E 02	8.8819E-02	8.7946E-02	1.6846E-01
3.0000E 02	8.7769E-02	8.6916E-02	1.3480E-01
3.6000E 02	8.1195E-02	8.0465E-02	1.1261E-01
4.2000E 02	7.6764E-02	7.6111E-02	9.6709E-02
4.8000E 02	7.3829E-02	7.3225E-02	8.4739E-02
5.4000E 02	6.7634E-02	6.7126E-02	7.5587E-02
6.0000E 02	6.2441E-02	6.2008E-02	6.8268E-02
6.6000E 02	5.8008E-02	5.7635E-02	6.2280E-02
7.2000E 02	5.9832E-02	5.9435E-02	5.9480E-02
7.8000E 02	5.7887E-02	5.7514E-02	5.7094E-02
8.4000E 02	6.0080E-02	5.9680E-02	5.4709E-02
9.0000E 02	5.8280E-02	5.7903E-02	5.2683E-02
9.6000E 02	5.6586E-02	5.6230E-02	5.0807E-02
1.0200E 03	5.4987E-02	5.4651E-02	4.9065E-02
1.0800E 03	5.3477E-02	5.3159E-02	4.7444E-02
1.1400E 03	5.2046E-02	5.1745E-02	4.5931E-02
1.2000E 03	5.0689E-02	5.0403E-02	4.4515E-02

TABLE D42

SAMPLE - NORTHFLEET SLURRY

MEAN SAT. DROP TEMPERATURE= 160.00 DEG.C

CRUST THERMAL CONDUCTIVITY= .7030 W/M/DEG. C

AIR TEMPERATURE = 200.00 DEG. C

INITIAL MOISTURE CONTENT = 0.300 KG/KG

GAS FILM TRANSFER COEFFICIENT= 4.9927 M/S

DRYING TIME(SEC)	KC	KT	KE
6.0000E 01	1.2821E 00	1.0202E 00	1.2171E 00
1.2000E 02	6.6722E-01	5.8857E-01	6.1244E-01
1.8000E 02	4.5813E-01	4.1963E-01	4.1084E-01
2.4000E 02	3.5054E-01	3.2754E-01	3.1002E-01
3.0000E 02	2.8593E-01	2.7044E-01	2.4947E-01
3.6000E 02	2.3918E-01	2.2825E-01	2.0917E-01
4.2000E 02	2.0489E-01	1.9681E-01	1.8040E-01
4.8000E 02	1.7858E-01	1.7241E-01	1.5883E-01
5.4000E 02	1.5938E-01	1.5445E-01	1.4199E-01
6.0000E 02	1.4228E-01	1.3833E-01	1.2859E-01
6.6000E 02	1.2808E-01	1.2488E-01	1.1763E-01
7.2000E 02	1.2185E-01	1.1895E-01	1.1287E-01
7.8000E 02	1.1481E-01	1.1223E-01	1.0859E-01
8.4000E 02	1.1079E-01	1.0838E-01	1.0450E-01
9.0000E 02	1.0586E-01	1.0366E-01	1.0080E-01
9.6000E 02	1.0127E-01	9.9258E-02	9.7379E-02
1.0200E 03	9.9879E-02	9.7920E-02	9.3993E-02
1.0800E 03	9.5792E-02	9.3988E-02	9.1035E-02
1.1400E 03	9.1963E-02	9.0299E-02	8.8277E-02
1.2000E 03	8.8368E-02	8.6831E-02	8.5698E-02

TABLE D43

SAMPLE - NORTHFLEET SLURRY

MEAN SAT. DROP TEMPERATURE= 220.00 DEG.C

CRUST THERMAL CONDUCTIVITY= .8741 W/M/DEG. C

AIR TEMPERATURE = 300.00 DEG. C

INITIAL MOISTURE CONTENT = 0.300 KG/KG

GAS FILM TRANSFER COEFFICIENT= 8.0655 M/S

DRYING TIME(SEC)	KC	KT	KE
6.0000E 01	1.3455E 00	1.1531E 00	1.4635E 00
1.2000E 02	7.7354E-01	7.0585E-01	7.3731E-01
1.8000E 02	5.0968E-01	4.7938E-01	4.9652E-01
2.4000E 02	3.9664E-01	3.7804E-01	3.7555E-01
3.0000E 02	3.5346E-01	3.3862E-01	3.0180E-01
3.6000E 02	2.9868E-01	2.8801E-01	2.5347E-01
4.2000E 02	2.5777E-01	2.4979E-01	2.1897E-01
4.8000E 02	2.2593E-01	2.1977E-01	1.9312E-01
5.4000E 02	2.0036E-01	1.9550E-01	1.7304E-01
6.0000E 02	1.7933E-01	1.7543E-01	1.5699E-01
6.6000E 02	1.6170E-01	1.5853E-01	1.4388E-01
7.2000E 02	1.5392E-01	1.5104E-01	1.3819E-01
7.8000E 02	1.4671E-01	1.4409E-01	1.3298E-01
8.4000E 02	1.4002E-01	1.3763E-01	1.2819E-01
9.0000E 02	1.3379E-01	1.3160E-01	1.2377E-01
9.6000E 02	1.2797E-01	1.2597E-01	1.1968E-01
1.0200E 03	1.2253E-01	1.2070E-01	1.1588E-01
1.0800E 03	1.1744E-01	1.1575E-01	1.1236E-01
1.1400E 03	1.1265E-01	1.1110E-01	1.0907E-01
1.2000E 03	1.0814E-01	1.0671E-01	1.0600E-01

TABLE D44

SAMPLE - NORTHFLEET SLURRY

MEAN SAT. DROP TEMPERATURE= 321.00 DEG.C

CRUST THERMAL CONDUCTIVITY= *1.1341 W/M/DEG. C

AIR TEMPERATURE = 400.00 DEG. C

INITIAL MOISTURE CONTENT = 0.300 KG/KG

GAS FILM TRANSFER COEFFICIENT= 12.9182 M/S

DRYING TIME(SEC)	KC	KT	KE
6.0000E 01	2.0038E 00	1.7347E 00	1.8319E 00
1.2000E 02	9.6528E-01	8.9816E-01	9.2911E-01
1.8000E 02	6.6015E-01	6.2806E-01	6.2770E-01
2.4000E 02	3.1058E-01	3.0329E-01	4.9331E-01
3.0000E 02	1.9280E-01	1.8996E-01	4.1314E-01
3.6000E 02	3.4450E-01	3.3555E-01	3.2580E-01
4.2000E 02	2.9309E-01	2.8658E-01	2.8285E-01
4.8000E 02	2.5302E-01	2.4816E-01	2.5071E-01
5.4000E 02	2.8718E-01	2.8094E-01	2.2027E-01
6.0000E 02	2.5569E-01	2.5072E-01	2.0029E-01
6.6000E 02	2.2926E-01	2.2526E-01	1.8398E-01
7.2000E 02	2.1758E-01	2.1398E-01	1.7690E-01
7.8000E 02	2.0677E-01	2.0351E-01	1.7042E-01
8.4000E 02	1.9673E-01	1.9378E-01	1.6447E-01
9.0000E 02	1.8738E-01	1.8471E-01	1.5899E-01
9.6000E 02	1.7867E-01	1.7623E-01	1.5392E-01
1.0200E 03	1.7052E-01	1.6830E-01	1.4922E-01
1.0800E 03	1.6288E-01	1.6085E-01	1.4485E-01
1.1400E 03	1.5571E-01	1.5386E-01	1.4078E-01
1.2000E 03	1.4897E-01	1.4728E-01	1.3699E-01

FIGURE D1

EXPERIMENTAL VERSUS THEORETICAL

MASS TRANSFER COEFFICIENT FOR

SHOREHAM SLURRY SAMPLE

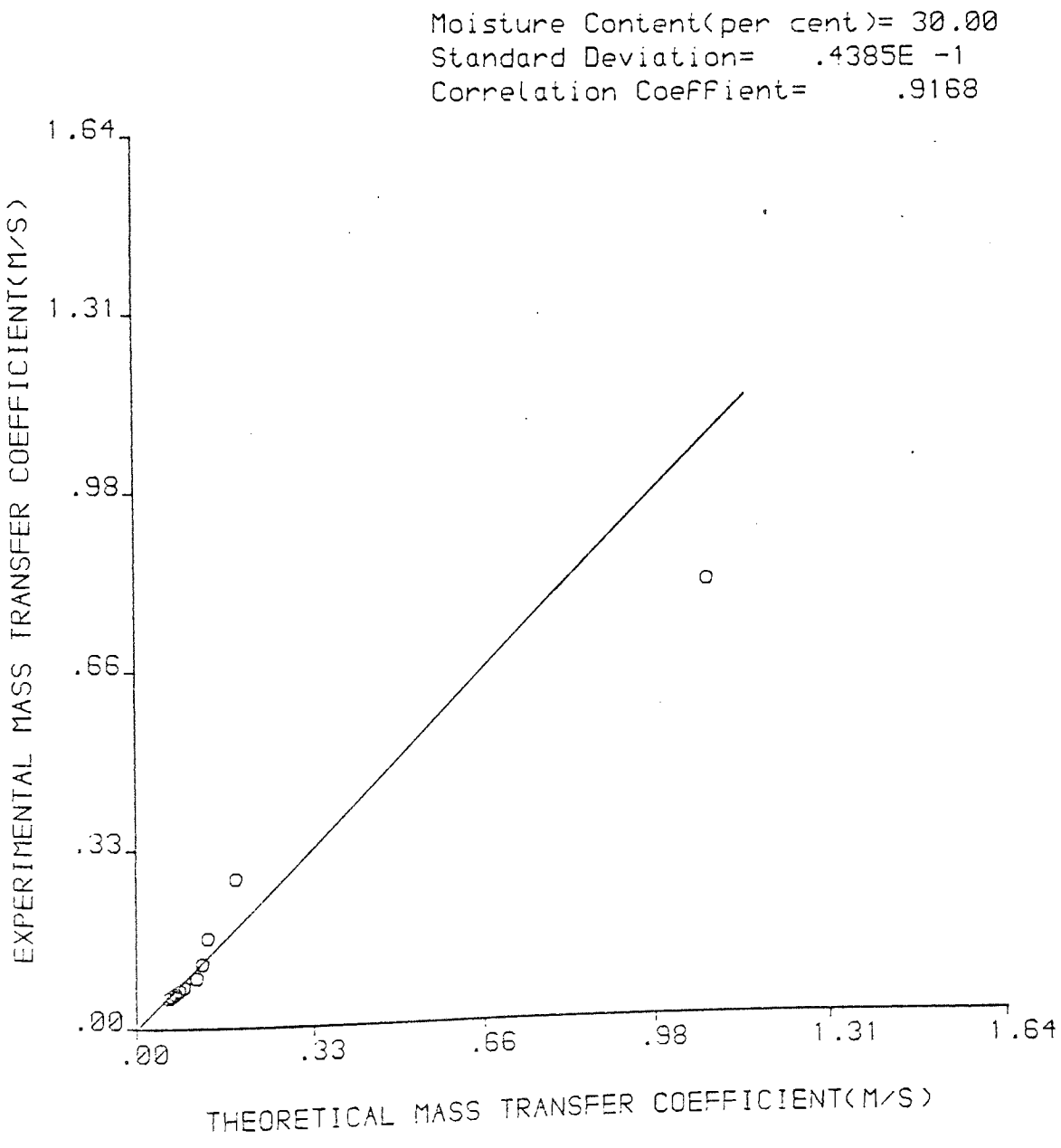

FIGURE D2

EXPERIMENTAL VERSUS THEORETICAL

MASS TRANSFER COEFFICIENT FOR

SHOREHAM SLURRY SAMPLE

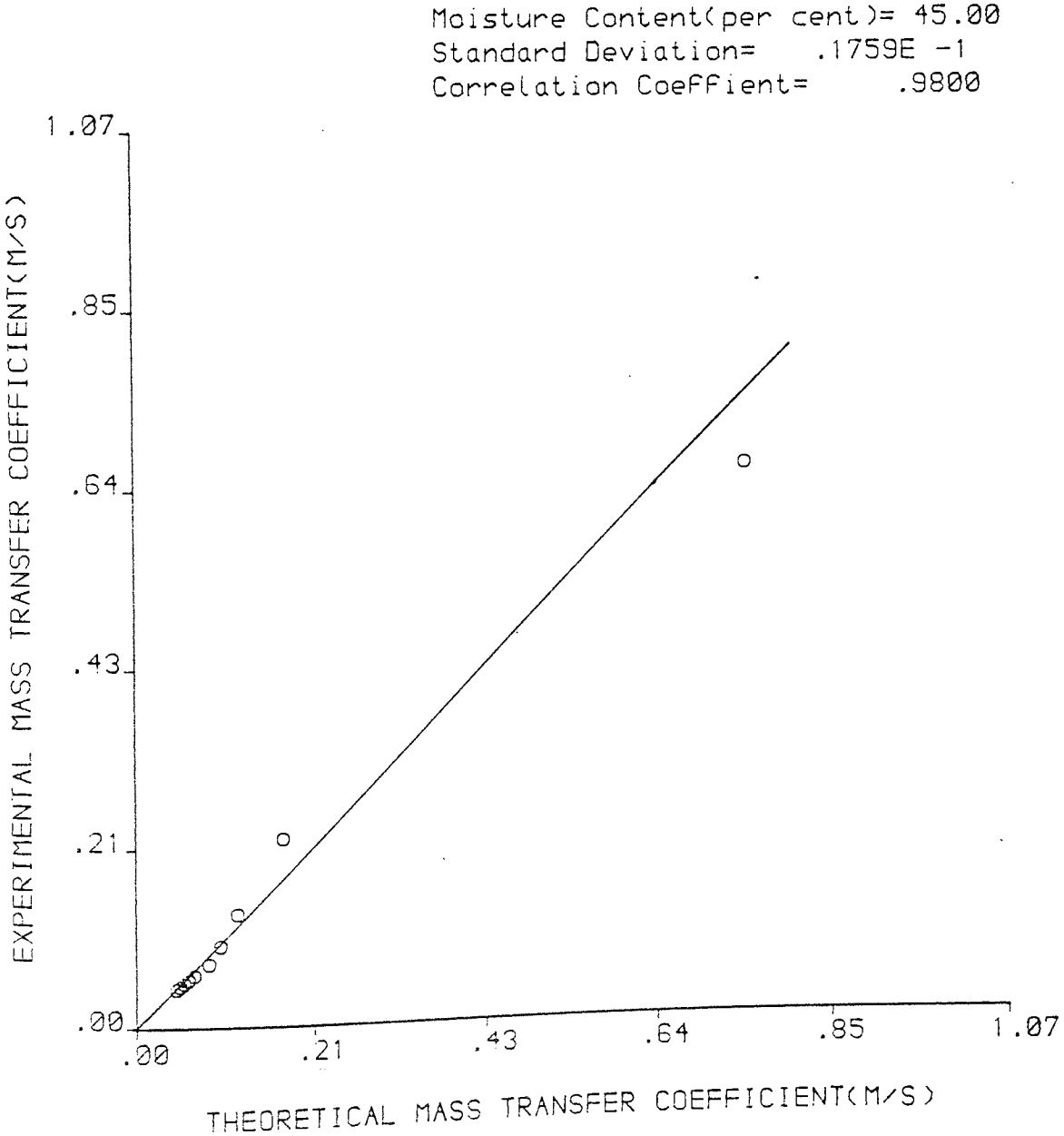

FIGURE D3

EXPERIMENTAL VERSUS THEORETICAL

MASS TRANSFER COEFFICIENT FOR

SHOREHAM SLURRY SAMPLE

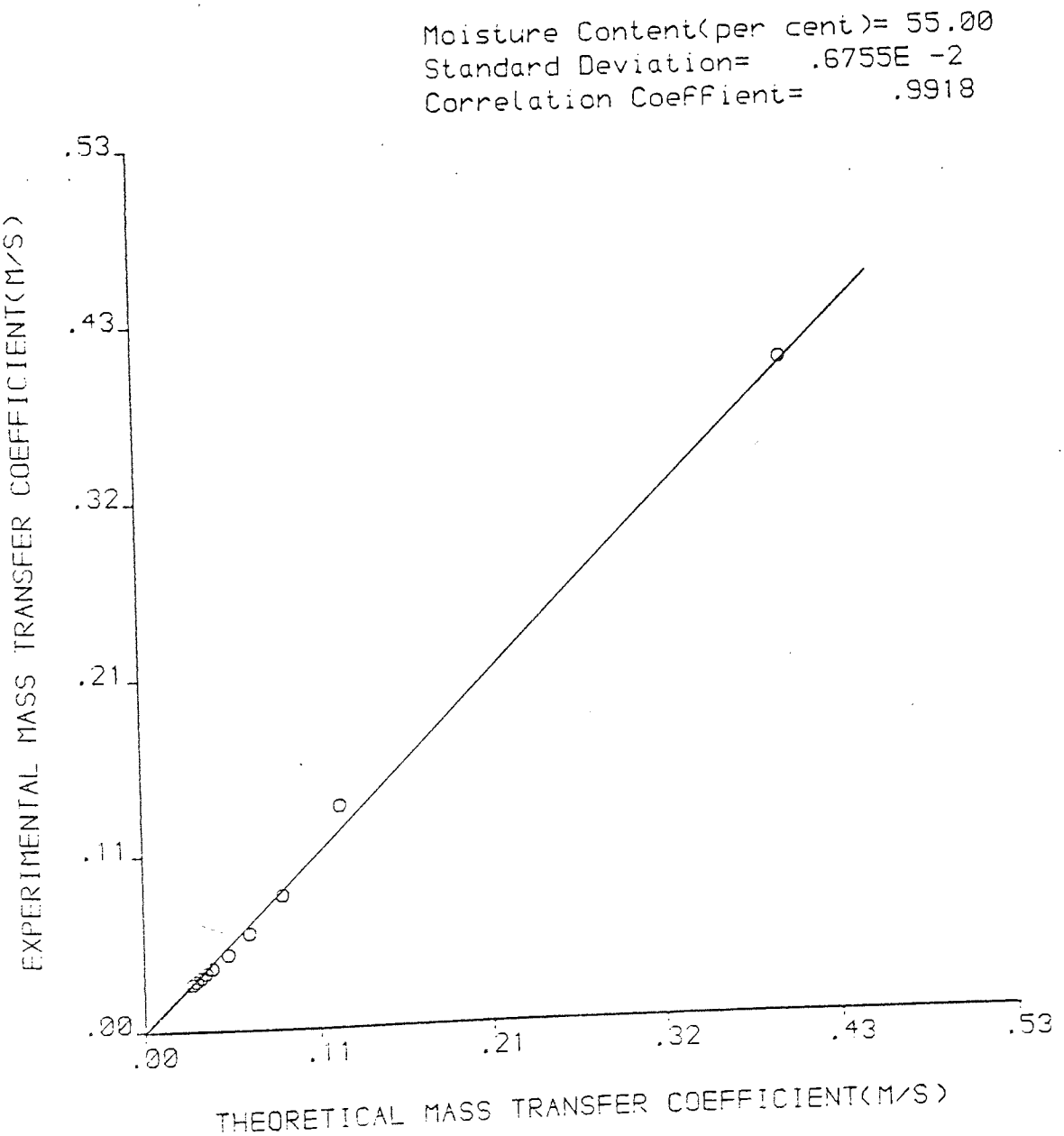

FIGURE D4

EXPERIMENTAL VERSUS THEOR-TICAL

MASS TRANSFER COEFFICIENT FOR

NORTHFLEET SLURRY SAMPLE

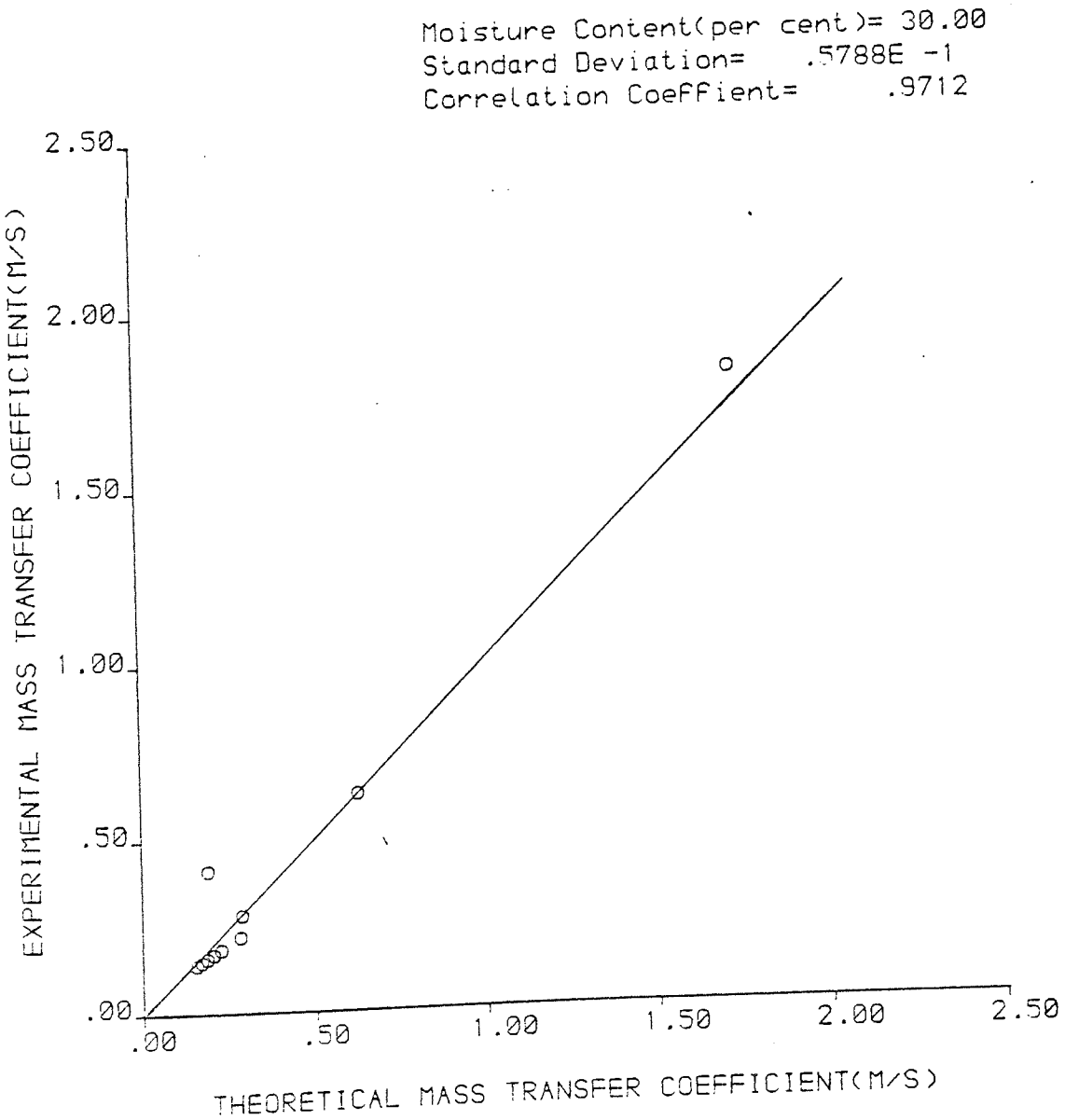

FIGURE D5

EXPERIMENTAL VERSUS THEORETICAL

MASS TRANSFER COEFFICIENT FOR

NORTHFLEET SLURRY SAMPLE

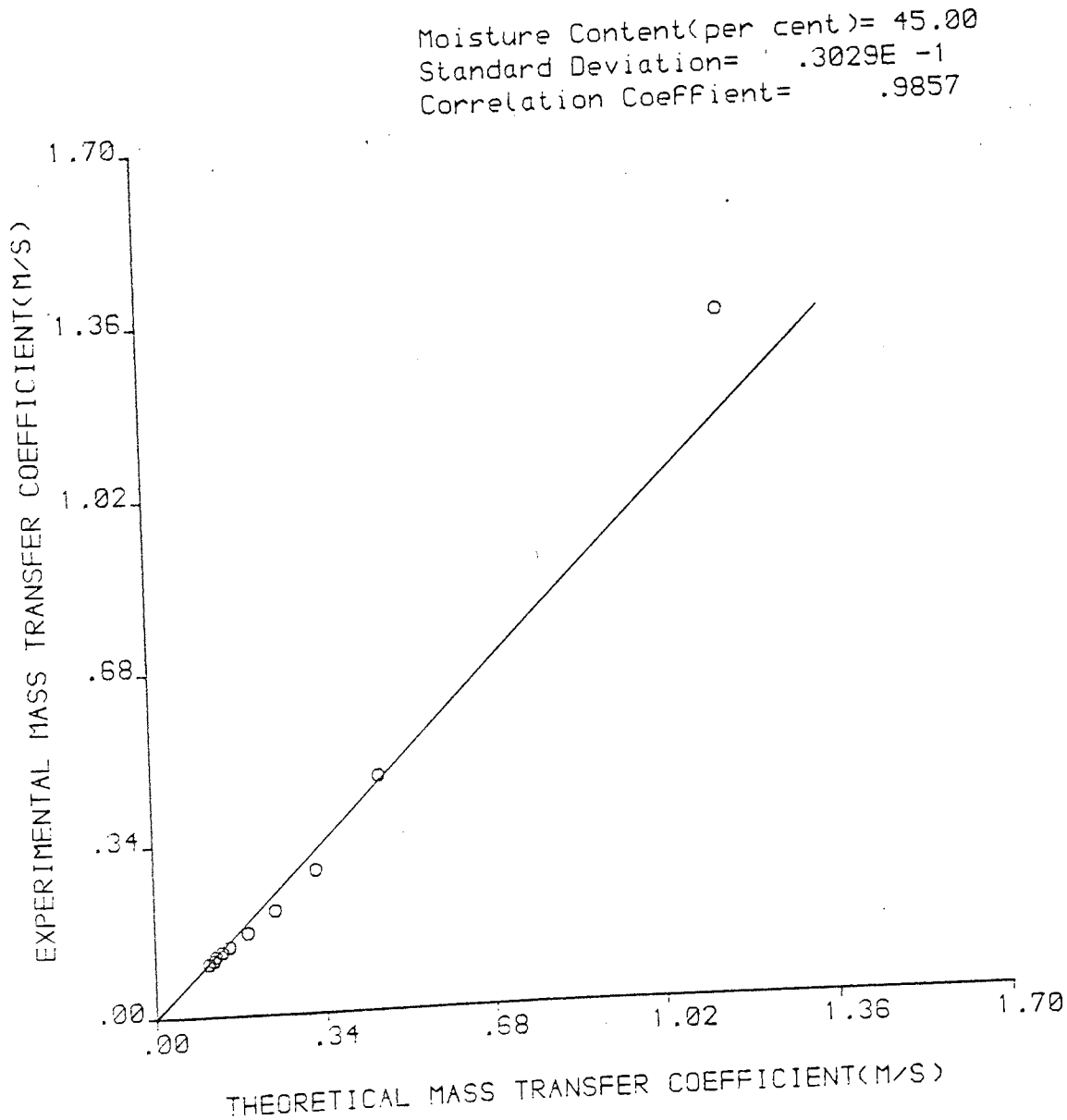

FIGURE D6

EXPERIMENTAL VERSUS THEOR-TICAL

MASS TRANSFER COEFFICIENT FOR

NORTHFLEET SLURRY SAMPLE

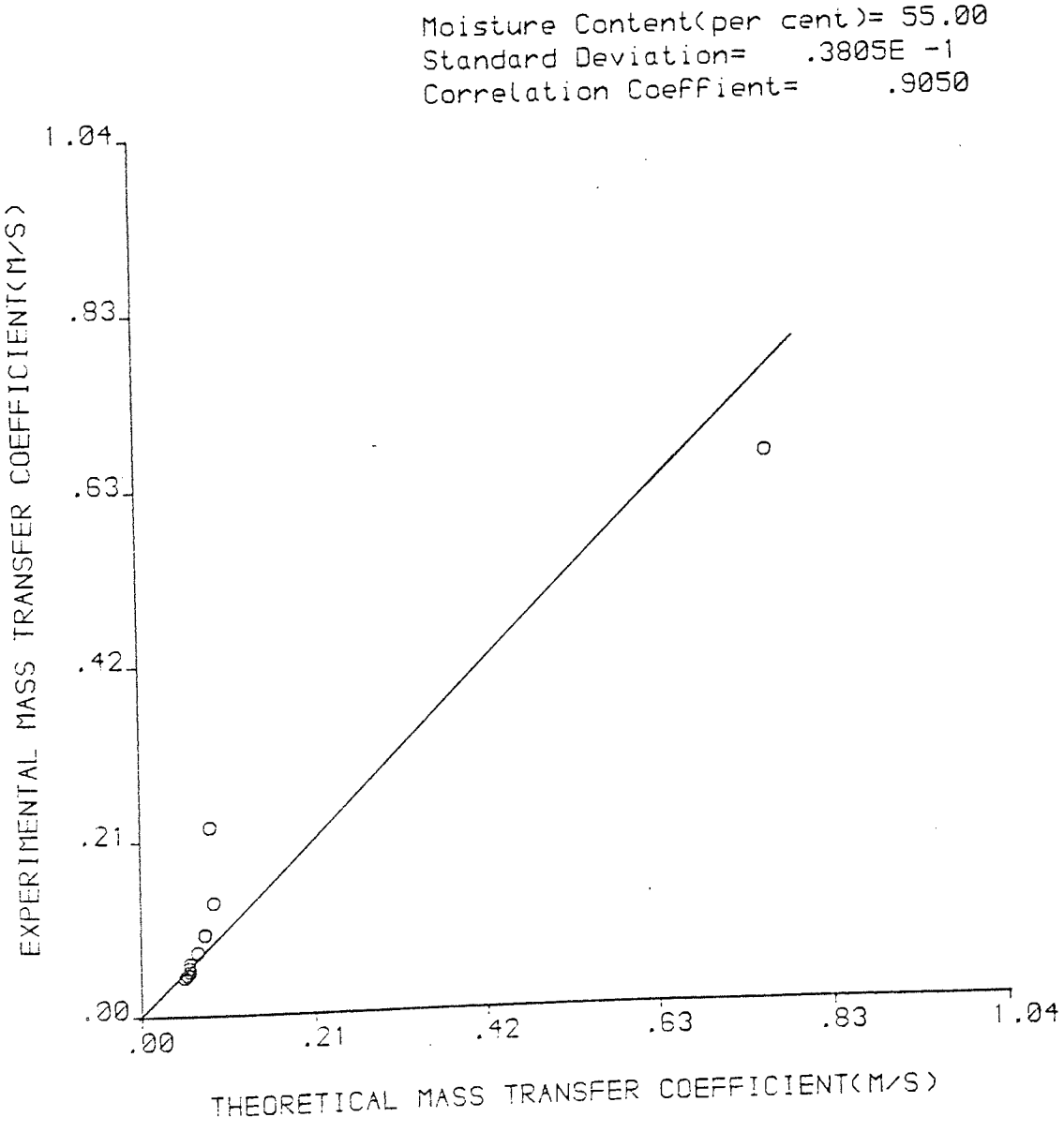

FIGURE D7

EXPERIMENTAL VERSUS THEORETICAL

MASS TRANSFER COEFFICIENT FOR

HUMBER SLURRY SAMPLE

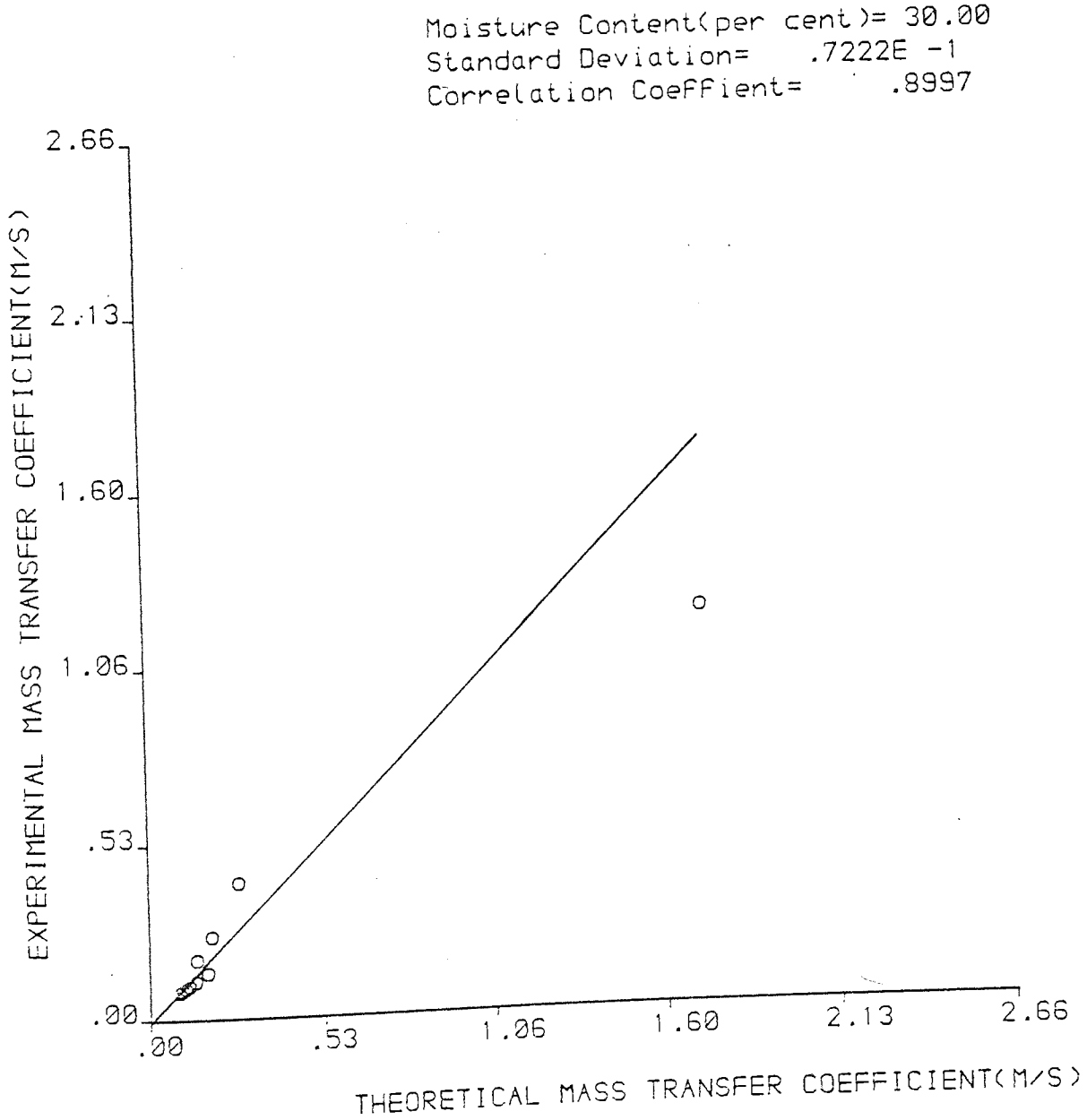

FIGURE D8

EXPERIMENTAL VERSUS THEORETICAL

MASS TRANSFER COEFFICIENT FOR

HUMBER SLURRY SAMPLE

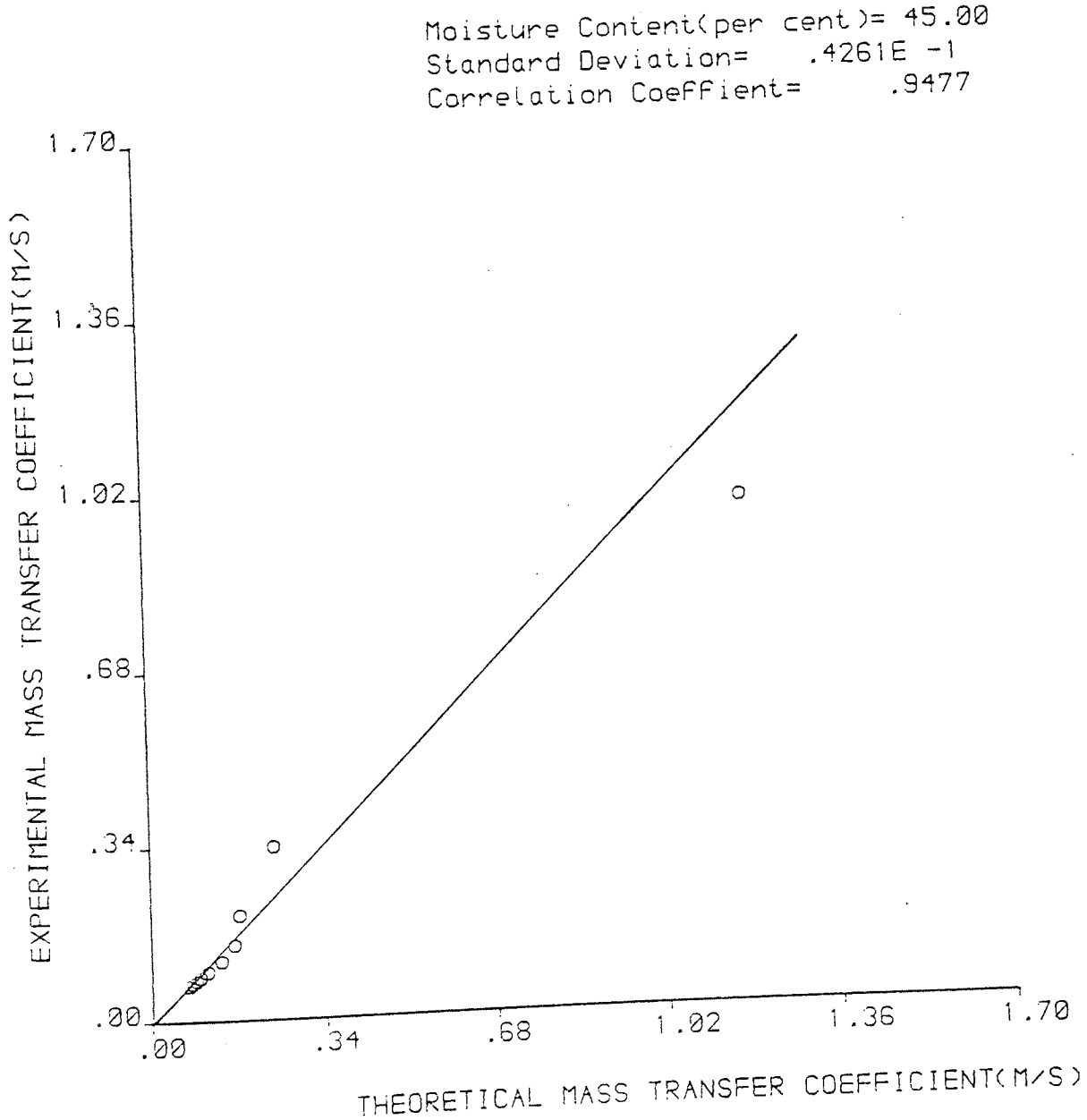

FIGURE D9

EXPERIMENTAL VERSUS THEORETICAL

MASS TRANSFER COEFFICIENT FOR

HUMBER SLURRY SAMPLE

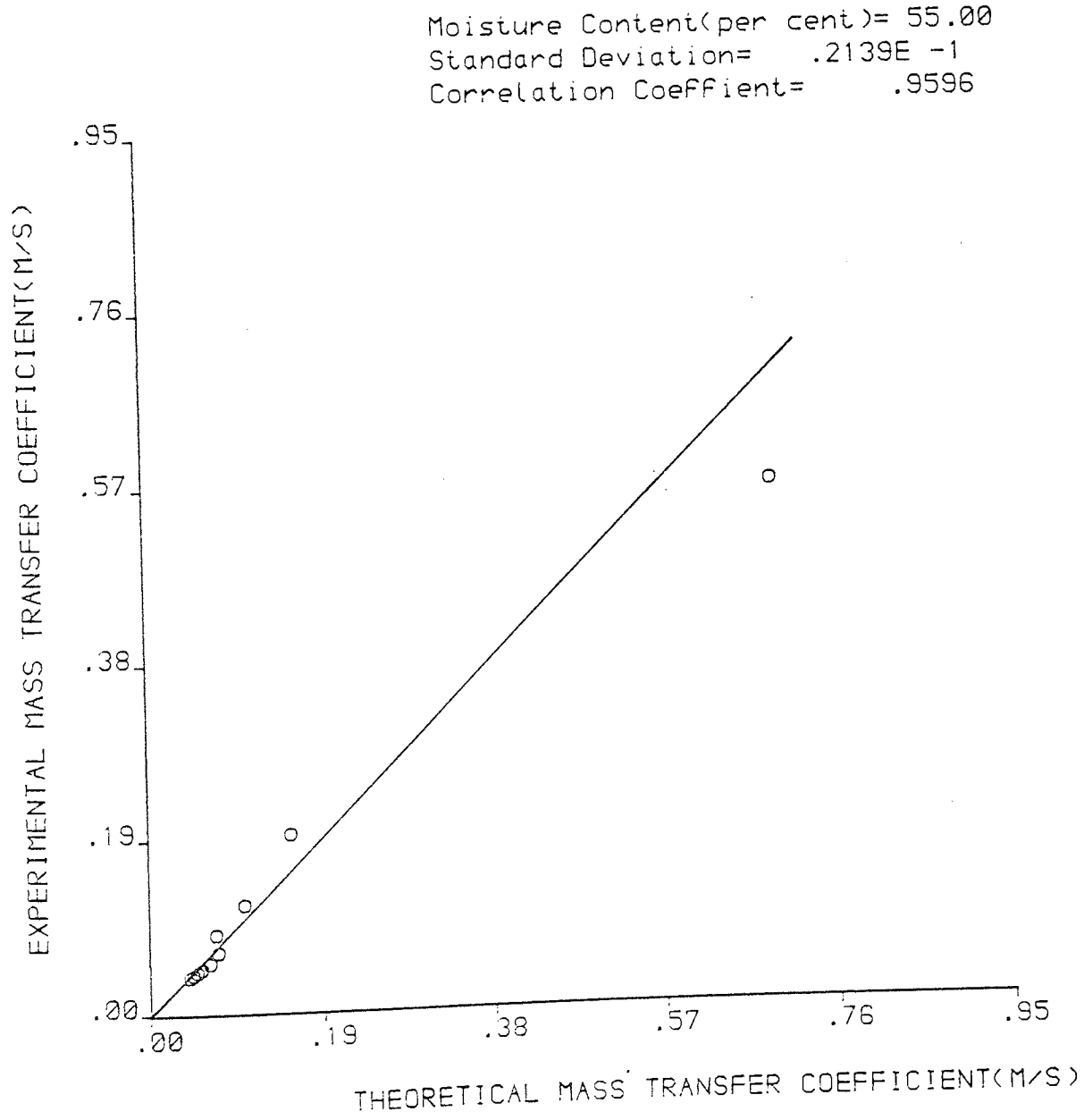

FIGURE D1O

EXPERIMENTAL VERSUS THEORETICAL

MASS TRANSFER COEFFICIENT FOR

MASON SLURRY SAMPLE

Moisture Content(per cent)= 30.00
Standard Deviation= .7296E -1
Correlation Coeffient= .8189

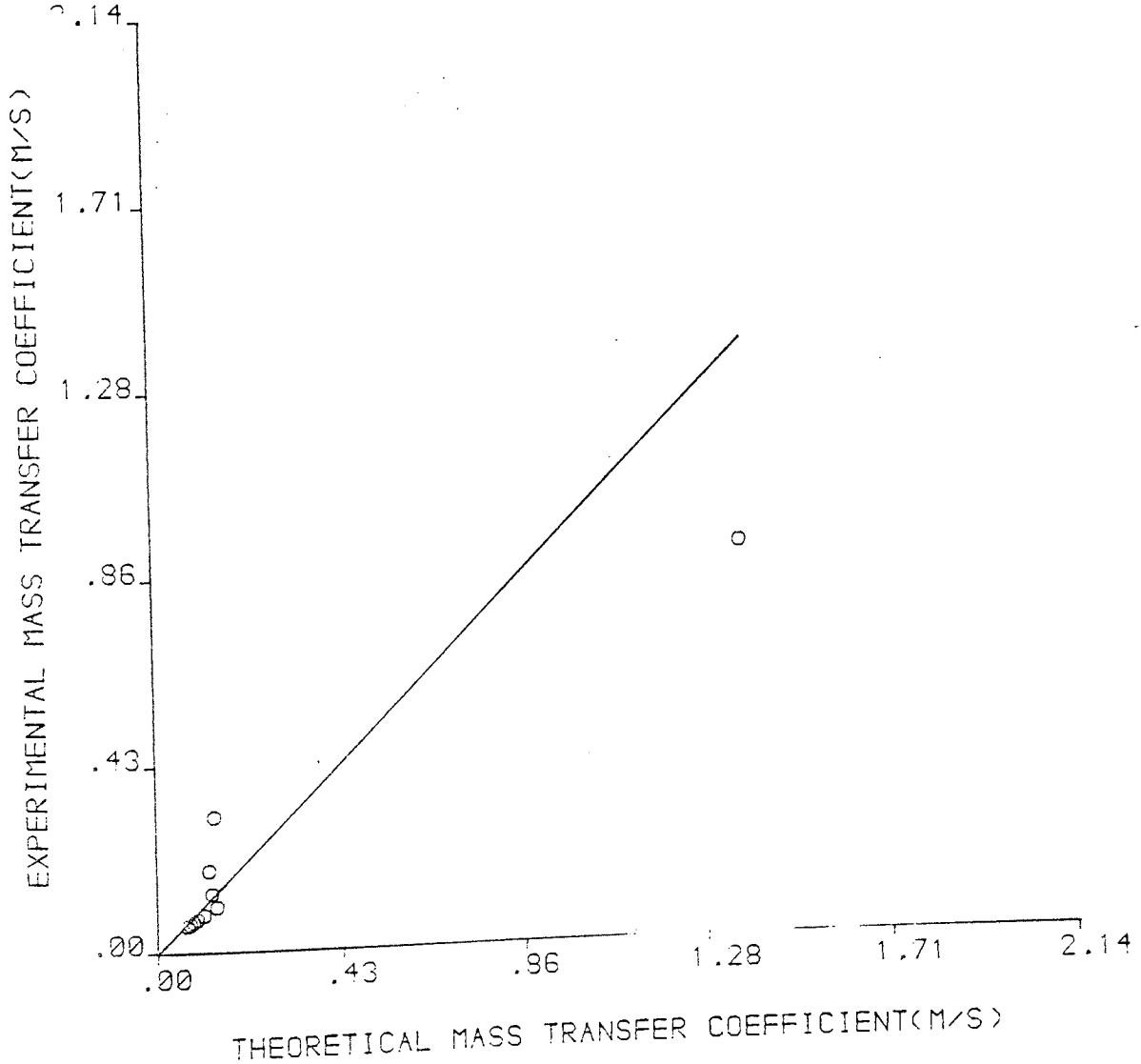

FIGURE D11

EXPERIMENTAL VERSUS THEORETI AL

MASS TRANSFER COEFFICIENT FOR

MASON SLURRY SAMPLE

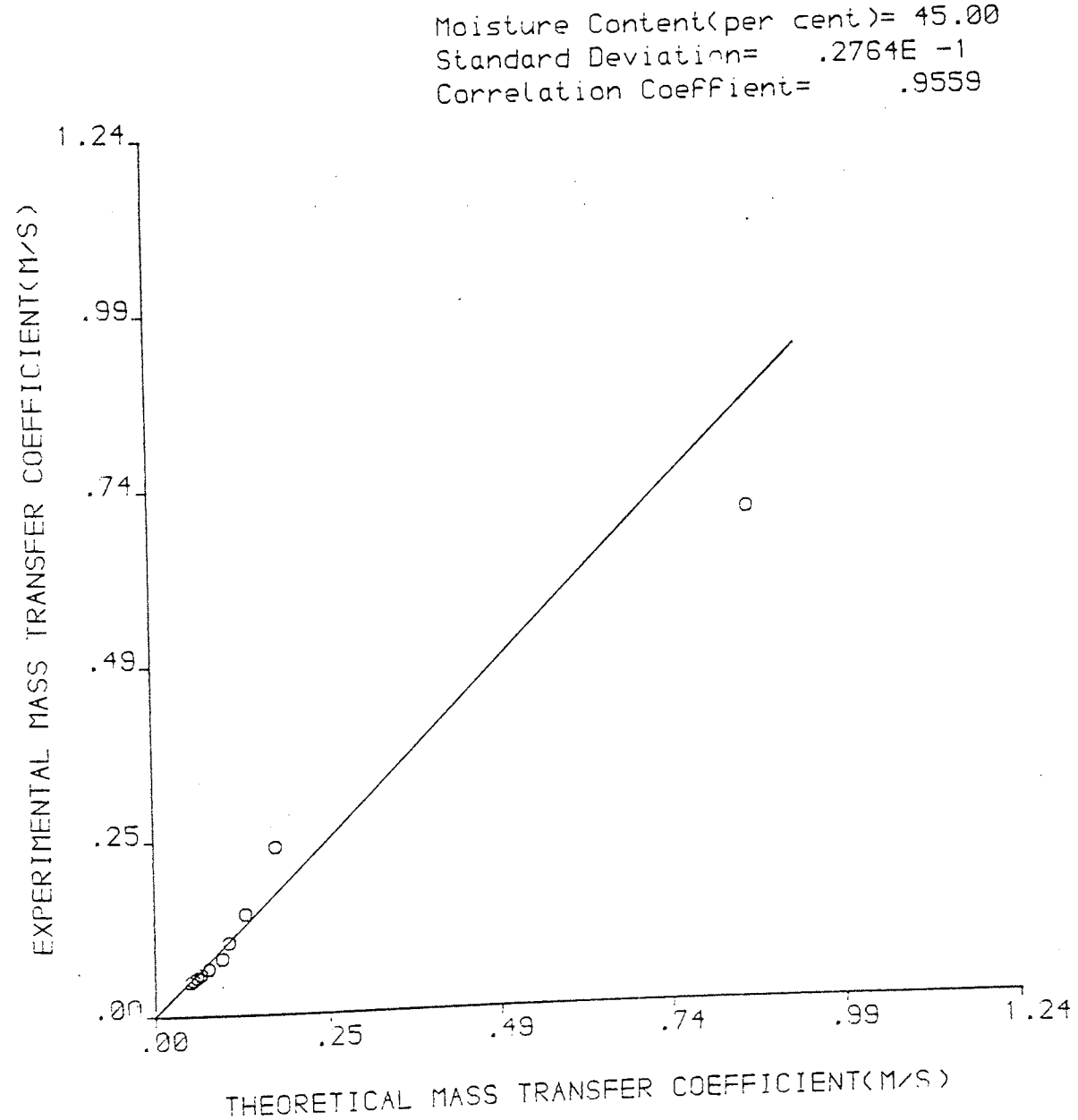

FIGURE D12

EXPERIMENTAL VERSUS THEORETICAL

MASS TRANSFER COEFFICIENT FOR

MASON SLURRY SAMPLE

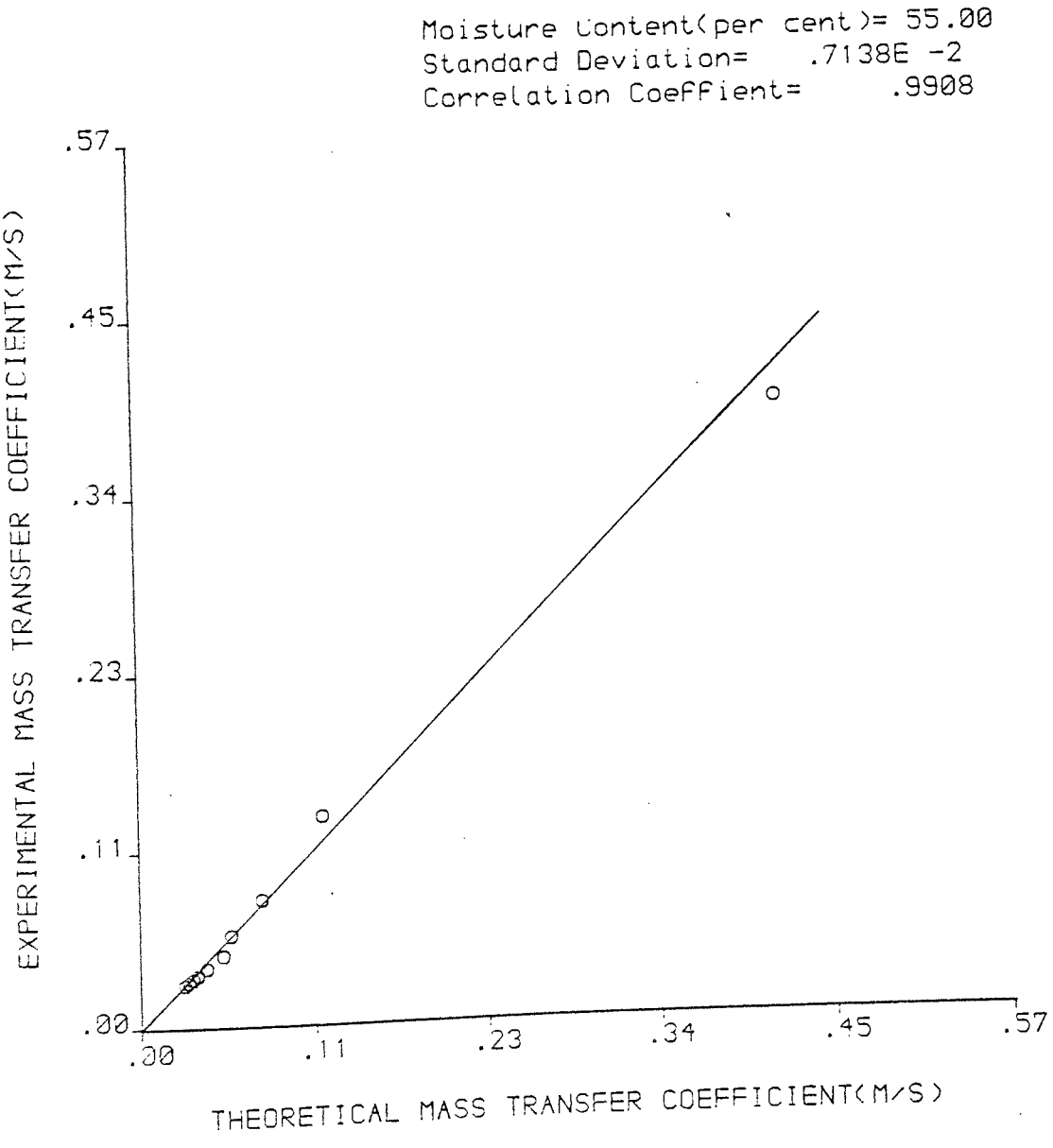

FIGURE D13

EXPERIMENTAL VERSUS THEORETICAL

MASS TRANSFER COEFFICIENT FOR

WESTBURY SLURRY SAMPLE

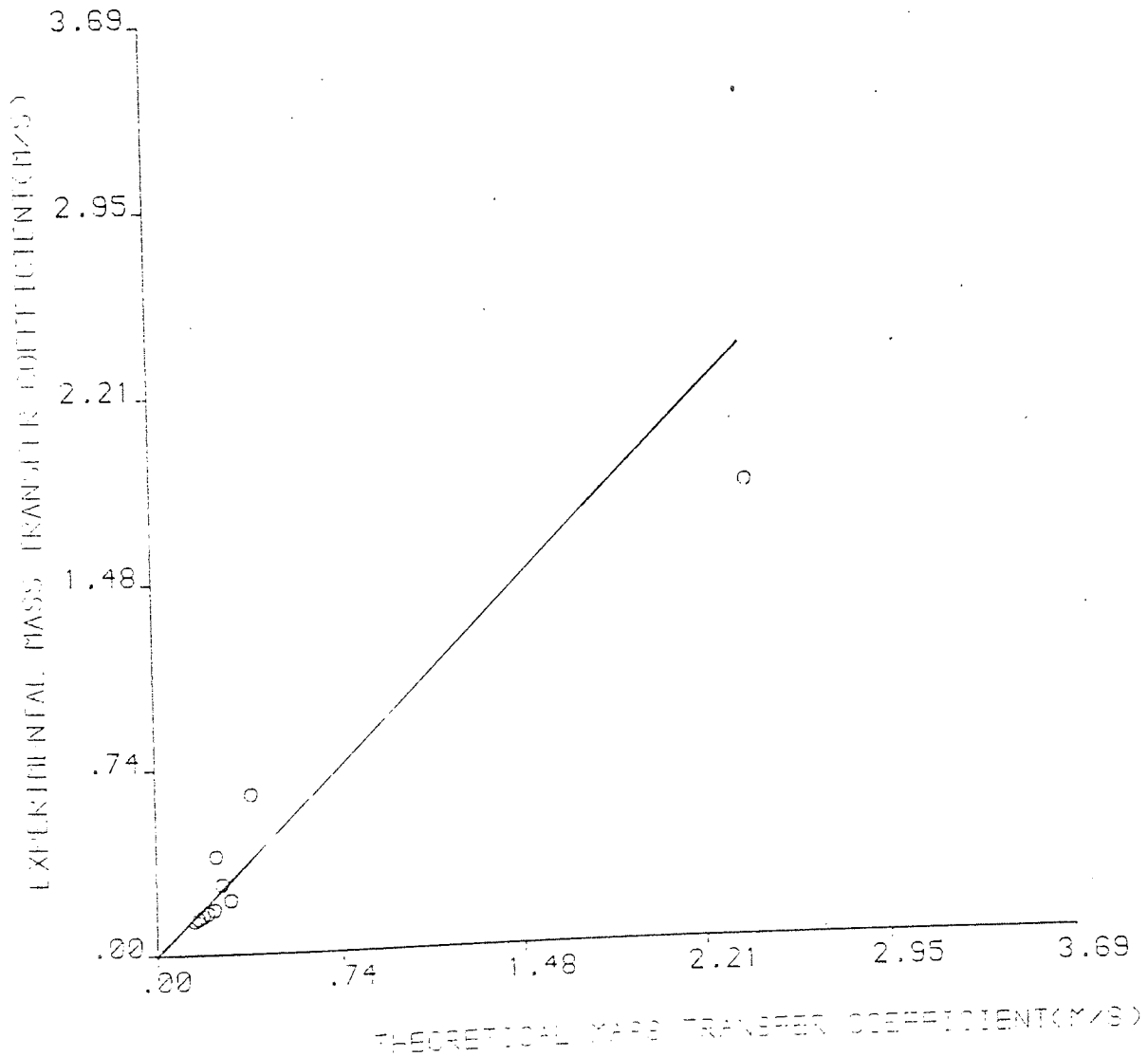

FIGURE D14

EXPERIMENTAL VERSUS THEORETICAL

MASS TRANSFER COEFFICIENT FOR

WESTBURY SLURRY SAMPLE

Moisture Content(per cent)= 45.00
Standard Deviation= .5499E -1
Correlation Coeffient= .9397

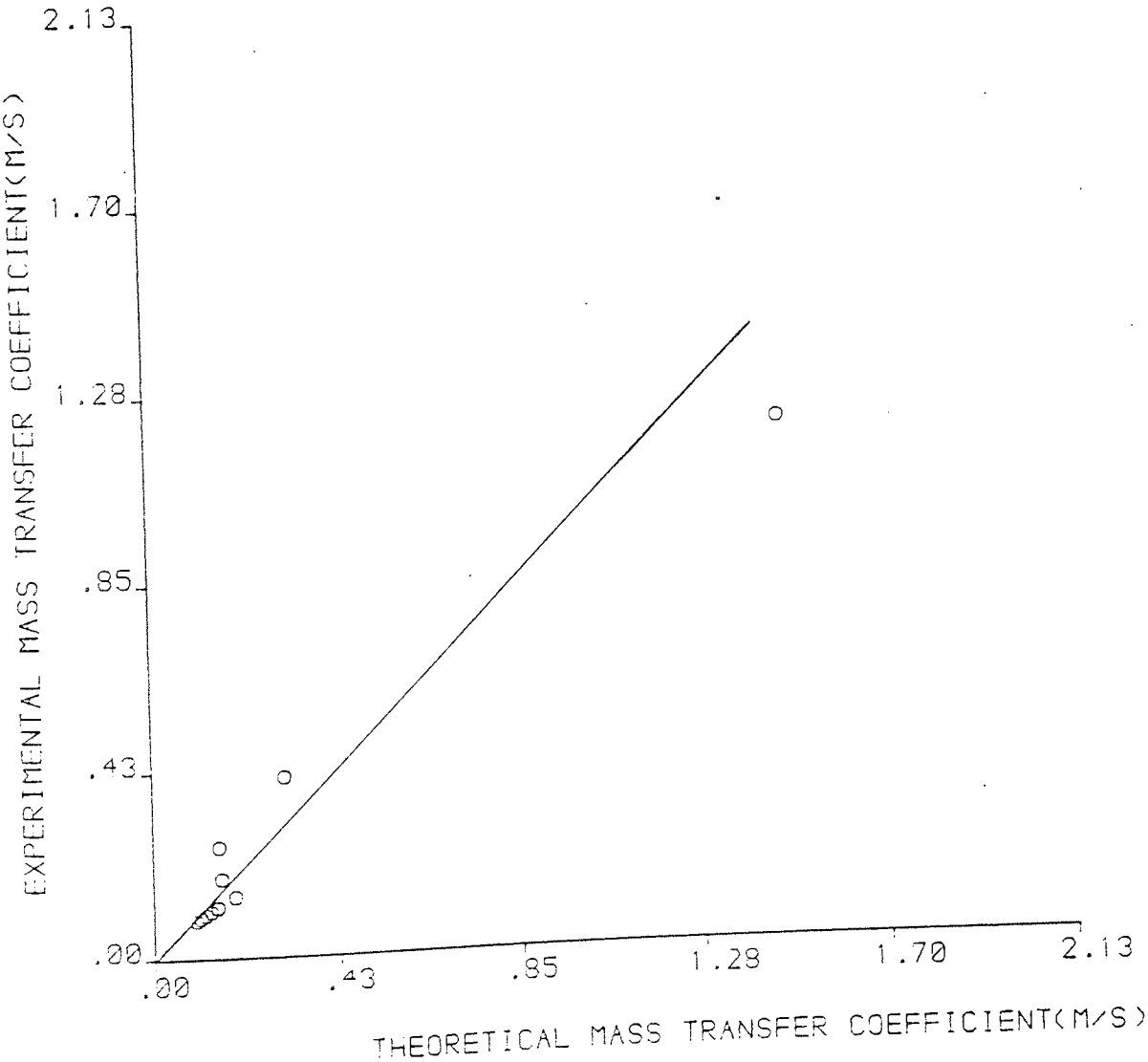

FIGURE D15

EXPERIMENTAL VERSUS THEORETICAL

MASS TRANSFER COEFFICIENT FOR

WESTBURY SLURRY SAMPLE

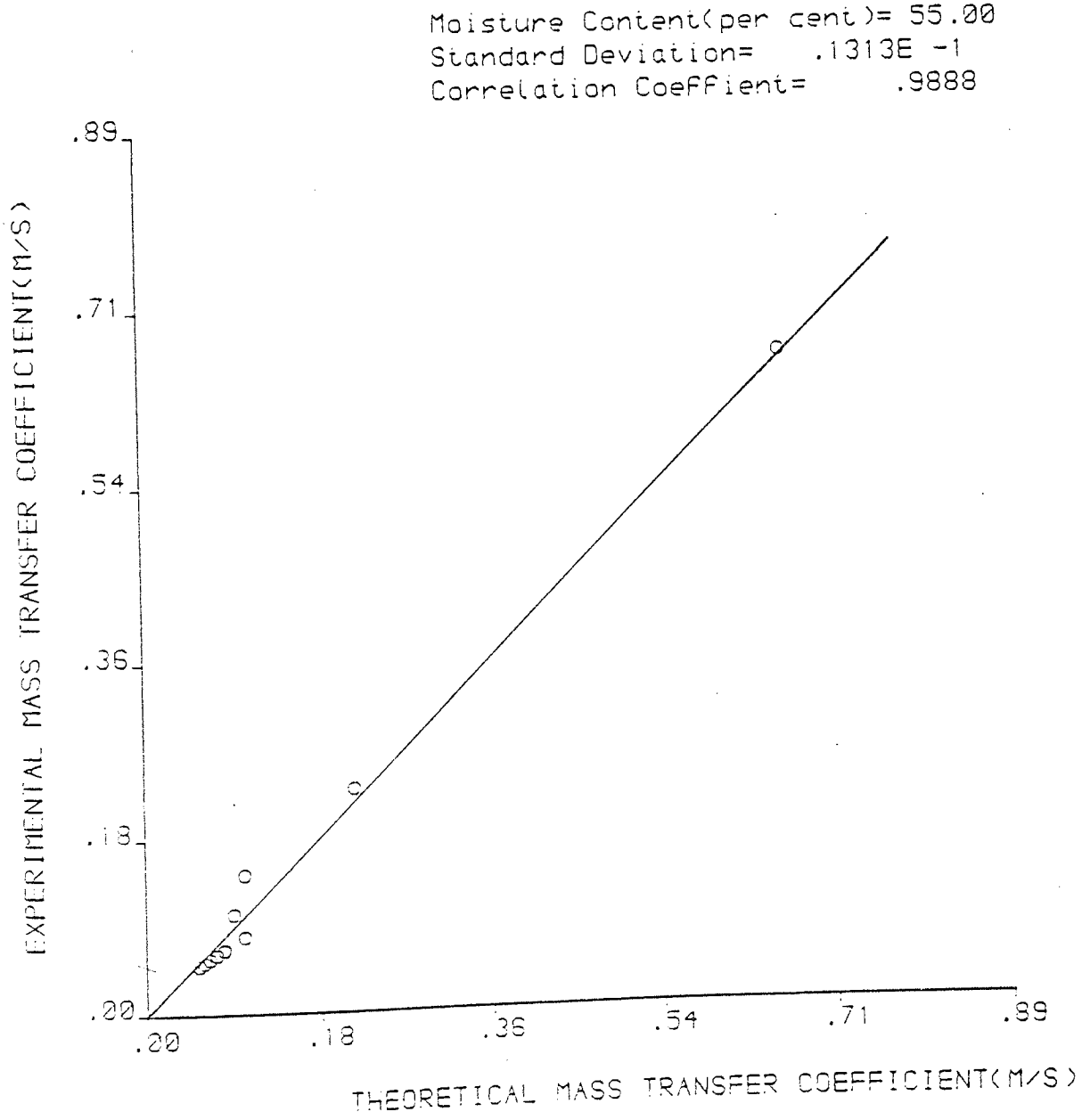

FIGURE D16

EXPERIMENTAL VERSUS THEORETICAL

MASS TRANSFER COEFFICIENT FOR

MASON SLURRY SAMPLE

Moisture Content(per cent)= 30.00
Standard Deviation= .2957E -1
Correlation Coeffient= .9700

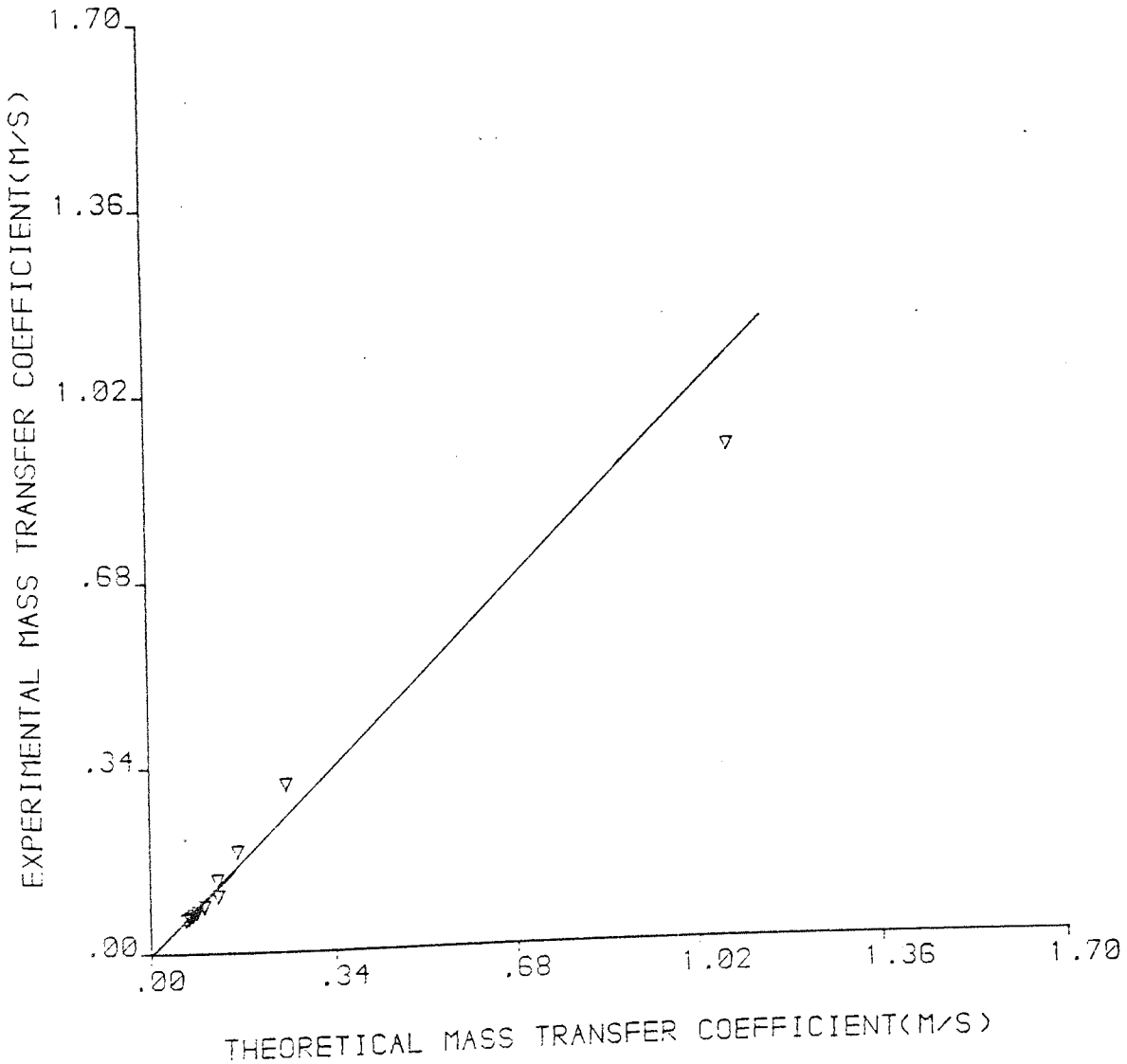

FIGURE D17

EXPERIMENTAL VERSUS THEORETICAL

MASS TRANSFER COEFFICIENT FOR

MASON SLURRY SAMPLE

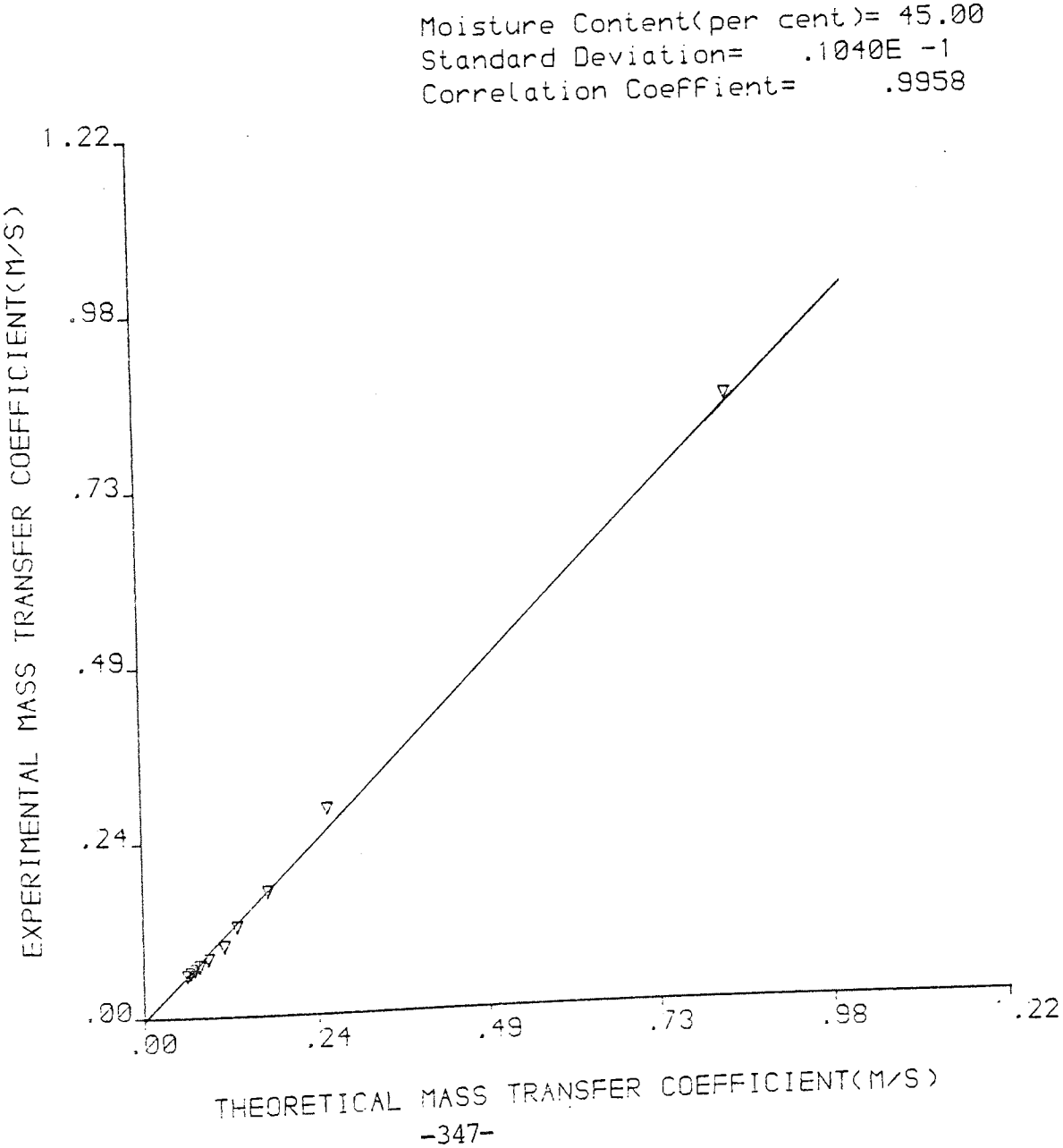

FIGURE D18

EXPERIMENTAL VERSUS THEORETICAL

MASS TRANSFER COEFFICIENT FOR

MASON SLURRY SAMPLE

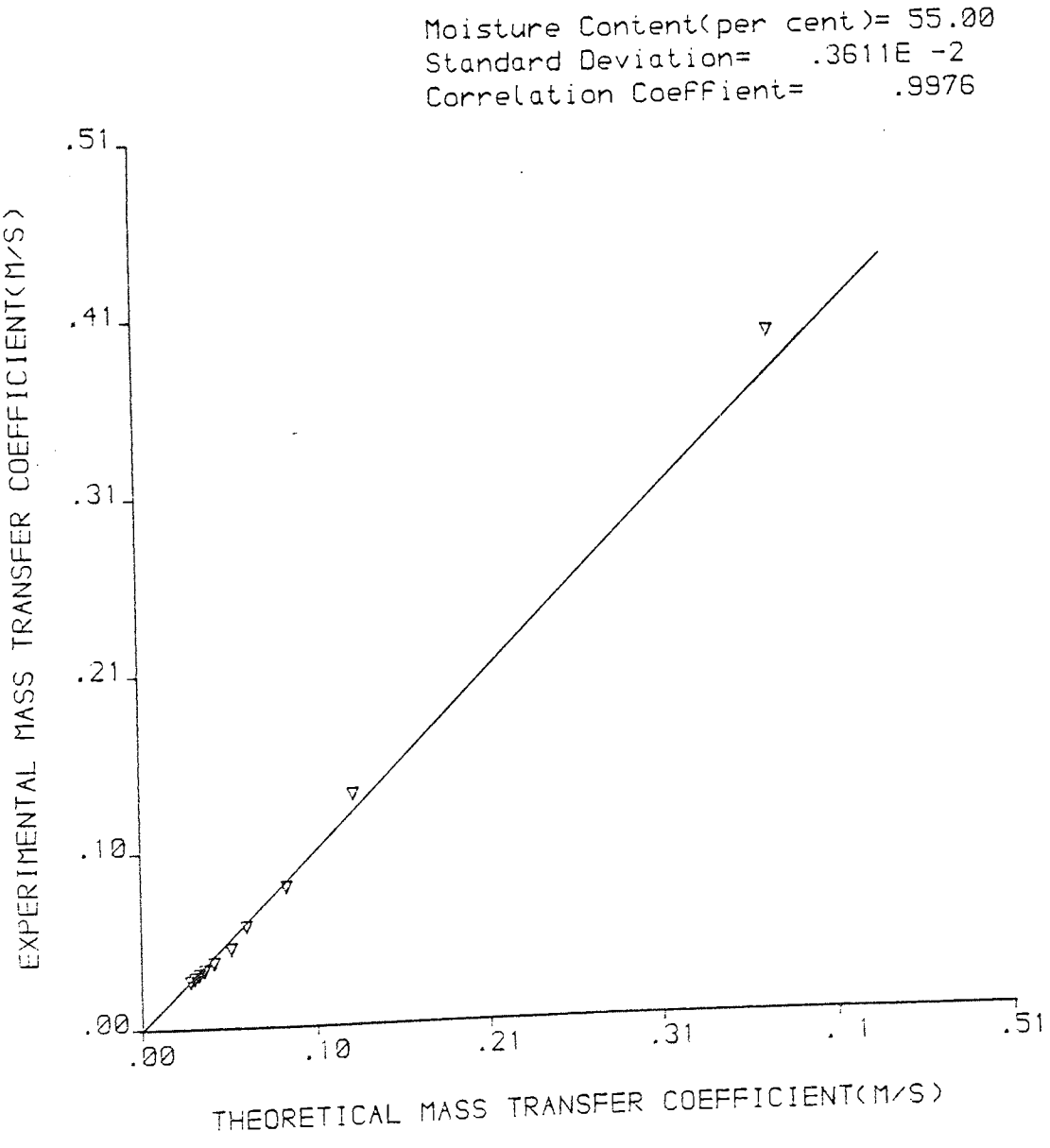

FIGURE D19

EXPERIMENTAL VERSUS THEORETICAL

MASS TRANSFER COEFFICIENT FOR

SHOREHAM SLURRY SAMPLE

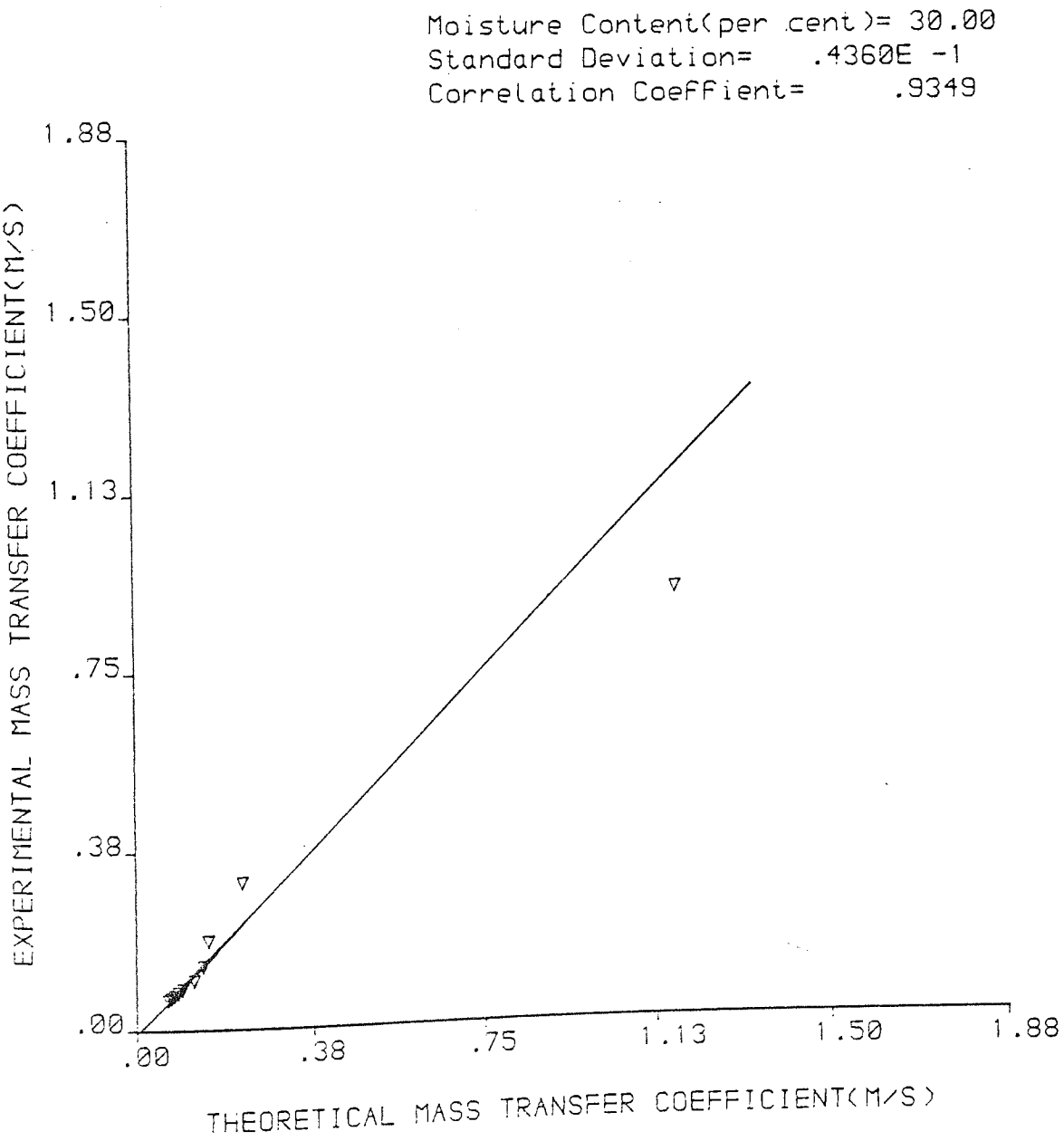

FIGURE D20

EXPERIMENTAL VERSUS THEORETICAL

MASS TRANSFER COEFFICIENT FOR

SHOREHAM SLURRY SAMPLE

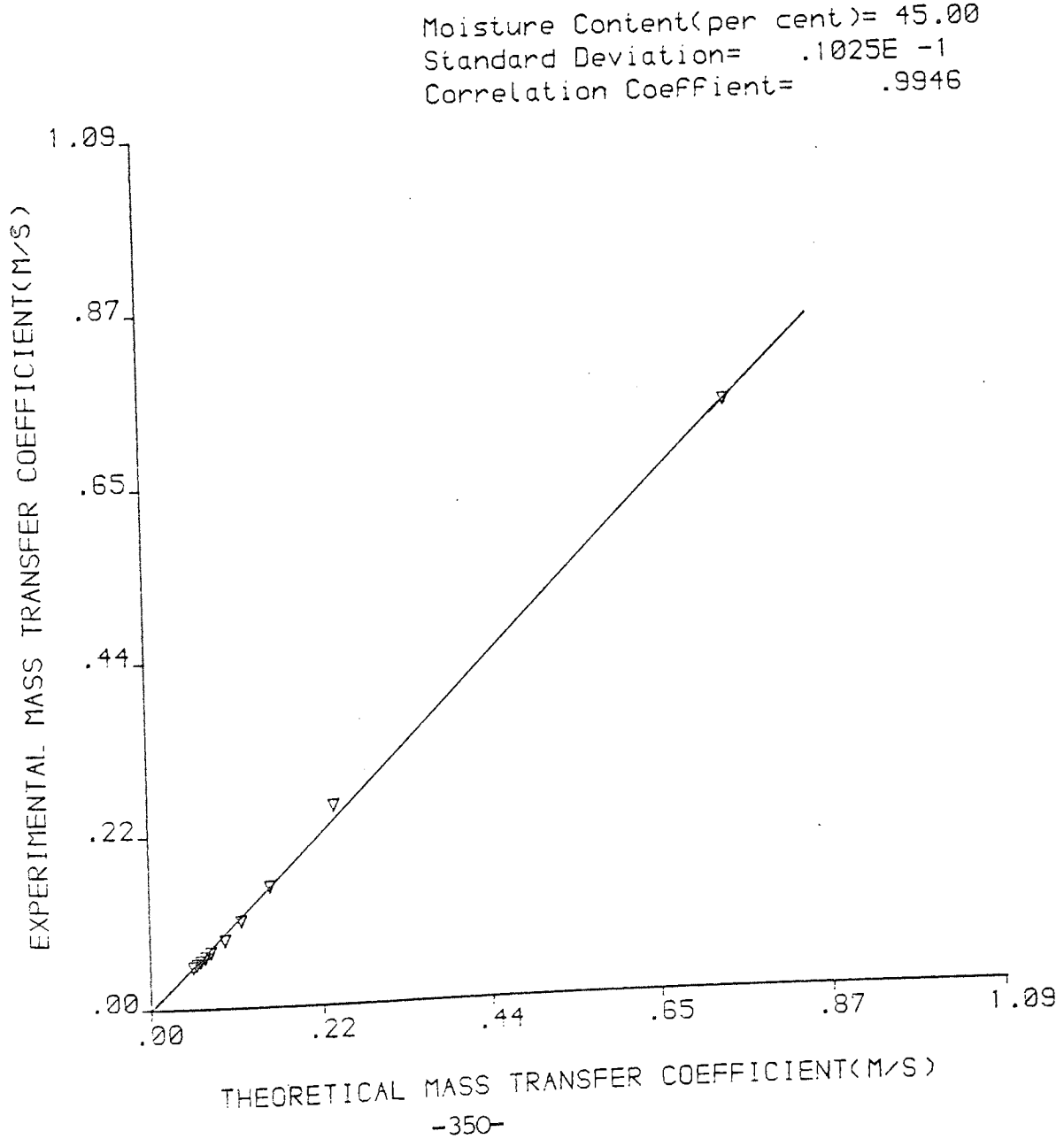

FIGURE D21

EXPERIMENTAL VERSUS THEORETICAL

MASS TRANSFER COEFFICIENT FOR

SHOREHAM SLURRY SAMPLE

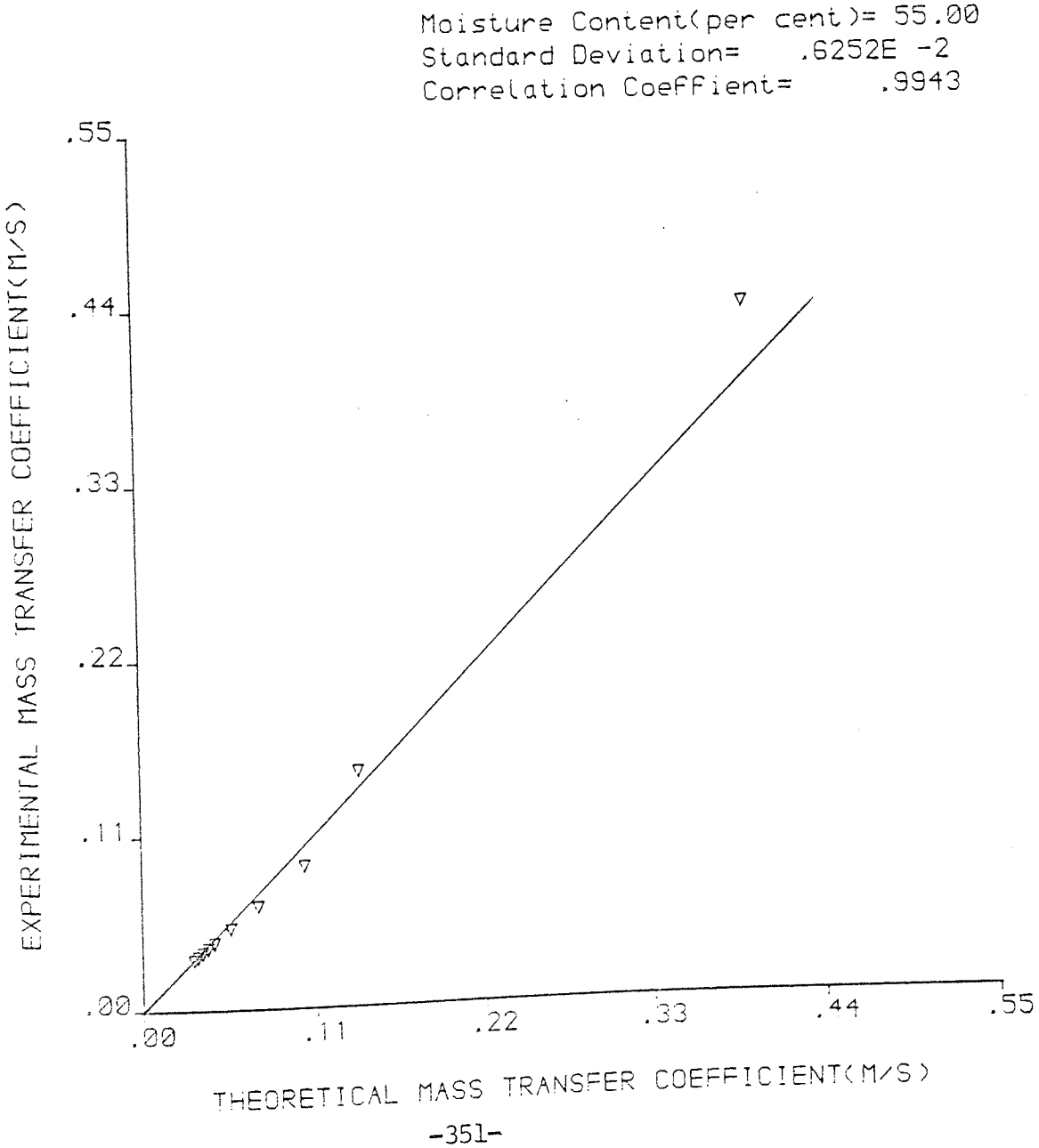

FIGURE D22

EXPERIMENTAL VERSUS THEORETICAL

MASS TRANSFER COEFFICIENT FOR

NORTHFLEET SLURRY SAMPLE

Moisture Content(per cent)= 30.00
Standard Deviation= .3798E -1
Correlation Coeffient= .9805

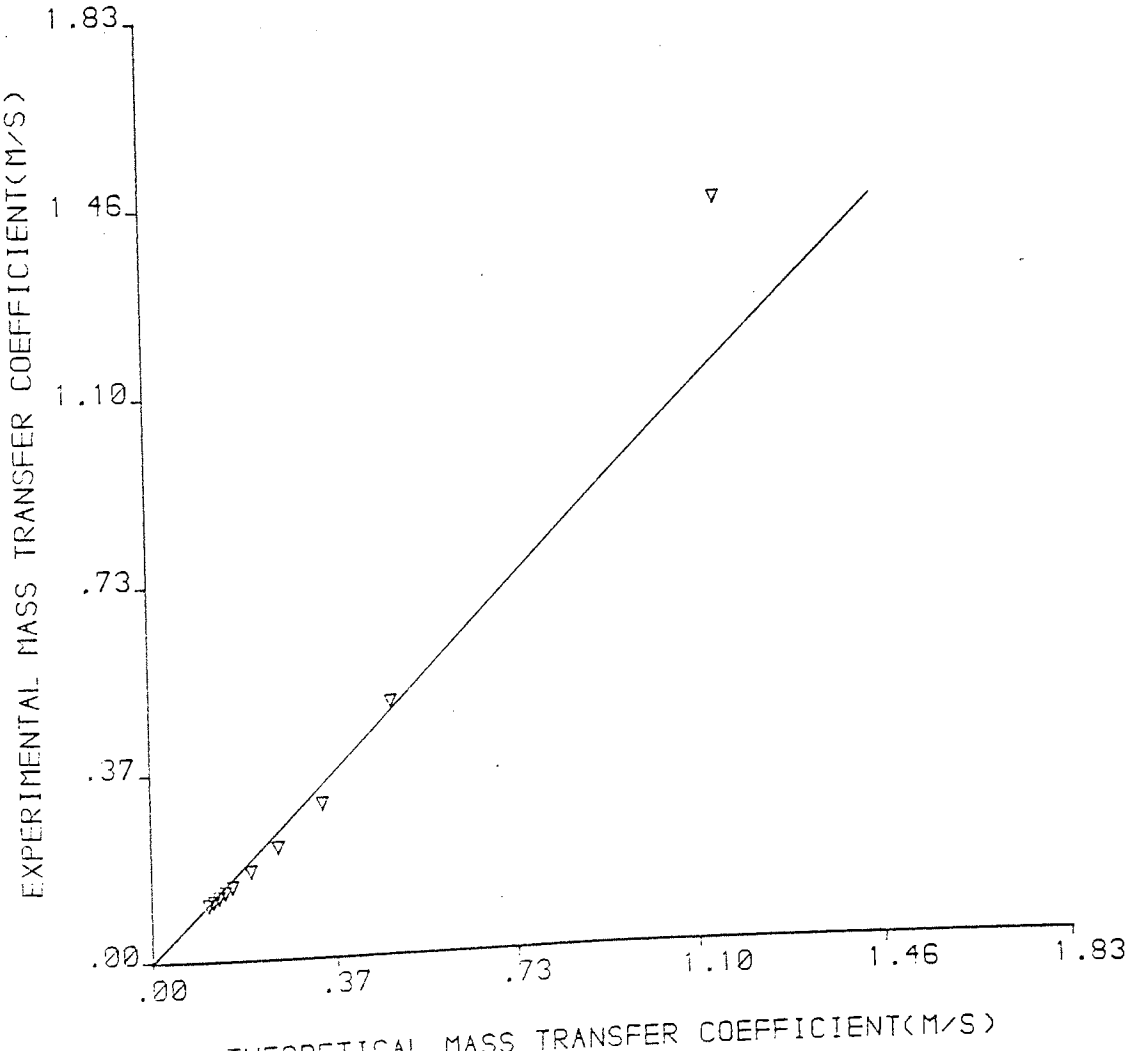

FIGURE D23

EXPERIMENTAL VERSUS THEORETICAL MASS TRANSFER COEFFICIENT FOR NORTHFLEET SLURRY SAMPLE

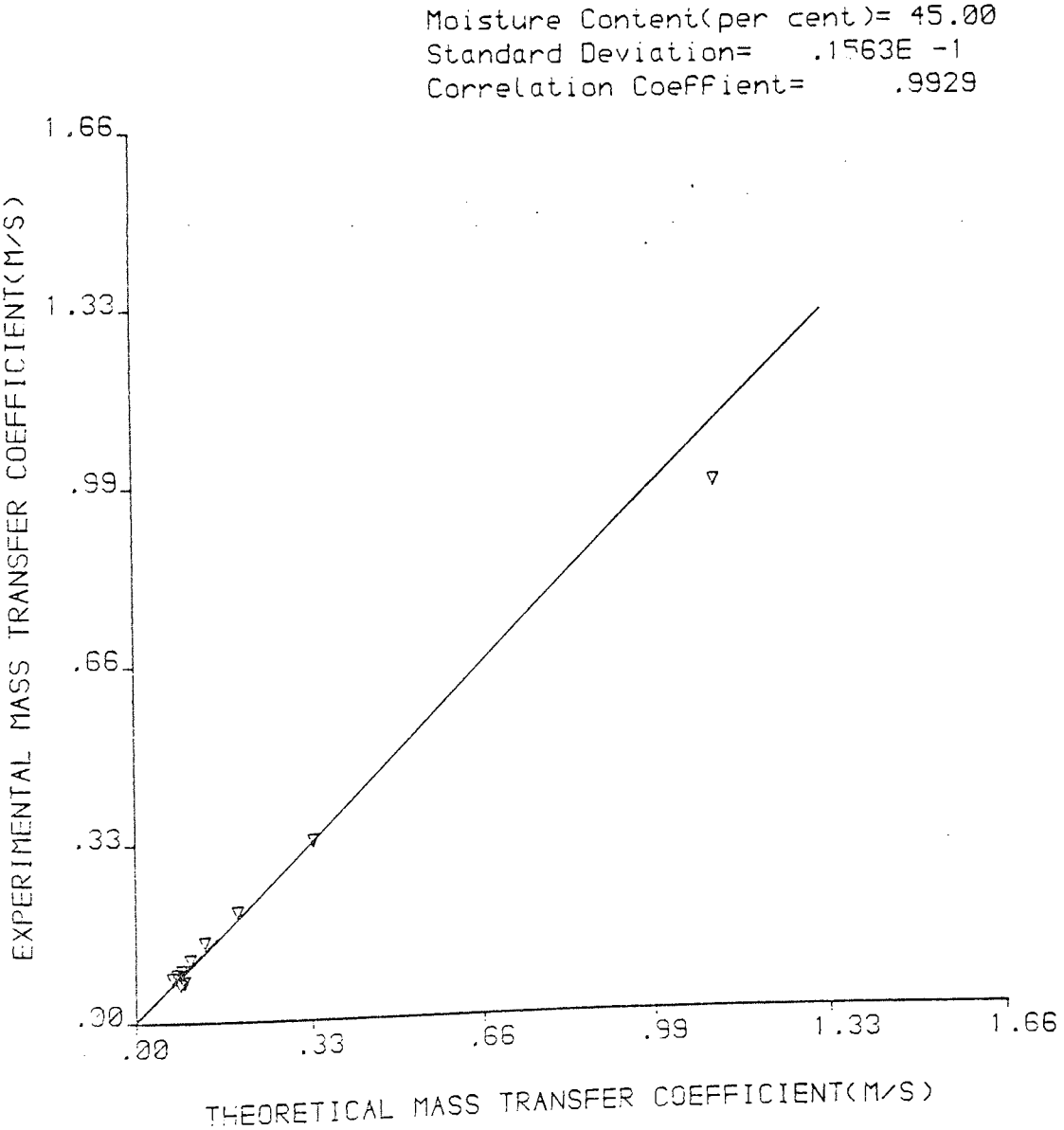

FIGURE D24

EXPERIMENTAL VERSUS THEORETICAL

MASS TRANSFER COEFFICIENT FOR

NORTHFLEET SLURRY SAMPLE

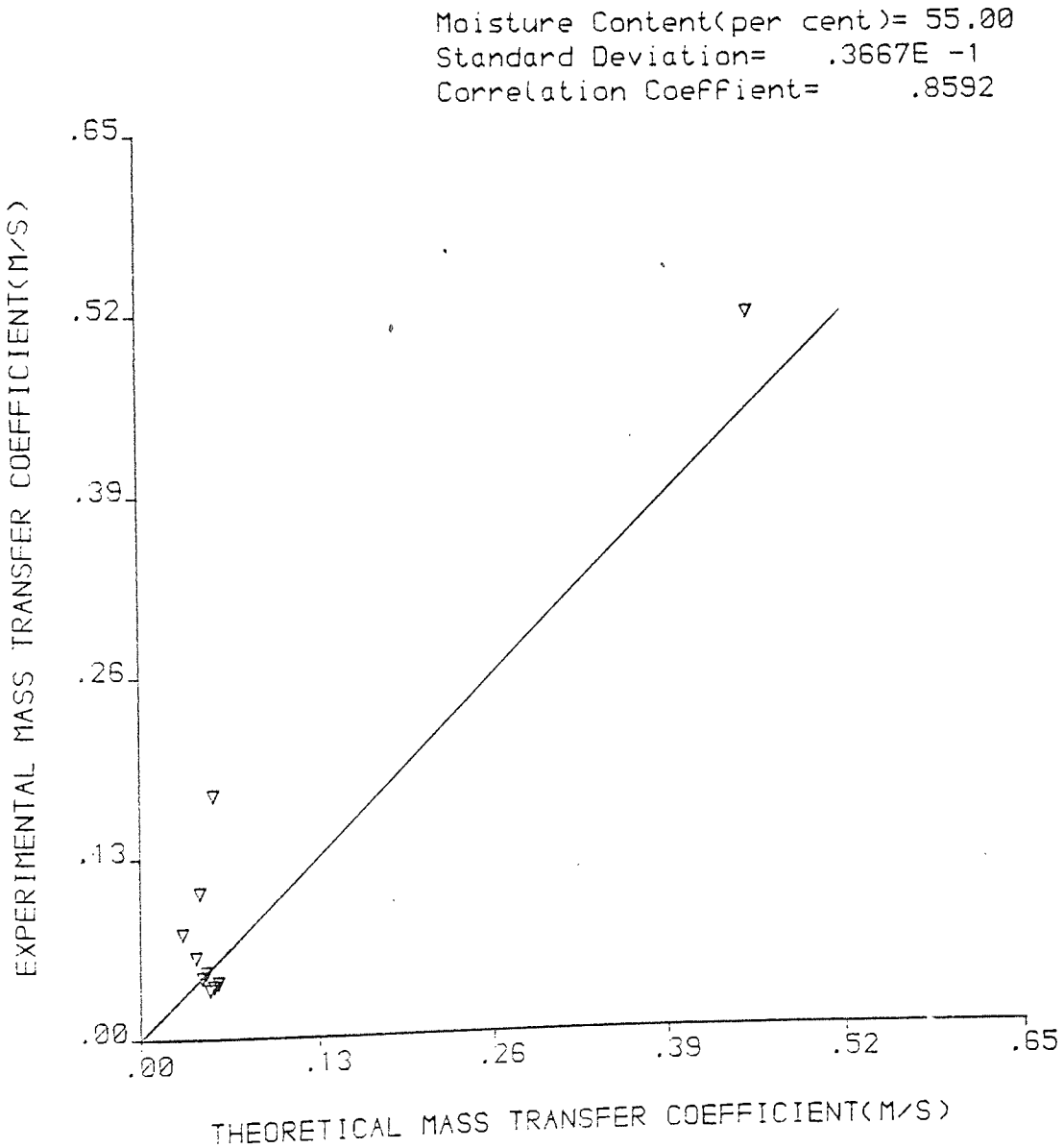

FIGURE D25

EXPERIMENTAL VERSUS THEORETICAL

MASS TRANSFER COEFFICIENT FOR

HUMBER SLURRY SAMPLE

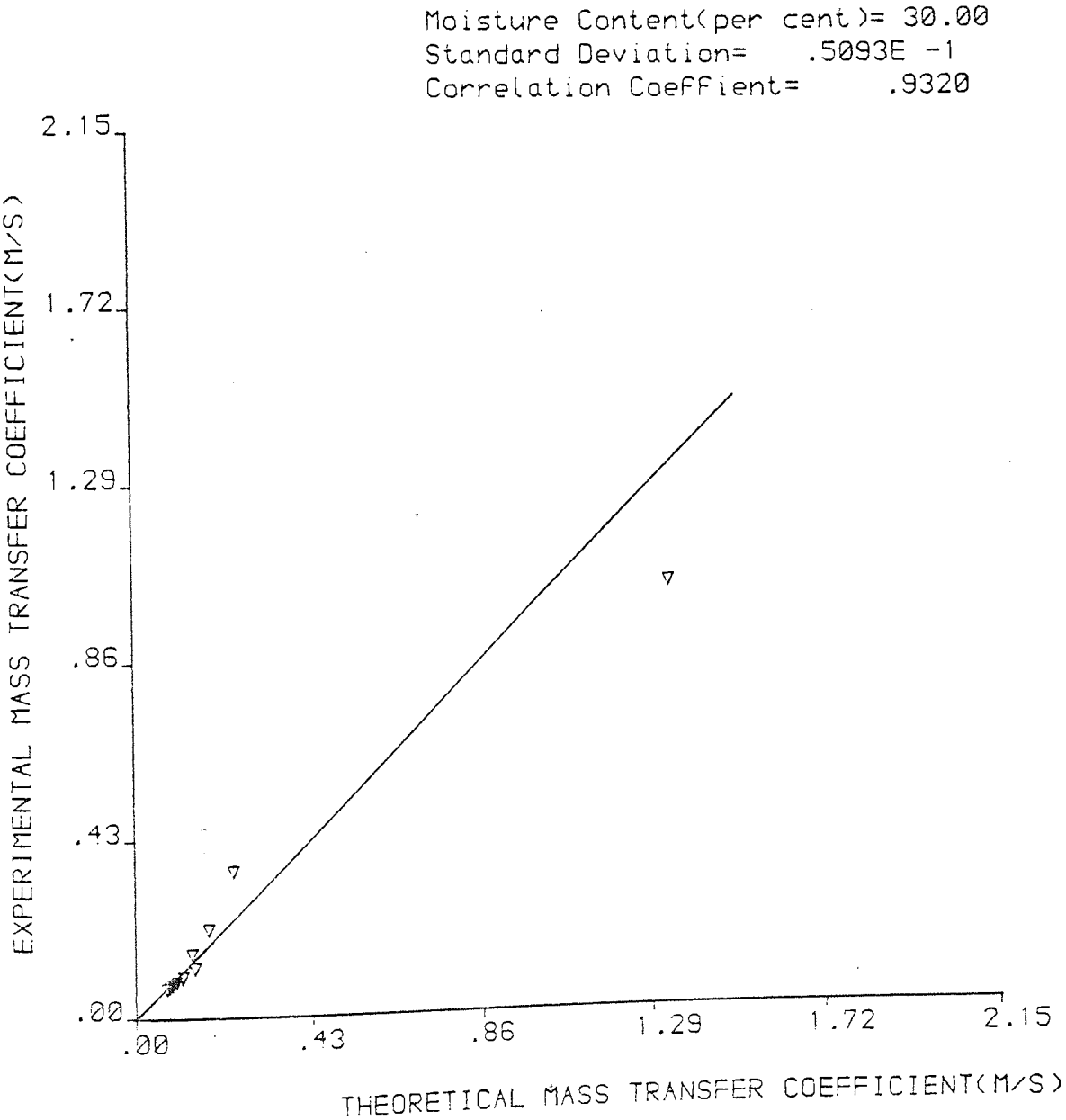

FIGURE D26

EXPERIMENTAL VERSUS THEORETICAL

MASS TRANSFER COEFFICIENT FOR

HUMBER SLURRY SAMPLE

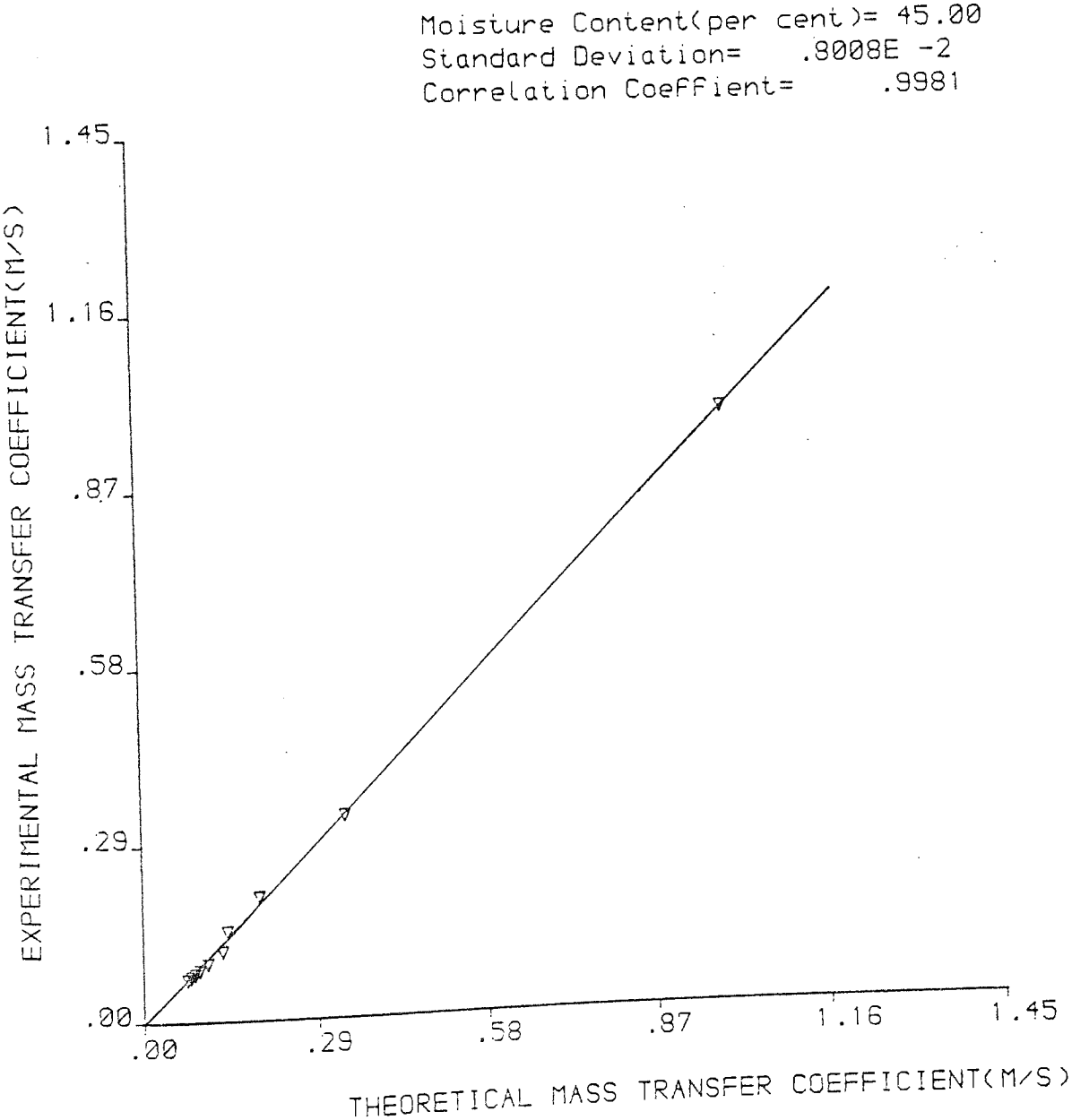

FIGURE D27

EXPERIMENTAL VERSUS THEORETICAL

MASS TRANSFER COEFFICIENT FOR

HUMBER SLURRY SAMPLE

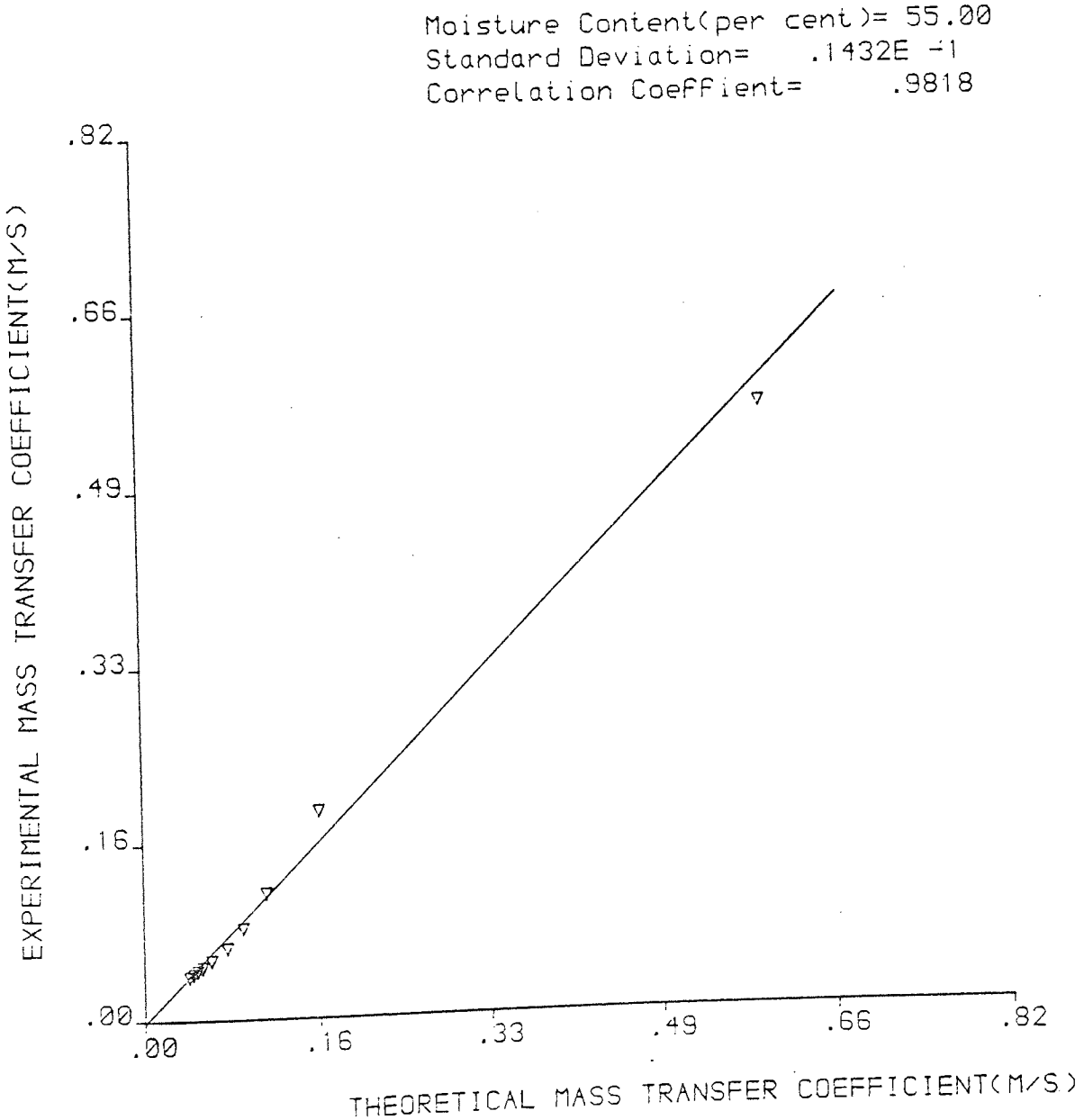

FIGURE D28

EXPERIMENTAL VERSUS THEORETICAL

MASS TRANSFER COEFFICIENT FOR

WESTBURY SLURRY SAMPLE

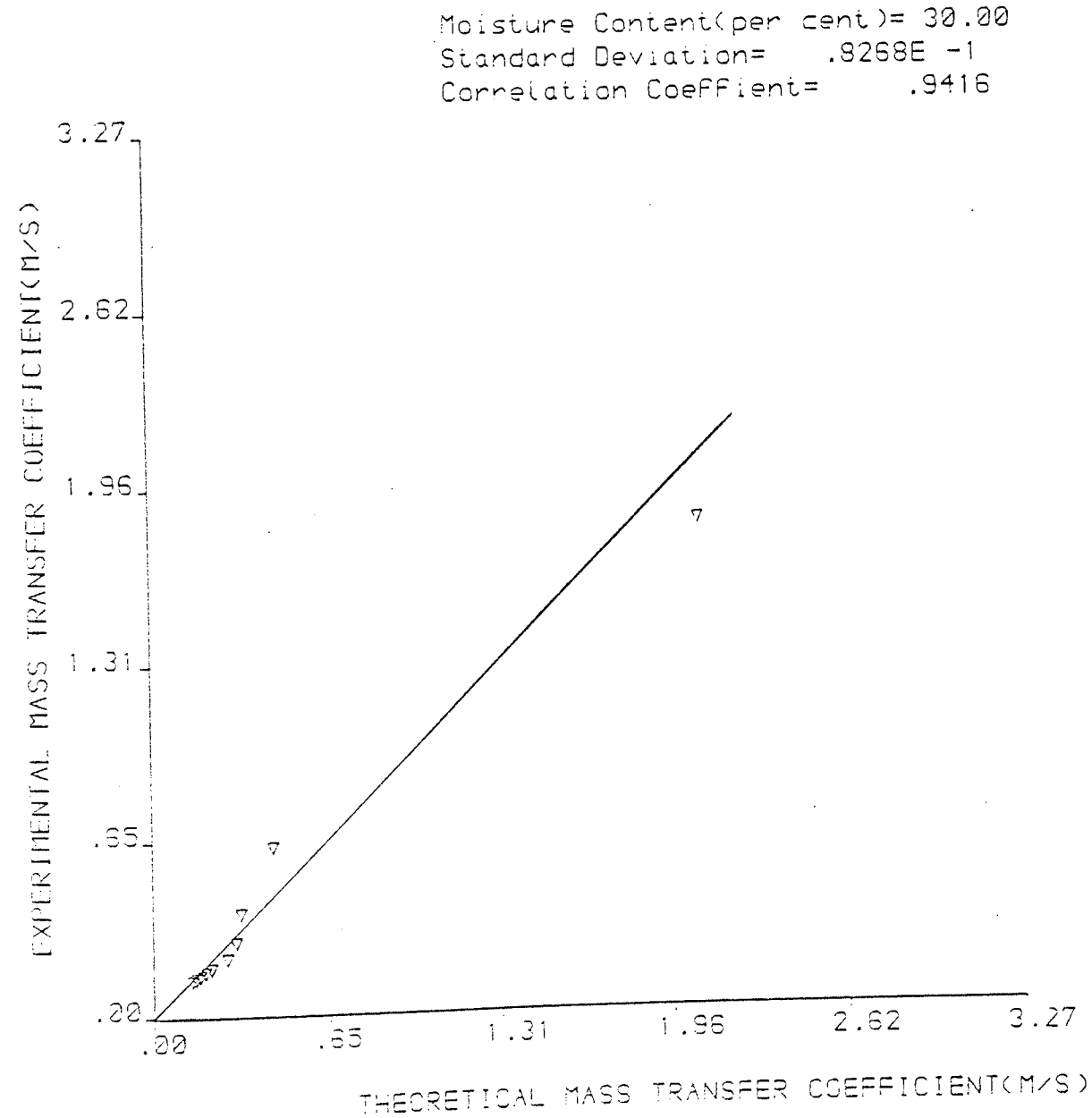

FIGURE D29

EXPERIMENTAL VERSUS THEORETICAL

MASS TRANSFER COEFFICIENT FOR

WESTBURY SLURRY SAMPLE

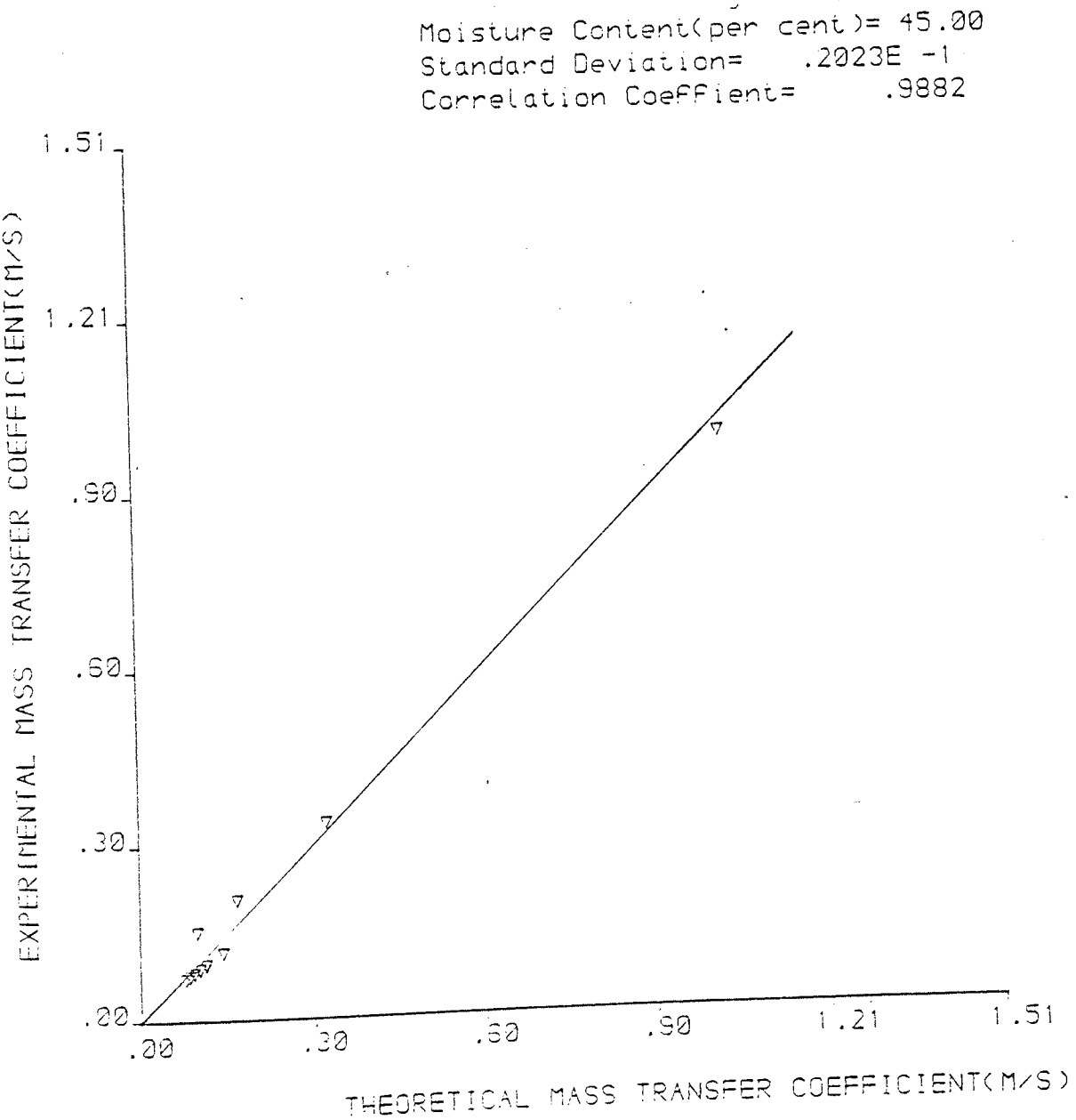

FIGURE D30

EXPERIMENTAL VERSUS THEORETICAL

MASS TRANSFER COEFFICIENT FOR

WESTBURY SLURRY SAMPLE

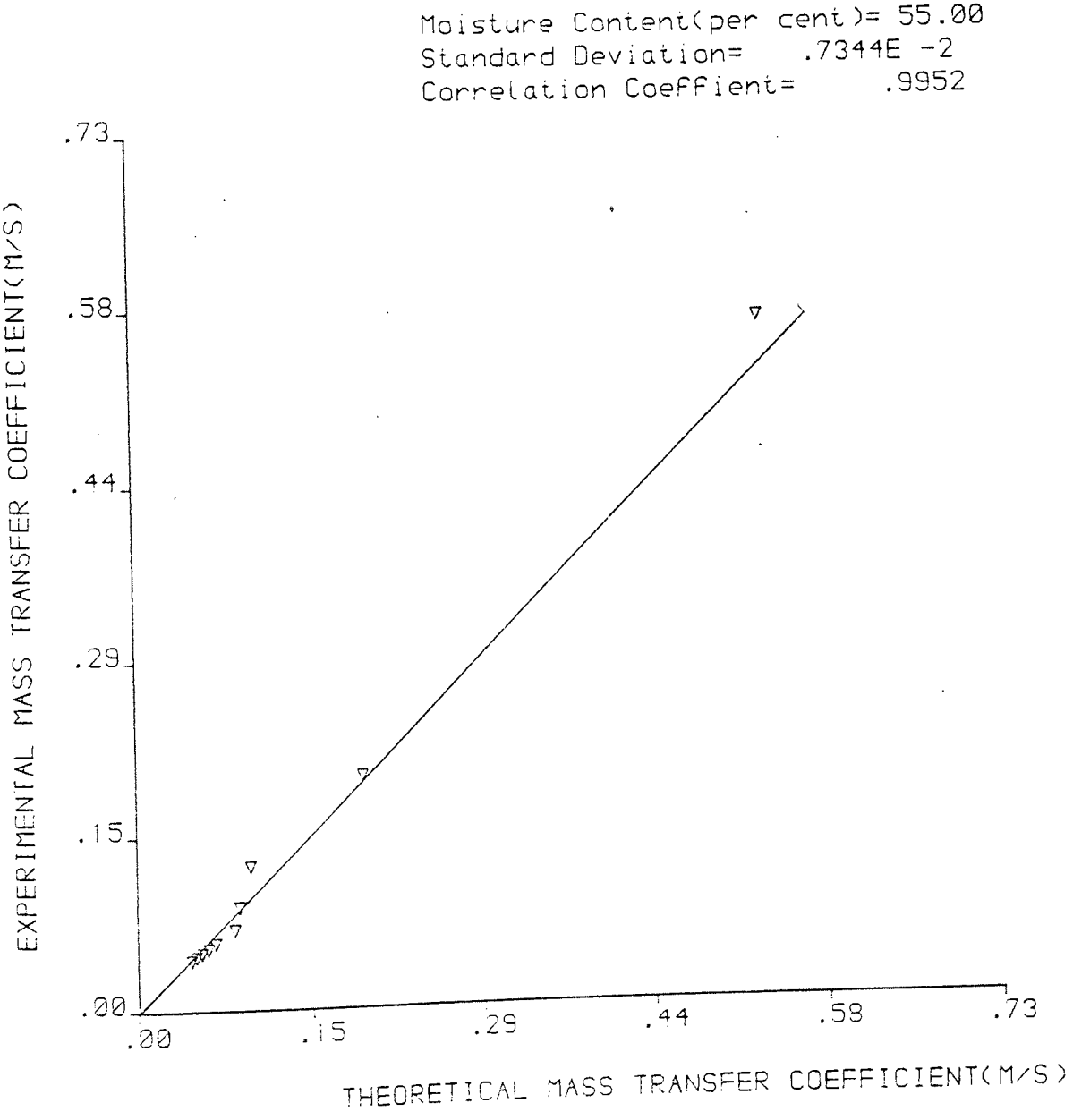

FIGURE D31

EXPERIMENTAL VERSUS THEORETICAL

MASS TRANSFER COEFFICIENT FOR

HUMBER SLURRY SAMPLE

Moisture Content(per cent)= 30.00
Standard Deviation= .1748E -1
Correlation Coeffient= .9941

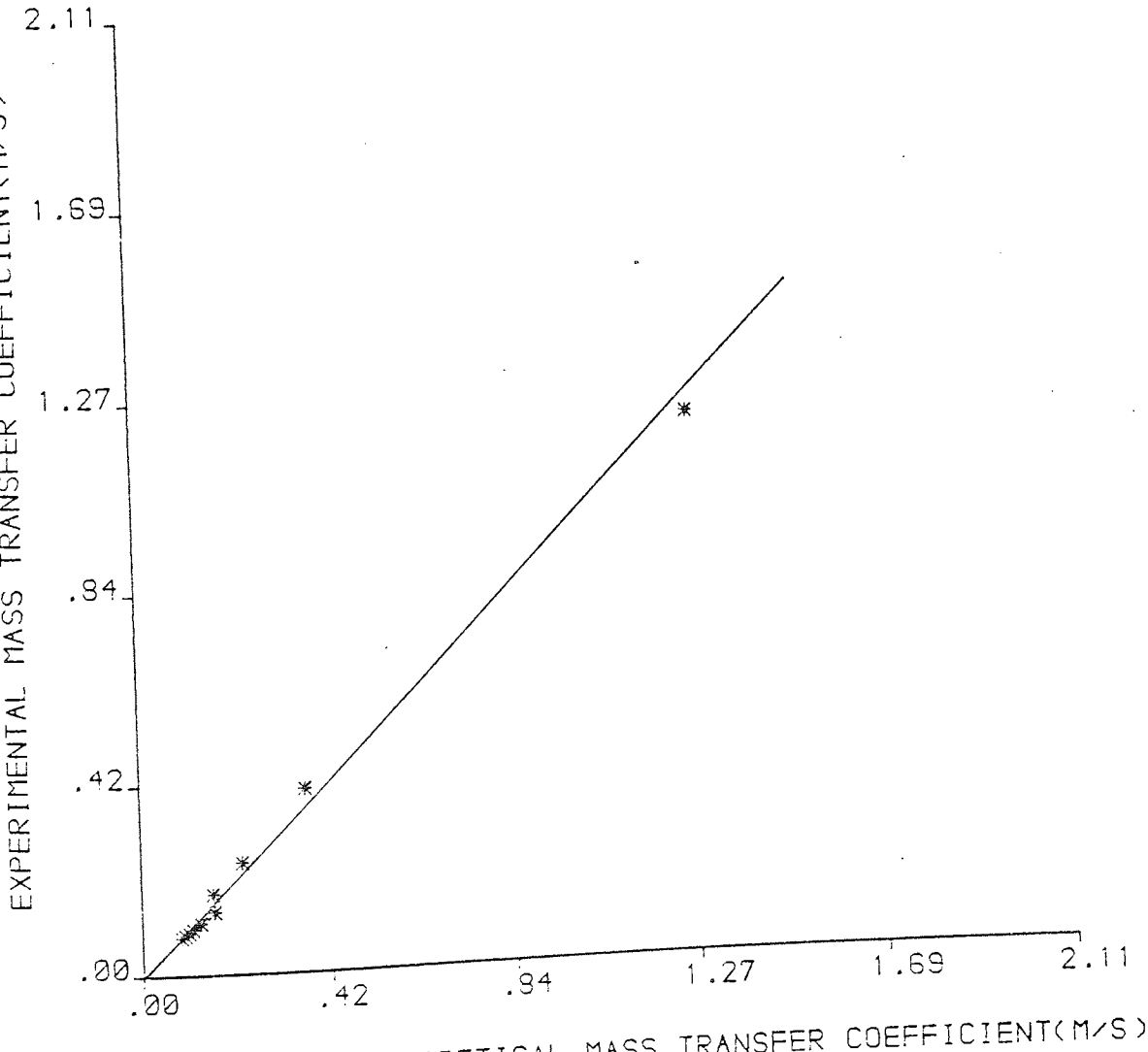

FIGURE D32

EXPERIMENTAL VERSUS THEORETICAL

MASS TRANSFER COEFFICIENT FOR

HUMBER SLURRY SAMPLE

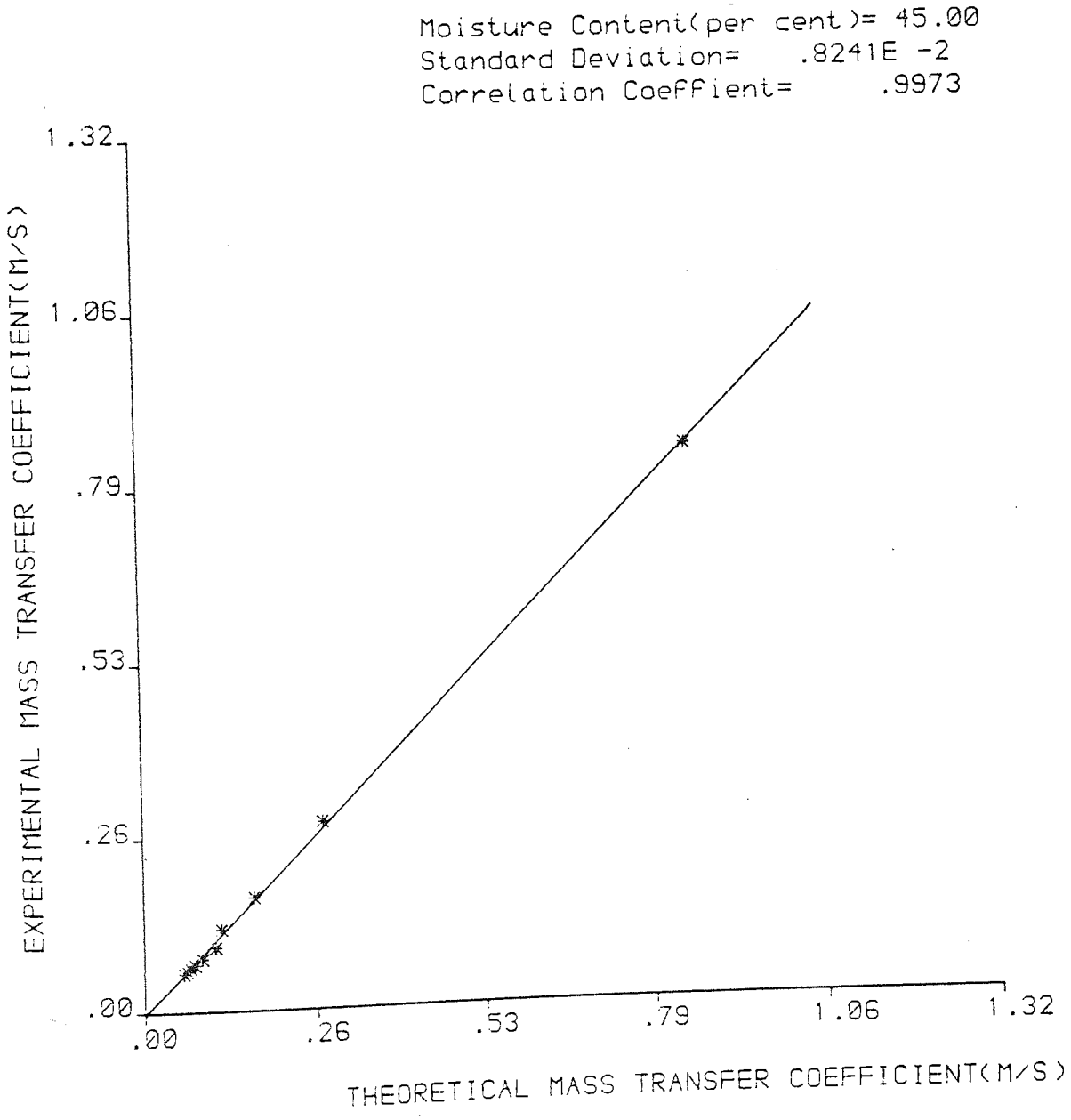

FIGURE D33

EXPERIMENTAL VERSUS THEORETICAL

MASS TRANSFER COEFFICIENT FOR

HUMBER SLURRY SAMPLE

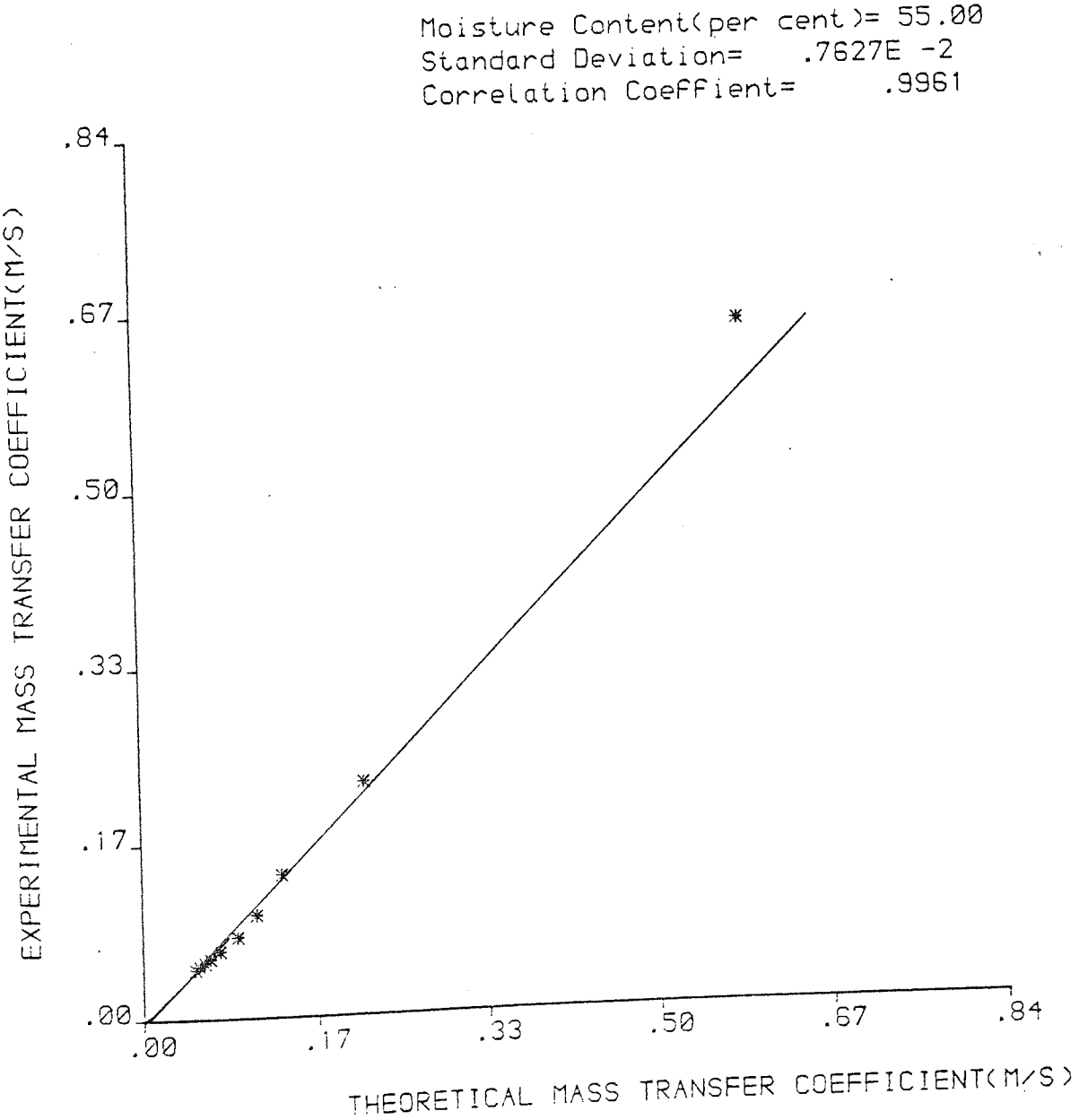

FIGURE D34

EXPERIMENTAL VERSUS THEORETICAL

MASS TRANSFER COEFFICIENT FOR

MASON SLURRY SAMPLE

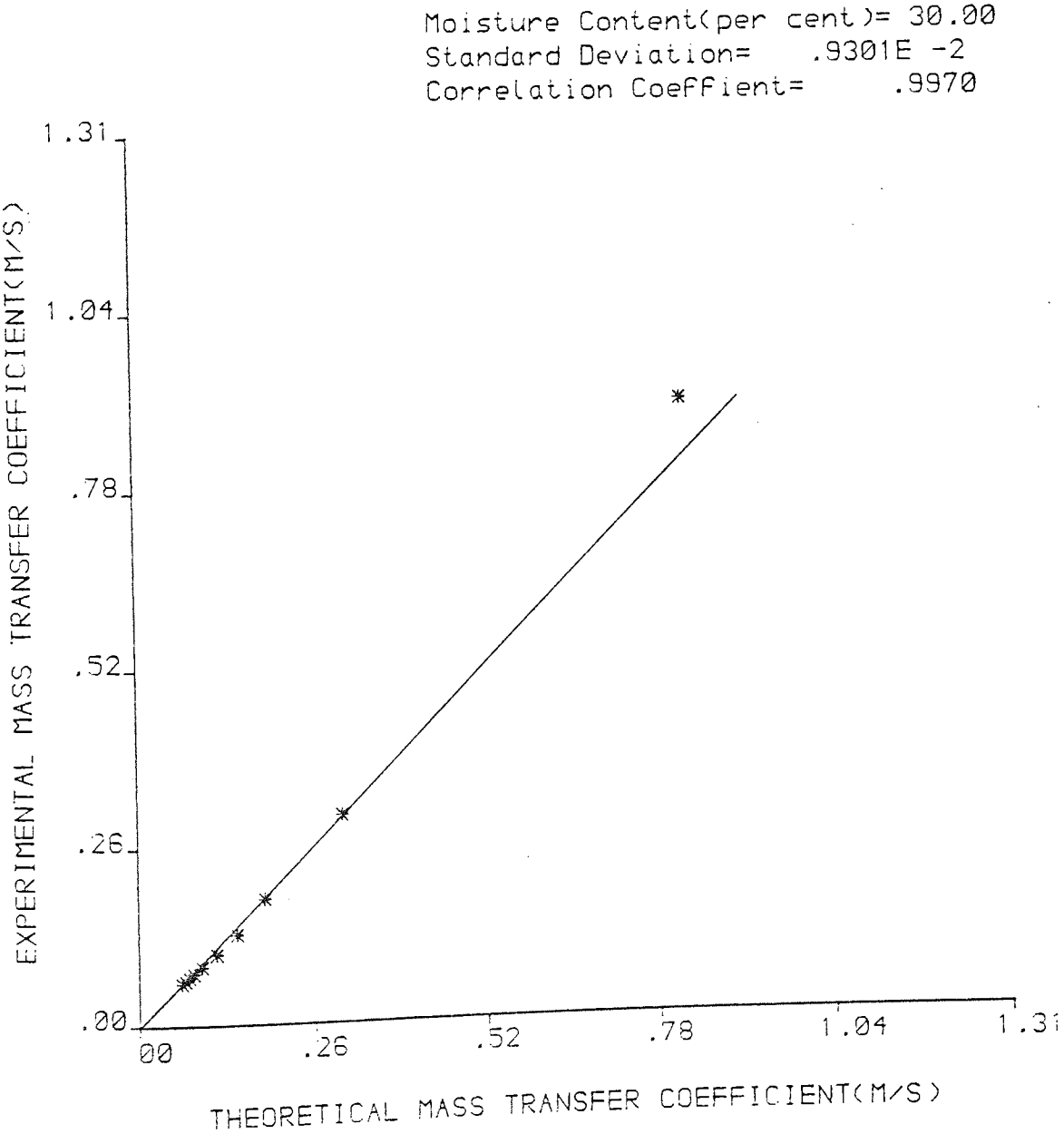

FIGURE D35

EXPERIMENTAL VERSUS THEORETICAL

MASS TRANSFER COEFFICIENT FOR

MASON SLURRY SAMPLE

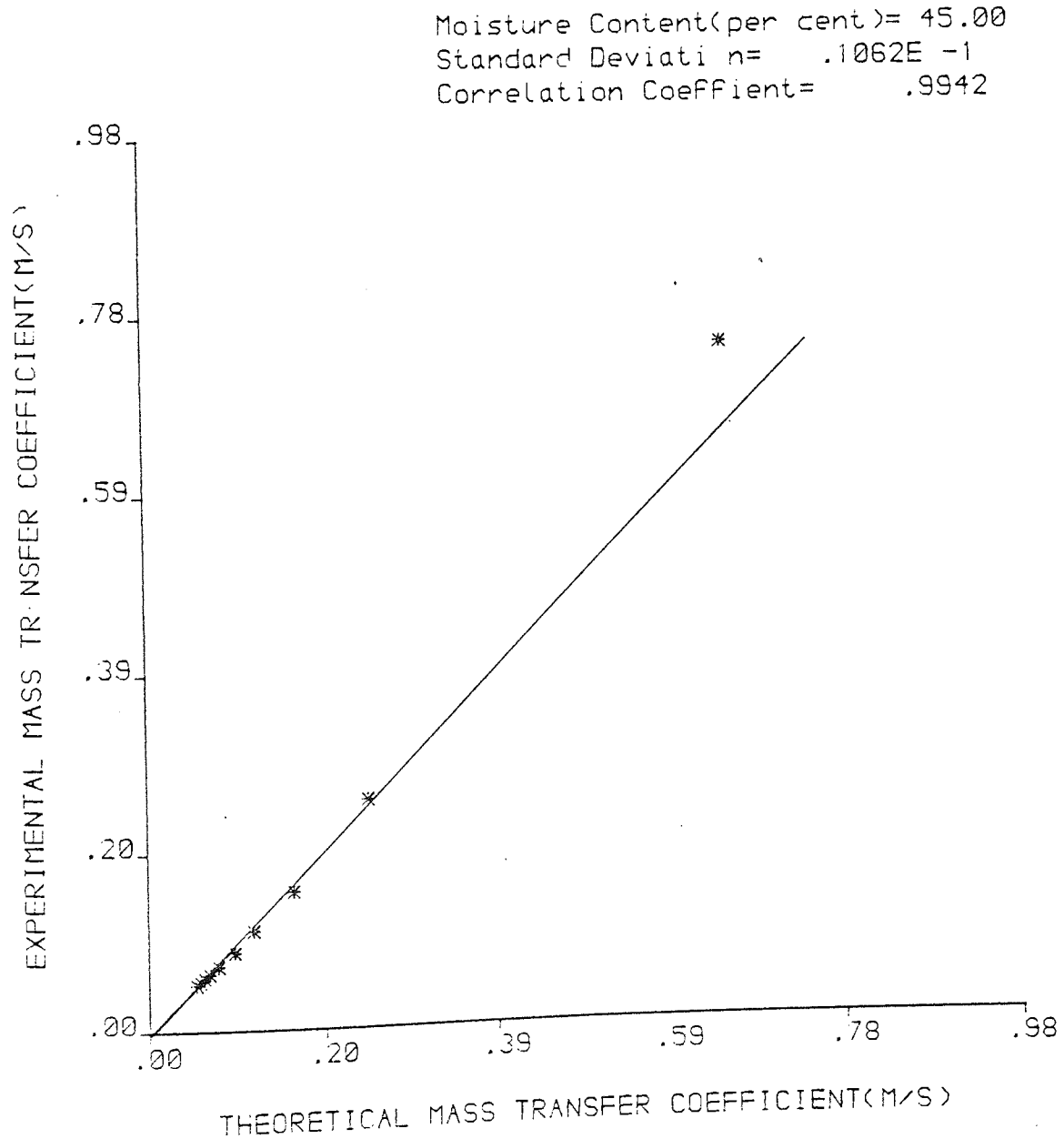

FIGURE D36

EXPERIMENTAL VERSUS THEORETICAL

MASS TRANSFER COEFFICIENT FOR

MASON SLURRY SAMPLE

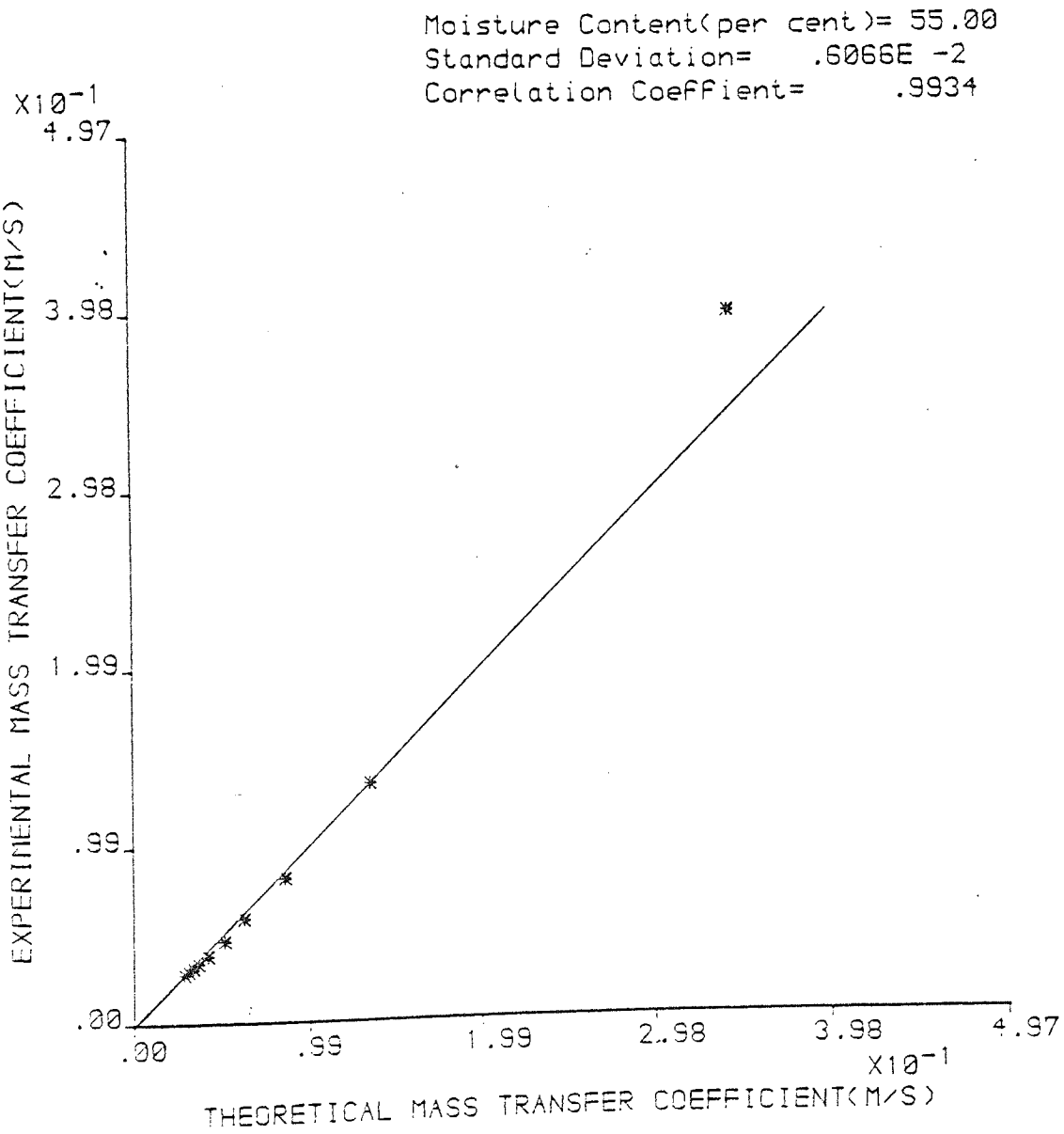

FIGURE D37

EXPERIMENTAL VERSUS THEORETICAL

MASS TRANSFER COEFFICIENT FOR

NORTHFLEET SLURRY SAMPLE

Moisture Content(per cent)= 30.00
Standard Deviation= .2407E -1
Correlation Coeffient= .9887

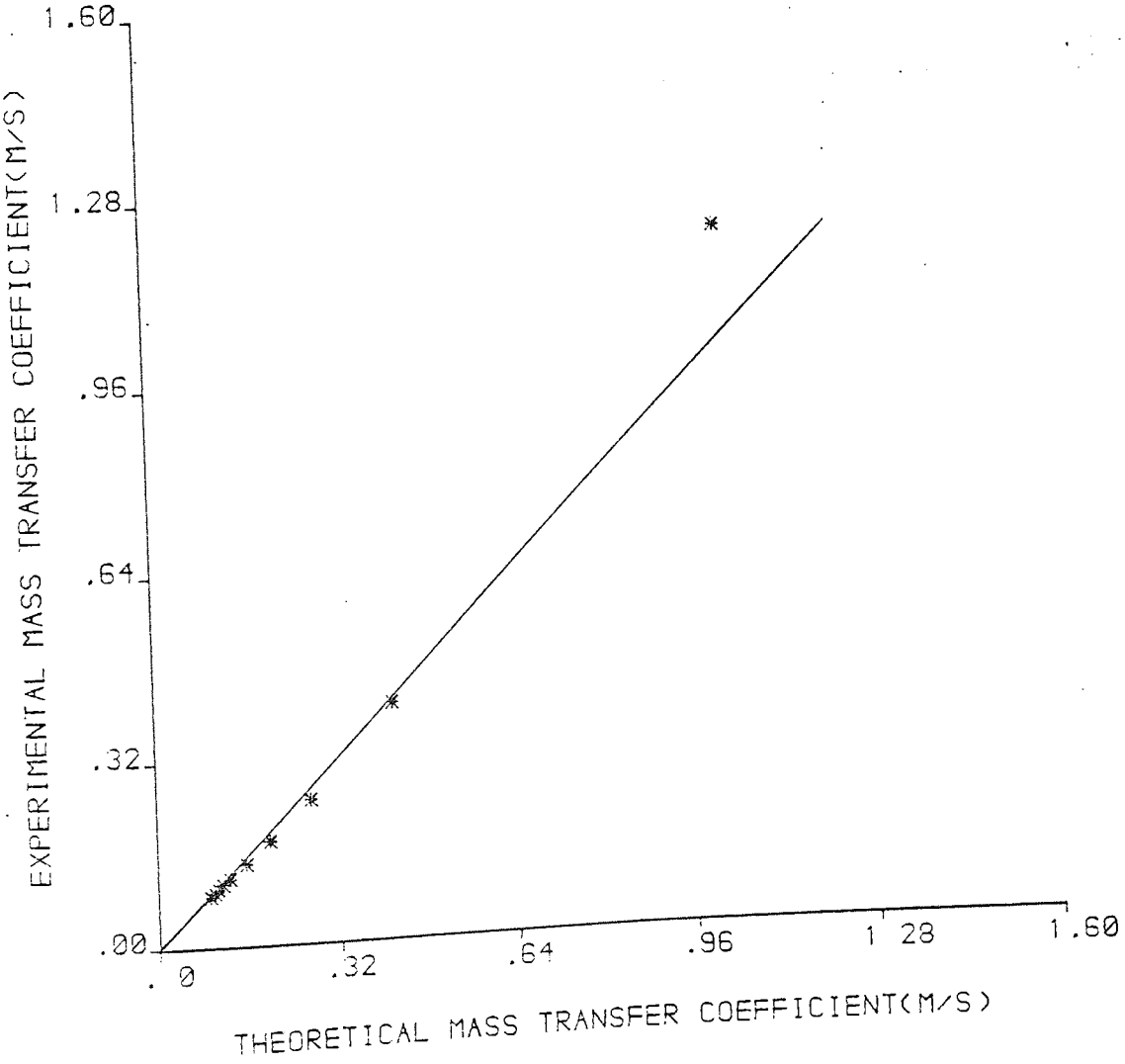

FIGURE D38

EXPERIMENTAL VERSUS THEORETICAL

MASS TRANSFER COEFFICIENT FOR

NORTHFLEET SLURRY SAMPLE

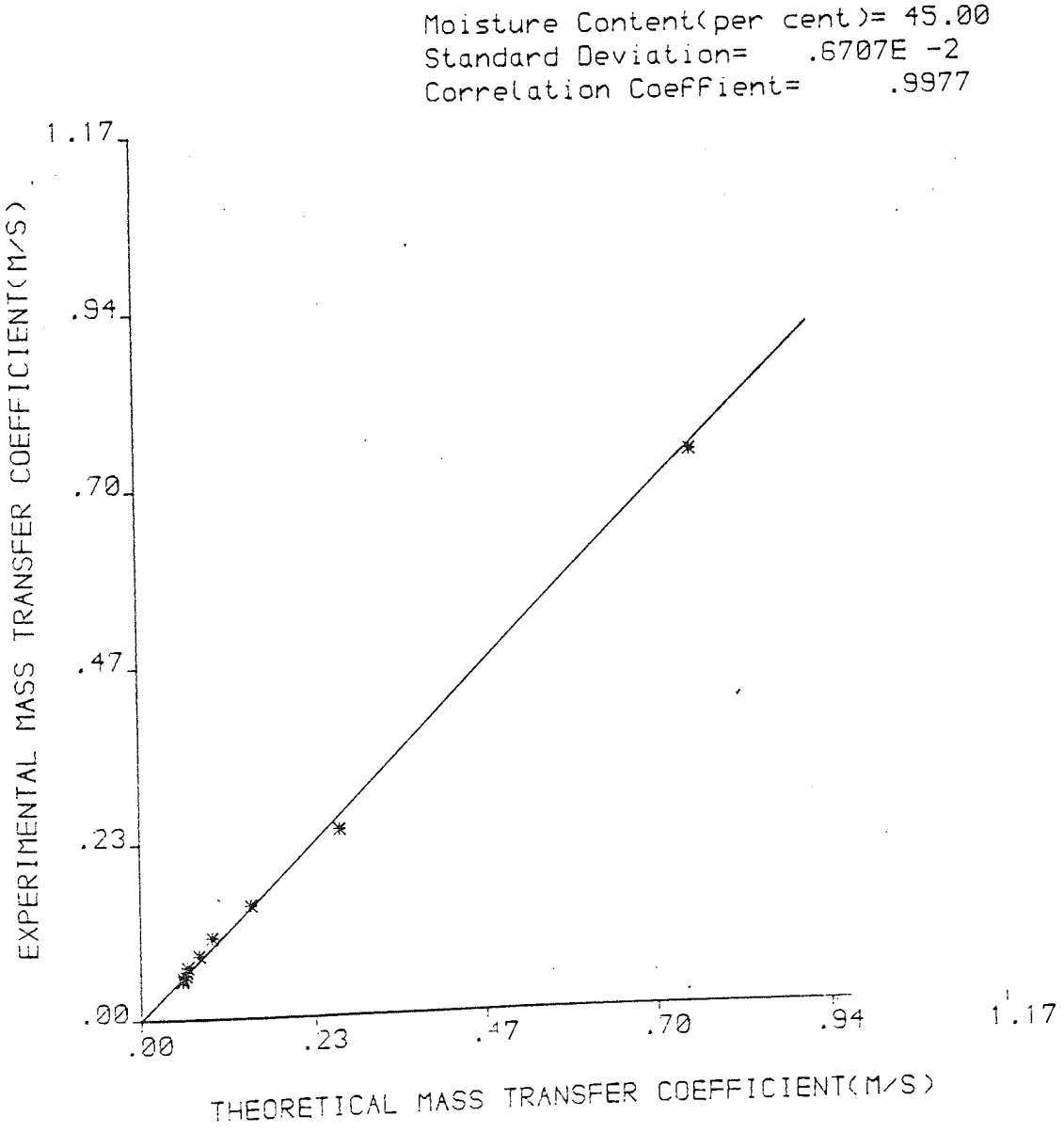

FIGURE D39

EXPERIMENTAL VERSUS THEORETICAL

MASS TRANSFER COEFFICIENT FOR

NORTHFLEET SLURRY SAMPLE

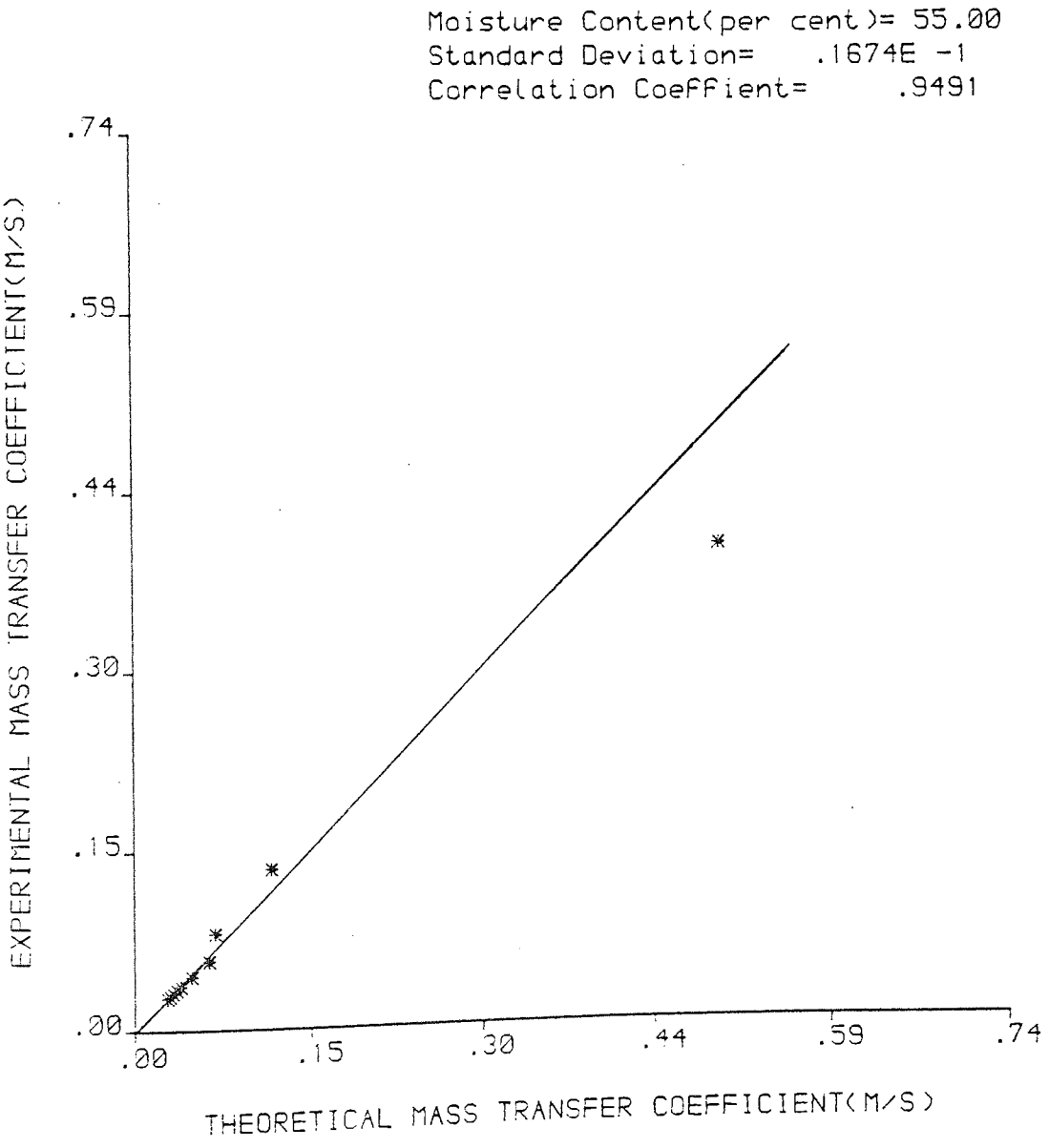

FIGURE D40

EXPERIMENTAL VERSUS THEORETICAL

MASS TRANSFER COEFFICIENT FOR

WESTBURY SLURRY SAMPLE

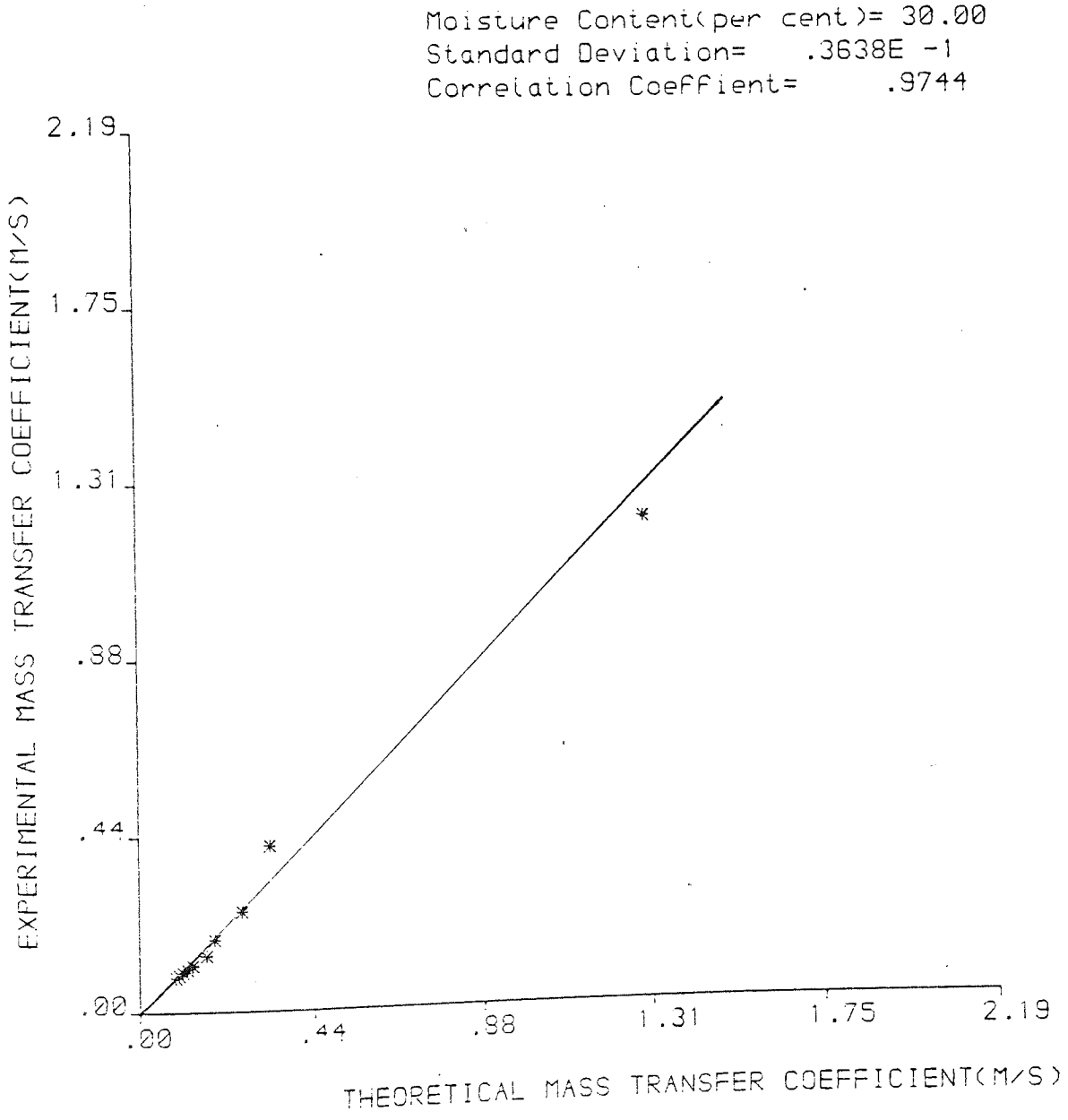

FIGURE D41

EXPERIMENTAL VERSUS THEORETICAL

MASS TRANSFER COEFFICIENT FOR

WESTBURY SLURRY SAMPLE

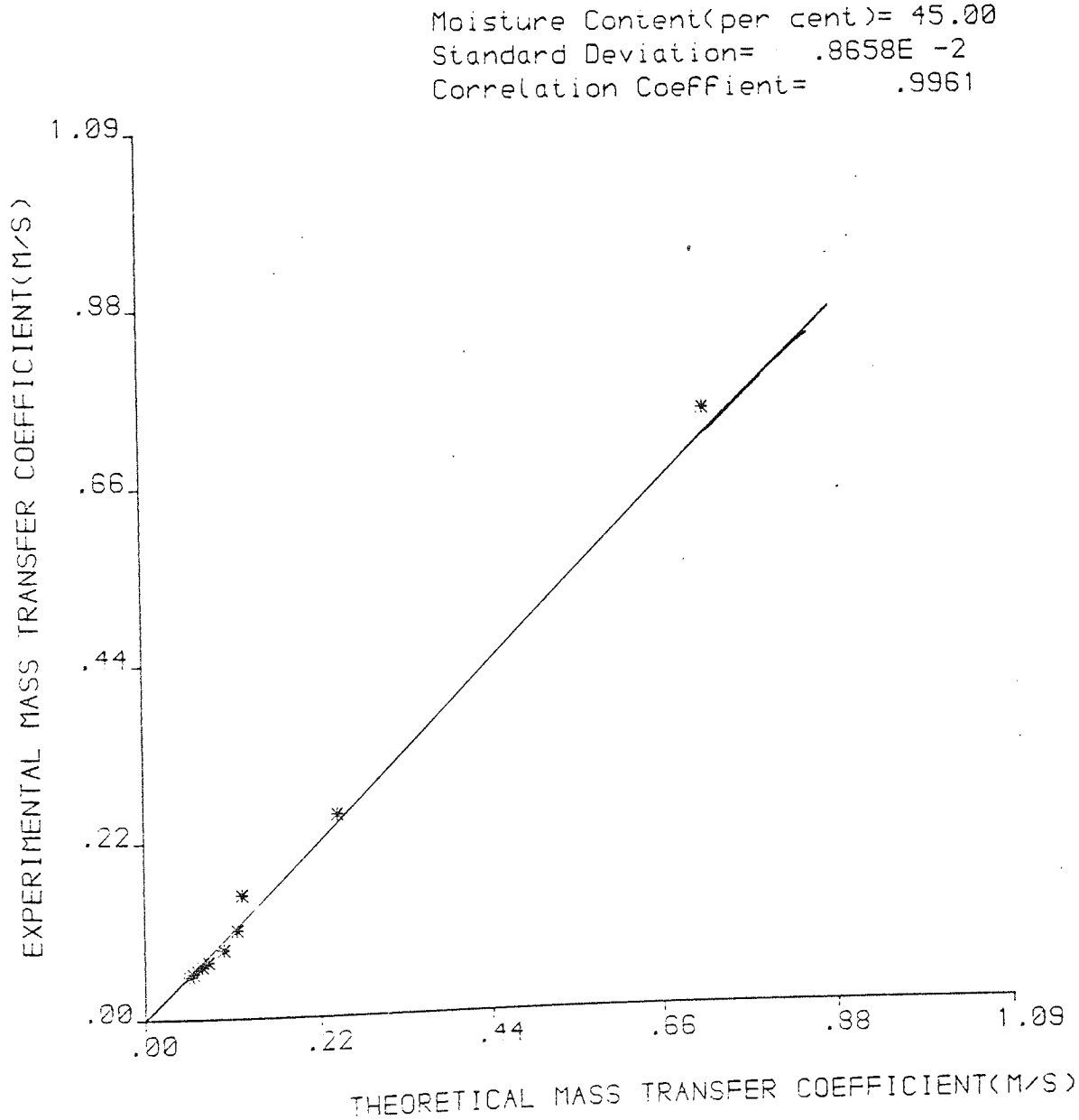

FIGURE D42

EXPERIMENTAL VERSUS THEORETICAL

MASS TRANSFER COEFFICIENT FOR

WESTBURY SLURRY SAMPLE

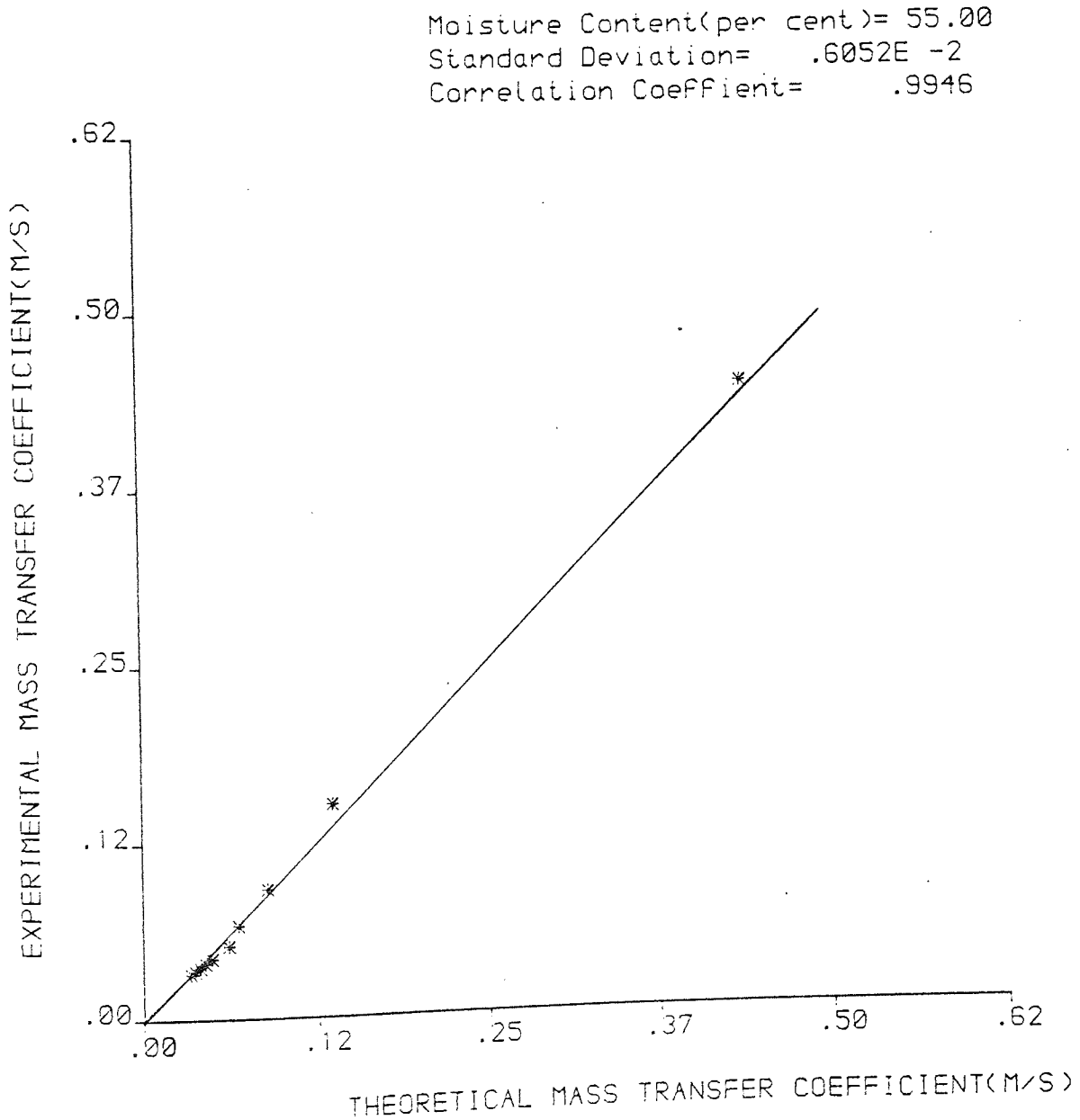

FIGURE D43

EXPERIMENTAL VERSUS THEORETICAL

MASS TRANSFER COEFFICIENT FOR

SHOREHAM SLURRY SAMPLE

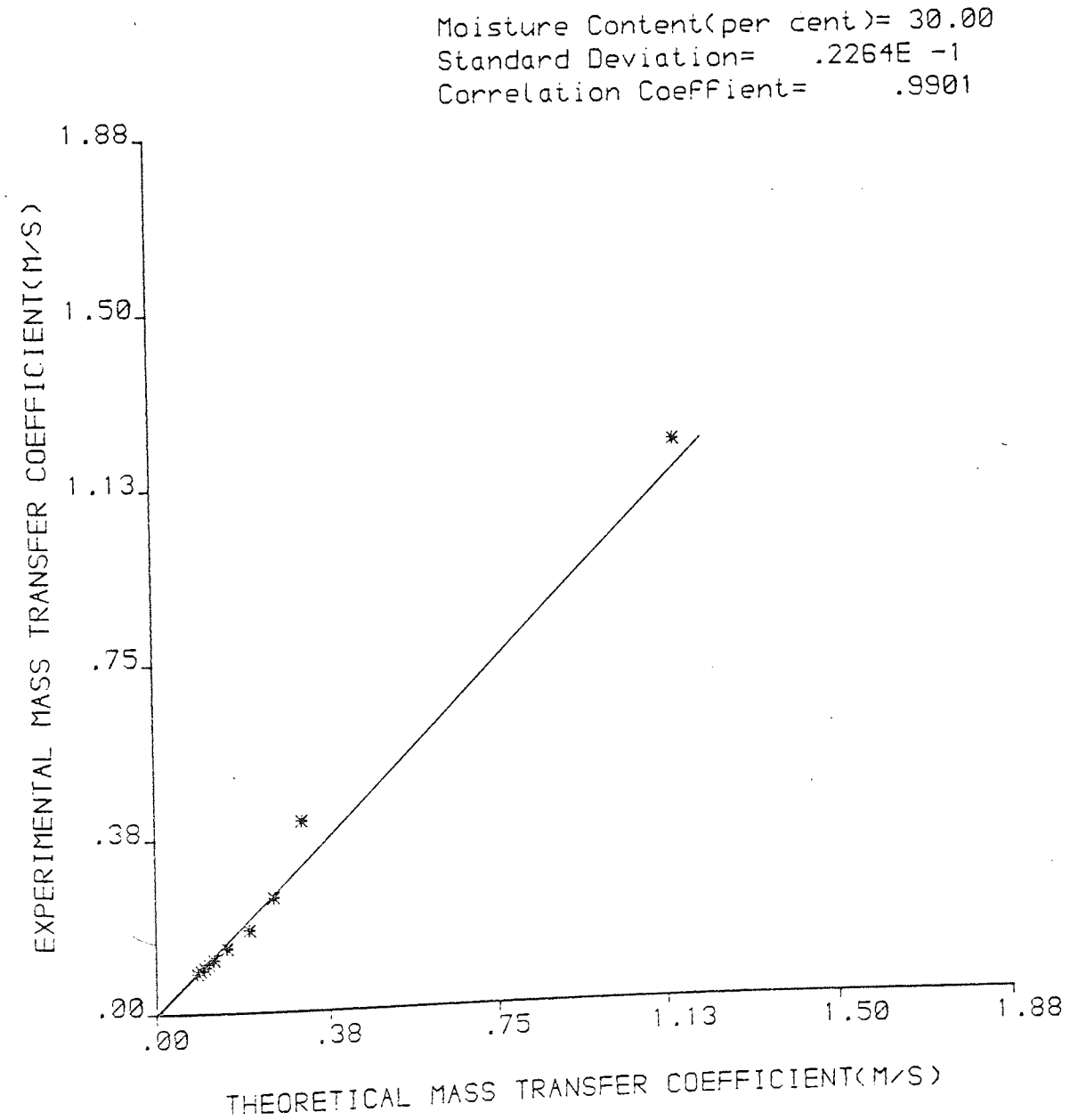

FIGURE D44

EXPERIMENTAL VERSUS THEORETICAL

MASS TRANSFER COEFFICIENT FOR

SHOREHAM SLURRY SAMPLE

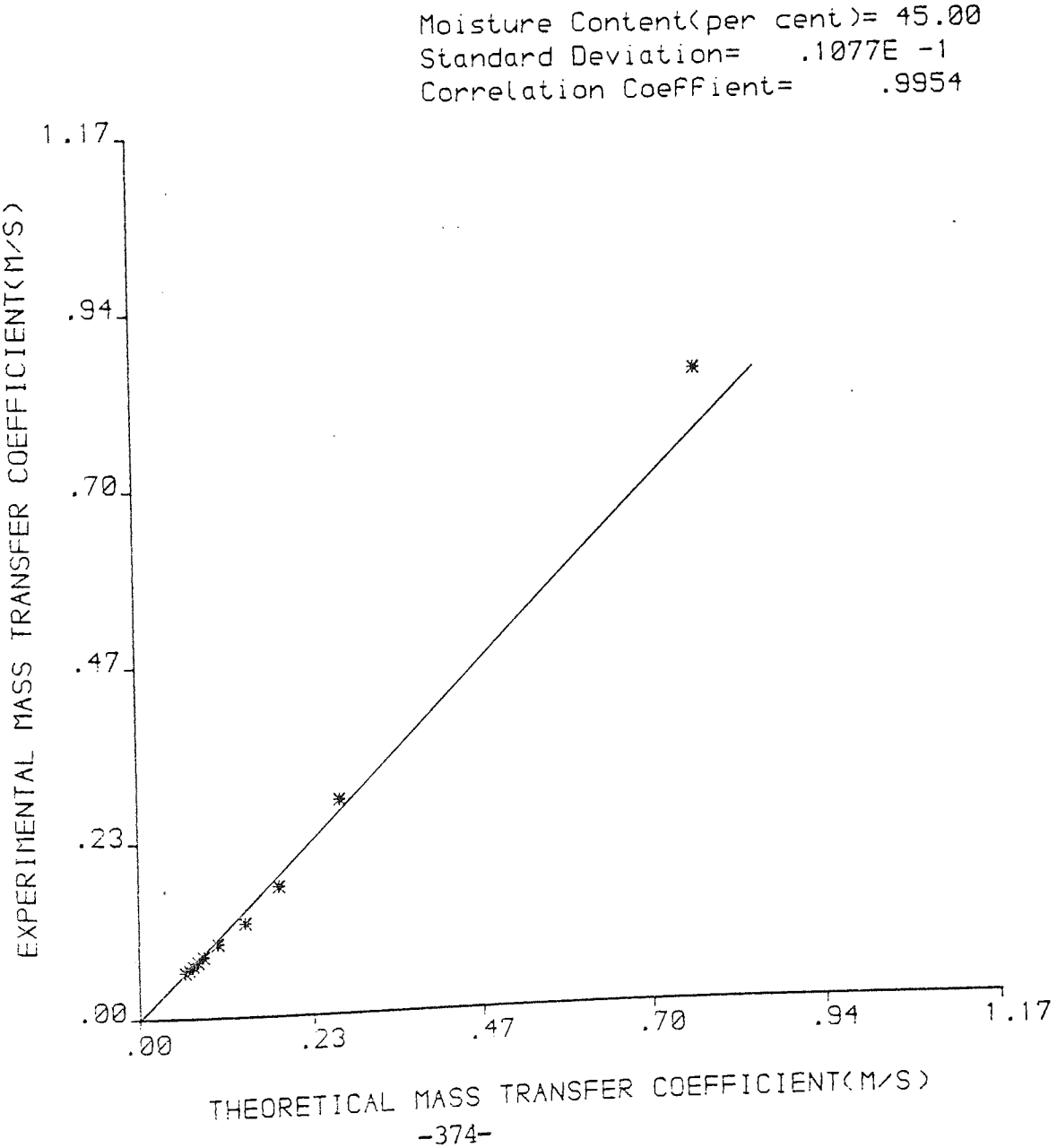

FIGURE D45

EXPERIMENTAL VERSUS THEORETICAL

MASS TRANSFER COEFFICIENT FOR

SHOREHAM SLURRY SAMPLE

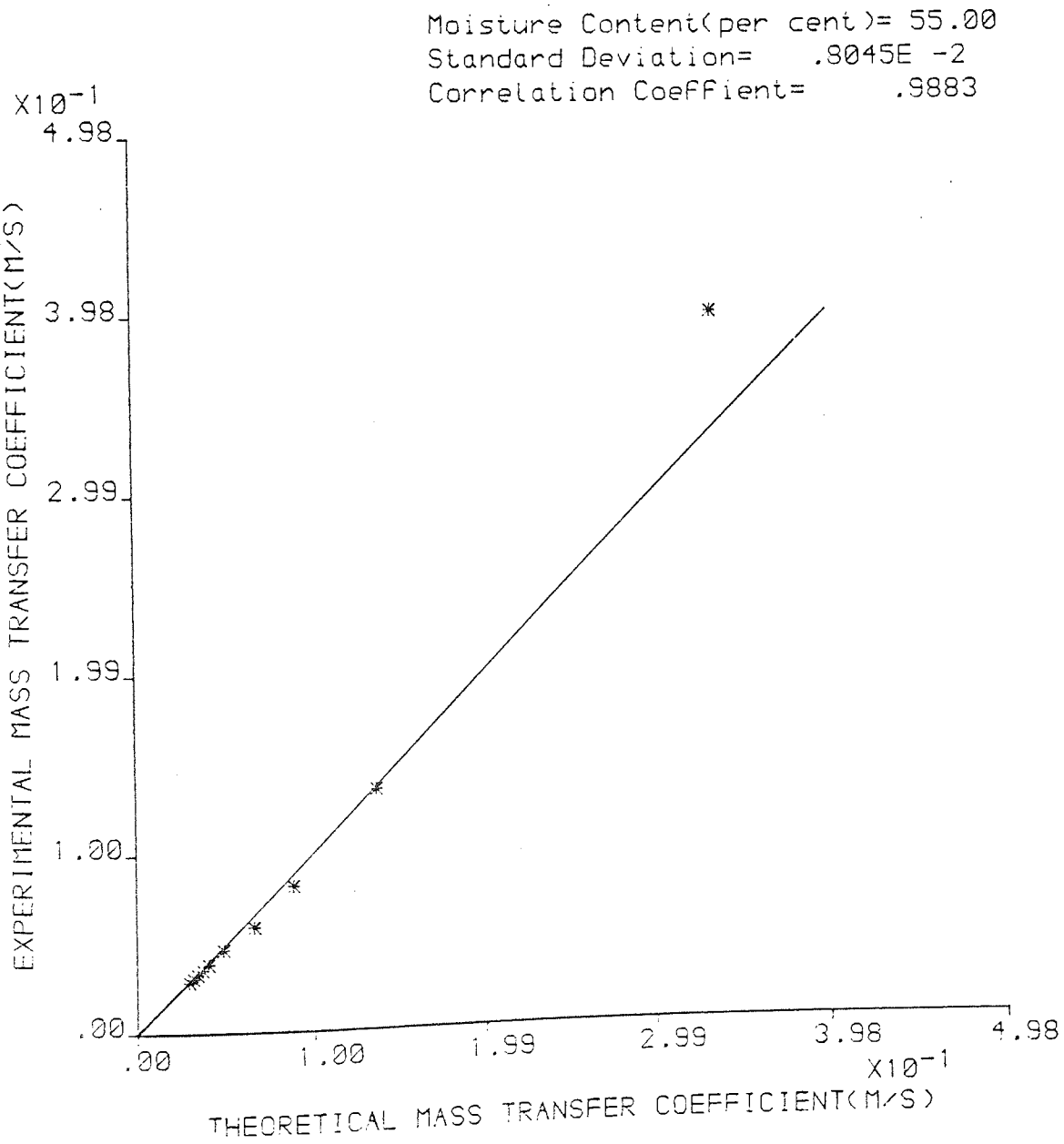

APPENDIX E

1. Tables E1-E10, Experimental Data from the Spray Drying of Water Drops.

2. Tables E11-E20, Experimental Data from Spray Drying of Cement Slurries.

3. Typical Mass Balance and Enthalpy Balance Calculations.

TABLE E1

EXPERIMENT NUMBER: SD 1

AIR

INLET FLOWRATE (KGS^{-1})	0.13
INLET TEMPERATURE (^{o}C)	170.0
INLET HUMIDITY (KG/KG)	5.9556×10^{-3}
OUTLET FINAL TEMPERATURE (^{o}C)	75.0
OUTLET INITIAL HUMIDITY (KG/KG)	8.1165×10^{-3}
OUTLET FINAL HUMIDITY	2.4960×10^{-2}

FEED

INLET FLOWRATE (KGS^{-1})	4.15×10^{-3}
INLET TEMPERATURE (^{o}C)	25.00
FEED SAMPLE	WATER
OUTLET TEMPERATURE (^{o}C)	40.0
DRYING TIME (minutes)	13.08
PRODUCT AMOUNT	2500 ml

TABLE E2

EXPERIMENT NUMBER: SD 2

AIR

INLET FLOWRATE (KGS^{-1})	0.13
INLET TEMPERATURE (^{o}C)	285.0
INLET HUMIDITY (KG/KG)	6.3841×10^{-3}
OUTLET FINAL TEMPERATURE (^{o}C)	140.0
OUTLET INITIAL HUMIDITY (KG/KG)	8.1165×10^{-3}
OUTLET FINAL HUMIDITY	2.6646×10^{-2}

FEED

INLET FLOWRATE (KGS^{-1})	4.5×10^{-3}
INLET TEMPERATURE (^{o}C)	20.0
FEED SAMPLE	WATER
OUTLET TEMPERATURE (^{o}C)	51.0
DRYING TIME (minutes)	10.683
PRODUCT AMOUNT	385.0ml

TABLE E3

EXPERIMENT NUMBER: SD 3

AIR	
INLET FLOWRATE (KGS^{-1})	0.16
INLET TEMPERATURE (^{o}C)	260.0
INLET HUMIDITY (KG/KG)	5.8322×10^{-3}
OUTLET FINAL TEMPERATURE (^{o}C)	135.0
OUTLET INITIAL HUMIDITY (KG/KG)	7.5820×10^{-3}
OUTLET FINAL HUMIDITY	2.4158×10^{-2}
FEED	
INLET FLOWRATE (KGS^{-1})	4.15×10^{-3}
INLET TEMPERATURE (^{o}C)	30.0
FEED SAMPLE	WATER
OUTLET TEMPERATURE (^{o}C)	49.0
DRYING TIME (minutes)	7.783
PRODUCT AMOUNT	90.0 ml

TABLE E4

EXPERIMENT NUMBER: SD 4

AIR	
INLET FLOWRATE (KGS^{-1})	0.16
INLET TEMPERATURE (^{o}C)	225.0
INLET HUMIDITY (KG/KG)	6.3841×10^{-3}
OUTLET FINAL TEMPERATURE (^{o}C)	113.0
OUTLET INITIAL HUMIDITY (KG/KG)	6.6088×10^{-3}
OUTLET FINAL HUMIDITY	2.4960×10^{-2}
FEED	
INLET FLOWRATE (KGS^{-1})	4.5×10^{-3}
INLET TEMPERATURE (^{o}C)	20.0
FEED SAMPLE	WATER
OUTLET TEMPERATURE (^{o}C)	47.0
DRYING TIME (minutes)	13.20
PRODUCT AMOUNT	740.0ml

TABLE E5

EXPERIMENT NUMBER SD 5

AIR

INLET FLOWRATE (KGS^{-1})	0.19
INLET TEMPERATURE (^{o}C)	$220^{o}C$
INLET HUMIDITY (KG/KG)	5.9556×10^{-3}
OUTLET FINAL TEMPERATURE (^{o}C)	102.0
OUTLET INITIAL HUMIDITY (KG/KG)	7.0801×10^{-3}
OUTLET FINAL HUMIDITY	2.4158×10^{-2}

FEED

INLET FLOWRATE (KGS^{-1})	4.15×10^{-3}
INLET TEMPERATURE (^{o}C)	28.5
FEED SAMPLE	WATER
OUTLET TEMPERATURE (^{o}C)	47.50
DRYING TIME (minutes)	7.90
PRODUCT AMOUNT	1900ml

TABLE E6

EXPERIMENT NUMBER: SD 6

AIR

INLET FLOWRATE (KGS^{-1})	0.19
INLET TEMPERATURE (^{o}C)	205.0
INLET HUMIDITY (KG/KG)	6.9834×10^{-3}
OUTLET FINAL TEMPERATURE (^{o}C)	90.0
OUTLET INITIAL HUMIDITY (KG/KG)	6.8407×10^{-3}
OUTLET FINAL HUMIDITY (KG/KG)	2.2631×10^{-3}

FEED

INLET FLOWRATE (KGS^{-1})	4.5×10^{-3}
INLET TEMPERATURE (^{o}C)	20.0
FEED SAMPLE	WATER
OUTLET TEMPERATURE (^{o}C)	45.0
DRYING TIME (minutes)	9.667
PRODUCT AMOUNT	3900ml

TABLE E7

EXPERIMENT NUMBER: SD 7

AIR

INLET FLOWRATE (KGS^{-1})	0.21
INLET TEMPERATURE (^{o}C)	245.0
INLET HUMIDITY (KG/KG)	6.3841×10^{-3}
OUTLET FINAL TEMPERATURE (^{o}C)	125.0
OUTLET INITIAL HUMIDITY (KG/KG)	7.3271×10^{-3}
OUTLET FINAL HUMIDITY	2.5790×10^{-2}

FEED

INLET FLOWRATE (KGS^{-1})	4.5×10^{-3}
INLET TEMPERATURE (^{o}C)	20.0
FEED SAMPLE	WATER
OUTLET TEMPERATURE (^{o}C)	47.0
DRYING TIME (minutes)	9.833
PRODUCT AMOUNT	265ml

TABLE E8

EXPERIMENT NUMBER: SD 8

AIR

INLET FLOWRATE (KGS^{-1})	0.21
INLET TEMPERATURE (^{o}C)	245.0
INLET HUMIDITY (KG/KG)	6.8407×10^{-3}
OUTLET FINAL TEMPERATURE (^{o}C)	122.0
OUTLET INITIAL HUMIDITY (KG/KG)	7.5820×10^{-3}
OUTLET FINAL HUMIDITY	2.5790×10^{-2}

FEED

INLET FLOWRATE (KGS^{-1})	4.15×10^{-3}
INLET TEMPERATURE (^{o}C)	195.0
FEED SAMPLE	WATER
OUTLET TEMPERATURE (^{o}C)	45.50
DRYING TIME (minutes)	10.633
PRODUCT AMOUNT	410.0 ml

TABLE E9

EXPERIMENT NUMBER: SD 9

AIR

INLET FLOWRATE (KGS^{-1})	0.23
INLET TEMPERATURE (^{o}C)	210.0
INLET HUMIDITY (KG/KG)	6.6088×10^{-3}
OUTLET FINAL TEMPERATURE (^{o}C)	128.0
OUTLET INITIAL HUMIDITY (KG/KG)	7.8450×10^{-3}
OUTLET FINAL HUMIDITY	2.4960×10^{-2}

FEED

INLET FLOWRATE (KGS^{-1})	4.50×10^{-3}
INLET TEMPERATURE (^{o}C)	20.0
FEED SAMPLE	WATER
OUTLET TEMPERATURE (^{o}C)	45.0
DRYING TIME (minutes)	11.350
PRODUCT AMOUNT	410.0ml

TABLE E10

EXPERIMENT NUMBER: SD 10

AIR

INLET FLOWRATE (KGS^{-1})	0.23
INLET TEMPERATURE (^{o}C)	200.0
INLET HUMIDITY (KG/KG)	6.3841×10^{-3}
OUTLET FINAL TEMPERATURE (^{o}C)	115.0
OUTLET INITIAL HUMIDITY (KG/KG)	6.3841×10^{-3}
OUTLET FINAL HUMIDITY (KG/KG)	2.4158×10^{-2}

FEED

INLET FLOWRATE (KGS^{-1})	4.5×10^{-3}
INLET TEMPERATURE (^{o}C)	20.0
FEED SAMPLE	WATER
OUTLET TEMPERATURE (^{o}C)	45.0
DRYING TIME (minutes)	10.323
PRODUCT AMOUNT	490.0 ml

TABLE E11

EXPERIMENT NUMBER: SD11

AIR

Inlet Flowrate (KGS^{-1})	0.13
Inlet Temperature (^{o}C)	250.0
Inlet Humidity (KG/KG)	4.9960×10^{-3}
Outlet Final Temperature (^{o}C)	115.0
Outlet Initial Humidity (KG/KG)	8.2275×10^{-3}
Outlet Final Humidity (KG/KG)	3.4649×10^{-2}

FEED

Sample:	Northfleet Slurry
Inlet Flowrate (KGS^{-1})	3.25×10^{-2}
Temperature at the Nozzle (^{o}C)	85.0
Inlet Temperature (^{o}C)	20.00
Initial Moisture content (%, wt/wt)	33.50
Final Moisture content (%, wt/wt)	24.56
Temperature of Powder (^{o}C)	$42^{o}C$
Drying Time (minutes)	20.00

TABLE E12

EXPERIMENT NUMBER: SD12

AIR

Inlet Flowrate (KGS^{-1})	0.13
Inlet Temperature (^{o}C)	255.0
Inlet Humidity (KG/KG)	4.9960×10^{-3}
Outlet Final Temperature (^{o}C)	115.0
Outlet Initial Humidity (KG/KG)	8.6857×10^{-3}
Outlet Final Humidity (KG/KG)	1.9223×10^{-2}

FEED

Sample:	Northfleet Slurry
Inlet Flowrate (KGS^{-1})	1.862×10^{-2}
Inlet Temperature (^{o}C)	15.00
Temperature at the Nozzle (^{o}C)	86.0
Initial Moisture content (%, wt/wt)	33.50
Final Moisture content (%, wt/wt)	26.30
Temperature of Powder (^{o}C)	$40^{o}C$
Drying Time (minutes)	21.00

TABLE E13

EXPERIMENT NUMBER: SD13

AIR

Inlet Flowrate (KGS^{-1})	0.16
Inlet Temperature (^{o}C)	240.0
Inlet Humidity (KG/KG)	4.9960×10^{-3}
Outlet Final Temperature (^{o}C)	100.0
Outlet Initial Humidity (KG/KG)	8.2275×10^{-3}
Outlet Final Humidity (KG/KG)	3.4649×10^{-2}

FEED

Sample:	Northfleet Slurry
Inlet Flowrate (KGS^{-1})	3.25×10^{-2}
Inlet Temperature (^{o}C)	15.00
Temperature of the Nozzle (^{o}C)	86.00
Initial Moisture content (%, wt/wt)	33.50
Final Moisture content (%, wt/wt)	22.10
Temperature of Powder (^{o}C)	41.0
Drying Time (minutes)	25.00

TABLE E14

EXPERIMENT NUMBER: SD14

AIR

Inlet Flowrate (KGS^{-1})	0.16
Inlet Temperature (^{o}C)	246.00
Inlet Humidity (KG/KG)	4.9960×10^{-3}
Outlet Final Temperature (^{o}C)	120.0
Outlet Initial Humidity (KG/KG)	8.9840×10^{-3}
Outlet Final Humidity (KG/KG)	1.9861×10^{-2}

FEED

Sample:	Northfleet Slurry
Inlet Flowrate (KGS^{-1})	1.862×10^{-2}
Inlet Temperature (^{o}C)	15.0
Temperature of the Nozzle (^{o}C)	88.0
Initial moisture content (%, wt/wt)	33.50
Final moisture content (%, wt/wt)	23.80
Temperature of Powder (^{o}C)	40.0
Drying Time (minutes)	18.00

TABLE E15

EXPERIMENT NUMBER: SD15

AIR

Inlet Flowrate (KGS^{-1})	0.19
Inlet Temperature (^{o}C)	225.0
Inlet Humidity (KG/KG)	5.1758×10^{-3}
Outlet Final Temperature (^{o}C)	125.0
Outlet Initial Humidity (KG/KG)	9.9373×10^{-3}
Outlet Final Humidity (KG/KG)	2.0520×10^{-2}

FEED

Sample:	Northfleet Slurry
Inlet Flowrate (KGS^{-1})	3.25×10^{-2}
Temperature at the Nozzle (^{o}C)	89.0
Inlet Temperature (^{o}C)	16.0
Initial Moisture content (%, wt/wt)	33.50
Final Moisture content (%, wt/wt)	26.89
Temperature of Powder (^{o}C)	41.0
Drying Time (minutes)	21.50

TABLE E16

EXPERIMENT NUMBER: SD16

AIR

Inlet Flowrate (KGS^{-1})	0.19
Inlet Temperature (^{o}C)	220.0
Inlet Humidity (KG/KG)	4.9960×10^{-3}
Outlet Final Temperature (^{o}C)	105.0
Outlet Initial Humidity (KG/KG)	8.2275×10^{-3}
Outlet Final Humidity (KG/KG)	2.2631×10^{-2}

FEED

Sample:	Northfleet Slurry
Inlet Flowrate (KGS^{-1})	1.862×10^{-2}
Inlet Temperature (^{o}C)	20.0
Temperature at the Nozzle (^{o}C)	87.0
Initial Moisture content (%, wt/wt)	33.50
Final Moisture content (%, wt/wt)	19.02
Temperature of Powder (^{o}C)	42.0
Drying Time (minutes)	10.00

TABLE E17

EXPERIMENT NUMBER: SD17

AIR

Inlet Flowrate (KGS^{-1})	0.21
Inlet Temperature (^{o}C)	208.0
Inlet Humidity (KG/KG)	4.6530×10^{-3}
Outlet Final Temperature (^{o}C)	112.5
Outlet Initial Humidity (KG/KG)	7.3271×10^{-3}
Outlet Final Humidity (KG/KG)	1.7427×10^{-2}

FEED

Sample:	Northfleet Slurry
Inlet Flowrate (KGS^{-1})	3.25×10^{-2}
Inlet Temperature (^{o}C)	16.0
Temperature at the Nozzle (^{o}C)	88.0
Initial Moisture content (%, wt/wt)	33.50
Final Moisture content (%, wt/wt)	27.50
Temperature of Powder (^{o}C)	40.0
Drying Time (minutes)	20.00

TABLE E18

EXPERIMENT NUMBER: SD18

AIR

Inlet Flowrate (KGS^{-1})	0.21
Inlet Temperature (^{o}C)	218.0
Inlet Humidity (KG/KG)	5.1758×10^{-3}
Outlet Final Temperature (^{o}C)	100.0
Outlet Initial Humidity (KG/KG)	8.3966×10^{-3}
Outlet Final Humidity (KG/KG)	2.4960×10^{-2}

FEED

Sample:	Northfleet Slurry
Inlet Flowrate (KGS^{-1})	1.862×10^{-2}
Inlet Temperature (^{o}C)	18.0
Temperature at the Nozzle (^{o}C)	90.0
Initial Moisture content (%. wt/wt)	33.50
Final Moisture content (%, wt/wt)	12.30
Temperature of Powder (^{o}C)	44.0
Drying Time (minutes)	26.0

TABLE E19

EXPERIMENT NUMBER: SD19

AIR

Inlet Flowrate (KGS^{-1})	0.23
Inlet Temperature (^{o}C)	200.0
Inlet Humidity (KG/KG)	4.8217×10^{-3}
Outlet Final Temperature (^{o}C)	127.0
Outlet Initial Humidity (KG/KG)	9.9373×10^{-3}
Outlet Final Humidity (KG/KG)	1.8605×10^{-2}

FEED

Sample:	Northfleet Slurry
Inlet Flowrate (KGS^{-1})	3.25×10^{-2}
Inlet Temperature (^{o}C)	19.0
Temperature at the Nozzle (^{o}C)	90.0
Initial moisture content (%, wt/wt)	33.50
Final moisture content (%, wt/wt)	26.32
Temperature of Powder (^{o}C)	46.0
Drying Time (minutes)	25.00

TABLE E20

EXPERIMENT NUMBER: SD20

AIR

Inlet Flowrate (KGS^{-1})	0.23
Inlet Temperature (^{o}C)	205.0
Inlet Humidity (KG/KG)	4.6530×10^{-3}
Outlet Final Temperature (^{o}C)	140.0
Outlet Initial Humidity (KG/KG)	8.3966×10^{-3}
Outlet Final Humidity (KG/KG)	2.9397×10^{-2}

FEED

Sample:	Northfleet Slurry
Inlet Flowrate (KGS^{-1})	1.862×10^{-2}
Inlet Temperature (^{o}C)	15.0
Temperature at the Nozzle (^{o}C)	92.0
Initial moisture content (%, wt/wt)	33.50
Final Moisture content (%. wt/wt)	13.50
Temperature of Powder (^{o}C)	45.0
Drying Time (minutes)	25.00

A TYPICAL MASS AND ENTHALPY BALANCE CALCULATION FOR THE PILOT PLANT SPRAY DRIER

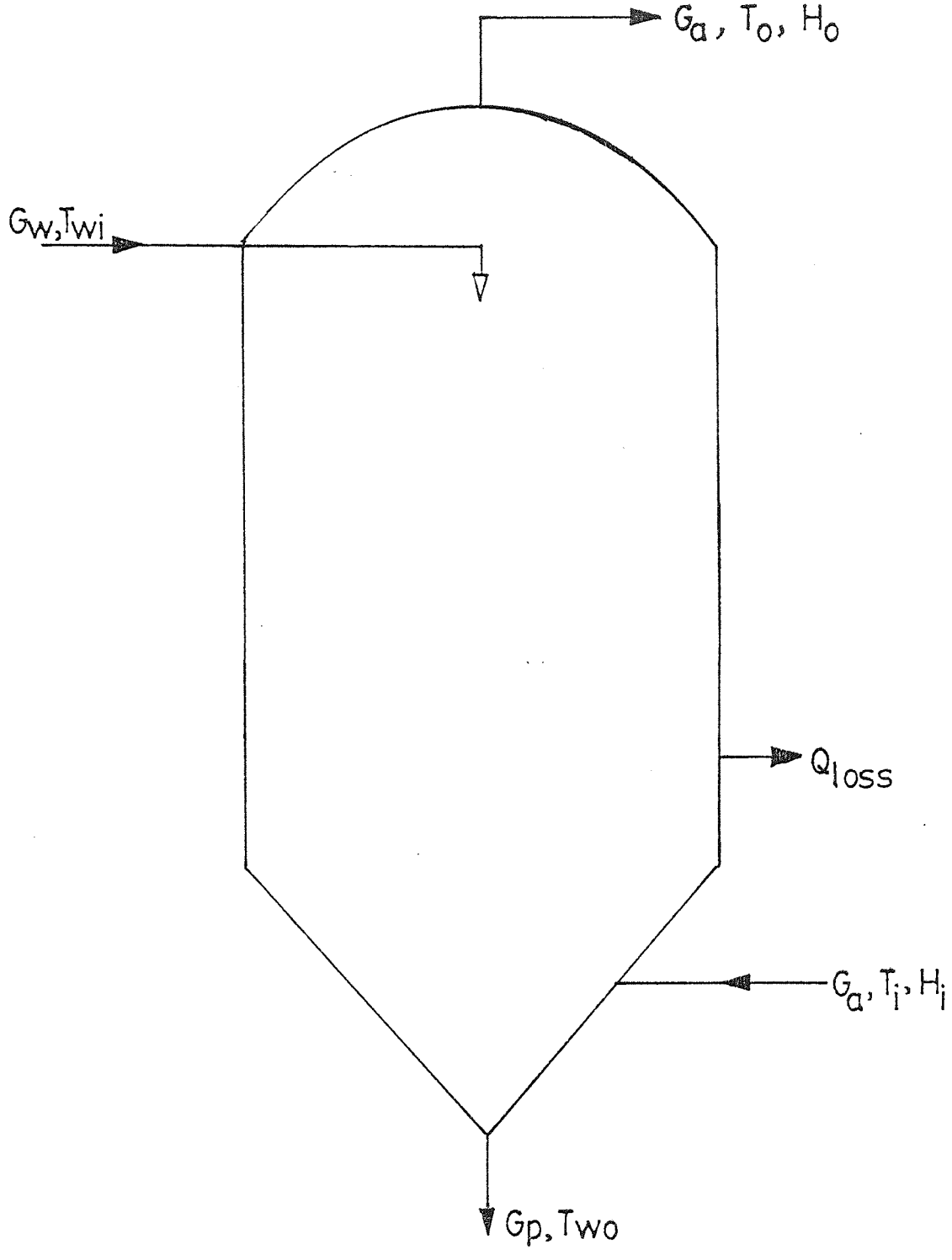

FIGURE E1 Data for Enthalpy and Mass Balances

The Enthalpy and Mass balances over the drier have been calculated with reference to Figure E1. G_a Kgs^{-1} of water at temperature T_{ω_i} is fed into the spray drying chamber. After evaporation, G_p Kgs^{-1} of the water is effluent unevaporated at a temperature T_{ω_o}. The drying air flowing at G_a Kgs^{-1} enters the chamber at a temperature T_i and humidity of H_i Kg/Kg. It is exhausted at an outlet humidity of H_o Kg/Kg and temperature T_o.

Mass Balance

Moisture entering in hot air = $G_a H_i$

Moisture entering in feed = G_ω

Moisture leaving in exhaust air = $G_a H_o$

Moisture leaving in unevaporated water = G_p

For no product accumulation, the following relationship holds.

Input = Output at Steady State

Then:

$$G_\omega + G_a H_i - (G_p + G_a H_o) = \text{Accumulation}$$

Using the data collected in experiment SD2, presented in Table E2, yields:

$$4.5\times10^{-3}+(0.13\times6.3841\times10^{-3})-(0.13\times2.6647\times10^{-2})-0.385 = \text{Accumulation}$$

Thus:

Total Moisture into the Drier = 5.3299×10^{-3} Kgs^{-1}

Total Moisture evaporated in Drier = 3.4641×10^{-3} Kgs^{-1}

Accumulation = 1.8658×10^{-3} Kgs^{-1}

Enthalpy Balance

Enthalpy of air entering drier $= G_a(Q_a)_i$

Enthalpy of feed entering drier $= G_\omega(Q_\omega)_i$

Enthalpy of exhaust drying air $= G_a(Q_a)_o$

Enthalpy of unevaporated water $= G_p(Q_\omega)_o$

Similarly:

Heat Input = Heat Output + Heat Loss

That is:

$$G_a(Q_a)_i + G_\omega(Q_\omega)_i = G_a(Q_a)_o + G_p(Q_\omega)_o + Q_L$$

where Q_a, the enthalpy of the drying air is expressed in terms of the humid heat, C_s, absolute humid heat, and the latent heat of evaporation of water, λ.

Thus:

$$Q_a = C_s\Delta T + H\lambda$$

and Q_ω the enthalpy of the water feed is expressed in terms of its flowrate, heat capacity, C_ω and temperature.

Thus:

$$Q_\omega = C_\omega\Delta T.$$

Using data collected from experiment number SD2, steam tables and a datum temperature of 0^oC.

$$(Q_a)_i = (285.0-0)\times 1.0398 + (2500.8\times 6.3841\times 10^{-3})$$

$$(Q_a)_o = (140.0-0)\times 1.0135 + (2500.8\times 2.6647\times 10^{-2})$$

$$(Q_\omega)_i = 4.5\times 10^{-3}\times 4.183\times (20.0-0)$$

$$(Q_\omega)_o = 1.8658\times 10^{-3}\times 4.183\times (51.0-0)$$

Thus:

Total Heat input into drier = 40.398 $KJKg^{-1}S^{-1}$

Total heat output from drier = 26.661 $KJKg^{-1}S^{-1}$

APPENDIX F

1. Tables F1-F5, Experimental Data from Tracer Response Analysis on Pilot Plant Spray Drier.

2. Tables F6-F7, Typical Experimental Data from Tracer Analysis on Humber Spray Drier.

3. "Fortran IV" pogram listing for Normalisation of RTD data.

4. "Basic 16" program listing of the mathematical model simulating tracer response from the spray drier.

TABLE F1

Experiment Number: SD21

Air Flowrate 0.13 Kgs^{-1}

Volume of Tracer Used, A_x 0.5053 m^3

Mean Residence Time; $\bar{t}$ 16.7879 seconds

TIME (S)	DIMENSIONLESS TIME (θ)	EXIT CONCENTRATION, C_E	
		EXPERIMENTAL	SIMULATED
0	0.0000	0.0000	0.0000
10	0.5957	0.0787	0.1582
20	1.1914	0.2698	0.2912
30	1.7870	0.3709	0.3413
40	2.3827	0.2726	0.3662
50	2.9784	0.2023	0.2689
60	3.5741	0.1349	0.1017
70	4.1698	0.1068	0.0647
80	4.7654	0.0731	0.0272
90	5.3611	0.0422	0.0118
100	5.9568	0.0337	0.0051
110	6.5525	0.0253	0.0022
120	7.1482	0.0197	0.0011
130	7.7438	0.0112	0.0004
140	8.3395	0.0112	0.0002
150	8.9352	0.0084	0.0001
155	9.2330	0.0028	0.0001

TABLE F2

Experiment Number: SD22

Air Flowrate: 0.16 Kgs^{-1}

Volume of Tracer Used, A_x: 0.5045 m^3

Mean Residence Time, $\bar{t}$: 14.0468 seconds

TIME (S)	DIMENSIONLESS TIME (θ)	EXIT CONCENTRATION, C_E	
		EXPERIMENTAL	SIMULATED
0	0.0000	0.0000	0.0000
10	0.7119	0.0701	0.2055
20	1.4238	0.2806	0.2813
30	2.1358	0.3354	0.3144
40	2.8477	0.2074	0.3292
50	3.5596	0.1464	0.2093
60	4.2715	0.0976	0.0755
70	4.9834	0.0793	0.0240
80	5.6954	0.0488	0.0081
90	6.4073	0.0366	0.0028
100	7.1192	0.0244	0.0010
110	7.8311	0.0183	0.0003
120	8.5430	0.0122	0.0002
130	9.2500	0.0122	0.0001
140	9.9669	0.0091	0.0001
150	10.6788	0.0030	0.0001
155	11.0348	0.0030	0.0001

TABLE F3

Experiment Number	SD23
Air Flowrate	0.19 Kgs^{-1}
Volume of Tracer Used, A_x	0.5039 m^3
Mean Residence Time, $\bar{t}$	12.1426 seconds

TIME t (S)	DIMENSIONLESS TIME (θ)	EXIT CONCENTRATION, C_E	
		EXPERIMENTAL	SIMULATED
0	0.0000	0.0000	0.0000
10	0.8236	0.0770	0.1932
20	1.6471	0.2337	0.2815
30	2.4707	0.3081	0.3045
40	3.2943	0.2231	0.2748
50	4.1178	0.1328	0.1097
60	4.9414	0.0691	0.0283
70	5.7649	0.0505	0.0073
80	6.5885	0.0319	0.0018
90	7.4121	0.0239	0.0005
100	8.2356	0.0159	0.0002
110	9.0592	0.0106	0.3248E-4
120	9.8828	0.0106	0.8394E-5
130	10.7063	0.0053	0.2170E-5
135	11.1181	0.0027	0.1103E-5

TABLE F4

Experiment Number	SD24
Air Flowrate	0.21 Kgs^{-1}
Volume of Tracer Used, A_x	0.5039 m^3
Mean Residence Time, $\bar{t}$	11.1453 seconds

TIME (S)	DIMENSIONLESS TIME (θ)	EXIT CONCENTRATION, C_E	
		EXPERIMENTAL	SIMULATED
0	0.0000	0.0000	0.0000
10	0.8973	0.1016	0.2222
20	1.7945	0.2272	0.2923
30	2.6198	0.3049	0.3079
40	3.5890	0.2152	0.1469
50	4.4863	0.1106	0.0382
60	5.3835	0.0598	0.0085
70	6.2808	0.0329	0.0038
80	7.1780	0.0239	0.0019
90	8.0753	0.0149	0.0002
100	8.9725	0.0090	0.0001
110	9.8693	0.0090	0.5627E-4
120	10.7671	0.0060	0.1342E-5
130	11.6643	0.0060	0.3230E-5
135	12.1129	0.0030	0.1580E-5

TABLE F5

Experiment Number SD25

Air Flowrate 0.23 Kgs^{-1}

Volume of Tracer Used, A_x 0.5041 m^3

Mean Residence Time, $\bar{t}$ 10.3475 seconds

TIME (S)	DIMENSIONLESS TIME (θ)	EXIT CONCENTRATION, C_E	
		EXPERIMENTAL	SIMULATED
0	0.0000	0.0000	0.0000
10	0.9664	0.0718	0.2134
20	1.9329	0.2154	0.2808
30	2.8993	0.2924	0.2922
40	3.8657	0.1821	0.1964
50	4.8322	0.0872	0.0446
60	5.7986	0.0590	0.0705
70	6.7651	0.0333	0.0014
80	7.7315	0.0272	0.0003
90	8.6979	0.0128	0.6768E-4
100	9.6644	0.0103	0.1583E-4
110	10.6308	0.0077	0.3759E-5
120	11.5972	0.0051	0.8990E-6
130	12.5637	0.0051	0.7089E-6
135	13.0469	0.0026	0.5588E-6

TABLE F6

Experiment Number H1

Air Flowrate 2.606×10^4 m^3/HR

Volume of Tracer Used, A_x 4.1295 m^3

Mean Residence Time, $\bar{t}$ 54.2616 seconds

TIME (S)	DIMENSIONLESS TIME (θ)	EXIT CONCENTRATION, C_E	
		EXPERIMENTAL	SIMULATED
0	0.0000	0.0000	0.0000
10	0.1843	0.0659	0.0663
20	0.3686	0.1648	0.1609
30	0.5529	0.2637	0.2439
40	0.7372	0.3955	0.3284
50	0.9215	0.4615	0.4651
60	1.1058	0.5274	0.5612
70	1.2900	0.5933	0.6581
80	1.4743	0.5933	0.6121
90	1.6586	0.6592	0.5633
100	1.8429	0.5274	0.5212
110	2.0272	0.3955	0.3986
120	2.2115	0.2307	0.3105
130	2.3958	0.1978	0.1672
140	2.5801	0.0659	0.1130
150	2.7644	0.0330	0.0820
160	2.9487	0.0330	0.0600
170	3.1330	0.0330	0.0469
178	3.2804	0.0330	0.0388

TABLE F7

Experiment Number H5

Air Flowrate 2.606×10^4 m^3/HR

Volume of Tracer Used, A_x 1.90 m^3

Mean Residence Time, $\bar{t}$ 54.2616 seconds

TIME t (S)	DIMENSIONLESS TIME (θ)	EXIT CONCENTRATION, C_E	
		EXPERIMENTAL	SIMULATED
0	0.0000	0.0000	0.0000
10	0.1843	0.1791	0.2030
20	0.3686	0.2686	0.2943
30	0.5529	0.3582	0.3450
40	0.7372	0.5373	0.5221
50	0.9215	0.6268	0.5770
60	1.1058	0.6268	0.6198
70	1.2900	0.4477	0.5449
80	1.4743	0.4477	0.4565
90	1.6586	0.3582	0.3990
100	1.8429	0.3134	0.3621
110	2.0272	0.2239	0.2190
120	2.2115	0.2239	0.1809
130	2.3958	0.1791	0.1377
140	2.5801	0.0895	0.1163
150	2.7644	0.0895	0.0989
168	2.0961	0.0895	0.0750

"Fortran IV" programm listing for

Normalisation of RTD data.

```
      TRACE 2
      MASTER HULL
      DIMENSION X(300),Y(300),PH(300)
      DIMENSION X1(200),Y1(200)
C     B - CORRECTION FACTOR FOR GAS RISER TEMPERATURE OF 650 DEG. C
      X(1)=0.0
      QT=7.239
      VT=3.928E2
      TBAR=VT/QT
      A=1.1E-2
      READ(1,100) N,ASH,DT,NRUN
      B=3.1502
  100 FORMAT(I3,2F0.0,I2)
      READ(1,110) (PH(I),I=1,N)
  110 FORMAT(10F0.0)
      N1=N-1
      D2=DT/TBAR
      DO 10 I=1,N
      Y(I)=A*QT*(PH(I)-ASH)/ASH
   10 CONTINUE
      DO 11 J=1,N1,2
      SUM=SUM+2.*Y(I)+2.*Y(J)+4.*Y(J+1)
   11 CONTINUE
      AREA=0.3333*DT*SUM
      DO 12 I=1,N
      X1(I+1)=X1(I)+D2
      Y1(I+1)=TBAR*Y(I)/AREA
   12 CONTINUE
      VOL=AREA*B
      WRITE(2,200) NRUN,TBAR,VOL,VT
      WRITE(2,210)(X(I),X1(I),Y(I),Y1(I),I=1,N)
      WRITE(6,300) (X1(I),Y1(I),I=1,N)
  300 FORMAT(2X,F10.5,',',F10.6)
  200 FORMAT(10X,I4,3F10.4)
  210 FORMAT(25X,4F10.4)
      STOP
      END
      FINISH
```

"Basic 16" program listing of the mathematical model simulating tracer response from the spray drier.

```
 9  READ P,E,I
 10  DIM U(150),Y(150),T(150),W(150),V(10,150),Z(10)
 11  I0=0: GOSUB 9000
 12  READ W,Y2,Y1
 14  B0=8:N0=48
 20  L2=INT(E/P+.5)
 21  GOSUB 7000
 22  PRINT "RUN ?": INPUT F4
 23  IF F4=0 THEN 25
 24  GOSUB 8020
 25  FOR I1=0,L2:U(I1),Y(I1),T(I1),W(I1)=0: NEXT I1
 26  IF F4=0 THEN 210
 27  PRINT "INPUT A,B,J,K,M,N,L": INPUT A,B,J,K,M,N,L
 28  PRINT "FULL DISPLAY ?": INPUT F3
 29  PRINT "ZERO STORAGE ?": INPUT F4
 30  IF F4=0 THEN 32
 31  GOSUB 7000
 32  GOSUB 4000
 33  IF A=0 THEN 100
 40  GOSUB 1000
 45  FOR I1=0,L2:T(I1)=W(I1): NEXT I1
 47  IF ABS(J+K+M+N+L-1)<.1E-02 THEN 55
 49  REM                                   CSTR A1
 50  K1=A/(1-J-K-M-N-L): GOSUB 2000
 52  GOSUB 5000
 55  FOR I1=0,L2:U(I1)=W(I1): NEXT I1
 60  IF J=0 THEN 80
 64  REM                                   DELAY A2
 65  FOR I1=0,L2:T(I1)=U(I1): NEXT I1
 70  D=INT(J/(A*P)+.5): GOSUB 3000
 71  GOSUB 5000
 75  FOR I1=0,L2:U(I1)=W(I1): NEXT I1
 84  REM                                   CSTR A3
 85  FOR I1=0,L2:T(I1)=U(I1): NEXT I1
 90  K1=A/K: GOSUB 2000
 91  GOSUB 5000
 95  FOR I1=0,L2:U(I1)=W(I1): NEXT I1
100  IF B=0 THEN 150
104  REM                                   DELAY B1
105  GOSUB 1000
110  FOR I1=0,L2:Y(I1),T(I1)=W(I1): NEXT I1
115  IF M=0 THEN 130
120  D=INT(M/(B*P)+.5): GOSUB 3000
121  GOSUB 5000
125  FOR I1=0,L2:Y(I1)=W(I1): NEXT I1
130  IF N=0 THEN 150
134  REM                                   CSTR B2
135  FOR I1=0,L2:T(I1)=Y(I1): NEXT I1
140  K1=B/N: GOSUB 2000
141  GOSUB 5000
145  FOR I1=0,L2:Y(I1)=W(I1): NEXT I1
150  GOSUB 1000
```

```
151  FOR I1=0,L2:T(I1)=W(I1): NEXT I1
152  IF ABS(1-A-B)<.1E-02 THEN 157
153  REM                                   DELAY C1
154  D=INT(L/(P*(1-A-B))+.5): GOSUB 3000
155  GOSUB 5000
156  REM                                   CALCULATE RESPONSE
157  FOR I1=0,L2:W(I1)=A*U(I1)+B*Y(I1)+(1-A-B)*W(I1): NEXT I1
158  GOSUB 5005
159  CALL (7,2,E/8,Y1/1.1,L1): CALL (8,7)
167  GOSUB 9020
168  CALL (9)
170  S=W(0)+W(L2)
172  FOR I1=1,L2-1,2:S=S+4*W(I1): NEXT I1
173  FOR I1=2,L2-2,2:S=S+2*W(I1): NEXT I1
174  PRINT : PRINT : PRINT : PRINT
175  S4=0
176  PRINT "A=";A: PRINT "B=";B: PRINT "J=";J: PRINT "K=";K
177  PRINT "M=";M: PRINT "N=";N: PRINT "L=";L
178  PRINT "TIME","EXPERIMENTAL","SIMULATED"
180  FOR N4=1,N5
185  PRINT C(N4),D(N4),W(N4)
190  S4=S4+(D(N4)-W(N4))*(D(N4)-W(N4))
195  NEXT N4
200  PRINT "SUM OF SQUARED ERRORS=";S4
205  S5=S4/(N5-1)
210  PRINT "VARIANCE=";S5
265  PRINT "STOP ?": INPUT P4
266  I0=0
270  IF P4=0 THEN 22
275  STOP
280  GOSUB 6000
285  IF I4=0 THEN 265
290  FOR I1=0,I4-1:I7=I7-1
295  FOR I2=0,L2+8:V(Z(I1),I2)=0: NEXT I2: NEXT I1
300  FOR I1=0,9
305  IF V(I1,7)<>0 THEN 330
310  FOR I2=I1+1,10
315  IF V(I2,7)=0 THEN 325
320  FOR I5=0,L2+8:V(I1,I5)=V(I2,I5
321  V(I2,I5)=0: NEXT I5: GOTO 330
325  NEXT I2: GOTO 335
330  NEXT I1
335  IF I8<>0 THEN 265
340  GOTO 175
345  DATA .3686E-01,4,4
350  DATA 1.2,.85,1
1000  FOR J2=0,L2
1005  IF J2>T2 THEN W(J2)=0: GOTO 1015
1010  W(J2)=Y2
1015  NEXT J2: RETURN
2000  J2=0:C=0
2005  CALL (1,T)
2010  D1=K1*(T(J2)-C)
2015  CALL (2,P,E,F1,F2)
```

```
2020  IF F2=1 THEN 2045
2025  W(J2)=C
2030  J2=J2+1
2035  IF J2>L2 THEN  RETURN
2040  IF F1=2 THEN  RETURN
2045  CALL (3,T,P,I)
2050  CALL (4,C,D1)
2055  GOTO 2010
3000  IF D<1 THEN  FOR J2=0,L2:W(J2)=T(J2): NEXT J2: RETURN
3005  IF D>L2 THEN  FOR J2=0,L2:W(J2)=0: NEXT J2: RETURN
3010  FOR J2=L2,0,-1: IF J2<D THEN 3020
3015  U1=T(J2-D): GOTO 3025
3020  U1=0
3025  W(J2)=U1: NEXT J2: RETURN
4000  CALL (5)
4002  CALL (6,-E/6,22*E/18+E/6,-.25,Y1+.25)
4005  REM                          18 CM=E 15 CM=Y1 (ON SCREEN)
4010  CALL (7,2,0,0,L1): CALL (7,1,E,0,L1)
4011  CALL (7,2,0,Y1,L1): CALL (7,1,0,0,L1)
4012  FOR I9=1,E+1
4013  N6=I9-1
4016  CALL (7,2,N6,0,L1): CALL (8,7): PRINT "!"
4017  CALL (7,2,(N6-E/12),-.75E-01,L1): CALL (8,7)
4018  PRINT N6: NEXT I9: FOR I9=1,6
4019  CALL (7,2,0,(I9-1)*.2,L1): CALL (8,7): PRINT "-"
4020  CALL (7,2,-E/6,(I9-1)*.2,L1): CALL (8,7)
4021  PRINT (I9-1)*.2
4022  RETURN
5000  IF F3=0 THEN  RETURN
5005  CALL (7,2,0,W(0),L1)
5010  FOR J2=1,L2
5012  IF I0=1 THEN  IF J2=I0+I1*5 THEN  CALL (8,Z(I1)+N0)
5013  CALL (7,2,(J2-1)*P,N(J2-1),L1)
5015  CALL (7,1,J2*P,W(J2),L1)
5020  NEXT J2:I0=0: RETURN
7000  FOR J1=0,10:Z(J1)=0: FOR J2=0,L2+8:V(J1,J2)=0
7002  NEXT J2: NEXT J1
7005  I7=0: RETURN
8020  T2=INT(W/P+.5)
8025  RETURN
9000  PRINT "INPUT TOTAL NO OF EXPERIMENTAL POINTS"
9005  INPUT N5
9010  FOR N4=1,N5
9012  INPUT N1,N2,:C(N4)=N1:D(N4)MN2: NEXT N4
9020  FOR N4=1,N5: CALL (7,2,C(N4),D(N4),L1)
9025  CALL (8,48)
9030  NEXT N4
9035  RETURN
```

NOMENCLATURE

A	area of hemispherical drop $(2\pi R^2)$ (m^2)
A_x	total volume of input tracer (m^3)
A_y	total volume of output tracer (m^3)
C	moisture content (kg moisture/m^3 solution)
C_o	initial drop moisture content (kg moisture/m^3 solution)
ΔC	concentration driving force
C_D	drag coefficient
c_p	specific heat (kJ/Kg/^oK)
D_G	dimensionless group $(p/\rho V_s^2)$
D_m, D_v	diffusivity of water vapour in air (m^2/s)
D_p	drop diameter (m)
D_{VS}	surface mean diameter (m)
d_o	outlet orifice diameter (m)
G	mass flowrate (kg/s)
Gr	Grashof Number $((D_p^3 \rho_g g_c \sigma \Delta\theta)/\mu^2)$
g_c	acceleration due to gravity m/s^{-2}
H	air humidity (kg/kg)
Hc	Henry's Law constant
k	thermal conductivity $(W/m^2 s^oK)$
K_C	crust mass transfer coefficient (m/s)
K_E	experimental mass transfer coefficient (m/s)
K_G	gas phase mass transfer coefficient (m/s)
K_T	theoretical mass transfer coefficient (m/s)
L	mean pore length (m)
L_s	sheet length (m)
N	number of pores
N_A	rate of mass transfer $(kg/m^2 s)$

N_D	drying rate (kg/s)
N_e	evaporative capacity of spray drier (kg/s)
n_i	number of drops in size range i
Nu	Nusselt Number for heat transfer $(h_c D_p/\rho_G)$
Nu'	Nusselt Number for mass transfer $(K_G M D_p P_f/D_V \rho_G)$
P	vapour pressure (N/m^2)
Pr	Prandtl Number $(C_p \mu/k)$
Q_a, Q_T	total air volumetric flowrate (m^3/s)
Q_s	slurry flowrate (kg/s)
R	external drop radius (m)
r	internal drop radius (m)
R_c	universal gas constant
Re	Reynold's Number $(\rho_G U D_p/\mu)$
S	specific surface area of pores (m^{-1})
s	humid heat (kJ/Kg^oK)
Sc	Schmidt Number $(\mu/\rho_G D_V)$
Sh	Sherwood Number $(K_G D_p/D_V)$
T	slurry temperature (^oC)
t	air temperature (^oC)
$\bar{t}$	mean residence time (S)
U	vapour velocity (m/s)
V_s	sheet velocity (m/s)
We	Weber Number $(\frac{d_o V_s^2}{\theta_c})$
X	dimensionless input tracer concentration
Y	dimensionless output tracer concentration

Greek Letters

β	crust thickness (m)
σ	radius of pore (m)
ε	porosity
θ	dimensionless time
θ_c	semi-cone angle
θ_D	droplets residence time (s)
$\theta_J, \theta_K, \theta_L \ldots$	residence time in zone, J,K,L.....(s)
θ_T	total residence time (s)
ρ	density (kg/m^3)
μ	viscosity (N/sm^2)
λ	latent heat (kJ/kg)
η	thermal efficiency
η_{drying}	drying efficiency
π	constant (3.1416)
σ	temperature coefficient of expansion for gas ($^oK^{-1}$)

Subscripts

a	air
amb	ambient
g	gas
d,ad	downstream
u,au	upstream
l	liquid
s	slurry
sat	saturation
i	inlet
o	outlet

REFERENCES

1. COULSON, J. M. and RICHARDSON, J. F., Chemical Engineering, Vol. 1; Second Edition, Pergamon Press, (1970).

2. WHITMAN, W. G., Chem. and Met. Eng.; 29, 147, (1923).

3. HIGBIE, R., Trans. Am. Inst. Eng. Chem.; 31, 365, (1935).

4. DANCKWERTS, P. V., Ind. Eng. Chem.; 43, 1460, (1951).

5. TOOR, H. L. and MARCHELO, J. M., A.I.Ch.E. Journal; 4, 97, (1958).

6. COLBURN, A. P., Trans. Am. Inst. Chem. Eng.; 29, 174, (1933).

7. CHILTON, T. H. and COLBURN, A. P., Ind. Eng. Chem.; 22, 967, (1930).

8. CHILTON, T. H. and COLBURN, A. P.,ibid; 26, 1183, (1934).

9. MAISEL, D. S. and SHERWOOD, T. K., Chem. Eng. Prog.; 46, 131, 172, (1950).

10. SHERWOOD, T. K., Trans. Am. Inst. Chem. Engnrs.; 36, 817, (1940).

11. GILLAND, E. R. and SHERWOOD, T. K., Ind. Eng. Chem.; 26, 516, (1934).

12. LINTON, W. H. and SHERWOOD, T. K., Chem. Eng. Prog., 46, 258, (1950).

13. SHERWOOD, T. K. and PIGFORD, R. L., "Absorption and Extraction", McGraw-Hill, (1952).

14. CHARLESWORTH, D. H. and MARSHALL, W. R., A.I.Ch.E. Journal; 6, 9, (1966).

15. PECK, R. E. and KAUH, J. Y., A.I.Ch.E. Journal; 15, 85, (1969).

16. KEEN, B. A., J. Agric. Sci.; 6, 456, (1914).

17. FISHER, E. A., idid; 13, 121, (1923).

18. FISHER, E. A., ibid; 17, 407 (1927).

19. SHERWOOD, T. K., Ind. Eng. Chem., 21, 12, 976, (1929).

20. SHERWOOD, T. K., ibid; 22, 132, (1930).

21. SHERWOOD, T. K., ibid; 24, 207, (1932).

22. SHERWOOD, T. K. and COMINGS, E. W., ibid; 25, 311, (1933).

23. AUDU, T. O. K., Ph.D. Thesis, University of Aston in Birmingham, U.K., (1973).

24. AUDU, T. O. K. and JEFFREYS, G. V., Trans. Inst. Chem. Eng.; 53, 165, (1975).

25. FUCHS, V. M., Phys. Z. Sowjet; 6, 224, (1934).

26. LANGSTROTH, G. O., et al., Can. J. Res.; 28A, 580, (1950).

27. LUCHAK, G., et al., ibid; 28A, 574, (1950).

28. FRÖESSLING, N., Gerlands Beitre Geophysics; 52, 70, (1938).

29. RANZ, W. E. and MARSHALL, W. R. Jnr., Chem. Eng. Prog.; 48, 41, 173, (1952).

30. McADAMS, W. H., "Heat Transmission", McGraw-Hill, New York, (1942).

31. DLOUHY, J. and GAUVIN, W. H., A.I.Ch.E. Journal; 6, 29, (1960).

32. PEI, D. C. T., et al., 3rd Congr. Euro. Fed. of Chem. Engnrs.; June (1962).

33. SHLÜNDER, E. U., Int. J. Ht. Transfr.; 7, 49, (1964).

34. CHARLESWORTH, D. H. and MARSHALL, W. R. Jnr., A.I.Ch.E. Journal; 6, 9, (1960).

35. WILLIAM, G. C. and SCHMIDT, R. O., Ind. and Eng. Chem.; 38, 967, (1946).

36. CHU, J. C., et al., Ind. Eng. Chem.; 45, 1586, (1953).

37. CHU, J. C., et al., ibid; 51, 275, (1959).

38. HUGHMARK, G. A., A.I.Ch.E. Journal; 13, 1219, (1967).

39. TOEI, R. M., et al., Chem. Eng. (Jap); 30, 43, (1966).

40. SANO, U., et al., ibid; 29, 294, (1965).

41. TROMMELEN, A. M. and CROSBY, E. J., A.I.Ch.E. Journal; 16, 5, 857, (1970).

42. LEE, K. and RYLEY, D. J., J. Heat Transfr.; Am. Soc. Mech. Engnrs., 90, 445, (1968).

43. WENZEL, R. B. and WHITE, R. R., Ind. Eng. Chem.; 43, 1829, (1951).

44. MASTERS, K., "Spray Drying Handbook"; 3rd Edition, (London: George Godwin), (1979).

45. KEEY, R. B. and PHAAM, Q. T., Chem. Engnr.; July/August, 516, (1976).

46. LUIKOV, A. V., Sushka Raspilenyijen, (Moskva: Pischepromizdat) (1955).

47. TURBA, J. and NEMETH, J., Brit. Chem. Eng.; 9, 457, (1959).

48. FEDER, A., Chem. Eng.; 66, 159, (1959).

49. LONGWELL, J. P. and WEISS, A. M., et al., Ind. Eng. Chem.; 45, 667, (1953).

50. BORDE, I. I., Proc. 2nd All Soviet Union Conference on Heat and Mass Transfer; Rand Report, 451-PR, 5, 649, (1964).

51. DOLINSKY, A. A., ibid; 5, 666, (1964).

52. SJENITZER, F., Chem. Eng. Sci.; 17, 309, (1962).

53. SJENITZER, F., ibid; 1, 101, (1952).

54. JOHNSTONE, H. F., and EADS, D. K., Ind. Eng. Chem.; 42, 2293, (1950).

55. MIESSE, C. C., Jet Propulsion, 24, 237, (1954).

56. MUGELE, R. A. and EVANS, H. D., Ind. Eng. Chem.; 43, 1317, (1951).

57. ROSIN, P., and RAMMLER, E., J. Inst. Fuel; 7, 29, (1933).

58. NUKIYAMA, S. and TASANAWA, Y., Trans. Soc. Mech. Engnrs. (Japan); 4, 86, (1938); 5, 63, 68, (1939); No. 22, II-7, No. 23, II-8, (1940).

59. SHAPIRO, A. H. and ERICKSON, A. T., Trans. A.S.M.E., 79, 775, (1957).

60. SCHLÜNDER, E. U., Ph.D. Dissertation, Technische Hochshule, Darmstadt,(1962).

61. MARONE, I. Ya., Theoretical Foundations of Chemical Engineering (English Translation), 5, 546, (1971).

62. YARON, I and GAL-OR, B., Internat. J. Heat and Mass Transfr.; 14, 727

63. HOPKINS, M. J. and EISENKLAM, P., Proc. Conf.Chemeca '70, Butterworths (Australia), Melbourne/Sydney, (1970).

64. MARSHALL, W. R., Trans. A.S.M.E.; 77, 1377, (1955).

65. DICKINSON, D. R., and MARSHALL, W. R., A.I.Ch.E. Journal; 41, 541, (1968).

66. DLOUGHY, J. and GUAVIN, W. H., Can. J. Chem. Eng.; 38, 113, (1960).

67. DLOUGHY, J. and GUAVIN, W. H., A.I.Ch.E. Journal, 6, 29, (1960).

68. KATTA, S. and GAUVIN, W. H., ibid; 21, 143, (1975).

69. VIEHWEG, H., BIESS, G., and WEBER, B., Chem. Tech.; 20, 620, (1968).

70. PARTI, M. and PALANCZ, B., Chem. Eng. Sci.; 29, 335, (1974).

71. GLUKERT, F. A., A.I.Ch.E. Journal; 8, 460, (1962).

72. NARASIMHAN, C., and GUAVIN, W. H., Can. J. Chem. Eng.; 46, 138, (1968).

73. KEEY, R. B., "Drying: Principles and Practice", Oxford: Pergamon Press; (International series of monograph in Chemical Engineering, Vol. 13), (1972).

74. BELCHER, D. W., et al., Chem. Eng.; 70, 20, 83, (1963).

75. MARSHALL, W. R., Chem. Eng. Prog.; Monograph Series; 2, 50 (1954).

76. MASTERS, K., Brit. Chem. Eng.; 13, 83, 242, (1968).

77. MASTERS, K., and MOHTADI, M. F., Chem. Eng., 12, 12, (1967).

78. FRIEDMAN, J. J., et al., Chem. Eng. Prog.; 48, 181, (1952).

79. KESSLER, H. G., Chem. Eng. Tech., 36, 479, (1964).

80. BUCKHAM, J. A., and MOULTON, R. W., Chem. Eng. Prog.; 51, 126, (1955).

81. CHALOUD, et al., ibid; 53, 593, (1957).

82. LEVENSPIEL, O. and BISCHOFF, K. B., Advan. Chem. Eng.; 4, 95, (1963).

83. WEN, C., and FAN, L. T., "Models for Flow Systems and Chemical Reactors", Chemical Process and Engineering Series, Vol. 3, Marcel Dekker Inc. New York, (1975).

84. LEVENSPIEL, O., and SMITH, W. K., Chem. Eng. Sci.; 6, 227, (1957).

85. VAN DER LAAN, E. Th., ibid; 7, 187, (1958).

86. ADE-JOHN, A. O., Ph.D. Thesis, University of Aston in Birmingham, (1976).

87. PARIS, J. R., et al., Ind. Eng. Chem. Proc. Des. Develop.; 10, 157-164, (1971).

88. KEEY, R. B. and PHAM Q. T., Chem. Eng. Sci.; 32, 1219, (1977).

89. KEEY, R. B. and PHAM, Q. T., ibid; 32, 786, (1977).

90. ESUBIYI, A. O., M.Sc. Thesis, University of Aston in Birmingham, (1977).

91. LEVENSPIEL, O., "Chemical Reaction Engineering", Wiley, New York.(1962).

92. HIMMELBLAU, D. M., and BISCHOFF, B. K., "Process Analysis and Simulation", Wiley, New York, (1968).

93. DANCKWERTS, P. V., Chem. Eng. Sci.; 2, 1, (1953).

94. PLACE, G., et al., Trans. Inst. Chem. Eng.; 37, 268, (1959).

95. JOHNSON, J. L., et al., Ind. Eng. Chem. Proc. Des. Dev.; 10, 4, 425, (1971).

96. CURTET, R., and RICOU, F. P., Trans. A.S.M.E.; 86, 765, (1963).

97. MASTERS, K., Ind. Eng. Chem.; 60, 53, (1968).

98. PHAM, Q. T. and KEEY, R. B., Can. J. Chem. Eng.; 55, 466, (1977).

99. BALTAS, L. and GUAVIN, W. H., A.I.Ch.E. Journal, 15, 764, (1969).

100. BALTAS, L. and GUAVIN, W. H., ibid; 15, 772, (1969).

101. SOO, S. L., Chem. Eng. Sci., 5, 57, (1956).

102. CHAO, B. T., Oester. Ing. Archv., 18, 7, (1964).

103. GAUVIN, W. H., et al., "Drop Trajectory Predictions and their importance in Deisgn of Spray Driers"; Interna. J. Multi-Phase Flow, (1974).

104. ESUBIYI, A. O., Private Communication with Blue Circle R and D (Engineering) Department, Barnstone.

105. BLARKE, F. C., Trans. A.I.Ch.E.; 14, 415, (1922).

106. KOZENY, J., Sber. Akaad, Wiss. Wein. (AbtIIa); 136, 271, (1922).

107. ERGUN, S., Chem. Eng. Prog.; 48, 89, (1952).

108. BURKE, S. P. and PLUMMER, W. B., Ind. Eng. Chem.; 20, 1196, (1928).

109. GUAVIN, W. H. and KATTA, S., A.I.Ch.E. Journal; 22, 713, (1976).

110. BAILEY, G. H., et al., Brit. Chem. Eng.; 15, 912-916, (1970).

111. DOMINGO, J. J. D. and RORIZ, L. F. C., "The Predication of Trajectories of Evaporating or Burning Droplets", Dept. of Mech. Eng., Intituto Superior, Technico, Lisbon, Portugal, RC/30, (1974).

112. FABIAN, J. M., Ph.D. Thesis, University of Washington, Seattle, (1974).

113. SEN, D. K., Ph.D. Thesis, University of Wisconsin, Madison, (1973).

114. ASHTON, C. J., Ph.D. Thesis, University of Aston in Birmingham, (1980).

115. PERRY, R. H. and CHILTON, C. H., "Chemical Engineers Handbook", 5th Edition, McGraw-Hill, (1973).

116. TILLER, F. M. and SHIRATO, M., A.I.Ch.E. Journal; 10, 61, (1964).

117. SHREVE, R. N. and BRINK, J. A., "Chemical Process Industries", 4th Edition, McGraw-Hill, (1977).